



Dublin City University  
Ollscoil Chathair Bhaile Átha Cliath

***An Investigation of Some Chromatographic  
and Electrophoretic Separations for Industrial  
and Clinical Applications***

by

**Gillian Whitaker B.Sc., M.Sc.**

**Thesis submitted for the Degree of Doctor of Philosophy**

**Supervisors:**

**Dr. Fiona Regan  
Prof. Raymond Leonard  
Prof. Malcolm R. Smyth**

## Declaration

I hereby certify that this material, which I now submit for assessment on the programme of study leading to the award PhD is entirely my own work and has not been taken from the work of others save and to the extent that such work has been cited and acknowledged within the text of my work.

Signed: gullu Butale

ID No.: 9914 0144

Date: 3rd October 2006

*For my Parents*

## Acknowledgements

I would like to thank all those who assisted me in completing this thesis.

I am especially grateful to my DCU supervisors, Prof. Malcolm R. Smyth and Dr. Fiona Regan for all their encouragement and assistance throughout the last four years. And also for giving me the opportunity to travel to Kansas, which was a memorable time.

To Prof. Craig Lunte, and all at Kansas University, especially Amy, Eric, Stacy and Stephanie, for all their help and guidance and really making me feel like I was an important member of their research group.

To Prof. Ray G. Leonard, for his excellent technical information and advice, and for his enthusiasm and encouragement.

I would also like to thank Adriano, Aoife (QFE), Blánaid, Geraldine, Kathleen, Máire, Michele, Tony and Xiliang for all their support, friendship and encouragement. Also for helping to make my time in DCU a most enjoyable experience. Special thanks to Blánaid whose friendship and unstinting support helped me through the course of my research. Thanks are also due to all the past members of the Sensors and Separations Research group.

A special word of thanks to all the technical staff at DCU for their support.

Finally, a note of thanks to all my family, for their love and encouragement, without whose support I could have not come this far. I dedicate this thesis in memory of my father, whose untimely death occurred as I was starting my research programme; and to my mother for all their love and support.



## ***Table of Contents***

Title Page	I
Declaration	II
Dedication	III
Acknowledgements	IV
Table of Contents	V
Abbreviations	XIII
Abstract	XVI

<b>Chapter One</b>	<b>1</b>
--------------------	----------

### ***A Comparison between Chromatographic and Electrophoretic Separations: A Literature Review***

<b>1.1 Introduction</b>	<b>2</b>
<b>1.2 Liquid Chromatography</b>	<b>3</b>
1.2.1 Theory of liquid chromatography	3
1.2.1.1 Separation efficiency	5
1.2.1.2 Separation factor and Resolution	7
1.2.1.3 Flow Profiles in HPLC and CE	8
<b>1.3 Modes of Separation in HPLC</b>	<b>10</b>
1.3.1 Normal Phase	10
1.3.2 Reverse Phase	10
1.3.3 Ion-exchange	11
<b>1.4 Capillary Electrophoresis</b>	<b>14</b>
1.4.1 Theory of Capillary Electrophoresis	15
1.4.1.1 Electroosmotic flow	15
1.4.1.2 Dispersion	18
1.4.1.3 Efficiency and Resolution	18

<b>1.5</b>	<b>Alternative Modes of CE</b>	<b>21</b>
1.5.1	MEKC	21
1.5.2	CEC	22
1.5.3	CITP	23
<b>1.6</b>	<b>Modes of detection in HPLC and CE</b>	<b>24</b>
1.6.1	UV-vis detection	25
1.6.1.1	Indirect UV detection	26
1.6.2	Electrochemical detection	27
1.6.2.1	Amperometric detection	28
1.6.3	Fluorescence detection	29
1.6.4	Mass Spectrometry detection	30
<b>1.7</b>	<b>Conclusions and Thesis Outline</b>	<b>32</b>
<b>1.8</b>	<b>References</b>	<b>34</b>

## **Chapter Two** **40**

### *Characterisation of an Acylphosphine oxide Photoinitiator*

<b>2.1</b>	<b>Introduction</b>	<b>41</b>
2.1.1	Theory of acylphosphine oxides	42
2.1.2	Photochemistry of acylphosphine oxides	43
2.1.2.1	UV spectroscopy	44
2.1.2.2	Time resolved spectroscopy	45
<b>2.2</b>	<b>Scope of Research</b>	<b>47</b>
<b>2.3</b>	<b>Materials and Methods</b>	<b>48</b>
2.3.1	Instrumentation	48
2.3.1.1	HPLC-UV-vis separations	48
2.3.1.2	HPLC-MS analysis	48
2.3.1.3	CE-UV separations	48

2.3.1.4	UV-vis analysis	49
2.3.2	Chemicals	49
2.3.3	Procedures	49
2.3.3.1	HPLC mobile phase preparation	49
2.3.3.2	CE background electrolyte preparation	50
2.3.3.3	Preconditioning of CE capillary	50
2.3.3.4	Preparation of stock solutions and standards	50
<b>2.4</b>	<b>Results and Discussion</b>	<b>51</b>
2.4.1	Characterisation of Irgacure	51
2.4.2	Development of HPLC separation	53
2.4.2.1	Choice of internal standard	55
2.4.2.2	Development of HPLC gradient method	57
2.4.3	Analysis of Light and Dark samples	61
2.4.3.1	Photodegradation of Irgacure	61
2.4.3.2	Addition of water	63
2.4.3.3	Comparison of strong and weak acid	65
2.4.3.4	Addition of stabiliser	66
2.4.3.5	Ethyl cyanoacetate analysis	71
2.4.4	HPLC-MS analysis of Irgacure	73
2.4.5	Optimisation of APCI parameters	74
2.4.5.1	Direct infusion analysis	74
2.4.5.2	Analysis of Irgacure with additives	77
2.4.5.3	Investigation of Irgacure cure mechanism	83
2.4.6	Development of CE separation	85
2.4.6.1	CE buffer selection	85
<b>2.5</b>	<b>Conclusion</b>	<b>89</b>
<b>2.6</b>	<b>References</b>	<b>90</b>

*Development and Application of a CE method for the analysis  
of Cyanoacrylate Adhesives*

<b>3.1</b>	<b>Introduction</b>	<b>93</b>
3.1.1	Choice of probe ion	96
<b>3.2</b>	<b>Scope of Research</b>	<b>99</b>
<b>3.3</b>	<b>Materials and Methods</b>	<b>100</b>
3.3.1	Instrumentation	100
3.3.1.1	CE-UV separations	100
3.3.1.2	Ion chromatography	100
3.3.2	Chemicals	100
3.3.3	Procedures	101
3.3.3.1	CE background electrolyte preparation	101
3.3.3.2	Preconditioning of CE capillary	101
3.3.3.3	Preparation of IC eluent	102
3.3.3.4	Preparation of stock solutions and standards	102
3.3.3.5	Quantification of Analytes	102
3.3.3.6	Adhesive sample preparation	102
<b>3.4</b>	<b>Results and Discussion</b>	<b>103</b>
3.4.1	Development of CE separation	103
3.4.2	Optimisation of CE separation	106
3.4.2.1	Effect of injection pressure and time	106
3.4.2.2	Electrolyte pH	108
3.4.2.3	Electrolyte concentration	109
3.4.2.4	Electrolyte surfactant composition and concentration	111
3.4.2.5	Development of chromate based buffered electrolytes	114
3.4.2.6	Effect of separation voltage	116
3.4.2.7	Effect of separation temperature	118
3.4.3	Optimum separation conditions	123

3.4.4	Quantification of Analytes	124
3.4.3.1	Internal standard method	124
3.4.5	Limits of detection and quantification	127
3.4.6	Application of CE method to Cyanoacrylate Adhesive samples	128
3.4.6.1	Ethyl cyanoacrylate adhesive samples	130
3.4.7	IC comparison	134
<b>3.5</b>	<b>Conclusion</b>	<b>139</b>
<b>3.6</b>	<b>References</b>	<b>140</b>

## **Chapter Four** **142**

### *An Investigation of the Stability of Cyanoacrylate Adhesive*

#### *Samples Using the Developed CE method*

<b>4.1</b>	<b>Introduction</b>	<b>143</b>
4.1.1	Cure chemistry of Cyanoacrylate Adhesives	143
<b>4.2</b>	<b>Scope of Research</b>	<b>149</b>
<b>4.3</b>	<b>Materials and Methods</b>	<b>150</b>
4.3.1	Instrumentation	150
4.3.1.1	CE-UV separations	150
4.3.2	Chemicals	150
4.3.3	Procedures	150
4.3.3.1	CE background electrolyte preparation	150
4.3.3.2	Preconditioning of CE capillary	151
4.3.3.3	Quantification of Analytes	151
4.3.3.4	Adhesive sample preparation	151
<b>4.4</b>	<b>Results and Discussion</b>	<b>152</b>
4.4.1	Sample preparation procedure	152

4.4.2	Chloride determination	157
4.4.3	Stability of Cyanoacrylate Adhesives	159
<b>4.5</b>	<b>Conclusion</b>	<b>163</b>
<b>4.6</b>	<b>References</b>	<b>164</b>
	<b>Chapter Five</b>	<b>165</b>
	<i>Analysis of Anthracycline Antibiotics by CE and HPLC</i>	
<b>5.1</b>	<b>Introduction</b>	<b>166</b>
<b>5.2</b>	<b>Analysis of Anthracyclines</b>	<b>170</b>
5.2.1	HPLC Analysis	170
5.2.1.1	HPLC-EC detection	170
5.2.1.2	HPLC-fluorescence detection	172
5.2.1.3	HPLC-UV detection	174
5.2.1.4	HPLC-MS detection	175
5.2.2	CE Analysis	176
5.2.2.1	CE-EC detection	176
5.2.2.2	CE-LIF detection	178
5.2.2.3	CE-UV detection	180
5.2.2.4	Alternative methods of analysis	181
<b>5.3</b>	<b>Scope of Research</b>	<b>182</b>
<b>5.4</b>	<b>Materials and Methods</b>	<b>184</b>
5.4.1	Instrumentation	183
5.4.1.1	CE-UV separations	183
5.4.1.2	CE-EC separations	183
5.4.1.3	CE-LIF separations	183
5.4.1.4	HPLC-UV separations	184
5.4.1.5	Electrochemical analysis	184
5.4.1.6	UV-vis analysis	184
5.4.2	Chemicals	184
5.4.3	Procedures	185

5.4.3.1	CE background electrolyte preparation	185
5.4.3.2	Preconditioning of CE capillary	185
5.4.3.3	Preparation of HPLC mobile phase	185
5.4.3.4	Preparation of plasma samples	186
5.4.3.5	Determination of free drug by VUF	186
5.4.3.6	Determination of bound drug by microdialysis	187
5.4.3.7	Preparation of stock solutions and standards	187
<b>5.5</b>	<b>Results and Discussion</b>	<b>188</b>
5.5.1	Development of CE separation	188
5.5.1.1	Addition of chiral selectors	189
5.5.1.2	Optimum separation conditions	193
5.5.2	Application to plasma samples	194
5.5.2.1	Direct injection of plasma samples	194
5.5.2.2	VUF of plasma samples	195
5.5.3	CE-Electrochemical detection	197
5.5.4	CE-LIF detection	201
5.5.5	Determination of protein binding of anthracyclines	202
5.5.6	Comparison of CE method with HPLC-UV analysis	205
<b>5.6</b>	<b>Conclusion</b>	<b>206</b>
<b>5.7</b>	<b>References</b>	<b>207</b>
<b>Chapter Six</b>		<b>213</b>
	<i>Conclusions</i>	
<b>6.1</b>	<b>Comparison of Electrophoresis vs Chromatography</b>	<b>214</b>
6.1.1	Sample matrix	214
6.1.2	Sample volume	215
6.1.3	Length of Analysis	215
6.1.4	Detection modes	216
6.1.5	Conclusion	216

<b>Chapter Seven</b>	<b>217</b>
<i>Appendices</i>	
<b>7.1 Appendix 1a – MS Parameters for positive APCI</b>	<b>218</b>
<b>7.2 Appendix 1b – IC Gradient method</b>	<b>219</b>
<b>7.3 Publications</b>	<b>220</b>
<b>7.4 Oral Presentations</b>	<b>221</b>
<b>7.5 Poster Presentations</b>	<b>222</b>



## Abbreviations

ACN	acetonitrile
Ag/AgCl	silver/silver chloride (reference electrode)
AE	auxiliary electrode
APCI	atmospheric pressure chemical ionisation
BAPO	bisacylphosphine oxide
BF <sub>3</sub> .2H <sub>2</sub> O	boron trifluoride dihydrate
BGE	background electrolyte
BQ	benzoquinone
CD	cyclodextrins
CEC	capillary electrochromatography
CE	capillary electrophoresis
CE-EC	capillary electrophoresis-electrochemical detection
CE-LIF	capillary electrophoresis-laser induced fluorescence detection
CE-MS	capillary electrophoresis-mass spectrometry detection
CE-UV	capillary electrophoresis-ultra-violet detection
CHP	cumene hydroperoxide
CIDNP	chemically induced dynamic nuclear polarisation
CITP	capillary isotachophoresis
CMC	critical micelle concentration
CTAB	cetyltrimethylammonium bromide
CV	cyclic voltammetry
CZE	capillary zone electrophoresis
DAN	daunorubicin
DAP	dialkyl phosphate
DDAB	didodecylammonium bromide
DEP	diethyl phosphate
DMEP	dimethoxy ethyl phosphate
DNA	DeoxyriboNucleic Acid
DOX	doxorubicin
EC	electrochemical detection
EIC	extracted ion chromatogram

EOF	electroosmotic flow
EPI	epirubicin
ESI	electrospray ionisation
ESR	electron spin resonance
FITC	fluorescein isothiocyanate
GC-MS	gas chromatography mass spectrometry
H <sub>2</sub> O <sub>2</sub>	hydrogen peroxide
H <sub>2</sub> SO <sub>4</sub>	sulphuric acid
HDV	hydrodynamic voltammogram
HETP	height equivalent to a theoretical plate
HPLC	high performance liquid chromatography
HPLC-EC	high performance liquid chromatography electrochemical detection
HPLC-MS	high performance liquid chromatography mass spectrometry detection
HPLC-UV	high performance liquid chromatography ultra-violet detection
HQ	hydroquinone
IC	ion chromatography
IEC	ion-exchange chromatography
IE-CEC	ion-exchange capillary electrochromatography
ITP	isotachopheresis
LC-MS/MS	liquid-chromatography tandem mass spectrometry
LE	leading electrolyte
LIF	laser-induced fluorescence
LLE	liquid-liquid extraction
LOD	limit of detection
LOQ	limit of quantification
MAPO	monoacylphosphine oxides
MEKC	micellar electrokinetic chromatography
MeOH	methanol
MS	mass spectrometry
MSA	methyl sulphonic acid

m/z	mass to charge ratio
NaOH	sodium hydroxide
NDA	naphthalene-2,3-dicarboxaldehyde
NMR	nuclear magnetic resonance
NP	normal-phase
ODS	octadecyl silane
PAN	polyacrylonitrile membrane
PDCA	pyridinedicarboxylic acid
PEEK	polyetheretherketone
PK	pharmacokinetic
PMA	pyromellitic acid
PTSA	<i>p</i> -toluene sulphonic acid
RE	reference electrode
RSD	relative standard deviation
RP	reverse-phase
SDS	sodium dodecyl sulphate
S/N	signal to noise ratio
TAPS	N-tris[Hydroxymethyl]methyl-3amino-propane sulphonic acid
THF	tetrahydrofuran
TE	terminating electrolyte
TIC	total ion chromatogram
TLC	thin-layer chromatography
TR-ESR	time-resolved electron spin resonance
TR-IR	time-resolved infra-red
TTAB	tetradecylammonium bromide
UV	Ultra-violet
VUF	vacuum ultrafiltration
WE	working electrode

## **An Investigation of the Chromatographic and Electrophoretic Separations for Industrial and Clinical Applications**

Chromatographic techniques, such as high performance liquid chromatography (HPLC) and ion chromatography (IC), have traditionally been employed in the analysis of a variety of analytes, such as inorganic anions, organic acids and pharmaceuticals. Capillary electrophoresis (CE) methods have recently been developed for their determination and can be ideal methods due to low sample and material consumption, reduced analysis times and increased separation efficiencies.

A HPLC method was developed and successfully applied to the analysis of the photoinitiator, bis(2,4,6-trimethylbenzoyl)phenyl-phosphine oxide. A comparison of its stability in samples, which were both kept in the dark and exposed to the light, was performed using the optimised HPLC-UV method. From this it was determined that complete degradation of the Irgacure had occurred by 60 min. for the samples exposed to the light. The curing mechanism of the Irgacure was determined using HPLC-MS, and it was determined that the Irgacure undergoes a free radical curing reaction.

There are a wide range of inorganic and acidic anions that may be present at different stages of the cyanoacrylate adhesive production process. A highly efficient CE separation was developed and applied to the simultaneous determination of inorganic and acidic anions, which are present in ethyl cyanoacrylate adhesive samples. The CE method developed was compared with IC, the method traditionally employed for their analysis. CE offers advantages over the IC method, namely reduced sample volumes and waste and also more rapid separation. From this investigation, CE was demonstrated to be an effective method for their quantification, as it enabled the sensitive monitoring of the cyanoacrylate production process.

A CE method was developed for the simultaneous analysis of the anthracyclines, daunorubicin, doxorubicin and epirubicin. Ultra-violet (UV), electrochemical (EC) and laser-induced fluorescence (LIF) detection coupled to CE were investigated. Improved detection limits ( $150\text{--}1400\text{ ng ml}^{-1}$ ) were obtained with LIF detection, which were capable of monitoring the therapeutic levels ( $5\text{--}50,000\text{ ng ml}^{-1}$ ) of anthracyclines. For the real time monitoring of anthracyclines in plasma, it was preferred that minimal sample pre-treatment was carried out. The feasibility of analysing plasma samples without sample pre-treatment was demonstrated. The degree of plasma protein binding of anthracyclines was determined using microdialysis, and the potential of this technique for the real time monitoring of plasma samples with on-line microdialysis coupled with CE was demonstrated. Microdialysis is suitable for coupling to CE as it generates sample volumes that are ideal for CE.

## ***Chapter One***

# ***A Comparison between Chromatographic and Electrophoretic Separations: A Literature Review***

## 1.1 INTRODUCTION

Traditional chromatographic techniques, such as High Performance Liquid Chromatography (HPLC) and Ion Chromatography (IC), have been applied to the analysis of numerous analytes, such as inorganic anions,<sup>[1-5]</sup> organic acids<sup>[6,7]</sup> and pharmaceuticals.<sup>[8-10]</sup> Capillary Electrophoresis (CE) methods have recently been developed as an alternative for the analysis of small charged species (inorganic anions)<sup>[11-14]</sup> and also in the analysis of pharmaceuticals.<sup>[15-18]</sup> Capillary Zone Electrophoresis (CZE), which is CE in its free zone form, is an ideal method for the analysis of anions due to its low sample consumption and compared to chromatography methods, its reduced analysis times and highly efficient separations makes it an attractive option for the determination of anions.<sup>[13]</sup>

As an introduction, a comparison between chromatographic and electrophoretic separation techniques for the determination of analytes in complex matrices, such as plasma and serum,<sup>[19]</sup> will be made. CE will be introduced as a powerful and potential alternative for their analyses. The different modes of separation available in HPLC and CE will also be discussed.

There are various modes of detection, which may be coupled to either HPLC or CE, *e g* ultra-violet (UV), fluorescence and electrochemical detection (EC). These modes of detection will be discussed and their application to the analysis of samples in complex matrices will be examined. Throughout this study, the advantages of CE over the traditional chromatographic techniques will be outlined.

## 1.2 LIQUID CHROMATOGRAPHY

Chromatography is a separation technique, which is based upon the distribution of analytes between two phases, a stationary and a mobile phase.<sup>[20]</sup> The stationary phase is either a solid or liquid, which is coated onto a solid surface. The mobile phase is either a liquid or a gas, and is known as the eluent. Analyte molecules are continually distributed between both phases. Whilst in the mobile phase, the analytes are carried forward with it and separation occurs due to differences in affinity for the stationary and mobile phases. Those with the greatest affinity for the stationary phase remain on the column the longest.

### 1.2.1 Theory of liquid chromatography

In HPLC, the mechanism of retention is based upon the development of an equilibrium between the stationary and mobile phase. The volume of mobile phase needed to elute an analyte from the column is the retention volume,  $V_R$ , which is described by Eqn 1.1:

$$V_R = t_R F \quad \text{Eqn 1.1}$$

where:       $t_R$       =      analyte retention time (min)  
               $F$         =      flow rate (ml/min)

A representation of a typical chromatogram is illustrated in Fig. 1.1. The dead volume,  $V_0$ , and its corresponding retention time,  $t_0$ , is defined as the volume of eluent required to elute unretained components (the void).

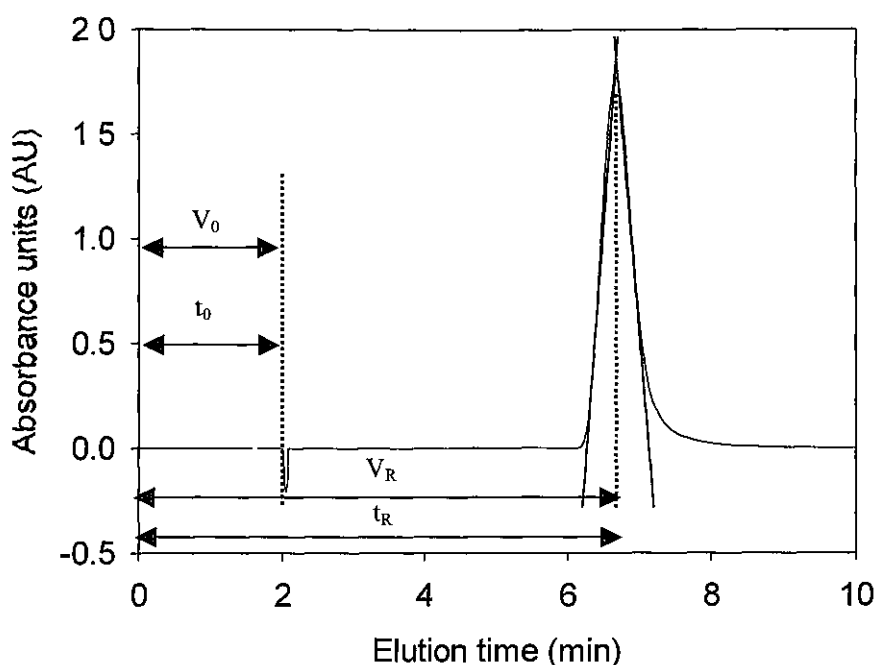


**Figure 1.1** Representation of a typical HPLC chromatogram<sup>[21]</sup>

The retention factor,  $k$ , is an essential factor in the retention mechanism of analytes. It is defined as a measure of the affinity that an analyte has for the stationary phase and is shown by Eqn. 1.2:

$$k = \frac{t_R - t_0}{t_0} \quad \text{Eqn. 1.2}$$

The optimal value for  $k$  lies in the range 2 and 5. If the value is below 2, this indicates that the analyte has been eluted too quickly, so that it is too close to the void and if the value is greater than 5, this illustrates that the analyte has been eluted too slowly, so that the run time is excessively long. The  $k$  value may be altered by modifying the eluent composition or pore size of the column.<sup>[21]</sup>



### 1.2.1.1 Separation efficiency

The efficiency of a chromatographic separation is commonly described by the term, theoretical plates (N). It may also be expressed as the height equivalent to a theoretical plate (HETP). N is determined by Eqn. 1.3:

$$N = \left( \frac{t_R}{\sigma} \right)^2 = \frac{L}{H} \quad \text{Eqn. 1.3}$$

where:  $\sigma$  = band variance (min)  
 $L$  = column length (m)  
 $H$  = plate height (HETP)

The efficiency may also be calculated experimentally using Eqn.'s 1.4 and 1.5:

$$N = 16 \left( \frac{t_R}{W} \right)^2 \quad \text{Eqn. 1.4}$$

where W is the baseline peak width of the analyte

$$N = 5.54 \left( \frac{t_R}{W_{1/2}} \right)^2 \quad \text{Eqn. 1.5}$$

where  $W_{1/2}$  is the peak width at half height

The concept of theoretical plates was first introduced by Martin and Synge;<sup>[22]</sup> however, a more realistic rate theory was developed by van Deemter.<sup>[23]</sup> This theory takes into account the diffusion effects of mass transfer and migration through a packed bed, with the resulting peak shape being affected by the rate of elution.<sup>[21]</sup> The van Deemter theory of HETP is described by Eqn. 1.6, where the factors A, B and C all contribute to peak broadening.

$$HETP = A + B/u + Cu \quad \text{Eqn. 1.6}$$

where:       $u$       =      average velocity of the mobile phase  
               $A$       =      eddy diffusion term  
               $B$       =      longitudinal diffusion term  
               $C$       =      kinetics of mass transfer term

Eddy diffusion is caused by the movement of molecules from the same analyte, which migrate through the stationary phase at random. This will result in broadening of the analyte band. Longitudinal diffusion is related to the length of time an analyte will spend in the mobile phase. Whilst, the third parameter,  $C$ , is dependant upon the amount of time an analyte needs in order to equilibrate between the stationary and mobile phase. A plot of plate height ( $H$ ) against the mobile phase velocity, known as a van Deemter plot, is commonly employed to determine the optimum flow rate for the mobile phase. A typical plot is illustrated in Fig. 1.2.

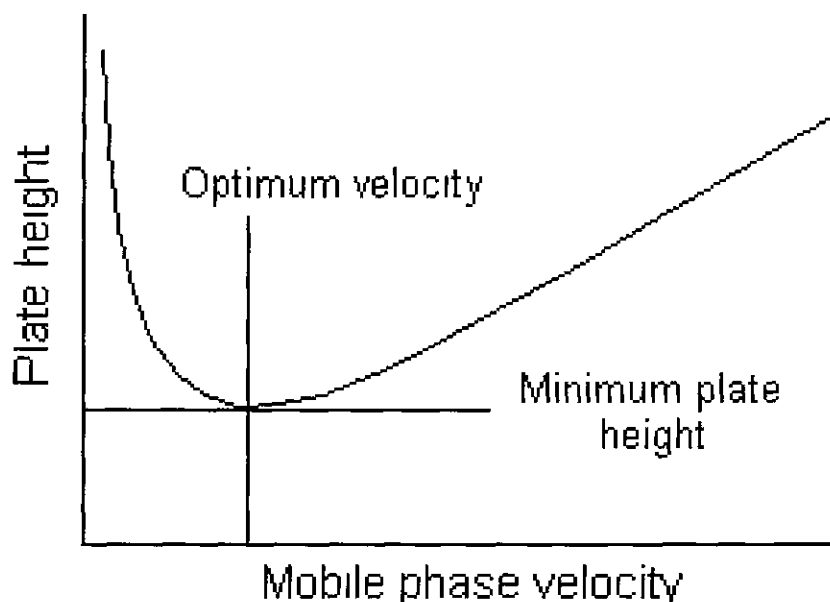


**Figure 1.2** Representation of a typical van Deemter plot<sup>[24]</sup>

### 1.2.1.2 Separation factor and Resolution

The separation factor ( $\alpha$ ) of a chromatographic separation is a measure of the band proximity of two adjacent analyte bands, which have  $k$  values of  $k_1$  and  $k_2$ . This is determined by Eqn. 1.7:

$$\alpha = \frac{k_2}{k_1} \quad \text{Eqn. 1.7}$$

This factor is identified with the selectivity of a chromatographic system, *i.e.*, the ability of the system to provide different retention times for two specific analytes. It may be determined experimentally using Eqn. 1.8:

$$\alpha = \frac{t_{R_2} - t_0}{t_{R_1} - t_0} \quad \text{Eqn. 1.8}$$

where:  $t_{R_2}$  = retention time of the second analyte  
 $t_{R_1}$  = retention time of the first analyte

The resolution,  $R$ , of a separation is another measure of the ability of a chromatographic system to separate two analytes. It is calculated using Eqn. 1.9:

$$R = \frac{2(t_{R_2} - t_{R_1})}{W_1 + W_2} \quad \text{Eqn. 1.9}$$

where  $W$  is the baseline peak width of components

It is also determined by Eqn. 1.10

$$R = \frac{\sqrt{N}}{4} \left( \frac{\alpha - 1}{\alpha} \right) \left( \frac{k_2}{1 + k_2} \right) \quad \text{Eqn. 1.10}$$

For quantitative analysis, baseline resolution is achieved when  $R=1.5$ .<sup>[24]</sup> From Eqn. 1.10, it is evident that  $R$  is dependant upon  $\alpha$ ,  $N$  and  $k$ . The optimum parameter with which to control resolution is  $\alpha$ ; however, this is primarily achieved by changing the stationary phase. Resolution is also proportional to both the square root of  $N$  and to  $k$ . It may be improved by increasing these parameters; however, these can lead to long analysis times and increased band broadening.

A comparison of the flow profiles generated in HPLC and CE is discussed in Section 1.2.1.3.

#### **1.2.1.3 Flow Profiles in HPLC and CE**

In CE, the plug-like flow profile generated within the capillary gives rise to a uniform flow throughout, electroosmotic flow (EOF), which produces a laminar flow profile. This is in contrast to the hydrodynamic flow that is produced from an external pump in HPLC (Fig. 1.3), which produces a parabolic flow profile. The theory of CE is discussed in detail in Section 1.4.

Hydrodynamic flow results in peak broadening and as a consequence the efficiency and resolution of the separation will be reduced, whilst the flow profile in CE reduces the velocity across the capillary, thereby decreasing the band-broadening due to slow mass transfer across the capillary.<sup>[25]</sup>

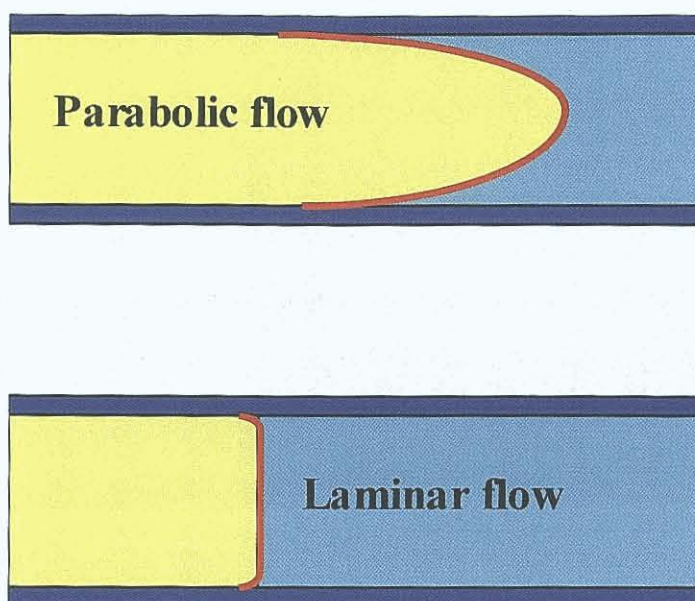


**Figure 1.3** Representation of the flow profiles generated in HPLC (parabolic) and CE (laminar flow)<sup>[24]</sup>

### 1.3 MODES OF SEPARATION IN HPLC

#### 1.3.1 Normal-phase

In normal-phase high-performance liquid chromatography (NP-HPLC), separation occurs through the interaction of analytes with a polar stationary phase (a cyano or amino bonded stationary phase) and a less polar mobile phase, such as hexane and heptane. Analytes are retained on the column based upon their polarity; the more polar the analyte, the more it will be retained on the column.

NP chromatography with fluorescence detection has been employed for the determination of some pharmaceuticals in plasma<sup>[26]</sup> and in blood, with limits of quantification (LOQ) in the range 2-20 ng ml<sup>-1</sup> obtained.<sup>[27]</sup> NP-HPLC has recently been applied to the chiral determination of zolmitriptan and any potential impurities in pharmaceutical formulations.<sup>[28]</sup> However, the applications of this mode of chromatography have become limited and reverse-phase chromatography is a more commonly used separation mechanism and is discussed in Section 1.3.2.

#### 1.3.2 Reverse-phase

Separation in reverse-phase HPLC (RP-HPLC) is based upon the distribution of analytes between a non-polar stationary phase and a polar mobile phase, such as methanol-water or acetonitrile-water organic aqueous mixtures. Typical stationary phases employed are hydrophobic bonded packings with octadecyl (C-18), octyl (C-8) or phenyl functional groups.<sup>[29]</sup>

In RP-HPLC, as the hydrophobic nature of the analytes increases, their retention on the column also increases. This retention may be reduced by the addition of an organic solvent to the mobile phase, which helps in reducing the polarity of the mobile phase. The less polar the organic solvent, such as tetrahydrofuran (THF), the less time the analyte is retained on the column.<sup>[29]</sup>

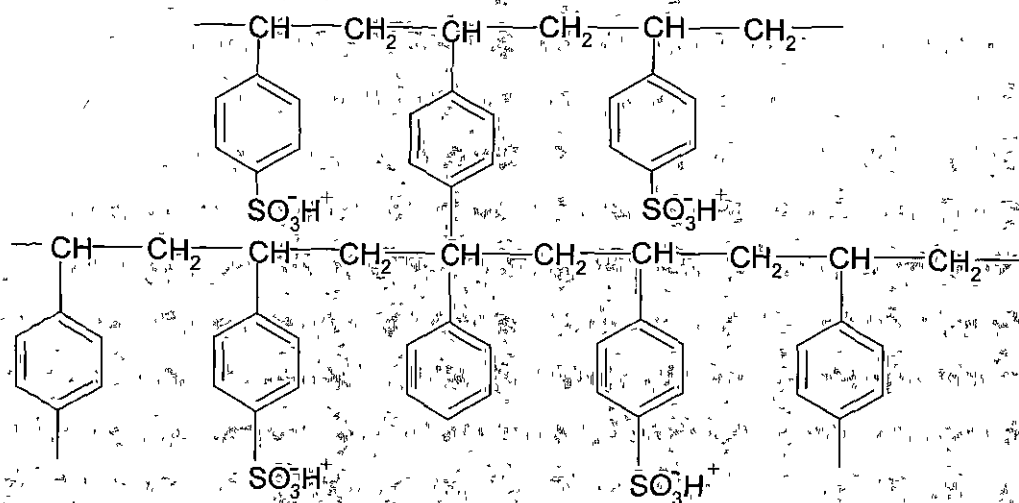
The application of RP-HPLC in the determination of pharmaceuticals in biological fluids has been widely reported in the literature, such as serum<sup>[30,31]</sup> and

plasma.<sup>[32,33]</sup> The use of reverse-phase columns has also been employed for the determination of inorganic anions in a process known as ion-pair chromatography.<sup>[5]</sup> An alternative method for the analysis of ions is ion-exchange chromatography (IEC) and is routinely employed for their determination.<sup>[34]</sup>

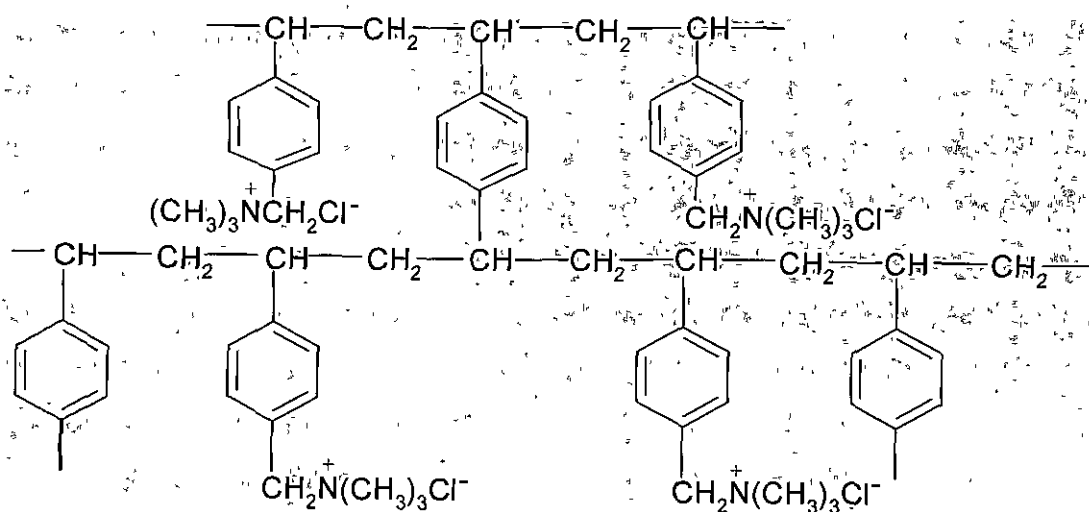
### 1.3.3 Ion-exchange

In IEC, the packing material possesses charge-bearing functional groups, which are capable of exchanging with ionic analytes in the mobile phase. The functional groups employed are permanently bonded ionic groups associated with counterions of the opposite charge, where retention occurs due to the exchange of analyte ions with ions of the opposite charge in the mobile phase.<sup>[29]</sup>

There are two modes of IEC; anion-exchange chromatography in which the packing material is a strongly basic quaternary ammonium group, and cation-exchange chromatography where the packing material is a strongly acidic sulphonic acid group. Examples of a cation-exchange resin (I) and an anion-exchange resin (II) are illustrated in Fig. 1.4. Both of these functional groups are totally dissociated, *i.e.*, their exchange properties are independent of pH. There are also exchangers that possess weakly acidic and basic functional groups, such as carboxylate and tertiary amine groups. In this instance, the retention mechanism of analyte ions is dependent upon the pH of the mobile phase.<sup>[29]</sup>



### I-Strongly acidic cation-exchange resin



### II-Strongly basic anion-exchange resin

Figure 1.4 Structures of styrene-divinylbenzene cross-linked ion-exchange resins<sup>[35]</sup>



The applications of IEC range from the analysis of amino acids on a cation exchanger to the simultaneous separation of inorganic anions and cations using anion and cation-exchange columns connected in tandem.<sup>[1,29]</sup> An alternative application of IEC is IC, which combines an ion-exchange separation with suppression of the mobile phase and in most cases detection is performed conductimetrically. IC has become the method of choice for the analysis of anions, and has been employed for the simultaneous separation of inorganic anions.<sup>[36]</sup> The trace analysis of anions in drinking water has also been reported by IC.<sup>[37-39]</sup>

## 1.4 CAPILLARY ELECTROPHORESIS

CE has also emerged as a powerful separation technique for the analysis of small charged species, such as anions and cations,<sup>[13,14,40-42]</sup> and also in the determination of pharmaceuticals in complex matrices.<sup>[18,43,44]</sup> This method of separation is discussed in greater detail in Section 1.4.

The term electrophoresis is used to describe the separation of charged species under the influence of an electric field. When an electric field is applied the charged species migrate into discrete zones that are separated. Performing electrophoresis in narrow-bore capillaries has been developed during the last twenty-five years.<sup>[11,45]</sup> This technique is an alternative to the traditional slab electrophoresis, which generally suffers from long analysis times, low efficiencies and difficulties in detection and automation.<sup>[46]</sup> Typical CE instrumentation is illustrated in Fig. 1.5.

The small internal diameter of the capillary (10 to 100  $\mu\text{m}$ ) leads to efficient heat dissipation, which allows for increased voltages to be applied. Typical applied voltages range from 5 kV to 30 kV. As a result of the increased voltages, high-resolution separations are achieved in shorter analysis times.<sup>[47]</sup>

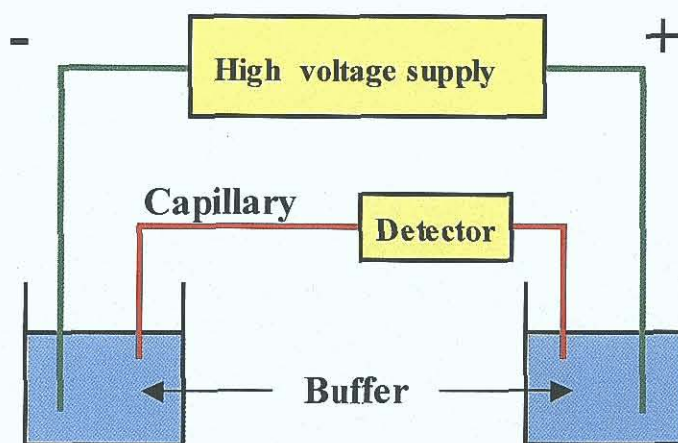


**Figure 1.5** Schematic showing capillary electrophoresis instrumentation, in reverse polarity. A capillary electrophoresis system consists of fused-silica capillary with an optical viewing window for detection, a high voltage power supply, two buffer reservoirs and a detector<sup>[24]</sup>

### 1.4.1 Theory of Capillary Electrophoresis

Separation in electrophoresis is based upon differences in solute velocity under the influence of an electric field,  $E$ . This solute velocity ( $v_{ep}$ ) is described by Eqn. 1.11:

$$v_{ep} = \mu_{ep} E \quad \text{Eqn. 1.11}$$

The electrophoretic mobility ( $\mu_{ep}$ ) depends upon the charge of the ionic species, the concentration of the electrolytes and the temperature. This is determined by Eqn. 1.12:

$$\mu_{ep} = \left( \frac{q}{6\pi} \right) \eta r \quad \text{Eqn. 1.12}$$

where:

$\mu_{ep}$	=	electrophoretic mobility
$q$	=	charge on the ion
$\eta$	=	buffer viscosity
$r$	=	ion radius

#### 1.4.1.1 Electroosmotic Flow (EOF)

A fundamental factor in CE is electroosmosis. This originates in the presence of an electric field when an ionic solution is in contact with a charged solid surface and gives rise to EOF.<sup>[47]</sup> The inner surface of the fused silica capillary contains silanol groups. Upon ionisation of these silanol groups, a negatively charged surface is created. This surface affects the distribution of nearby ions in solution, forming a double layer of ions on the capillary surface.<sup>[48]</sup>

The counter ions in the double layer are arranged into two zones, a diffuse and fixed zone, with a surface of shear just beyond the interface. When a voltage is applied across the capillary, the solvated cations in the diffuse layer migrate towards the cathode.<sup>[48]</sup>

As a result of this movement, the solvent molecules are pulled along with them, as represented in Fig. 1.6.

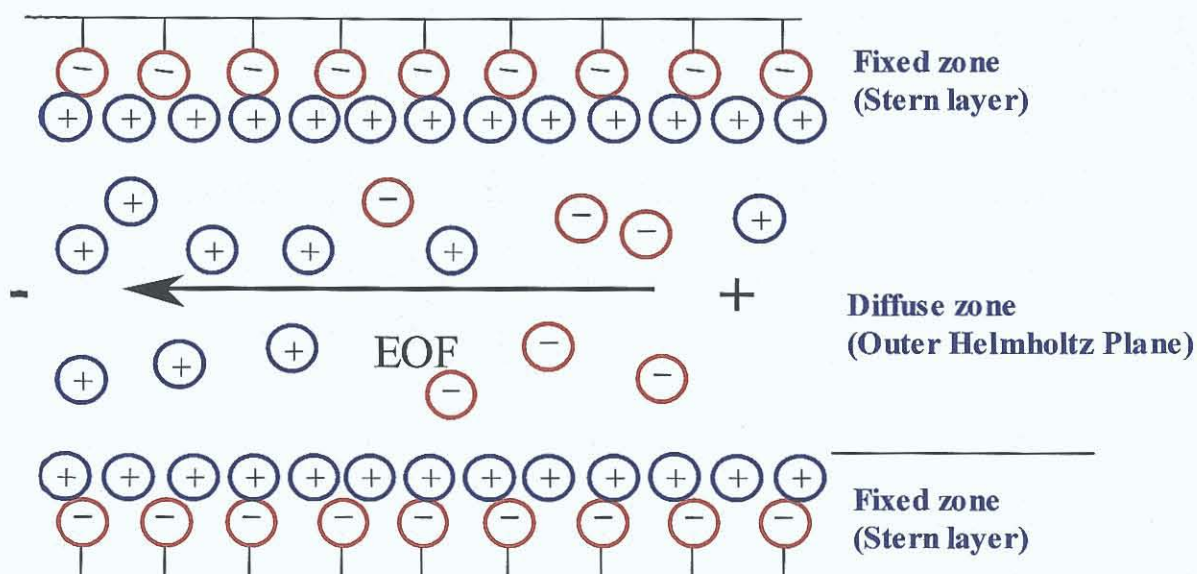


**Figure 1.6** Representation of the ionic layer in a fused silica capillary, in normal polarity with the detector at the cathode<sup>[24]</sup>

All species, regardless of charge, will move in the same net direction due to the EOF. In normal polarity, cations will migrate the fastest because the electrophoretic attraction is towards the cathode and the EOF is in the same direction. Anions migrate against the EOF and are detected last.<sup>[49]</sup> With reverse polarity, the direction of the EOF is opposite to the detector and only anions with an electrophoretic mobility greater than the EOF will be detected. Under these conditions, the capillaries are generally coated with EOF modifiers, which reverse the net charge of the inner wall and therefore the EOF will be reduced.<sup>[50]</sup>

The mobility of the EOF, ( $\mu_{EOF}$ ), is calculated by Eqn 1.13:

$$\mu_{EOF} = \left( \frac{\epsilon \xi}{4\pi\eta r_c} \right) \quad \text{Eqn. 1.13}$$

where:  $\mu_{EOF}$  = mobility of the EOF  
 $\varepsilon$  = dielectric constant  
 $\zeta$  = zeta potential  
 $\eta$  = solution viscosity  
 $r_c$  = radius of capillary

The velocity of the EOF, ( $V_{EOF}$ ), is described by Eqn. 1.14:

$$V_{EOF} = \mu_{EOF} E \quad \text{Eqn. 1.14}$$

The migration time of analytes, ( $t$ ), is dependent upon the mobility of the solute and the EOF. This is used to determine the apparent solute mobility, ( $\mu_a$ ), using Eqn. 1.15:

$$\mu_a = \frac{1}{tE} = \frac{lL}{tV} \quad \text{Eqn. 1.15}$$

where  $\mu_a$  =  $\mu_{ep} + \mu_{EOF}$   
 $t$  = migration time (min)  
 $E$  = electric field  
 $l$  = effective capillary length  
 $L$  = total capillary length  
 $V$  = applied voltage

The EOF decreases as the concentration of the background electrolyte (BGE) increases. In general, high buffer concentrations reduce the overall adsorption of analytes to the capillary wall.<sup>[48]</sup> This reduction may be caused by a number of factors including the charge of ion, ( $q$ ), buffer viscosity, ( $\eta$ ) and the zeta potential, ( $\zeta$ ).<sup>[51]</sup>

EOF is dependent upon the pH of the electrolyte. At high pH, the EOF is considerably larger than at low pH. This is due to the deprotonation of the silanol groups on the capillary wall. At low pH the EOF is reduced because protons convert the charged  $\text{SiO}^-$  surface to  $\text{SiOH}$ , causing a decrease in  $\zeta$ . If the EOF is too fast the analytes will migrate too quickly through the capillary and will be poorly separated by

the time they reach the detector. It is therefore, important that the EOF is sufficient to allow for adequate separation of the charged species in a short time.<sup>[51]</sup>

Electroosmosis and electrophoresis are closely related phenomena, which often occur together in CE. The presence of electroosmosis in the capillaries reduces the analysis times and allows for the operation of the device in a continuous mode.<sup>[52]</sup>

#### 1.4.1.2 Dispersion

Electrophoresis is the separation of charged species into discrete zones under the influence of an electric field. Dispersion results from differences in solute velocity within that zone. Peak dispersion,  $\sigma^2$ , is determined by Eqn. 1.16:

$$\sigma^2 = 2D_m t \quad \text{Eqn. 1.16}$$

where  $D_m$  is the diffusion coefficient of the solute ( $\text{cm}^2\text{s}^{-1}$ ).

Dispersion in CE can be caused by a number of factors including Joule heating, injection plug length or sample adsorption to the capillary wall. These parameters may be controlled, *e.g.* applying a lower separation voltage or employing a capillary with a small internal diameter reduces the effects of Joule heating. This will limit the amount of heat produced and aid in the dissipation of the heat formed.

#### 1.4.1.3 Efficiency and Resolution

Due to the flow profile produced in CE, high separation efficiencies are obtained. The separation efficiency, can be expressed in terms of theoretical plates,  $N$ , and is determined by Eqn. 1.17:

$$\frac{L^2}{\sigma^2} = \frac{\mu_{ep} V}{2D_m} \quad \text{Eqn. 1.17}$$

where:  $\mu_{ep}$  = electrophoretic mobility

$D_m$	=	diffusion coefficient of the solute
$V$	=	voltage applied
$L$	=	total capillary length

The efficiency of a separation is dependent upon the high voltage applied. As the voltage is increased, the separation efficiency will also increase (Eqn. 1.18). Efficiency can also be calculated experimentally using Eqn. 1.19, just as with HPLC:

$$N = \frac{\mu_{ep} El}{2D_m} \quad \text{Eqn. 1.18}$$

where:	$E$	=	electric field
	$l$	=	effective capillary length

$$N = 5.54 \left( \frac{L}{W_{1/2}} \right)^2 \quad \text{Eqn. 1.19}$$

where  $W_{1/2}$  is the peak width at half height.

In CE,  $R$  of two components is dependent on the solute mobilities of the components. It can be affected significantly by peak sizes and shapes.<sup>[25]</sup> Again as with HPLC, it is determined experimentally using Eqn. 1.9.

It is also determined by Eqn. 1.20

$$R = \frac{I}{4} \Delta\mu_{ep} \sqrt{\frac{V}{(\mu_{ep} + \mu_{eo})D_m}} \quad \text{Eqn. 1.20}$$

From Eqn. 1.20, it is evident that the resolution of two peaks decreases with the magnitude of the EOF provided the EOF has the same direction as the electrophoretic migration.<sup>[53]</sup>

Resolution is dependent on capillary length at constant field strength and can be improved by increasing the length of the capillary and by applying reduced voltages. However, extreme magnitudes of both these variables can lead to long analysis times and Joule heating.<sup>[25]</sup>

The mode of CE described above is commonly known as CZE and the quantification of charged analytes has regularly been performed using this method of separation.<sup>[54,55]</sup> Alternative modes for their analysis are discussed in Section 1.5.



## 1.5 ALTERNATIVE MODES OF SEPARATION IN CE

### 1.5.1 Micellar Electrokinetic Chromatography (MEKC)

MEKC is a mode of electrokinetic chromatography, in which ionic surfactants are added to the BGE. It was first developed as a separation technique for CE by S. Terabe *et al.*<sup>[56,57]</sup> The most commonly used anionic surfactant is sodium dodecyl sulphate (SDS), whose structure is composed of a hydrophobic tail and a negatively charged, hydrophilic head, as shown in Fig. 1.7. Above their critical micelle concentration (CMC), the surfactants will form micelles. These have hydrophobic, non-polar moieties at their interior and charged polar groups at the surface.

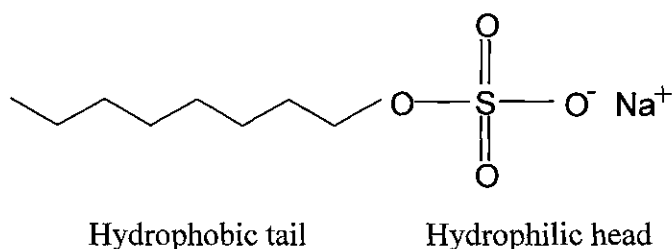


**Figure 1.7** Structure of sodium dodecyl sulphate<sup>[50]</sup>

Separation is obtained due to differences in electrophoretic mobilities and partitioning. The degree to which the separation is based upon partitioning is dependent upon the type of surfactant added.<sup>[58]</sup> MEKC has applications in the analysis of illicit drug substances<sup>[59]</sup> and also in the determination of pharmaceuticals.<sup>[60]</sup> In order to improve the poor concentration sensitivity of ultra-violet (UV) detection with MEKC, on-line preconcentration techniques have been employed. These include sample stacking and sweeping.<sup>[61-63]</sup> MEKC separations are also possible in the absence of EOF. This is particularly useful for acidic species which would be ionised at high pH and therefore will not interact with a negatively charged SDS micelle.<sup>[64]</sup> Cyclodextrins (CD), such as  $\beta$  or  $\gamma$ -cyclodextrins, have been incorporated in the buffer solution and have been successfully applied for the analysis of enantiomers, particularly neutral CDs with achiral surfactants.<sup>[65,66]</sup>

Although it was originally developed for the analysis of neutral substances, MEKC also allows for the separation of anionic species.<sup>[67,68]</sup> The selectivity of the separation is controlled by the type of surfactant added. Generally the structure of the polar group of the surfactant will affect selectivity more than the hydrophobic core of the micelle, as most analytes interact with the micelle at the surface. Also, selectivity is influenced by the combination of ionic and non-ionic micelles or ionic and zwitterionic micelles. MEKC has been shown to be effective for the separation of small molecules, which traditionally had been impossible by gel electrophoresis.<sup>[65]</sup>

### 1.5.2 Capillary Electrochromatography (CEC)

Capillary electrochromatography is a hybrid of the techniques of CE and HPLC. This process combines the high peak efficiency of electrically driven separation techniques with the high selectivity of chromatographic techniques.<sup>[69]</sup> The electrically driven flow transports the analytes through the capillary, which is packed with a stationary phase material. For neutral analytes, separation is achieved by differential partition between the stationary and mobile phase, and are transported through the capillary by the EOF. The separation of charged analytes is achieved by the combined effects of partitioning and electrophoresis.<sup>[70]</sup>

The capillaries are generally packed with a traditional HPLC reverse phase packing material, *e.g.* octadecyl silane (ODS). Separations are conducted at a high pH ( $\text{pH} > 7$ )<sup>[70]</sup> to ensure a fast EOF, which reduces analysis times. Alternatively a low pH may be employed, although, this will increase the total analysis time.<sup>[64]</sup>

Many of the applications of CEC are in the analysis of pharmaceuticals.<sup>[70-72]</sup> The separation of anions is achieved mainly by ion-exchange CEC (IE-CEC). In this mode, silica based ion-exchangers rather than silica based reversed phase sorbents are packed into the capillary. The first report for the separation of anions was by Li *et al.*<sup>[73]</sup> Subsequently, CEC methods have been developed for the analysis of anions with a variety of stationary phases, such as a polymer ion-exchangers<sup>[74]</sup> and quaternary ammonium anion-exchange latex particles.<sup>[75,76]</sup> The separation of acidic analytes is possible if a sulphonic acid-containing phase is employed.<sup>[64]</sup>

CEC is a highly efficient mode of CE, with efficiencies in the region 150,000-200,000 plates/m obtained.<sup>[50]</sup> However, as the application of CEC to charged analytes has only recently been developed, more research in this area is required.<sup>[76]</sup>

### 1.5.3 Capillary Isotachopheresis (CITP)

Isotachopheresis (ITP) is based upon the movement of a charged molecule in an electric field, which is dependent upon the mobility of the fastest moving ion. The analyte is introduced into the capillary between two electrolyte solutions, a leading electrolyte (LE) and a terminating electrolyte (TE). The LE and TE are fast and slow moving electrolytes respectively. When a high voltage is applied, the analyte ions will move through the capillary at a certain speed. The speed at which the analyte ions reach the detector is dependent upon the LE.<sup>[50]</sup> A steady state is achieved in which the analytes are separated into discrete zones, arranged in order of decreasing mobility with the same speed.

With CITP, samples are preconcentrated in one step and as a result, the improvement in detection sensitivity can be two orders of magnitude or higher. The most important parameter in ITP is the pH. This controls the degree of dissociation of an analyte in its zone and therefore its resulting effective mobility. By using a suitable pH range the anions of weak acids have been separated according to their  $pK_a$  values. However, for the anions of strong acids a complex forming equilibria is employed, due to difficulties in the pH optimisation of separation conditions. Therefore, their separation is not as readily achieved.<sup>[77]</sup>

This technique has been employed for the determination of nitrite and nitrate in biological samples,<sup>[78]</sup> inorganic anions in serum and urine, with a limit of detection (LOD) of  $1.4 \text{ ng ml}^{-1}$  obtained,<sup>[79]</sup> and for the determination of inorganic anions in saliva.<sup>[80]</sup> An assay was also recently developed for the determination of acebutolol in pharmaceuticals.<sup>[81]</sup>

## 1.6 MODES OF DETECTION IN HPLC AND CE

The detection mode principally used in capillary electrophoresis is UV-vis absorbance detection, which includes diode-array detectors. Alternative modes, which have advantages and disadvantages with respect to selectivity and sensitivity are shown in Table 1.1.

**Table 1.1** Methods of detection in capillary electrophoresis <sup>[46]</sup>

Method	Mass Det. Limit (moles)	Conc. Det. Limit (molar)	Advantages/ Disadvantages
UV –vis absorption	$10^{-13}$ - $10^{-18}$	$10^{-5}$ - $10^{-8}$	<ul style="list-style-type: none"> <li>•Chromophore must be present</li> <li>•Diode array offers spectral information</li> </ul>
Fluorescence	$10^{-15}$ - $10^{-17}$	$10^{-7}$ - $10^{-9}$	<ul style="list-style-type: none"> <li>•Sensitive</li> <li>•Usually requires derivatisation</li> </ul>
Laser-Induced Fluorescence (LIF)	$10^{-18}$ - $10^{-20}$	$10^{-14}$ - $10^{-16}$	<ul style="list-style-type: none"> <li>•Sensitive and expensive</li> <li>•Sample derivatisation required</li> </ul>
Amperometry	$10^{-18}$ - $10^{-20}$	$10^{-10}$ - $10^{-11}$	<ul style="list-style-type: none"> <li>•Sensitive</li> <li>•For electroactive species only</li> <li>•For CE requires capillary modification, for HPLC mobile phase must be electrochemically conductive</li> </ul>
Conductivity	$10^{-15}$ - $10^{-16}$	$10^{-7}$ - $10^{-8}$	<ul style="list-style-type: none"> <li>•Universal</li> <li>•Requires special electronics and capillary modification</li> </ul>
Mass Spectrometry	$10^{-16}$ - $10^{-17}$	$10^{-8}$ - $10^{-9}$	<ul style="list-style-type: none"> <li>•Universal</li> <li>•Interface between CE and MS complicated</li> </ul>
Indirect detection	10-100 times less than direct methods	-	<ul style="list-style-type: none"> <li>•Universal but lower in sensitivity than direct methods</li> </ul>

Whilst Laser-Induced Fluorescence (LIF) is the most sensitive mode of detection, not all analytes possess native fluorescence and sample derivatisation is usually required. The fluorescence derivatising agent, fluorescein isothiocyanate (FITC), was applied to the determination of amines in food samples.<sup>[82,83]</sup> The analysis of amines was also determined using 3-(2-furoyl)quinoline-2-carboxaldehyde as the derivatisation agent.<sup>[84]</sup> The determination of amino acids in brain samples was achieved using naphthalene-2,3-dicarboxaldehyde (NDA) as the derivatising agent.<sup>[85]</sup>

### 1.6.1 UV-vis detection

In CE, UV-vis detection is usually employed on-capillary by removing a small length of the polyimide coating on the capillary and directing a light beam through it. The pathlength is limited to the inner diameter of the capillary, usually 50  $\mu\text{m}$  or 75  $\mu\text{m}$ .<sup>[25]</sup> With fused silica capillaries, detection below 200 nm through the visible spectrum is possible.<sup>[46]</sup> UV-vis detection is used for molecules that contain a chromophore, *i.e.* absorb UV-vis light. This method of detection usually requires no chemical modification of the sample prior to analysis and is therefore, an extremely convenient detection scheme.<sup>[51]</sup>

CE-UV detection has been applied to the analysis of inorganic anions in serum samples, with a run time of 6 min. achieved<sup>[86]</sup> and also in the determination of nitrate and nitrite in rainwater samples.<sup>[87]</sup> A CE-UV method was developed for the simultaneous determination of some inorganic anions and carboxylic acids, which was successfully applied to the analysis of soil and plant extracts.<sup>[88]</sup> However, most inorganic anions, including those commonly found in adhesives, cannot be detected with direct modes. Therefore UV detection has been modified to allow for the determination of analytes that do not contain a chromophore by the addition of a UV absorbing probe ion, such as chromate.<sup>[89,90]</sup> This mode of UV detection is discussed in Section 1.6.1.1.

UV detectors are the most commonly used detectors in HPLC. Samples must absorb in the UV region (190-600 nm) to be detected. The concentration of sample is related to the fraction of light transmitted through the cell by Beer's law using Eqn. 1.21.<sup>[20]</sup>

$$\log \frac{I_o}{I} = \epsilon cl \quad \text{Eqn. 1.21}$$

where:

$I_o$	=	incident light intensity
$I$	=	intensity of the transmitted light
$\epsilon$	=	molar extinction coefficient ( $M^{-1}cm^{-1}$ )
$l$	=	cell pathlength (cm)
$c$	=	sample concentration (M)

HPLC-UV detectors provide a response in absorbance, which is linearly proportional to the sample concentration in the flow cell,<sup>[20]</sup> Eqn. 1.22:

$$A = \log \frac{I_o}{I} = \epsilon cl \quad \text{Eqn 1.22}$$

where A is the absorbance

HPLC coupled with UV detection has been applied to the analysis of pharmaceuticals in plasma.<sup>[91-95]</sup> A comparison of HPLC with CE for the determination of acetaminophen and diazepam has been made. In both cases comparable run times and LOD's were obtained.<sup>[96,97]</sup>

#### 1.6.1.1 Indirect UV detection

Indirect absorbance detection in CE, is performed by adding an absorbing species, or probe ion, to the separation buffer, which creates a background absorbance signal. As the analyte species, with lower absorbance than the probe ion passes through the optical detection window, a reduction in the background absorbance signal occurs.<sup>[25]</sup> The sensitivity of the method is controlled by the choice and

concentration of the probe ion. The concentration LOD of an indirect method is shown in Eqn. 1.23.

$$C_{LOD} = \frac{C_R}{T_R D_R} \quad \text{Eqn. 1.23}$$

where:

$C_{LOD}$	=	concentration LOD
$C_R$	=	concentration of reagent
$T_R$	=	transfer ratio
$D_R$	=	dynamic reserve

Indirect UV detection has been applied to the analysis of inorganic anions, organic acids and cations <sup>[98-101]</sup> and in the determination of pharmaceutical substances.<sup>[102]</sup> This mode of detection is discussed in greater detail in Chapter 3.

## 1.6.2 Electrochemical detection

Electrochemical (EC) detection methods are suited to the analysis of analytes, which have no UV or fluorescent chromophores but are redox active. However, there are challenges to coupling EC to CE, namely the interference of the high voltage electric field with the detection circuit.<sup>[103]</sup> Several approaches have been reported to isolate the electrochemical cell from the current.<sup>[104]</sup> An illustration of an EC detection system for CE is shown in Fig. 1.8. In HPLC, electrochemical detection may only be applied if the mobile phase is electrochemically conductive. This limitation may be overcome by the addition of a salt to the mobile phase. There are three modes of EC detection in HPLC and CE: amperometric, potentiometric and conductimetric. Amperometric detection is discussed in detail in Section 1.6.2.1.

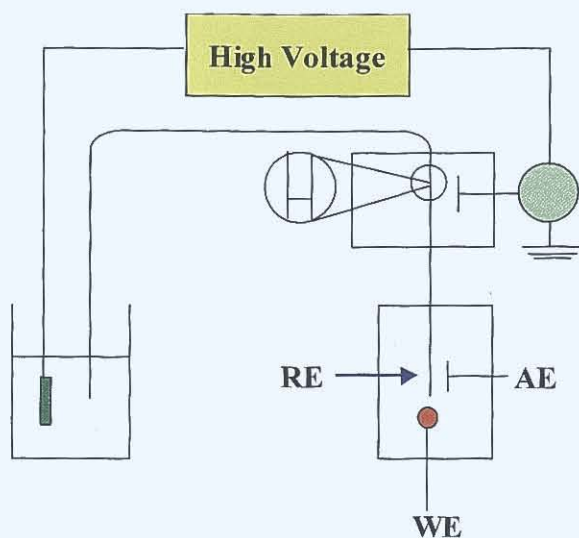


**Figure 1.8** Representation of an electrochemical detection system with an electric field decoupler; where HV: high voltage supply, RE: reference electrode, WE: working electrode and AE: auxiliary electrode<sup>[103]</sup>

#### 1.6.2.1 Amperometric detection

In amperometry, a potential is applied to the sensing or working electrode and the faradaic current resulting from the oxidation or reduction of the analyte is measured.<sup>[103]</sup> Amperometric detection methods maintain a high sensitivity and as they involve measurements that are not dependent upon the path length, amperometry is suited to the detection of analytes in very narrow capillaries.<sup>[105]</sup> Amperometric detection will only detect analytes that undergo either reduction or oxidation at the applied potential. However, this drawback may be overcome in HPLC by either pre- or post column derivatisation.<sup>[20]</sup>

In 1993, Lu *et al.*, introduced amperometric end-column detectors for the CE analysis of some metal ions and inorganic anions, with carbon fiber and mercury-film electrodes.<sup>[106,107]</sup> In end-column detection, the applied voltage generates a separation current which results in increased noise detected by the working electrode. This is minimised by use of low separation currents. In order to maintain low currents, the analysis is limited to small inner diameter capillaries, low concentration or non-aqueous buffers and reduced applied voltages.<sup>[108]</sup> In end-column detection, the



placement of the electrode is critical, as the detector noise decreases as the electrode is positioned further from the capillary. However, this will also reduce the sensitivity of the detector due to loss of analyte through diffusion in the detector cell.<sup>[109]</sup> This effect may be minimised through the application of on-column detection. In this mode of detection, the separation potential must be grounded prior to the capillary outlet.<sup>[108]</sup> The first amperometric on-column CE detector was reported by Wallingford and Ewing for the determination of catechol and catecholamines using a porous glass decoupler.<sup>[110]</sup> Alternative designs include bare fractures,<sup>[111]</sup> or casting a polymer (Nafion, cellulose acetate) over the fracture.<sup>[108,112,113]</sup> On-column detection reduces LOD by minimising loss of sample and band broadening. However, it has suffered from reproducibility issues and lack of robustness. CE coupled with amperometric detection was employed for the determination of the anthracycline, daunorubicin, in urine.<sup>[114]</sup>

In HPLC-EC, several different electrodes have been employed including carbon paste, glassy carbon, gold and mercury. Both glassy carbon and carbon paste electrodes are preferred due to lower background currents generated.<sup>[20]</sup> Amperometric detection with HPLC was also employed for the therapeutic monitoring of anthracyclines in plasma.<sup>[33,115]</sup>

### 1.6.3 Fluorescence detection

On-line fluorescence detection is achieved with a deuterium, tungsten or a xenon arc lamp. The excitation wavelength is chosen using a grating monochromator and fluorescence emission wavelengths are measured with a photomultiplier tube. Fluorescence detection is an extremely sensitive and selective mode of analysis; however, as not all compounds fluoresce, derivatisation is usually required.<sup>[20]</sup>

Fluorescence detection has been employed for the determination of some pharmaceuticals in plasma.<sup>[116-119]</sup> In CE, most inorganic anions and cations do not possess native fluorescence, indirect detection is therefore employed for their analysis. In this format, the BGE contains a fluorescent probe (*e.g.* eosin) in order to enable their detection. Detection limits in the range 0.008-0.037  $\mu\text{g ml}^{-1}$  were

obtained. This method was successfully applied to the determination of anions in tap water.<sup>[120]</sup>

LIF detection coupled with CE and HPLC has been shown to result in a high sensitivity that is greater than that achieved by absorbance-based methods.<sup>[121]</sup> A HPLC-LIF method was developed for the determination of amino acids, which enabled their detection at subfemtomole levels.<sup>[122]</sup> CE-LIF detection was utilised for the analysis of the cations, lithium and potassium with a fluorescein sodium salt incorporated in the buffer solution.<sup>[123]</sup> Alternatively, a violet diode laser was employed for the analysis of anions as demonstrated by Melanson *et al.*<sup>[124]</sup> CE-LIF has also been employed for the simultaneous determination of anthracyclines in plasma.<sup>[115,125]</sup>

Although indirect LIF detection is high in sensitivity, ( $10^{-13}$ - $10^{-15}$  M) it has limited applications. This is due to the cost of the lasers, the lack of appropriate probes and more importantly the instability of gas-based lasers. Whilst LIF would be the ultimate mode of detection, sensitivity is lost when miniaturised due to the reduced pathlength.<sup>[124]</sup>

#### 1.6.4 Mass spectrometry detection

Mass spectrometry is a widely used detection technique for gas and liquid chromatography that provides quantitative and qualitative information regarding the components of a mixture. In this technique gaseous molecules are ionised, accelerated by an electric field, and then separated according to their mass. The energy generated during ionisation causes the molecule to fragment.<sup>[35]</sup> The two main soft ionisation techniques are Electrospray Ionisation (ESI) and Atmospheric Pressure Chemical Ionisation (APCI) which is discussed in Chapter 2.

The simultaneous determination of four anthracyclines, epirubicin, doxorubicin, daunorubicin and idarubicin, was performed using HPLC coupled with electrospray mass spectrometry.<sup>[126]</sup> Detection limits in the range of 0.5-2 ng ml<sup>-1</sup> were obtained and this method was successfully applied to the analysis of serum

samples. CE-MS was also applied to the analysis of pharmaceuticals, such as steroids and anthracyclines in biological samples.<sup>[127]</sup>

## 1.7 CONCLUSIONS AND THESIS OUTLINE

From this Literature Review, the underlying theories of the separation techniques chromatography and electrophoresis were investigated. The separation principles of the two modes of separation are very different; however, they are complementary techniques.

Detection modes, such as fluorescence, electrochemical and mass spectrometric detection, have been successfully applied to the analysis of a wide range of samples. These modes of detection have been shown to be more sensitive than the traditional mode of detection of UV, and have enabled the therapeutic monitoring of pharmaceuticals in biological matrices. However, UV is still an important mode of detection both for method development and also for the analysis of samples where the LOD's are not the deciding factor.

The aim of this thesis was the development of chromatography and electrophoresis methodologies for the analysis of a wide range of analytes in variety of matrices and a comparison was made between these developed methods. HPLC-MS was also used for mechanism elucidation.

In *Chapter 2*, a HPLC method was developed and was successfully applied to the analysis of the photoinitiator, bis(2,4,6-trimethylbenzoyl)phenyl-phosphine oxide, (Irgacure 819). A comparison of its stability in samples, which were both maintained in the dark and exposed to the light, was performed using the optimised HPLC-UV method. From this it was determined that complete degradation of the Irgacure had occurred by 60 min. for the samples exposed to the light. For the samples maintained in the dark, only an 8% reduction in the Irgacure peak height was obtained. The curing mechanism of the Irgacure was determined using HPLC-MS, and it was determined that the Irgacure undergoes a free radical curing reaction.

In *Chapter 3*, a highly efficient CE separation was developed and applied to the simultaneous determination of inorganic and acidic anions, which are present in ethyl cyanoacrylate adhesive samples. The CE method developed was compared with

IC, the method traditionally employed for their analysis. The limits obtained by CE were capable of determining the expected concentrations in the adhesive samples.

In *Chapter 4*, a simple and reproducible sample preparation method was developed and successfully applied to the analysis of cyanoacrylate adhesives. Chloroform was determined to be the optimum solvent for their extraction as it enabled full dissolution of the sample. The efficiency of the production process was demonstrated and shows its effectiveness in the purification of the adhesive samples.

In *Chapter 5*, a CE method was successfully developed for the separation of the anthracyclines DAN, DOX and EPI coupled with UV, EC and LIF detection. Detection limits were obtained which were capable of monitoring the therapeutic levels of anthracyclines. The degree of plasma protein binding of anthracyclines was determined using microdialysis, and demonstrates the potential of this technique for the real time monitoring of plasma samples with on-line microdialysis coupled with CE.

In *Chapter 6*, electrophoretic separations were compared with chromatographic separations in terms of the matrix of the sample to be analysed, the volume of sample required, the length of analysis developed and the detection methods preferred. CE was clearly demonstrated as an alternative mode of separation capable of equalling, and in many cases improving the corresponding chromatographic analysis

## 1.8 REFERENCES

- [1] Abd Karim, K. J. B., Jin, J-Y., Takeuchi, T., *J. Chromatogr. A*, **2003**, 995, 153.
- [2] Fernandez-Garcia, R., Alonso-Garcia, J. I., Sanz-Medel, A., *J. Chromatogr. A*, **2004**, 1033, 127.
- [3] Di Matteo, V., Esposito, E., *J. Chromatogr. A*, **1997**, 789, 213.
- [4] Sarzanini, C., *J. Chromatogr. A*, **2002**, 956, 3.
- [5] Gennaro, M. C., Angelino, S., *J. Chromatogr. A*, **1997**, 789, 181.
- [6] Tormo, M., Izco, J. M., *J. Chromatogr. A*, **2004**, 1033, 305.
- [7] Alcazar, A., Fernandez-Caceres, P. L., Martin, M. J., Pablos, F., Gonzalez, A. G., *Talanta*, **2003**, 61, 95.
- [8] Alvarez-Cedron, L., Sayalero, M. L., Lanao, J. M., *J. Chromatogr. B*, **1999**, 721, 271.
- [9] Arnold, R. D., Slack, J. E., Straubinger, R. M., *J. Chromatogr. B*, **2004**, 808, 141.
- [10] Gilbert, C. M., Mc Geary, R. P., Filippich, L. J., Norris, R. L. G., Charles, B. G., *J. Chromatogr. B*, **2005**, 273.
- [11] Mikkers, F. P., Everaerts, F. M., Verheggen, Th. P. E. M., *J. Chromatogr.*, **1979**, 169, 11.
- [12] Isaaq, H. J., *Electrophoresis*, **2000**, 21, 1921.
- [13] Paull, B., King, M., *Electrophoresis*, **2003**, 24, 1892.
- [14] Timerbaev, A. R., *Electrophoresis*, **2002**, 23, 3884.
- [15] Perez-Ruiz, T., Martinez-Lozano, C., Sanz, A., Bravo, E., *Electrophoresis*, **2001**, 22, 134.
- [16] Gavenda, A., Sevic, J., Psotova, J., Bednar, P., Bartak, P., Adams, P., Simanek, V., *Electrophoresis*, **2001**, 22, 2782.
- [17] Simeon, N., Chatelut, E., Canal, P., Nertz, M., Couderc, F., *J. Chromatogr. A*, **1999**, 853, 449.
- [18] Altria, K. D., *LCGC*, **December 2001**, 2.
- [19] Glatz, V., Novakova, S., Sterbova, H., *J. Chromatogr. A*, **2001**, 916, 273.
- [20] Snyder and Kirkland, *Introduction to Modern Liquid Chromatography*, 2nd Edition, John Wiley and Sons, New York, **1979**.

- [21] Szepesi, G., *How To Use Reverse Phase HPLC*, VCH Publishers, New York, **1992**.
- [22] Martin, A. J. P., Synge, R. L. M., *J. Biochem* , **1941**, 35, 1358.
- [23] Van Deemter, J. J., Zuiderweig, F. J., Klinkenberg, A., *A Chem. Eng. Soc.*, **1956**, 5, 271.
- [24] [www.schu.ac.uk](http://www.schu.ac.uk)
- [25] Cooper, C. L., *J. Chem. Ed.*, **1998**, 75, 343.
- [26] Dua, V. K., Kar, P. K., Gupta, N. C., Sharma, V. P., *J. Pharm. Biomed. Anal.*, **1999**, 21, 199.
- [27] Liu, S-Y., Liu, K-S., Kuei, C-H., Tzeng, J-I., Ho, S-T., Wang, J-J., *J. Chromatogr. B*, **2005**, 818, 233.
- [28] Srinivasu, M. K., Mallikarjuna Rao, B., Sridhar, G., Rajender Kumar, P., Chandrasekhar, K. B., Islam, A., *J. Pharm. Biomed. Anal.*, **2005**, 37, 453.
- [29] Willard, H. H., Merritt, L. L., Dean, J. A., Settle, F. A., *Instrumental Methods of Analysis*, 7th Edition, Wadsworth Publishing Company, California, **1988**.
- [30] Bahrami, G., Kiani, A., Mirzaeei, S., *J. Chromatogr. B*, **2006**, 832, 197.
- [31] Bahrami, G., Kiani, A., *J. Chromatogr. B*, **2006**, 835, 123.
- [32] Fahmy, O. T., Korany, M. A., Maher, H. M., *J. Pharm. Biomed. Anal.*, **2004**, 34, 1099.
- [33] Ricciarello, R., Pichini, S., Pacifici, R., Altieri, I., Pellegrini, M., Fattorossi, A., Zuccaro, P., *J. Chromatogr. B*, **1998**, 707, 219.
- [34] Ruiz-Lopez, B., *J. Chromatogr. A*, **2000**, 881, 607.
- [35] Harris, D.C., *Quantitative Chemical Analysis*, 5th Edition, W. H. Freeman and Company, New York, **1998**.
- [36] Nesterenko, P., *Trends in Anal. Chem.*, **2001**, 20, 311.
- [37] Jackson, P. E., *Trends in Anal. Chem.*, **2001**, 20, 320.
- [38] Zhu, B., Zhixiong, Z., Yao, J., *J. Chromatogr. A*, **2006**, 1118, 106.
- [39] Barron, L., Nesterenko, P. N., Paull, B., *J. Chromatogr. A*, **2005**, 1072, 207.
- [40] Kaniansky, D., Masar, M., Marak, J., Bodor, R., *J. Chromatogr. A*, **1999**, 834, 133.
- [41] Kuban, P., Kuban, P., Kuban, V., *J. Chromatogr. A*, **1999**, 836, 75.
- [42] Fung, Y. S., Lau, K. M., *Electrophoresis*, **2003**, 24, 3224.
- [43] Lloyd, D. K., *J. Chromatogr. A*, **1996**, 735, 29.

- [44] Taga, A., Du, Y., Suzuki, S., Honda, S., *J. Pharm. Biomed Anal* , **2003**, 30, 1587.
- [45] Jorgenson, J. W., Dearman Lukacs, K., *Anal. Chem.*, **1981**, 53, 1298.
- [46] Heiger, D., *High Performance Capillary Electrophoresis-An Introduction*, Agilent Manual, Germany, **2000**.
- [47] Tagliaro, F., Manetto, G., Crivellente, F., Smith, F. P., *Forensic Science International*, **1998**, 92, 75.
- [48] Cikalo, M. G., Bartle, K. D., Robson, M. M., Myers, P., Euerby, M. R., *Analyst*, **1998**, 123, 87R.
- [49] Altria, K. D., *Capillary Electrophoresis Guidebook-Principles, Operations and Applications*, Human Press, Totowa, **1995**.
- [50] Landers, J. P., *Handbook of Capillary Electrophoresis*, CRC Press, Boca Raton, **1997**.
- [51] St. Claire, R. L., *Anal. Chem* , **1996**, 68, 569R.
- [52] Ghosal, S., *Electrophoresis*, **2004**, 25, 214.
- [53] Kuhn, R., *Capillary Electrophoresis. Principles and Practice*, Springer Verlag Telos, **1993**.
- [54] O' Flaherty, B., Yang, W-P., Sengupta, S., Cholli, A. L., *Food Chemistry*, **2001**, 74, 111.
- [55] Haumann, I., Boden, J., Mainka, A., Jegle, U., *J. Chromatogr. A*, **2000**, 895, 269.
- [56] Terabe, S., Otsuka, K., Ichikawa, K., Tsuchiya, A., Ando, T., *Anal. Chem.*, **1984**, 56, 111.
- [57] Terabe, S., Otsuka, K., Ando, T., *Anal. Chem.*, **1985**, 57, 834.
- [58] Harakuwe, A. H., Haddad, P. R., *Trends in Anal Chem.*, **2001**, 20, 375.
- [59] Weinberger, R., Lurie, I. S., *Anal. Chem.*, **1991**, 63, 823.
- [60] Nevado Berzas, J. J., Flores Rodriguez, J., Penalvo Castenada, G., Dorado Rodriguez, R. M., *Anal. Bioanal. Chem.*, **2006**, 384, 208.
- [61] Kim, J-B., Terabe, S., *J. Pharm. Biomed. Anal.*, **2003**, 30, 1625.
- [62] Wu, C-H., Chen, M-C., Su, A-K., Shu, P-Y., Chou, S-H., Lin, C-H., *J Chromatogr. B*, **2003**, 785, 317.
- [63] Monton, M. R. N., Quirino, J. P., Otsuka, K., Terabe, S., *J. Chromatogr. A*, **2001**, 939, 99.
- [64] Altria, K. D., *J. Chromatogr. A*, **1999**, 856, 443.



- [65] Terabe, S., *Anal. Chem.*, **2004**, 76, 240A.
- [66] Razak, J. L., Doyen, H. J., Lunte, C. E., *Electrophoresis*, **2003**, 24, 1764.
- [67] Bjergegaard, C., Moller, P., Sorensen, H., *J Chromatogr. A*, **1995**, 717, 409.
- [68] Kaneta, T., Tanaka, S., Taga, M., Yoshida, H., *Anal. Chem.*, **1992**, 64, 798.
- [69] Scriba, G. K. E., *Electrophoresis*, **2003**, 24, 2409.
- [70] Dermaux, A., Sandra, P., *Electrophoresis*, **1999**, 20, 3027.
- [71] Enlund, A. M., Hagman, G., Isaksson, R., Westerlund, D., *Trends in Anal. Chem.*, **2002**, 21, 412.
- [72] Bartle, K. D., Myers, P., *J. Chromatogr. A*, **2001**, 916, 3.
- [73] Li, D., Knobel, H. H., Remcho, V. T., *J. Chromatogr. B*, **1997**, 695, 169.
- [74] Hilder, E. F., Klampfl, C. W., Haddad, P. R., *J. Chromatogr. A*, **2000**, 890, 337.
- [75] Fritz, J. S., Breadmore, M. C., Hilder, E. F., Haddad, P. R., *J. Chromatogr. A*, **2002**, 942, 11.
- [76] Breadmore, M. C., Hilder, E. F., Macka, M., Haddad, P. R., *Trends in Anal. Chem.*, **2001**, 20, 355.
- [77] Valaskova, I., Havranek, E., *J. Chromatogr. A*, **1999**, 836, 201.
- [78] Szoko, E., Tabi, T., Halasz, A. S., Palfi, M., Magyar, K., *J. Chromatogr. A*, **2004**, 1051, 177.
- [79] Hirokawa, T., Yoshioka, M., Okamoto, H., Timerbaev, A. R., Blaschke, G., *J. Chromatogr. B*, **2004**, 811, 165.
- [80] Sadecka, J., Polonsky, J., *Talanta*, **2003**, 59, 643.
- [81] Pospisilova, M., Kavalirova, A., Polasek, M., *J. Chromatogr. A*, **2005**, 1081, 72.
- [82] Rodriguez, I., Lee, H. K., Li, S. F. Y., *J. Chromatogr. A*, **1996**, 745, 255.
- [83] Ramirez-Cortacero, S., Roman-Arreaez, D., Carretero-Segura, A., Gutierrez-Fernandez, A., *Food Chemistry*, **2007**, 100, 383.
- [84] Lin, X., Yang, L-X., Lu, Y-T, *J. Chromatogr. A*, **2003**, 998, 213.
- [85] Benturquina, N., Parrot, S., Sauvinet, V., Renaud, B., Denoroy, L., *J. Chromatogr. B*, **2004**, 806, 237.
- [86] Miyado, T., Nagai, H., Takeda, S., Saito, K., Fukushi, K., Yoshida, Y., Wakida, S., Niki, E., *J. Chromatogr. A*, **2003**, 1014, 197.
- [87] Padarauskas, A., Paliulionyte, V., Pranaitye, B., *Anal. Chem.*, **2001**, 73, 267.
- [88] Xu, J., Chen, Z., Yu, J. C., Tang, C., *J. Chromatogr. A*, **2002**, 942, 289.

- [89] King, M., Paull, B., Haddad, P. R., Macka, M., *Analyst*, **2002**, 127, 1564.
- [90] Sullivan, J., Douek, M., *J. Chromatogr. A*, **2004**, 1039, 215.
- [91] Ramachandran, G., Kumar, A. K., Swaminathan, S., Venkatesan, P., Kumaraswami, V., Greenblatt, D. J., *J. Chromatogr. B*, **2006**, 835, 131.
- [92] Zarghi, A., Shafaati, A., Foroutan, S. M., Khoddam, A., *J. Chromatogr. B*, **2006**, 835, 100.
- [93] Kirstein, M. N., Hassan, I., Guire, D. E., Weller, D. R., Dagit, J. W., Fisher, J. E., Pommel, R. P., *J. Chromatogr. B*, **2006**, 835, 136.
- [94] Deporte, R., Amiand, M., Moreau, A., Charbonnel, C., Campion, L., *J. Chromatogr. B*, **2006**, 834, 170.
- [95] Yeniceli, D., Dogrukol-Ak, D., Tuncel, M., *J. Pharm. Biomed. Anal.*, **2006**, 40, 197.
- [96] Marin, A., Barbas, C., *J. Pharm. Biomed. Anal.*, **2004**, 35, 769.
- [97] Prado, M. S., Steppe, M., Tavares, M., Kedor-Hackman, E., Santoro, M., *J. Pharm. Biomed. Anal.*, **2005**, 37, 273.
- [98] Bord, N., Cretier, G., Rocca, J-L., Bailby, C., Souchez, J-P., *J. Chromatogr. A*, **2005**, 1100, 223.
- [99] Padarauskas, A., *Anal. Bioanal. Chem.*, **2006**, 384, 132.
- [100] Doble, P., Macka, M., Haddad, P. R., *Trends in Anal. Chem.*, **2000**, 19, 10.
- [101] Johns, C., Yang, W., Macka, M., Haddad, P. R., *J. Chromatogr. A*, **2004**, 1050, 217.
- [102] Denis, C. M., Baryla, N. E., *J. Chromatogr. A*, **2006**, 1110, 268.
- [103] Matsyik, F. M., *Electroanalysis*, **2000**, 12, 1349.
- [104] Mesaros, J. M., Ewing, A. G., Gavin, P. F., *Anal. Chem.*, **1994**, 66, 527A.
- [105] Ye, J., Baldwin, R. P., *Anal. Chem.*, **1993**, 65, 3525.
- [106] Lu, W., Cassidy, R. M., Baranski, A. S., *J. Chromatogr.*, **1993**, 640, 433.
- [107] Lu, W., Cassidy, R. M., *Anal. Chem.*, **1993**, 65, 1649.
- [108] Osbourn, D. M., Lunte, C. E., *Anal. Chem.*, **2001**, 73, 5961.
- [109] Osbourn, D. M., Lunte, C. E., *Anal. Chem.*, **2003**, 75, 2710.
- [110] Wallingford, R. A., Ewing, A. G., *Anal. Chem.*, **1987**, 59, 1762.
- [111] Zhou, L., Lunte, S. M., *Electrophoresis*, **1995**, 16, 498.
- [112] Whang, C.-W., Chen, I.-C., *Anal. Chem.*, **1992**, 64, 2461.
- [113] Chen, I.-C., Whang, C.-W., *J. Chromatogr.*, **1993**, 644, 208.
- [114] Hu, Q., Zhang, L., Zhou, T., Fang, Y., *Anal. Chim. Acta*, **2000**, 416, 15.

- [115] Mou, C., Ganju, N., Sridhar, K.S., Krishan, A., *J. Chromatogr. B*, **1997**, 703, 217.
- [116] Ulu, S. T., *J. Chromatogr. B*, **2006**, 834, 62.
- [117] Andersen, A., Warren, D. J., Slordal, L., *Cancer Chemotherapy and Pharmacology*, **1994**, 34, 197.
- [118] De Jong, J., Bast, A., Van Der Vijgh, W. F., *Trends in Anal. Chem.*, **1993**, 12, 422.
- [119] Andersen, A., Warren, D. J., Slordal, L., *Ther. Drug Monit.*, **1993**, 15, 455.
- [120] Lista, A. G., Arce, L., Rios, A., Valcarcel, M., *J. Chromatogr. A*, **2001**, 919, 407.
- [121] Simonet, B. M., Rios, A., Valcarcel, M., *Trends in Anal. Chem.*, **2003**, 22, 605.
- [122] Roach, M. C., Harmony, M. D., *Anal. Chem.*, **1987**, 59, 411.
- [123] Desbene, P. L., Morin, C. J., Desbene Monvernay, A. M., Groult, R. S., *J. Chromatogr. A*, **1995**, 689, 135.
- [124] Melanson, J. E., Boulet, C. A., Lucy, C. A., *Anal. Chem*, **2001**, 73, 1809.
- [125] Hempel, G., Schulze-Westhoff, P., Flege, S., Boos, J., *J. Chromatogr. B*, **2001**, 758, 221.
- [126] Lachatre, F., Marquet, P., Ragot, S., Gaulier, J. M., Cardot, P., Dupuy, J. L., *J. Chromatogr. B*, **2000**, 738, 281.
- [127] Smyth, W. F., *Electrophoresis*, **2005**, 26, 1334.

## *Chapter Two*

### *Characterisation of an Acylphosphine oxide Photoinitiator*

## 2.1 INTRODUCTION

Ultra-violet (UV) curing is a process which converts a multifunctional monomer into a cross-linked polymer, through a mechanism initiated by a reactive species, under the influence of UV light. A schematic illustrating this polymerisation mechanism is shown in Fig. 2.1. However, most monomers do not generate an initiating species with sufficiently high yields when exposed to UV light. Therefore, a photoinitiator must be added to the mixture.<sup>[1]</sup>

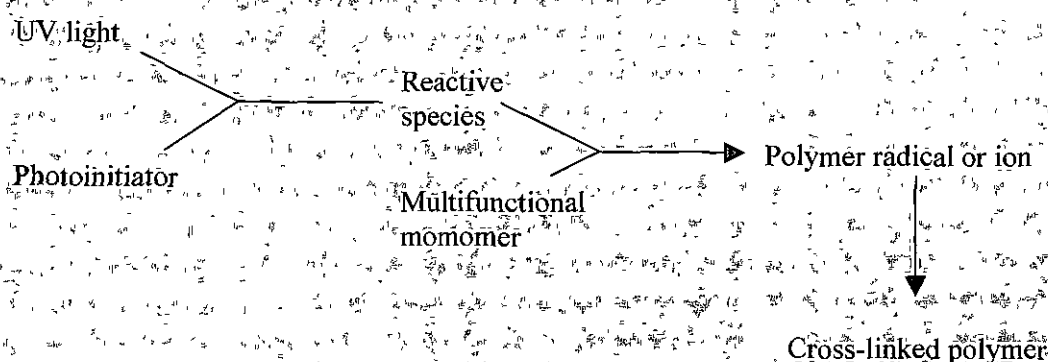


*Figure 2.1 Illustration of the UV curing process<sup>[1]</sup>*

The photoinitiator is an essential part of the formulation as it generates the reactive species and therefore aids in the completion of the curing process. The photoinitiator must possess a good stability in the formulation and its excited states must have a short lifetime to avoid quenching by atmospheric oxygen. Acylphosphine oxides are one such group of photoinitiators, which are capable of initiating the polymerisation of monomers such as acrylates.<sup>[2]</sup>

The two most important factors in deciding which photoinitiator to employ are curing efficiency and shelf life. In this section, the development of acylphosphine oxides as alternative photoinitiators, and their photochemistry will be discussed.

### 2.1.1 Theory of Acylphosphine oxides

Acylphosphine oxides belong to a class of  $\alpha$ -cleavable photoinitiators, which have been applied to the curing of both white and pigmented coatings, such as furniture coatings.<sup>[1]</sup> They possess low volatility, and also a high solubility in acrylate monomers, in particular the monoacylphosphine oxides (MAPO). They have been used in a variety of applications;<sup>[3,4]</sup> however, they are most suited to white lacquer applications, such as in furniture coatings.<sup>[5]</sup> The development of a new class of photoinitiators, bisacylphosphine oxides (BAPO), has led to their introduction in the photopolymerisation of pigmented coatings. BAPO contain two acyl substituents attached to the phosphine oxide unit.<sup>[6]</sup> The structures of some acylphosphine oxides are illustrated in Fig. 2.2.

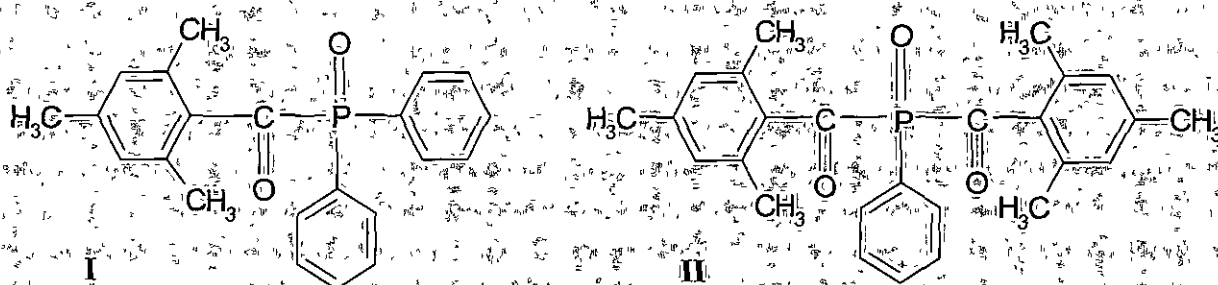
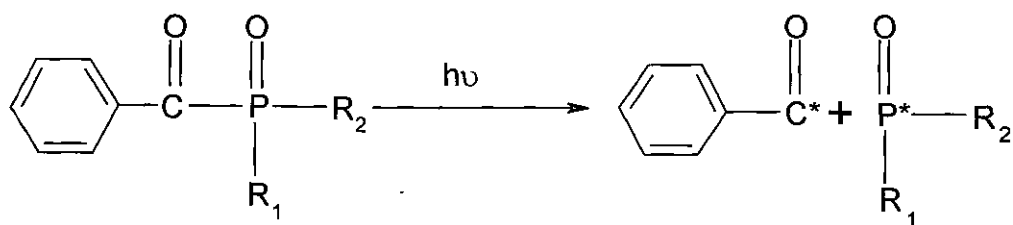


**Figure 2.2** The structure of the photoinitiators, *I*- monoacylphosphine oxide (MAPO) and *II*- bisacylphosphine oxide (BAPO)<sup>[7]</sup>.

The absorption of these compounds extends into the visible part of the spectrum, 250-400 nm. Therefore, this enables the absorption of sufficient light in order to generate the benzoyl and phosphinoyl radicals, as shown in Fig. 2.3.<sup>[6]</sup> These radicals are both very reactive and therefore initiate the polymerisation of a wide range of monomers, e.g. acrylates, styrenes, thiolene systems and maleimides.<sup>[2]</sup>



where:       $R_1, R_2 =$       alkyl, aryl for MAPO  
                   $R_1 =$           acyl for BAPO  
                   $R_2 =$           alkyl or aryl for BAPO

**Figure 2.3**  $\alpha$ -cleavage of MAPO and BAPO<sup>[8]</sup>

BAPO are superior photoinitiators to MAPO, and are extremely effective as they can produce four reactive species, each of which is an efficient initiator.<sup>[8]</sup> Whilst the application of MAPO photoinitiators has been limited to white pigmented coatings,<sup>[6]</sup> BAPO have been applied to more complex applications such as pigmented coatings and composite materials.<sup>[2]</sup> The investigation of the photochemistry of these photoinitiators is discussed in detail in Section 2.1.2.

### 2.1.2 Photochemistry of Acylphosphine oxides

Monoacylphosphine oxides undergo  $\alpha$ -cleavage from a triplet-excited state to produce two radicals, the benzoyl and phosphinoyl radicals. The photochemistry of bisacylphosphine oxides is similar; however, four radicals are produced from the  $\alpha$ -cleavage of the triplet excited state.<sup>[9]</sup>

Their photochemistry was investigated using a wide range of techniques including UV<sup>[4,9-11]</sup> and time resolved spectroscopy<sup>[6-8]</sup> which are discussed in Section 2.1.2.1

### 2.1.2.1 Ultraviolet (UV) spectroscopy

UV spectroscopy has been extensively applied to the investigation of the photochemistry of acylphosphine oxides. Jacobi and Henne first reported on their development as photoinitiators and demonstrated their effectiveness in the curing of some coatings, such as white furniture coatings.<sup>[4]</sup> A typical UV spectrum of a BAPO is shown in Fig. 2.4.

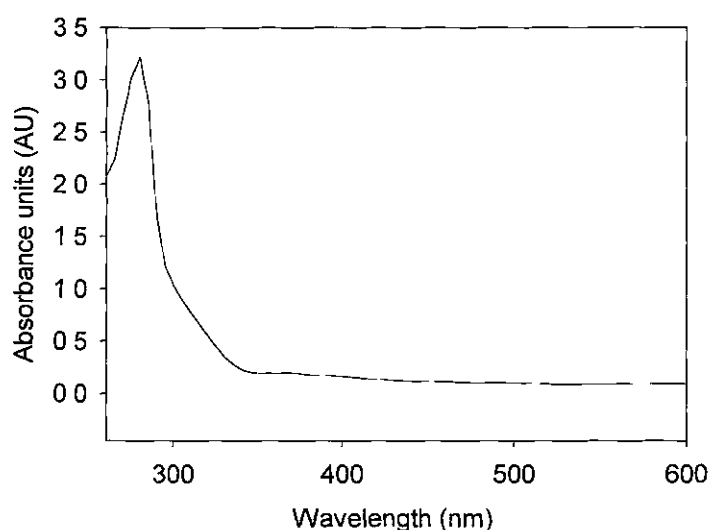


**Figure 2.4** UV-vis absorption spectrum for the bis(2,4,6-trimethylbenzoyl)phenyl-phosphine oxide

Baxter *et al.*,<sup>[10-12]</sup> have also investigated the efficiency of these photoinitiators with respect to alternative photoinitiators, such as acylphosphonates. From their investigations it was concluded that, although acylphosphine oxides are efficient photoinitiators, there was no distinct advantage in their application in either acrylate and unsaturated polyester resins, when compared to acetophenones,<sup>[10]</sup> or in pigmented acrylic resins.<sup>[11]</sup> However, acylphosphine oxides were determined to be more efficient photoinitiators than acylphosphonates, and this curing efficiency was shown to be further increased by the addition of amines.<sup>[12]</sup>

The role of the amine in the photodecomposition of acylphosphine oxides was investigated by both High Performance Liquid Chromatography (HPLC) and Gas



Chromatography Mass Spectrometry (GC-MS).<sup>[13]</sup> It was determined that although photodecomposition occurs in the presence and absence of an amine, the curing efficiency is significantly decreased in the absence of amines. However, the presence of an amine may also reduce the shelf life of the pigmented resin. In order to investigate and characterise further these photoinitiators, time resolved spectroscopy was applied and is discussed in Section 2.1.2.2.

#### 2.1.2.2 Time-resolved spectroscopy

Time-resolved spectroscopy provides information on the excited state of a material, *e.g.* the triplet excited state of acylphosphine oxides. The most powerful technique, which follows the time development of radicals, is Electron Spin Resonance (ESR).<sup>[7]</sup> ESR is similar to Nuclear Magnetic Resonance (NMR), the fundamental difference being that ESR describes the magnetically induced splitting of electronic spin and NMR is concerned with the splitting of nuclear spin sites.

Time-resolved ESR (TR-ESR) provides clear and concise structural information on the material under investigation, by allowing for the direct observation of the radicals.<sup>[7]</sup> TR-ESR has been applied for the analysis of the radicals formed and demonstrates the ability of BAPO to generate four radicals upon irradiation.<sup>[14]</sup> TR-ESR has also been employed in conjunction with time-resolved infra-red (TR-IR) and UV spectroscopies to determine further the photochemistry of acylphosphine oxides and also the reactivity of the radicals produced.<sup>[6,9,15]</sup> From this work, it was determined that BAPO is a more effective photoinitiator to MAPO, due to its ability to produce four highly reactive radicals.

ESR techniques were also successfully applied in combination with NMR spectroscopies, such as chemically induced dynamic nuclear polarisation (CIDNP), for the further investigation of the photochemistry of acylphosphine oxides. CIDNP is a powerful technique as it provides information on the elucidation of the radical reactions.<sup>[6]</sup>

Acylphosphine oxides have been determined to be highly efficient photoinitiators, which undergo a fast photolysis to generate very reactive free radicals. They are efficient in a number of systems, e.g. curing of pigmented coatings, and it is hoped that the potential of these photoinitiators for industrial applications will be realised.<sup>[2]</sup>

## 2.2 SCOPE OF RESEARCH

In this chapter, the characterisation of the BAPO photoinitiator, bis(2,4,6-trimethylbenzoyl)phenyl-phosphine oxide, (Irgacure 819) was carried out using UV spectroscopy, HPLC and CE. The solubility of the photoinitiator was investigated using various organic solvents, *e.g.* tetrahydrofuran (THF), chloroform, methanol (MeOH) and acetonitrile (ACN). A time stability study was performed, with various analytes added such as inhibitors and weak and strong acids, using HPLC-UV, and a comparison of its stability was determined in samples, which were kept under dark and light conditions. An investigation of the fragmentation pathway and hence the curing mechanism of the photoinitiator was performed using HPLC coupled with mass spectrometry detection (HPLC-MS), with Atmospheric Pressure Chemical Ionisation (APCI) as the source. A CE method was developed for the analysis of the Irgacure and was compared with the HPLC-UV method.

## 2.3 MATERIALS AND METHODS

### 2.3.1 Instrumentation

#### 2.3.1.1 HPLC- UV separations (HPLC-UV)

The HPLC system consisted of a Varian ProStar 230 solvent delivery module, and a Varian ProStar 310 UV detector module (Palo Alto, CA, USA). The system was operated using Varian ProStar 6.0 chromatography software. A Zorbax Eclipse XDB-C-18 reversed phase column (2.1 x 150 mm, particle size 5  $\mu\text{m}$ , Agilent Technologies Ireland) equipped with a Zorbax SB-C8 guard cartridge (2.1 x 12.5 mm, particle size 5  $\mu\text{m}$ , Agilent Technologies Ireland) was employed. A gradient elution was employed at a flow rate of 0.25 ml min<sup>-1</sup>. All sample analyses were carried out using UV detection at 270 nm with a deuterium lamp.

#### 2.3.1.2 HPLC- mass spectroscopy analysis (HPLC-MS)

The HPLC system consisted of an Agilent 1100 LC module with photodiode array (PDA) detector, (Agilent Technologies Ireland). A Bruker Daltronics Esquire 3000 LC-MS (ion trap) was used. A Zorbax Eclipse XDB-C-18 reversed phase column (2.1 x 150 mm, particle size 5  $\mu\text{m}$ , Agilent Technologies Ireland) equipped with a Zorbax SB-C8 guard cartridge (2.1 x 12.5 mm, particle size 5  $\mu\text{m}$ , Agilent Technologies Ireland) was employed. A gradient elution was employed at a flow rate of 0.25 ml min<sup>-1</sup>. APCI conditions were optimised using positive ion polarity with accompanying software.

#### 2.3.1.3 Capillary electrophoresis separations

All CE separations were performed on Beckman P/ACE MDQ instrument (Fullerton, CA), equipped with a UV absorbance detector. Polyimide-coated fused silica capillaries of 50  $\mu\text{m}$  internal diameter (i.d.) were employed. The effective length of the capillary utilised was 0.50 m, with a total length of 0.56 m. All sample analyses were carried out using direct UV detection at 280 nm with a deuterium lamp. Sample introduction was performed hydrodynamically (0.5 psi) for 5 s. Data analysis was

performed using Beckman (version 3.4) software. Separations were performed with normal polarity at 15 kV and the temperature maintained at 25 °C.

### 2.3.1.3 UV-vis analysis

All UV spectra were obtained on Cary Win UV 50, dual beam with 2 nm resolution.

## 2.3.2 Chemicals

MeOH (LC-MS Chromasolv, 34966 and Anhydrosolv grade, 322415), were purchased from Sigma Aldrich (Tallaght, Dublin). HPLC grade MeOH, ACN, chloroform and toluene were purchased from Labscan Ltd. (Dublin, Ireland). All other chemicals were of reagent grade. Ethyl cyanoacetate, (28429), biphenyl (B34656), triphenylmethane (93050), boric acid (B0394) and sodium hydroxide (48,0878, NaOH), were obtained from Sigma Aldrich (Tallaght, Dublin). Ferrocene, methyl sulphonic acid (MSA), boron trifluoride dihydrate, cumene hydroperoxide, hydroquinone, 1,4-benzoquinone and bis(2,4,6-trimethylbenzoyl)phenyl-phosphine oxide (Irgacure 819), samples were obtained from Henkel Technologies (Irl.) Ltd. Deionised water was treated with a Hydro Nanopure system to specific resistance > 18 MΩ cm (Millipore, Bedford, MA, USA).

## 2.3.3 Procedures

### 2.3.3.1 HPLC mobile phase preparation

The mobile phases for HPLC-UV and HPLC-MS consisted of solvent A 90:10 MeOH:H<sub>2</sub>O and solvent B 50:50 MeOH:H<sub>2</sub>O. The HPLC-MS mobile phases were prepared using LC-MS Chromasolv grade MeOH. All mobile phases were vacuum filtered using 47 mm Pall Nylaflo nylon membranes with 0.45 µm pore size and stirred overnight prior to use to ensure complete degassing.

### 2.3.3.2 CE Background electrolyte (BGE) preparation

Electrolytes were prepared using deionised water. Two BGE solutions were prepared, which consisted of a boric acid solution. A stock solution of 500 mM boric acid was prepared, from which 250 mM and 50 mM borate solutions were obtained by dilution of the stock with deionised water. The pH of the electrolytes were adjusted to 9.0 using 1 M NaOH solution. All electrolyte solutions were filtered with a 0.45  $\mu$ m swinny filter (Gelman Nylon Acrodisc, 4438) prior to use.

### 2.3.3.3 Preconditioning of the CE separation capillary

The capillary was rinsed each day with MeOH and 0.1 M NaOH for 2 min. each, followed by BGE for 3 min. Between each analysis, the capillary was rinsed with MeOH, 0.1 M NaOH and BGE for 1, 1 and 2 min. respectively. When the BGE or capillary was changed, the capillary was conditioned with a 5 min. rinse with MeOH, 10 min. rinse with 1 M HCl, 1 min. rinse with H<sub>2</sub>O, 20 min. rinse with 0.1 M NaOH, 1 min. rinse with H<sub>2</sub>O and a 5 min. rinse with BGE.

### 2.3.3.4 Preparation of stock solutions and standards

A stock (1000  $\mu$ g ml<sup>-1</sup>) solution of each analyte was prepared using deionised water. Standards of known concentration were prepared by dilution of the stock with deionised water.

## 2.4 RESULTS AND DISCUSSION

### 2.4.1 Characterisation of Irgacure 819

The structure of the Irgacure 819 is shown in Fig. 2.5. In order to determine the optimum solvent in which to perform the HPLC characterisation of this Irgacure, its solubility was investigated. Solvents of different polarities, such as toluene, acetone and MeOH, were employed, and the solvents, which enabled the full dissolution of the Irgacure, are illustrated in Table 2.1.

A UV study of the Irgacure was performed in ACN, ethyl acetate, THF and MeOH, as shown in Fig. 2.6. From Fig. 2.6, it was evident that the solvent THF resulted in the largest absorptivity at 270 nm. However, for HPLC analysis, it was not recommended to use THF as it causes the polyetheretherketone (PEEK) tubing to swell. An investigation of the fragmentation pathway of Irgacure 819 was performed using HPLC-APCI-MS.

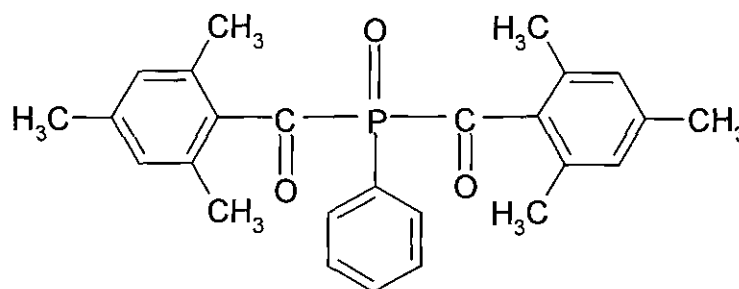


**Figure 2.5** Structure of bis(2,4,6-trimethylbenzoyl)phenyl-phosphine oxide (Irgacure 819), as provided by Henkel Loctite (Irl.)

**Table 2.1** Solubility of bis(2,4,6-trimethylbenzoyl)phenyl-phosphine oxide ( $100 \mu\text{g ml}^{-1}$ ) in different organic solvents of varying polarity

Solvent	Polarity <sup>[16]</sup>	Solubility of Irgacure
Toluene	2.3	Fully dissolved
Chloroform	3.4-4.4	Fully dissolved
THF	4.2	Fully dissolved
Ethyl acetate	4.3	Fully dissolved
Acetone	5.4	Fully dissolved
Acetonitrile	6.2	Fully dissolved
MeOH	6.6	Fully dissolved
Water	9.0	Not dissolved

For APCI-MS, protic solvents, such as MeOH are preferred for measurement in the positive ion mode. As a result MeOH was chosen as the optimum sample matrix and mobile phase solvent in which to perform the HPLC analysis.



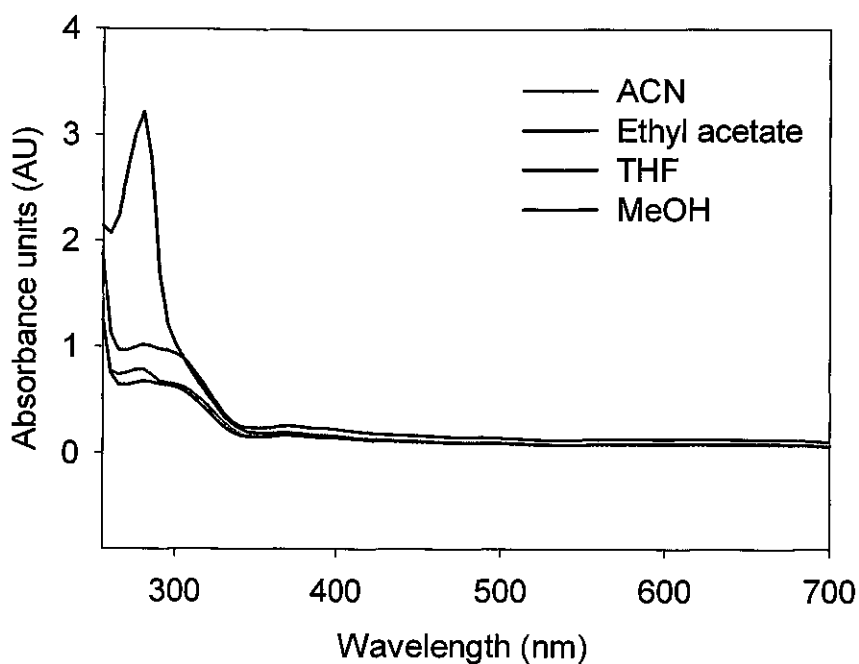


**Figure 2.6** UV-vis absorption spectra for Irgacure 819 ( $100 \mu\text{g ml}^{-1}$ ) in each of the organic solvents ACN, ethyl acetate, THF and MeOH

#### 2.4.2 Development of HPLC separation

Reverse-phase chromatography is the most widely reported mode of HPLC, with applications in the analysis of pharmaceutical and environmental samples.<sup>[17-20]</sup> For the analysis of the Irgacure, reverse-phase chromatography was chosen due to factors, such as its molecular weight and solubility. A schematic of a guide to selecting a HPLC method is illustrated in Fig. 2.7.

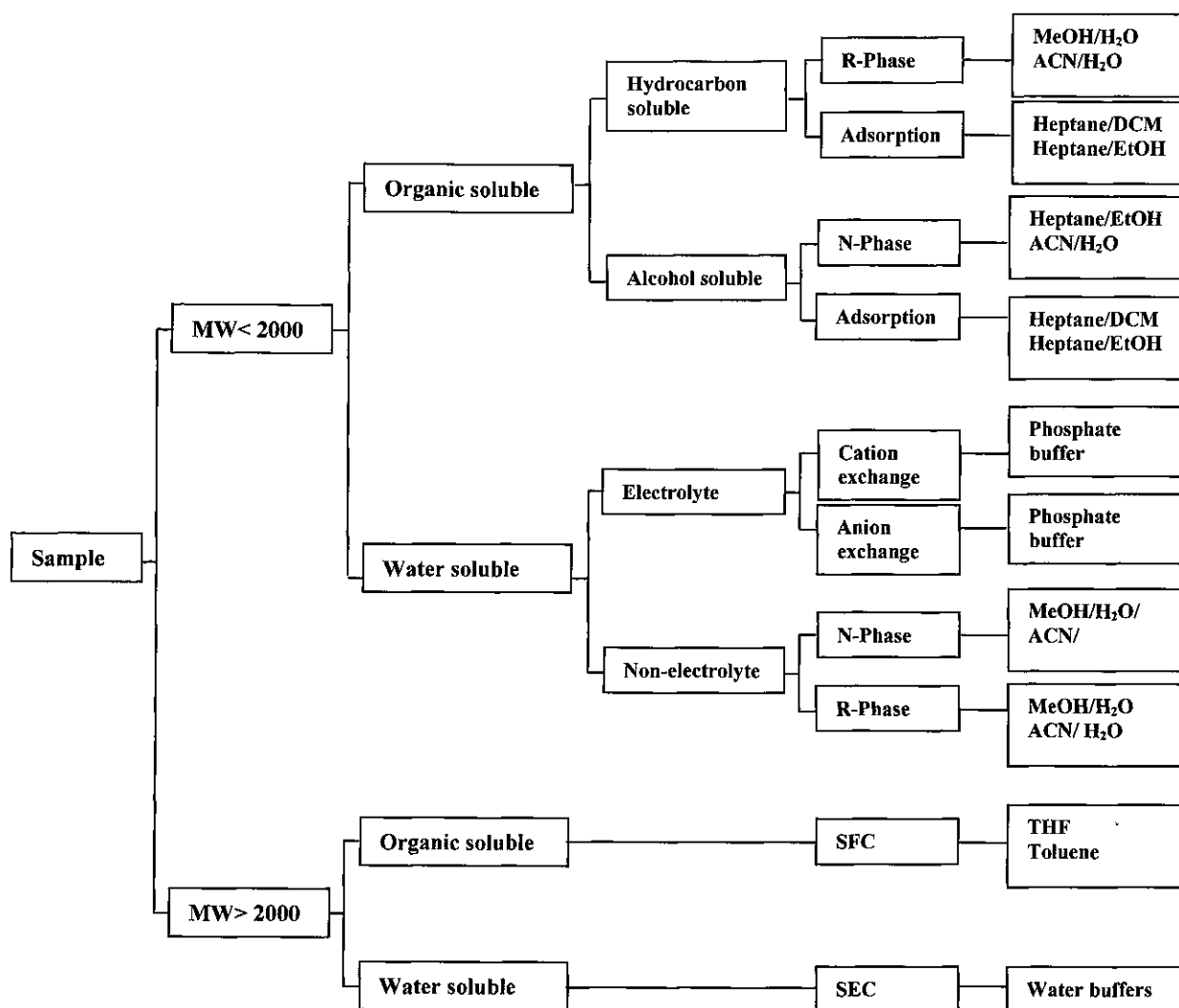


**Figure 2.7** Schematic of a guide to selecting a HPLC method<sup>[21]</sup>

The analyte under investigation, Irgacure 819, has a molecular weight of less than 2000, and is also soluble in organic solvents. Therefore, following the schematic highlighted in red in Fig. 2.7, the mode of HPLC employed for this research was reverse-phase chromatography with either an ACN or MeOH water mobile phase. A MeOH water mobile phase was chosen, as MeOH is the preferred solvent for APCI-MS, discussed in Section 2.4.4.

#### 2.4.2.1 Choice of internal standard

The addition of an internal standard in this analysis was essential, in order to provide an illustration of the degradation of the Irgacure under investigation. An internal standard must be similar to the analyte under investigation and must undergo similar losses during the process. It also must be completely resolved from the other components present in the sample. In Fig. 2.8, the HPLC separation of the Irgacure is shown; the slight fronting evident is probably due to overloading.

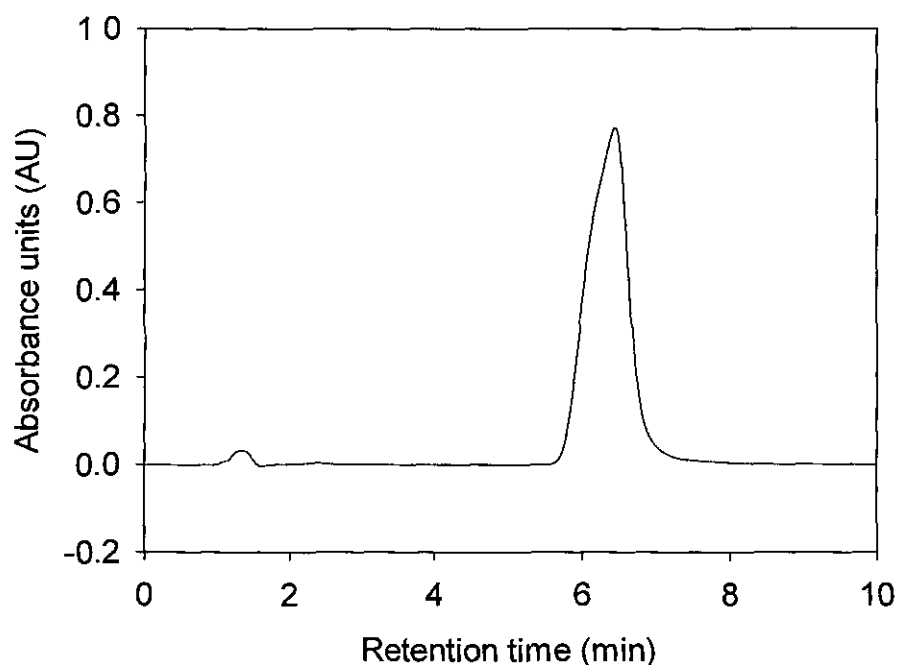


**Figure 2.8** HPLC separation of Irgacure 819 ( $250 \mu\text{g ml}^{-1}$ ) with UV detection at 270 nm using a Zorbax Eclipse XDB-C-18 reversed phase column (2.1 x 150 mm, particle size 5  $\mu\text{m}$ ). Mobile phase of 85:15 MeOH:H<sub>2</sub>O. Flow rate 0.25 ml min<sup>-1</sup>

Two closely structurally related analytes, triphenyl methane and biphenyl, were investigated as potential internal standards in the determination of Irgacure 819. Their structures are illustrated in Fig. 2.9.

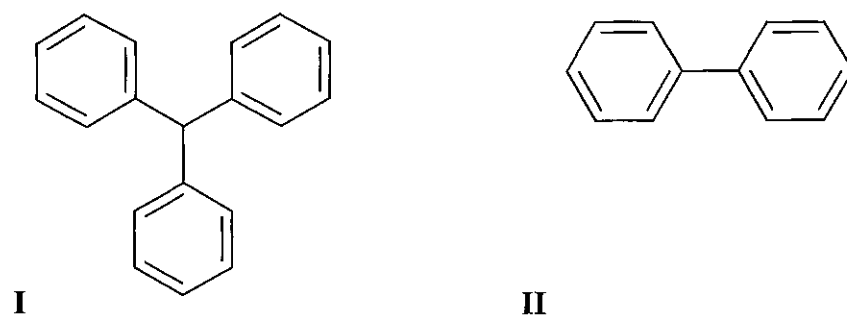


**Figure 2.9** Structures of I-triphenyl methane and II-biphenyl

Triphenyl methane co-eluted with the Irgacure and was therefore unsuitable as an internal standard. As illustrated in Fig. 2.10, biphenyl was clearly separated from the Irgacure and was therefore employed as the internal standard in subsequent work.

In order to improve the peak shape of both the Irgacure and biphenyl, and also to reduce the total analysis time, a gradient elution was employed, as discussed in Section 2.4.2.2.

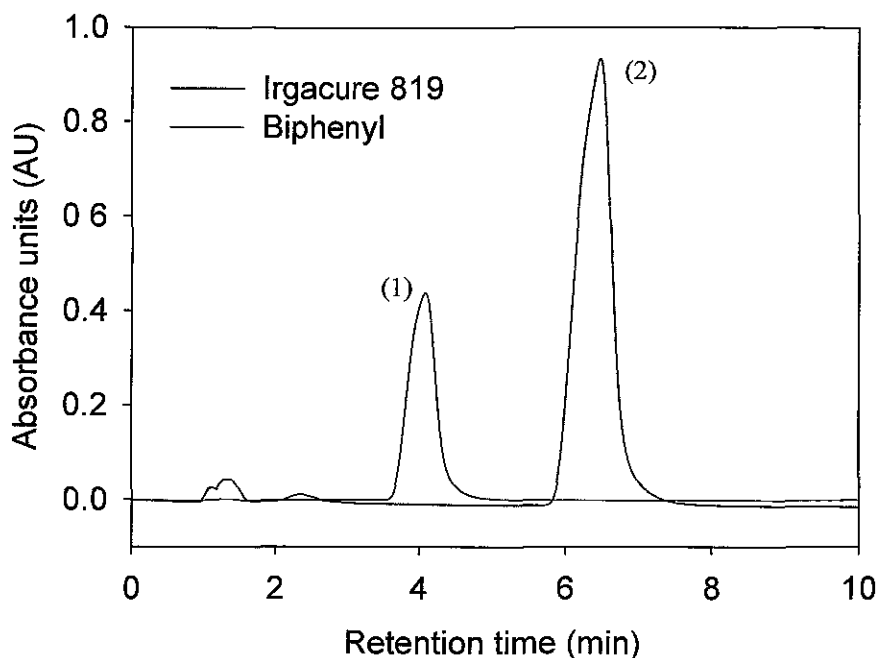


**Figure 2.10** HPLC separation of (1) biphenyl ( $50 \mu\text{g ml}^{-1}$ ) and (2) Irgacure 819 ( $250 \mu\text{g ml}^{-1}$ ) with UV detection at 270 nm. All operating conditions as in Fig. 2.8

#### 2.4.2.2 Development of gradient method

Initially the separation of the Irgacure was performed using the gradient method as illustrated in Fig. 2.11, with either 85:15 MeOH  $\text{H}_2\text{O}$  or 90:10 MeOH  $\text{H}_2\text{O}$ . In this method, the column was initially ramped from 0 min. to 6 min. from 98% C to 2% C, where A was 70:30 MeOH  $\text{H}_2\text{O}$  and C was either 85:15 MeOH  $\text{H}_2\text{O}$  or 90:10 MeOH  $\text{H}_2\text{O}$ . The separation of Irgacure and biphenyl was performed using this gradient method and the resulting chromatograms are shown in Fig. 2.12.

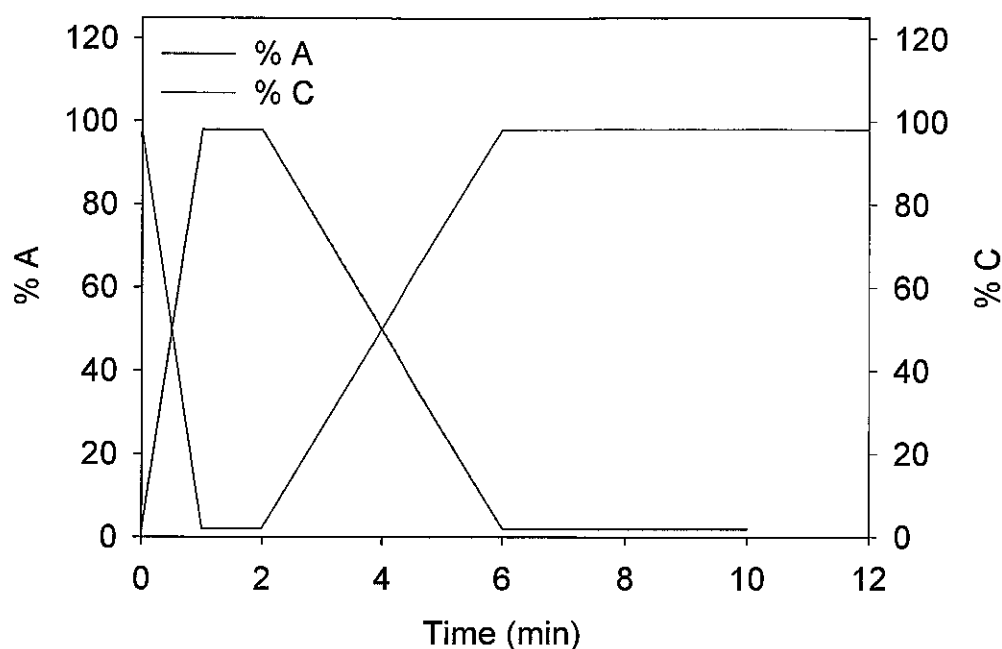


**Figure 2.11** Graphical illustration of the gradient method employed for the HPLC separation of Irgacure 819 and the internal standard, biphenyl, where Line A is 70:30 MeOH:H<sub>2</sub>O and Line C is either 85:15 MeOH:H<sub>2</sub>O or 90:10 MeOH:H<sub>2</sub>O

The internal standard, biphenyl, is less polar than the Irgacure, and is therefore expected to elute first, as illustrated in Fig. 2.12. With 85:15 MeOH:H<sub>2</sub>O, the Irgacure was retained on the column for approximately 12 min. and its peak shape was asymmetrical, with fronting of the peak evident. This indicates that the Irgacure required a more organic mobile phase in order to cause its elution. The run time was also excessively long (15 min.), as shown in Fig. 2.12. It was found that increasing the MeOH composition by 5% improved the peak shape of the Irgacure and also significantly reduced the run time from 15 min. to 10 min., as shown in Fig. 2.12. The resolution (R) between the two analytes was calculated according to Eqn. 1.9, and was determined to be 1.02. In order to improve the resolution further a gradient with lower organic content was employed, *i.e.*, 50:50 MeOH:H<sub>2</sub>O, as illustrated in Fig 2.13.

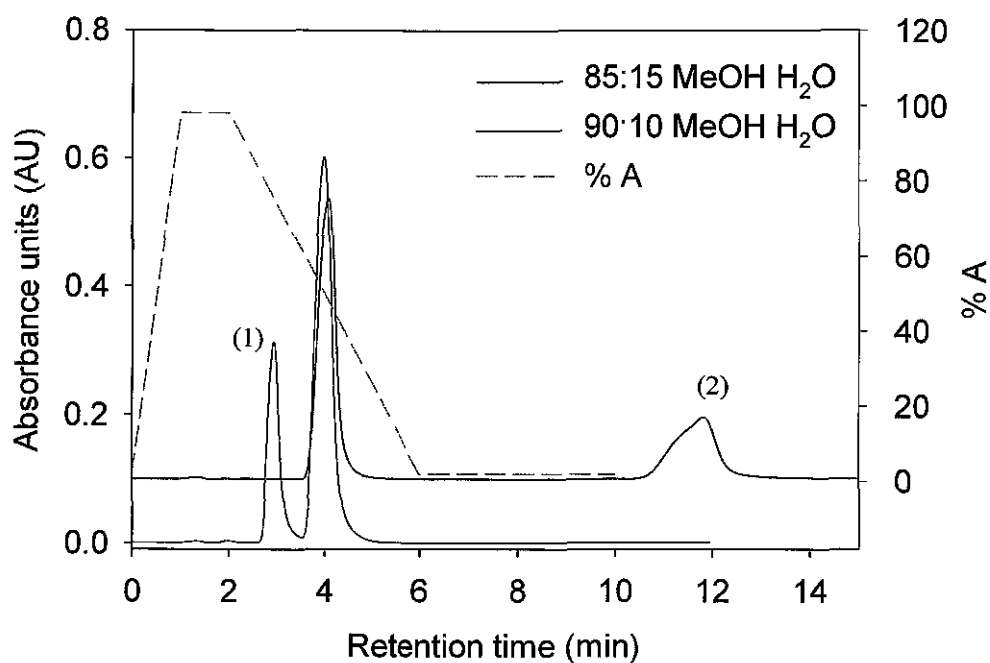


**Figure 2.12** Gradient elution of mobile phase (A) 70:30 MeOH:H<sub>2</sub>O with mobile phase (B) 85:15 MeOH:H<sub>2</sub>O or 90:10 MeOH:H<sub>2</sub>O for the HPLC separation of (1) biphenyl (50  $\mu\text{g mL}^{-1}$ ) and (2) Irgacure 819 (250  $\mu\text{g mL}^{-1}$ ) with UV detection at 270 nm. Gradient method as in Fig. 2.11. Unless stated otherwise all operating conditions as in Fig. 2.8. The 85:15 MeOH:H<sub>2</sub>O chromatogram is offset by 0.1 AU

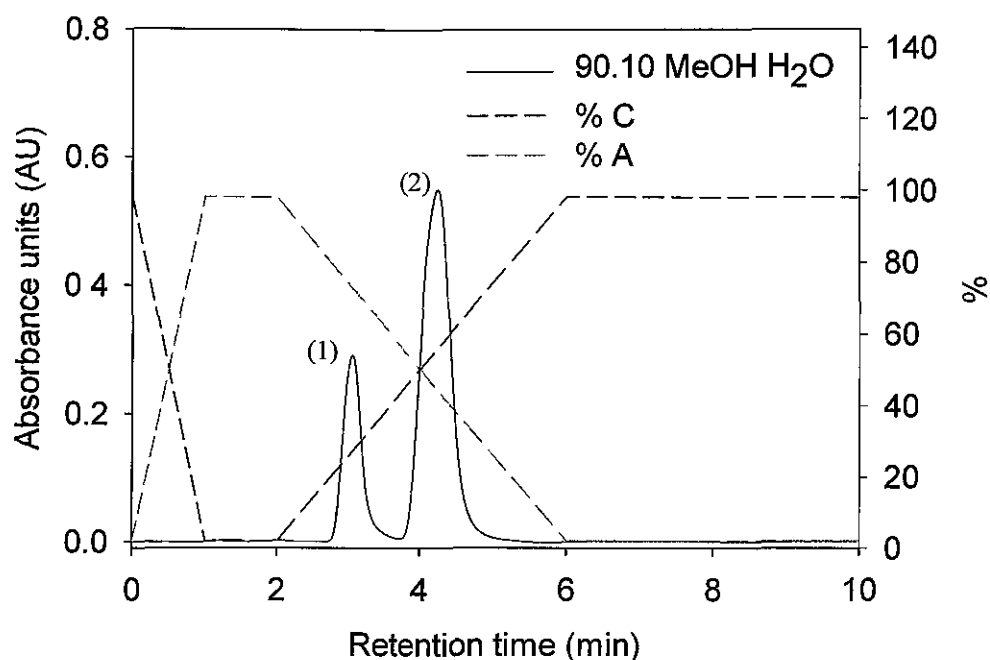


**Figure 2.13** Optimised gradient elution of mobile phase (A) 50:50 MeOH:H<sub>2</sub>O with mobile phase (B) 90:10 MeOH:H<sub>2</sub>O for the HPLC separation of (1) biphenyl (50 µg ml<sup>-1</sup>) and (2) Irgacure 819 (250 µg ml<sup>-1</sup>) with UV detection at 270 nm. Gradient method as in Fig. 2.11. Flow rate 0.25 ml min<sup>-1</sup>, Zorbax Eclipse XDB-C-18 reversed phase column (2.1 x 150 mm, particle size 5 µm)

The peak shape of the Irgacure had become slightly broader with 50:50 MeOH:H<sub>2</sub>O; however, an increased resolution of 1.16 was obtained, as shown in Fig. 2.13. Therefore, an optimised gradient method of 50:50 MeOH:H<sub>2</sub>O with 90:10 MeOH:H<sub>2</sub>O was employed in subsequent work. A time stability study was performed, with various analytes added such as inhibitors and weak and strong acids, using the optimised HPLC-UV method, as discussed in Section 2.4.3.1.



### 2.4.3 Analysis in light and dark conditions of Irgacure samples

#### 2.4.3.1 Photodegradation of the Irgacure

A stability study of the Irgacure was performed over a 24 hour time frame, and a comparison between samples stored under dark and light conditions was obtained, with anhydrous MeOH as the sample matrix. Fig. 2.14 illustrates the separation of the internal standard and the Irgacure, of samples which were preserved in the dark. It was determined that from 0 min. to 24 hours there was an 8% reduction in the peak height of the Irgacure, as shown in Fig. 2.14. Peak height was chosen due to difficulties associated with calculating peak area of the asymmetric peak shape of the Irgacure.

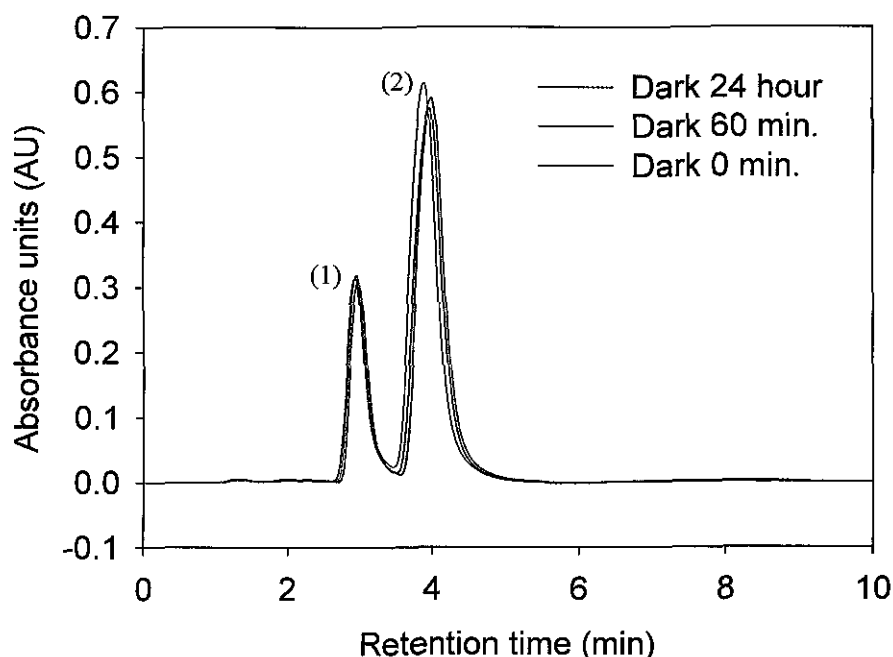


**Figure 2.14** HPLC separation of (1) biphenyl ( $50 \mu\text{g mL}^{-1}$ ) and (2) Irgacure 819 ( $250 \mu\text{g mL}^{-1}$ ) with UV detection at 270 nm for samples maintained in the dark over a 24 hour time frame. All operating conditions as in Fig. 2.13

In a comparison with the samples exposed to the light, it was found that the Irgacure had almost degraded completely by 60 min., and in addition the appearance of a peak at 1.8 min., which corresponded to the products of degradation of the Irgacure was obtained, as illustrated in Fig. 2.15. This was also observed in the appearance of the solution, as at 0 min. the Irgacure solution was yellow in colour; however, at 60 min. it had turned to clear. An overlay of the light and dark samples at 60 min. is illustrated in Fig. 2.16. It was therefore determined that the Irgacure was extremely photosensitive, undergoing a fast photolysis upon UV exposure.

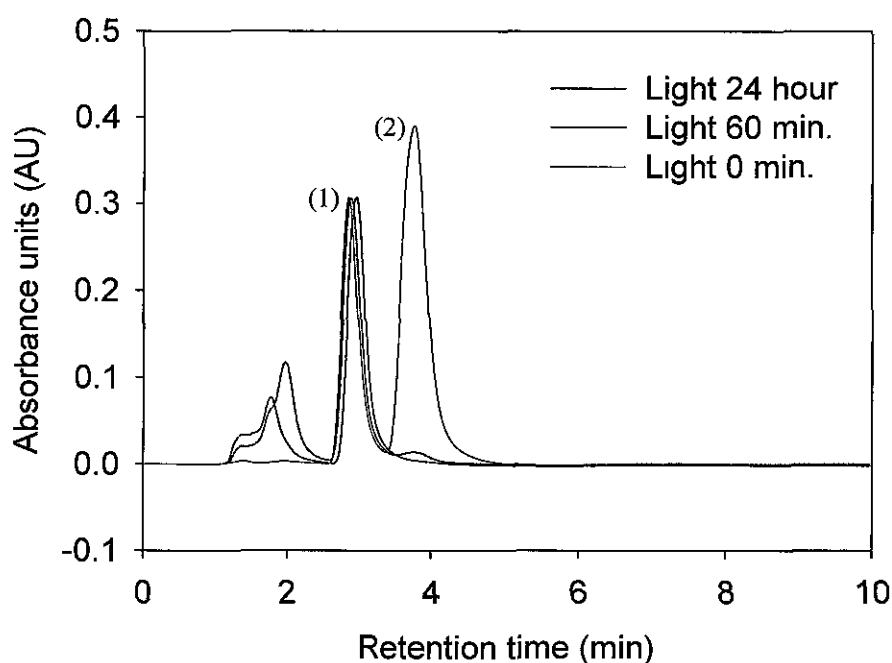


**Figure 2.15** HPLC separation of (1) biphenyl ( $50 \mu\text{g ml}^{-1}$ ) and (2) Irgacure 819 ( $250 \mu\text{g ml}^{-1}$ ) with UV detection at 270 nm for samples exposed to the light over a 24 hour time frame. All operating conditions as in Fig. 2.13

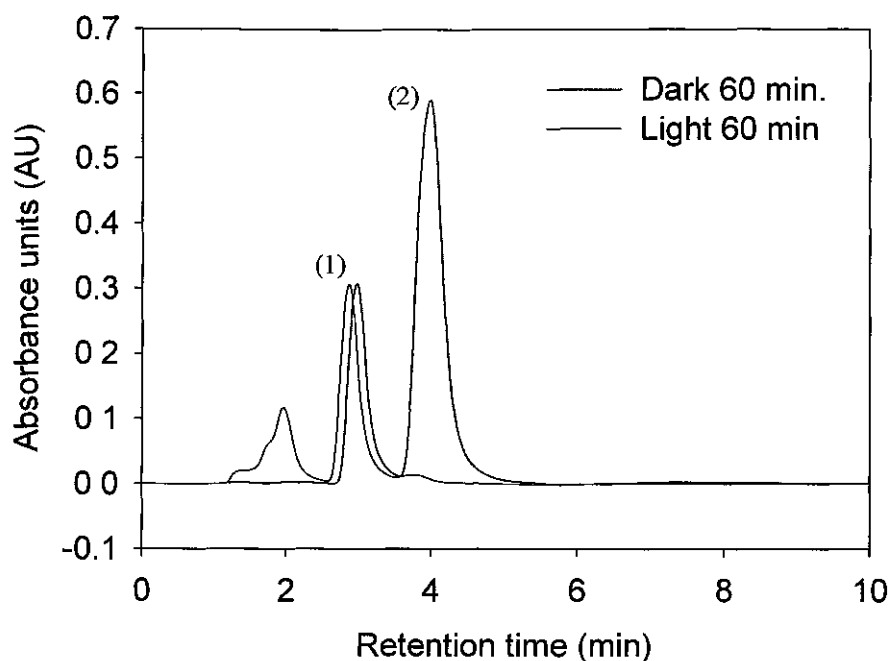


**Figure 2.16** Comparison of light and dark condition for the HPLC separation of (1) biphenyl ( $50 \mu\text{g ml}^{-1}$ ) and (2) Irgacure 819 ( $250 \mu\text{g ml}^{-1}$ ) with UV detection at 270 nm. All operating conditions as in Fig. 2.13

#### 2.4.3.2 Addition of water

The analysis of the stability of the Irgacure was performed with the addition of deionised water in the range 0.01-0.1%. Over this entire range, all the samples exposed to light were completely degraded by 60 min. As a result, these samples were not analysed further. All samples maintained in the dark degraded to the same extent, *i.e.*, the % water did not affect the rate of degradation. However, a slight effect on the separation efficiency of the Irgacure samples kept in the dark was determined, as plotted in Fig. 2.17, *e.g.* the separation efficiency for the 24 hour sample increased from 2040 plates  $\text{m}^{-1}$  to 2140 plates  $\text{m}^{-1}$  with 0.1% water added. The separation efficiencies were calculated according to Eqn. 1.5 and are dependent upon the peak width at half height ( $W_{1/2}$ ) and the elution time.

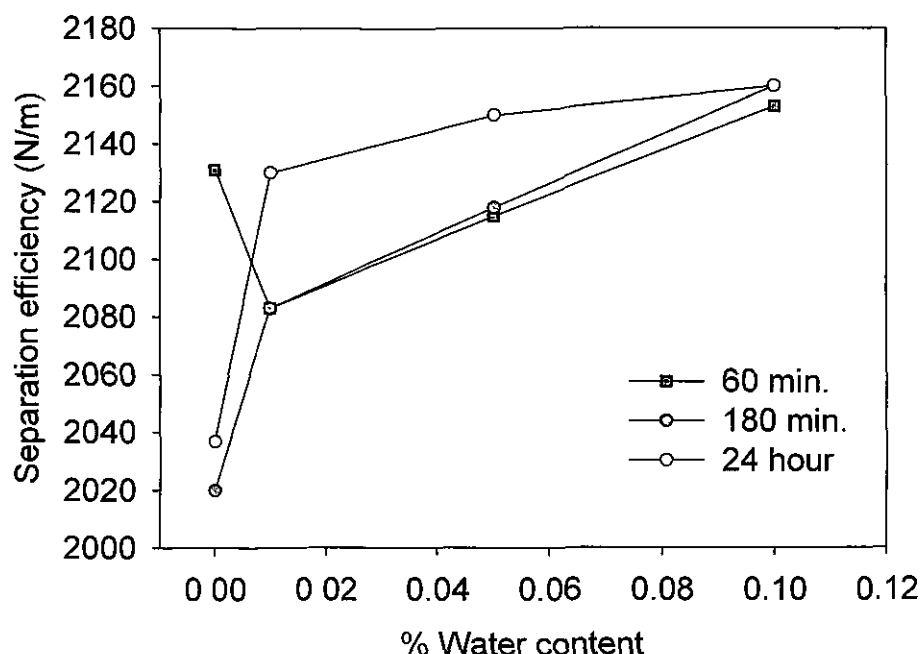


**Figure 2.17** Graphical illustration of the separation efficiencies calculated for 0%, 0.01%, 0.05% and 0.1% water added to the 60 min., 180 min and 24 hour Irgacure dark sample. All operating conditions as in Fig. 2.13

From this study, it was found that the separation efficiency increased with increasing amounts of water. This is illustrated in Fig. 2.17. However, for the 60 min. sample the separation efficiency calculated at 0% water was slightly higher than for the 180 min. and 24 hour samples, and this was contributed to a slight change in the elution time of the Irgacure as the  $W_{1/2}$  was similar for all samples. This increase though was not significant, and accounted only for an increase of 53 plates  $m^{-1}$ .

It was also concluded from results shown in Fig. 2.17, that from 0.05% to 0.1% water for the 24 hour sample the change in separation efficiency was not considerable, (10 plates  $m^{-1}$ ). However, for the same % water range, the change in separation efficiency for both the 60 and 180 min. samples resulted in a greater increase (42 plates  $m^{-1}$ ). As the separation efficiency increased with increasing % water; therefore it may be concluded that increasing the water content further will improve the symmetry of the peak.

### 2.4.3.3 Comparison of strong and weak acid

The addition of a strong acid versus a weak acid in the Irgacure sample was investigated. The strong acid employed was methyl sulphonic acid (MSA) and the weak acid utilised was boron trifluoride dihydrate ( $\text{BF}_3 \cdot 2\text{H}_2\text{O}$ ). MSA is a protonic acid, which generally exists as a salt and as a result is very acidic, while  $\text{BF}_3 \cdot 2\text{H}_2\text{O}$  is a Lewis acid. For the analysis of the light samples, the separation was the same as in Fig.'s 2.15 and 2.16, with complete degradation of the Irgacure occurring at 60 min., so that further analysis was not possible at this point. Therefore, neither the strong or weak acid significantly inhibited the photo-induced degradation.

For the samples, which were kept in the dark, again there was no difference in the rate of degradation upon the addition of either acid. The effect of their addition upon the separation efficiency of the Irgacure was determined, as plotted in Fig. 2.18.

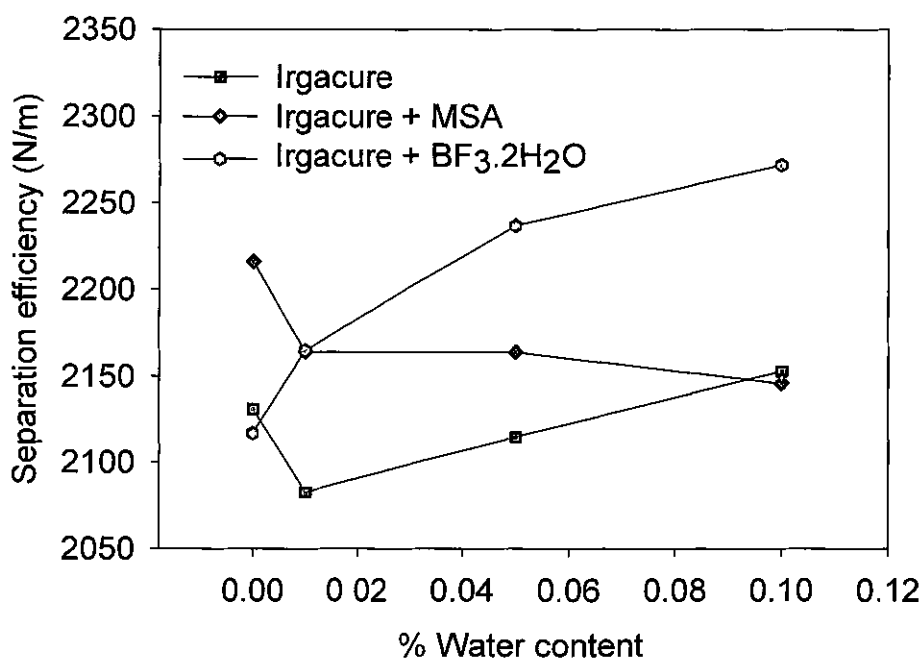


**Figure 2.18** Graphical illustration of the separation efficiencies calculated for 0%, 0.01%, 0.05% and 0.1% water added to the 60 min. Irgacure dark sample for the Irgacure, Irgacure and MSA and Irgacure and  $\text{BF}_3 \cdot 2\text{H}_2\text{O}$ . All operating conditions as in Fig 2.13

MSA was added with water in the range 0.01-0.1%. The separation efficiency decreased from 2216 plates  $\text{m}^{-1}$  in the 0% water sample to 2146 plates  $\text{m}^{-1}$  in the 0.1% water sample.  $\text{BF}_3 \cdot 2\text{H}_2\text{O}$  was also added with water in the range 0.01-0.1%. In contrast to the protonic acid, the addition of the Lewis acid caused the reverse effect, *i.e.*, the separation efficiency increased with increasing water content in the sample. This trend was also observed for the Irgacure sample with no weak or strong acid added. As discussed in Section 2.4.3.2, the separation efficiency calculated at 0% water was as a direct result of a change in the elution time of the Irgacure, as illustrated in Fig. 2.18.

#### 2.4.3.4 Addition of stabiliser and curing additives

Ferrocene, which acts as a stabiliser, protects the Irgacure from undergoing further hydrolysis. The analysis of the Irgacure with the addition of ferrocene plus either a weak or strong acid was performed for samples, which were exposed to the light. Fig. 2.19 illustrates the effect of the presence of these additives on the separation of the Irgacure by HPLC-UV. From Fig.'s 2.15 and 2.16, it was observed that degradation of the Irgacure had occurred by 60 min. The addition of ferrocene in the Irgacure sample reduced the degradation of the Irgacure, and the appearance of a peak at 1.8 min. was obtained, as illustrated in Fig. 2.19. However, as shown in Fig. 2.19, degradation of the Irgacure was not complete by 60 min, as had previously been observed. A very small peak was observed at 4.1 min.; therefore, the presence of ferrocene resulted in a decrease in the rate of degradation of the Irgacure.

When the strong and weak acids were added, they affected the rate of degradation in different ways. The addition of the weak acid,  $\text{BF}_3 \cdot 2\text{H}_2\text{O}$  increased the rate of Irgacure degradation, so that the Irgacure was completely degraded by 60 min., as shown in Fig. 2.19. With the addition of MSA in the Irgacure sample, the Irgacure had degraded with the appearance too of the peak at 1.8 min. This corresponded to the degradation of the Irgacure and this peak possessed a greater absorbance response than with the addition of just ferrocene or ferrocene in conjunction with the weak acid. However, the photodegradation of the Irgacure at 4.1 min. was significantly reduced than when just ferrocene was added, with an increased Irgacure peak height obtained. Therefore the addition of both MSA and ferrocene resulted in a decrease in the rate of Irgacure degradation.

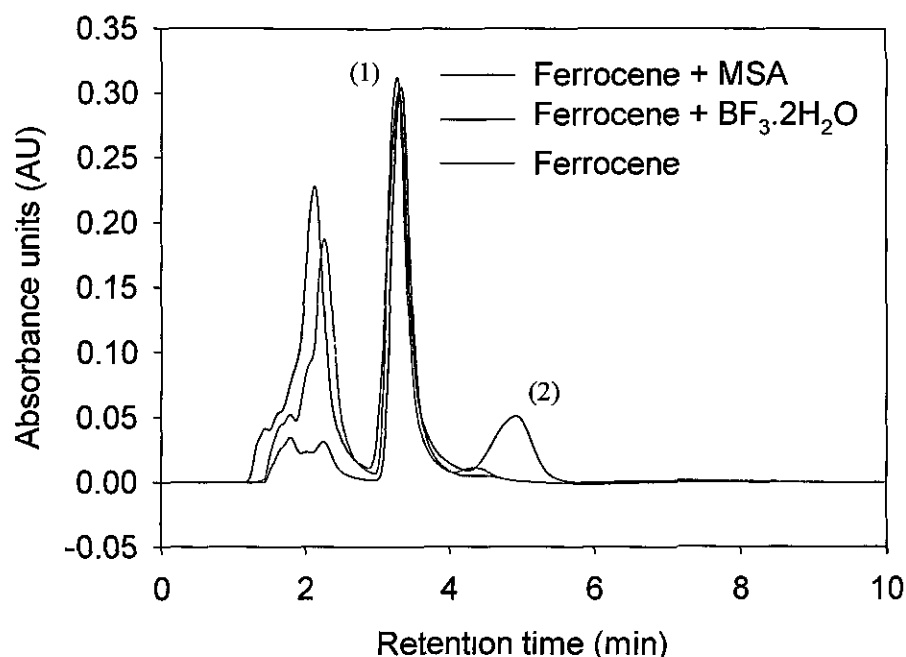


**Figure 2.19** HPLC separation of (1) biphenyl ( $50 \mu\text{g mL}^{-1}$ ) and (2) Irgacure 819 ( $250 \mu\text{g mL}^{-1}$ ) with UV detection at 270 nm for samples exposed to the light with ferrocene, ferrocene and MSA and ferrocene and  $\text{BF}_3 \cdot 2\text{H}_2\text{O}$  added to the 60 min. sample. All operating conditions as in Fig. 2.13

For the samples, which were maintained in the dark, there was no difference obtained in the peak height or peak area of the Irgacure and as a result showed no difference in the rate of degradation upon the addition of either acid in conjunction with ferrocene. The effect of their addition upon the separation efficiency of the Irgacure was investigated, and plotted in Fig. 2.20.

The addition of ferrocene to the Irgacure samples kept in the dark caused a reduction in the separation efficiency, which represented a 13.7% decrease from the sample with no additions to the sample with ferrocene added. However, the addition of MSA with ferrocene to the Irgacure sample resulted in an increase of the separation efficiency to a similar level to that of the Irgacure sample with no additions. The weak acid,  $\text{BF}_3 \cdot 2\text{H}_2\text{O}$ , was added to the Irgacure sample with ferrocene, and this again increased the separation efficiency, although an asymmetrical Irgacure peak was obtained. Therefore, for the samples maintained in the dark, the addition of ferrocene

alone caused an unexpected decrease in separation efficiency. The addition of either a weak or strong acid with ferrocene, did not affect the separation efficiency to the same degree as the addition of ferrocene alone, as shown in Fig. 2.20.

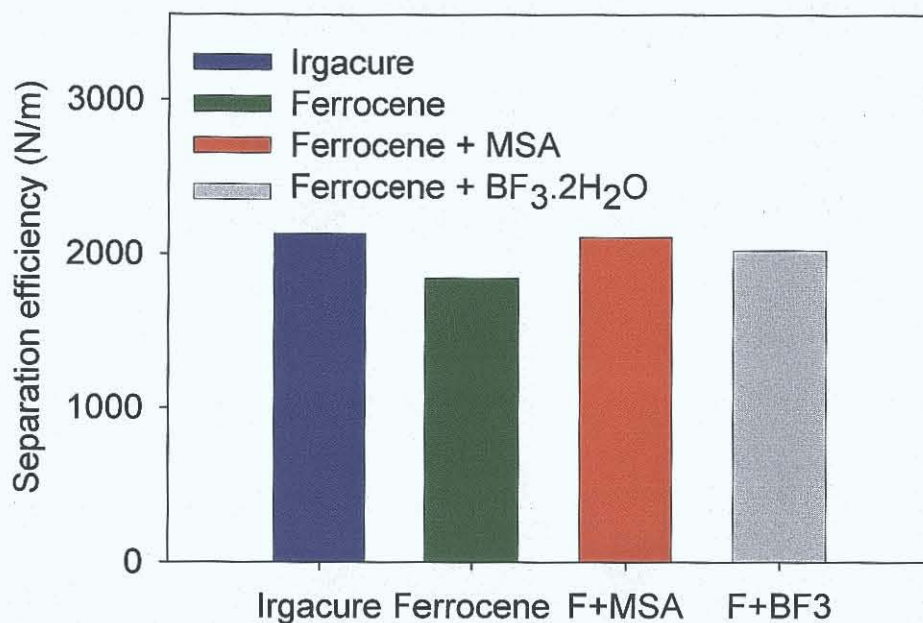


**Figure 2.20** Graphical illustration of the separation efficiencies calculated for the Irgacure with no ferrocene in the sample, ferrocene, ferrocene and MSA and ferrocene and  $\text{BF}_3 \cdot 2\text{H}_2\text{O}$  added to the 60 min. Irgacure dark sample. Where F: ferrocene and  $\text{BF}_3$ :  $\text{BF}_3 \cdot 2\text{H}_2\text{O}$ . All operating conditions as in Fig. 2.13

As both MSA and  $\text{BF}_3 \cdot 2\text{H}_2\text{O}$  affected the rate of degradation, for samples exposed to the light when added in conjunction with ferrocene, a number of other additives were also analysed. The analysis of the Irgacure samples exposed to the light, with ferrocene with either cumene hydroperoxide (CHP), 1,4-benzoquinone (BQ) or hydroquinone (HQ) added, were analysed by the optimised HPLC-UV method.

From results shown in Fig.'s 2.15 and 2.16 it was evident that the degradation of the Irgacure occurs by 60 min. The appearance of a peak at 1.8 min. was observed for the ferrocene samples as shown in Fig. 2.21. For the ferrocene sample with CHP, there



was evidence of a significant decrease of Irgacure at 4.1 min. and a corresponding peak at 1.8 min. possessed the greatest absorbance response. CHP, instead of inhibiting Irgacure degradation, actually increased the rate of degradation. The analysis of the Irgacure sample with ferrocene on its own also illustrated the presence of a peak at 4.1 min., as illustrated in Fig. 2.21.

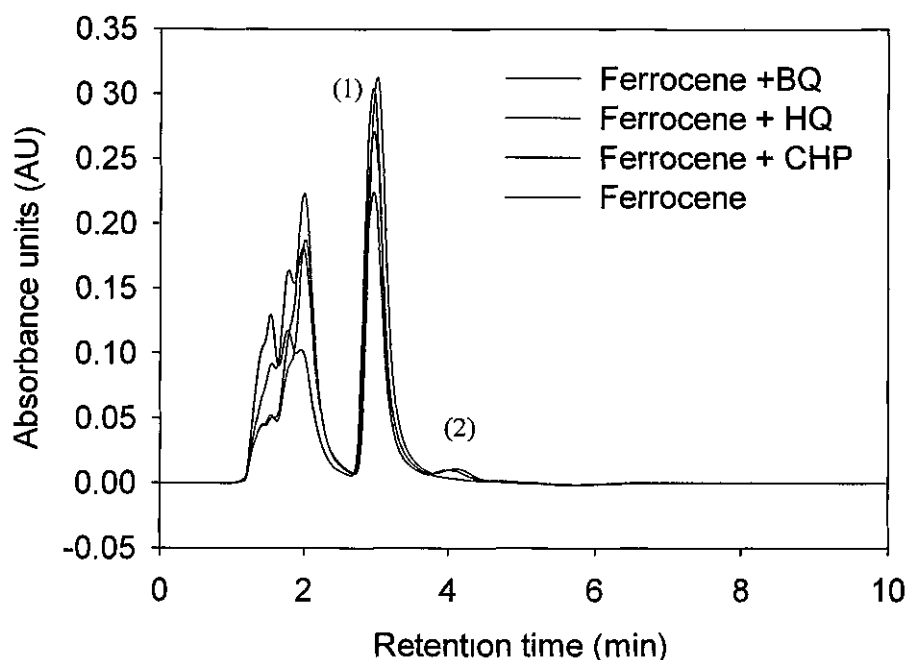


**Figure 2.21** HPLC separation of (1) biphenyl ( $50 \mu\text{g mL}^{-1}$ ) and (2) Irgacure 819 ( $250 \mu\text{g mL}^{-1}$ ) with UV detection at 270 nm for samples exposed to the light with ferrocene, ferrocene and CHP, ferrocene and HQ and ferrocene and BQ added to the 60 min. sample. All operating conditions as in Fig. 2.13

Hydroquinone and 1,4-benzoquinone act as inhibitors, which oxidise quickly. In the analysis of the Irgacure sample with HQ and BQ added, the Irgacure sample had completely degraded by 60 min., with the appearance again of the peak at 1.8 min. Therefore, it can be concluded that the addition of both HQ and BQ in conjunction with ferrocene, did not affect the rate of Irgacure photodegradation, however, the addition of ferrocene and CHP resulted in an increase in the rate of Irgacure degradation.

The Irgacure samples kept in the dark showed no significant differences in the peak height or peak area of the Irgacure and therefore resulted in no considerable difference in the rate of its degradation. The effect upon the separation efficiency of the Irgacure of each of the additives was obtained and is illustrated in Fig. 2.22. As discussed previously, the addition of ferrocene to the sample caused a reduction in the separation efficiency; however, the addition of CHP and HQ resulted in the separation efficiency to increase to a similar level to that of the Irgacure sample with no additions.

A comparison between HQ and BQ was investigated and from Fig. 2.22, it was found that the addition of BQ caused a slight reduction in the separation efficiency; however, this reduction was not considerable and represented an 8% reduction in separation efficiency.

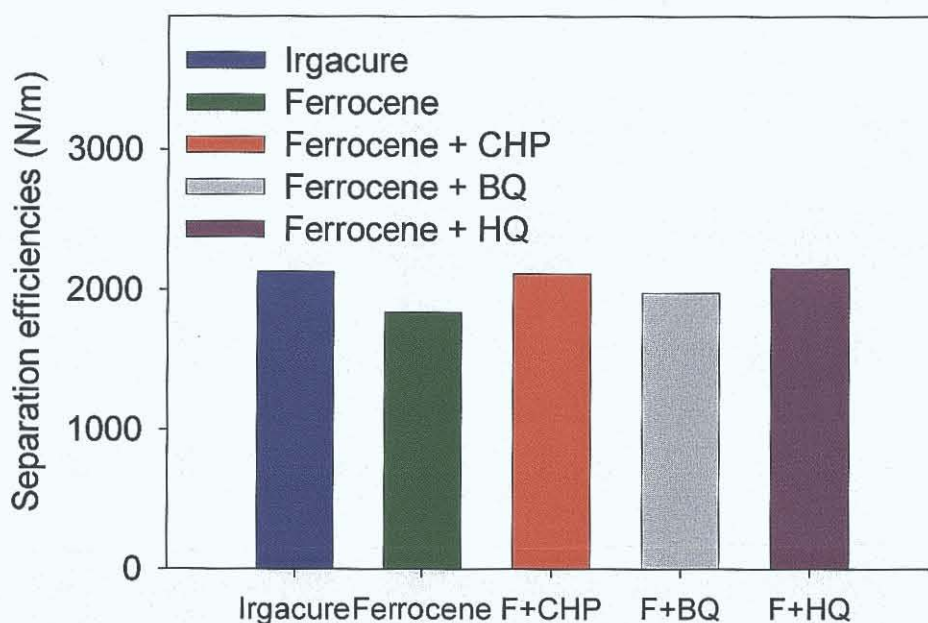


**Figure 2.22** Graphical illustration of the separation efficiencies calculated for the Irgacure with no ferrocene in the sample, ferrocene, ferrocene and CHP, ferrocene and BQ and ferrocene and HQ added to the 60 min. Irgacure dark sample. All operating conditions as in Fig. 2.13

Following the investigation of Irgacure degradation in MeOH, the analysis of the Irgacure in an ethyl cyanoacetate sample matrix was performed and is discussed in Section 2.4.3.5.

#### 2.4.3.5 Ethyl cyanoacetate analysis

The stability study of the Irgacure was performed in an ethyl cyanoacetate matrix over a 24 hour time frame. A comparison between samples maintained in the dark and light was made. Initially the analysis of an ethyl cyanoacetate sample was performed, with and without the Irgacure and internal standard, as illustrated in Fig. 2.23. It was determined that the ethyl cyanoacetate matrix peak eluted in the same region (1-3 min.) in which the degradation peak of the Irgacure occurs, and it also closely eluted with the internal standard, as shown in Fig. 2.23. The separation of the internal standard and the Irgacure, of samples which were maintained in the dark, is shown in Fig. 2.24.

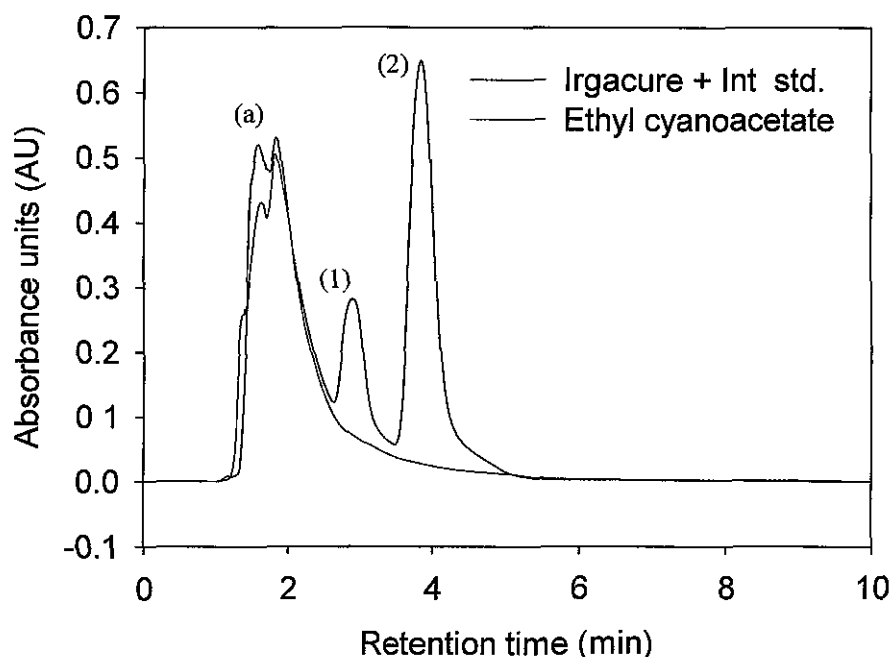


**Figure 2.23** HPLC separation of (1) biphenyl ( $50 \mu\text{g ml}^{-1}$ ) and (2) Irgacure 819 ( $250 \mu\text{g ml}^{-1}$ ) in an ethyl cyanoacetate sample matrix with UV detection at 270 nm, where (a) corresponds to the ethyl cyanoacetate matrix. All operating conditions as in Fig. 2.13

It was determined that from 0 min. to 24 hours there was only a slight reduction in the peak height of the Irgacure, from 0.64 AU in the 0 min. sample to 0.60 AU in the 24 hour sample, as shown in Fig. 2.24. A comparison was made with the Irgacure samples exposed to the light, and it was observed that the degradation of the Irgacure had occurred by 60 min., as illustrated in Fig. 2.25. In the region of the ethyl cyanoacetate matrix, a shoulder was observed at 2.2 min. This may correspond to the products of degradation of the Irgacure, but it was not possible to accurately establish this, as shown in Fig. 2.25. The addition of various analytes, such as inhibitors and weak and strong acids to the Irgacure sample in an ethyl cyanoacetate matrix, was performed; however, these separations also resulted in a similar trend. Therefore, only a comparison was possible between the analysis of the samples exposed to the light and maintained in the dark, as illustrated in Fig.'s 2.24 and 2.25.

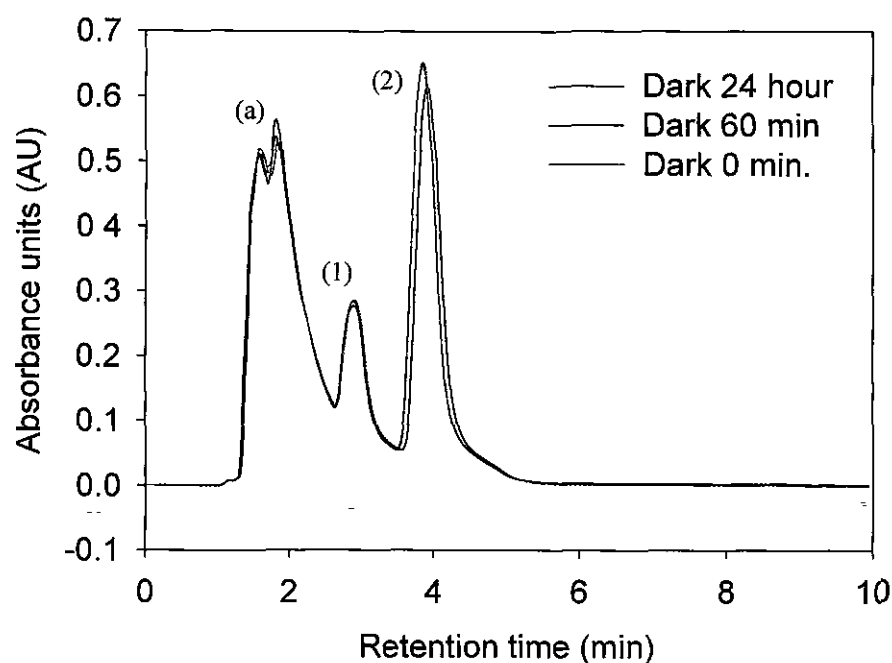


**Figure 2.24** HPLC separation of (1) biphenyl ( $50 \mu\text{g ml}^{-1}$ ) and (2) Irgacure 819 ( $250 \mu\text{g ml}^{-1}$ ) in an ethyl cyanoacetate sample matrix for samples maintained in the dark at 60 min with UV detection at 270 nm, where (a) corresponds to the ethyl cyanoacetate matrix. All operating conditions as in Fig. 2.13

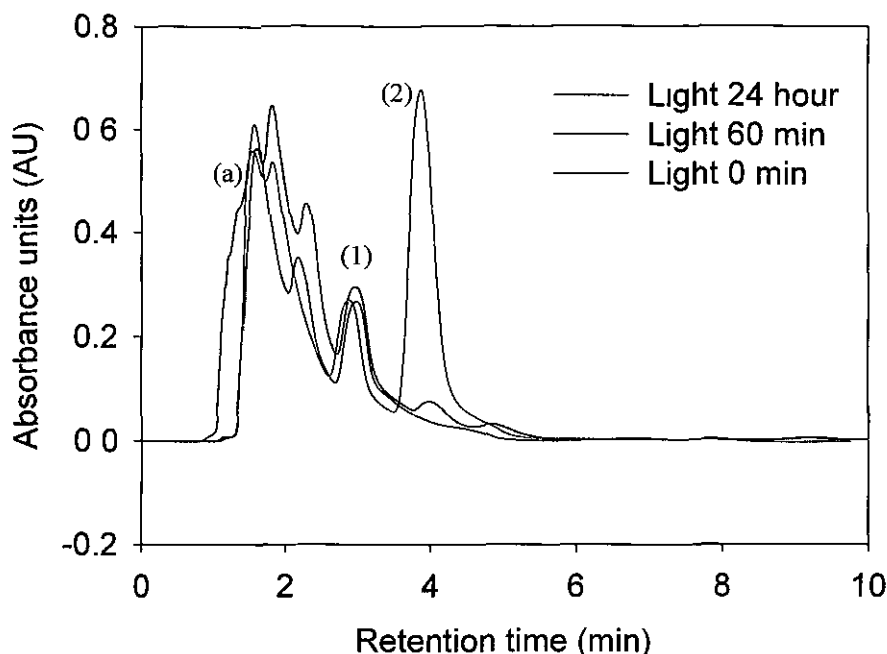


**Figure 2.25** HPLC separation of (1) biphenyl ( $50 \mu\text{g ml}^{-1}$ ) and (2) Irgacure 819 ( $250 \mu\text{g ml}^{-1}$ ) in an ethyl cyanoacetate matrix for samples exposed to the light at 60 min. with UV detection at 270 nm, where (a) corresponds to the ethyl cyanoacetate matrix. All operating conditions as in Fig. 2.13

#### 2.4.4 Irgacure degradation product determination by HPLC-MS

The analysis of the Irgacure samples was performed using HPLC-APCI-MS. The photolysis can give rise to three possible different cure mechanisms with an acrylic monomer in the presence of ferrocene. Firstly, a free radical mechanism, with the phosphinoyl ( $m/z$  125) and benzoyl ( $m/z$  147) radicals generated may take place. An anionic mechanism is also possible. Finally, a nucleophilic mechanism, due to the presence of a source of hydrogen ions, such as hydroquinone, may occur. APCI was the favoured ionisation technique due to the low molecular weight and the polarity properties of the Irgacure. Fig. 2.26 illustrates the applications of HPLC-MS ionisation techniques.

In APCI, the mobile phase containing the analyte, *i.e.*, the sample (*e.g.* Irgacure), is sprayed into a heated chamber at atmospheric pressure. In this chamber, the

solvents evaporate, and neutral analyte molecules are ionised by collision with reagent ions by interaction of the source gases with a corona discharge. Ionisation occurs either by proton transfer or charge exchange.<sup>[22]</sup> It was found that either MeOH water or ACN water were the preferred mobile phases for the analysis of the Irgacure, as illustrated in Fig. 2.7. However, as APCI was employed for MS analysis, a protic solvent such as MeOH is the preferred solvent because it helps improve positive ionisation.<sup>[22]</sup>

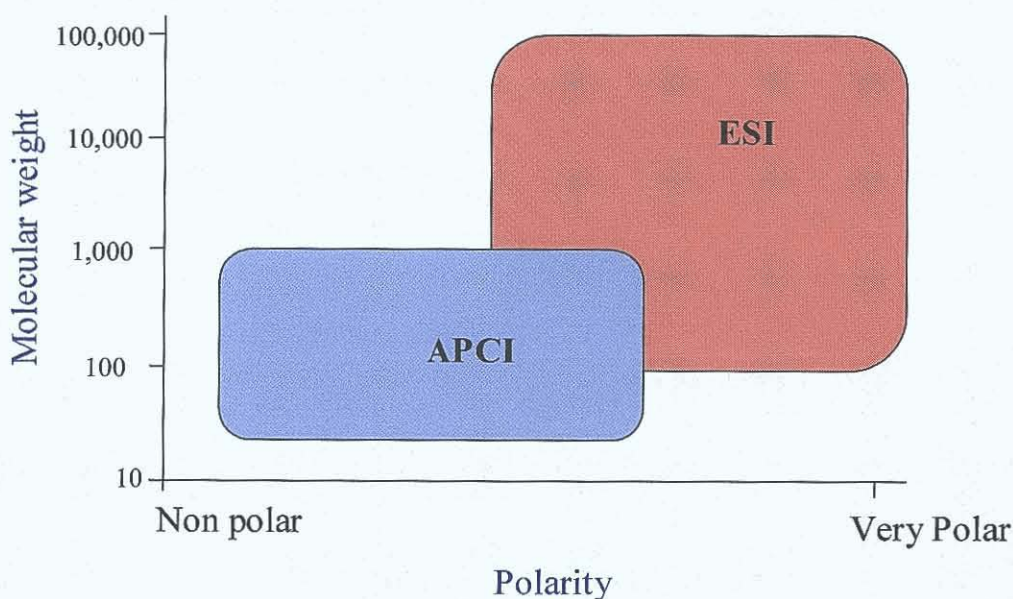


**Figure 2.26** Illustration of the applications of different ionisation techniques, where ESI: electrospray ionisation and APCI: atmospheric pressure chemical ionisation<sup>[23]</sup>

## 2.4.5 Optimisation of APCI parameters

### 2.4.5.1 Direct infusion analysis

For the optimisation of the parameters for APCI, an Irgacure sample, not containing an internal standard or additives, was injected directly into the APCI source. This was performed using a three-port tee piece. One end of the tee piece was connected to the HPLC pump, which was flowing a 100% MeOH mobile phase through the tee piece. This was subsequently mixed with an Irgacure sample from a syringe pump and

flowed towards the APCI source, whereupon ionisation of the sample occurred. Fig. 2.27 illustrates a mass spectrum of the Irgacure sample, following direct infusion of the sample into the APCI source. Optimum APCI-MS conditions are shown in Appendix 1a. Under these ionisation conditions the molecular ion, of  $m/z$  419, is of low intensity. This is most likely a consequence of the fragmentation conditions applied to the molecular ion, and it is possible this effect may be minimised by applying softer ionisation conditions such as reducing the dry temperature.

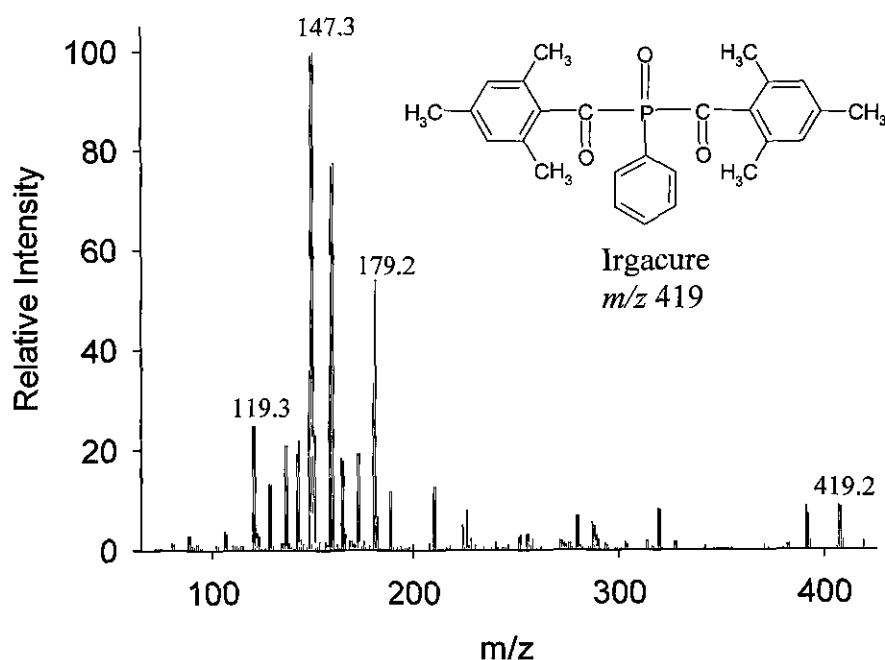


**Figure 2.27** APCI-MS of Irgacure 819 ( $100 \mu\text{g ml}^{-1}$ ) in MeOH. Flow rate  $0.19 \text{ ml min}^{-1}$

Upon UV irradiation, the Irgacure undergoes  $\alpha$ -cleavage of carbonyl-phosphorus bond and results in the production of benzoyl and phosphinoyl radicals, as shown in Fig. 2.28.

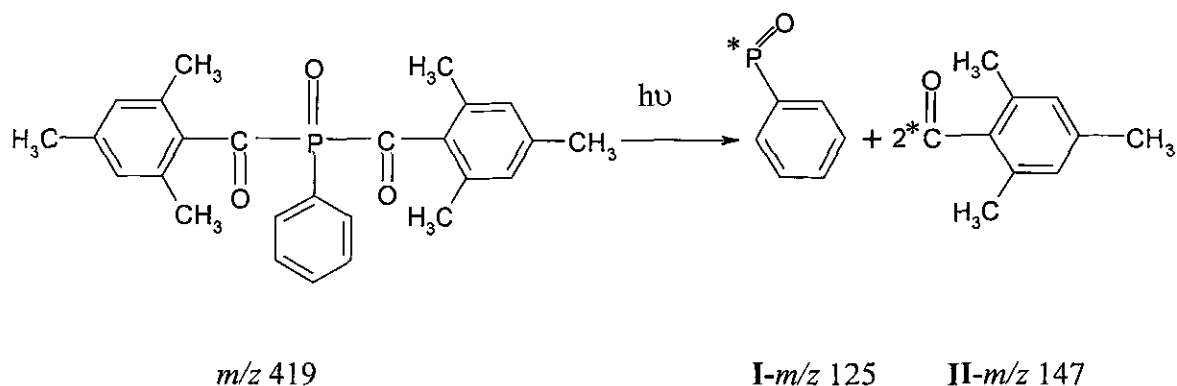


**Figure 2.28**  $\alpha$ -cleavage of Irgacure 819, to produce I-phosphinoyl radical and II-benzoyl radical<sup>[24]</sup>

From Fig. 2.27, it was found that the  $m/z\ 147.3$  was identified as the benzoyl radical, which is shown in Fig. 2.28. This fragmentation pathway corresponds to that shown in Fig. 2.28. In order to investigate any further fragmentation APCI-MS/MS was performed, as shown in Fig. 2.29. From the APCI/MS of the  $m/z\ 147.3$ , fragments of 119.1 and 91.3 resulted, which are illustrated in Fig. 2.29.

The analysis of the Irgacure samples, exposed to the light and maintained in the dark was performed using the optimised HPLC method with APCI-MS. A time stability study was also carried out, and the curing mechanism of the Irgacure was investigated with various additives, such as weak and strong acids, contained in the Irgacure sample.



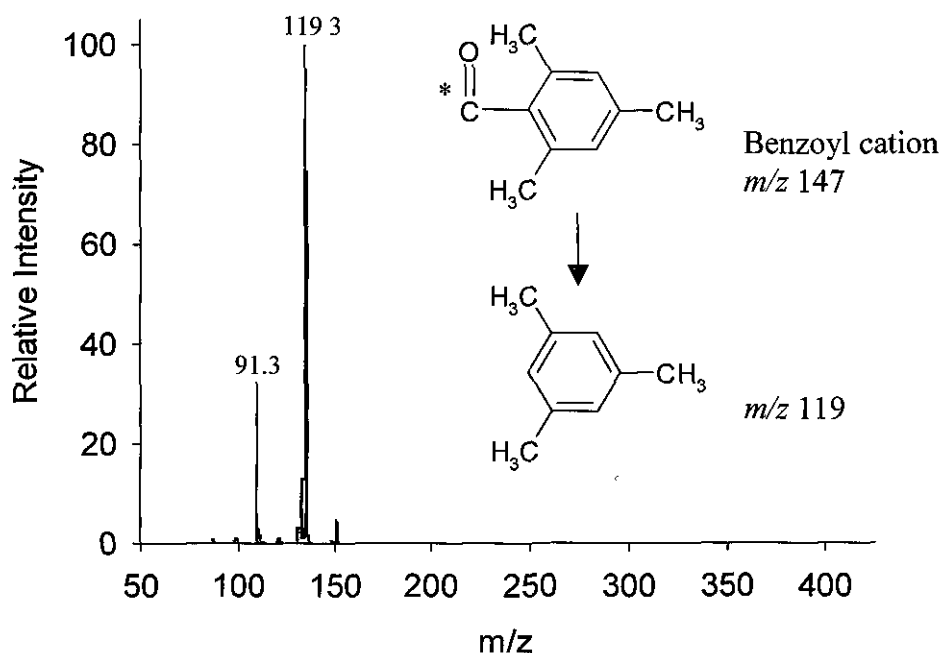


**Figure 2.29** APCI-MS/MS of Irgacure 819 ( $100 \mu\text{g ml}^{-1}$ ) in MeOH. Flow rate  $0.19 \text{ ml min}^{-1}$

#### 2.4.5.2 Analysis of Irgacure with additives

A stability study of the Irgacure was performed from 0 min. to 24 hours, and a comparison between samples maintained in the dark and light was obtained. It was determined from the HPLC-UV investigation that photodegradation of the Irgacure did not occur for samples maintained in the dark, as shown in Fig. 2.14. A comparison was performed, with samples maintained in the dark and exposed to the light; however, the results were similar for both. The results shown in this section correspond to studies for the light 0 min. and 24 hour analyses.

Initially, the analysis of the internal standard and the Irgacure was performed. Using the accompanying software, a Total Ion Chromatogram (TIC) was obtained from which Extracted Ion Chromatograms (EIC) were acquired. As the % water was shown not to affect the rate of degradation, water was added at its greatest quantity (0.1%). The ions detected in both investigations were the same,  $m/z$  147, 163 and 179. An overlay of

the TIC and EIC's obtained for the analysis of the Irgacure with and without water are illustrated in Fig. 2.30.

The ion of  $m/z$  147 corresponded to the benzoyl radical, as discussed in Section 2.4.5.1. This ion was also evident in the internal standard, which was identified by its elution time at 2.2 min. The ion of  $m/z$  163 was present in the Irgacure sample and also in the peak of retention time at 1.8 min., which corresponds to the degradation of the Irgacure. In a comparison with the Irgacure samples with 0.1% water this peak at 1.8 min. possessed a greater intensity in the sample with no water added, which indicates that the presence of water in the sample reduced the Irgacure degradation, as illustrated in Fig. 2.30. In contrast, the ion of  $m/z$  179, which was present in the Irgacure, possessed a greater intensity for the sample with water added, as shown in Fig 2.30. For the analysis of samples exposed to light for 24 hours, no significant photodegradation was obtained. In order to investigate further the cure mechanism of the Irgacure, the analysis of the Irgacure was performed with additives such as ferrocene and MSA in the Irgacure sample.

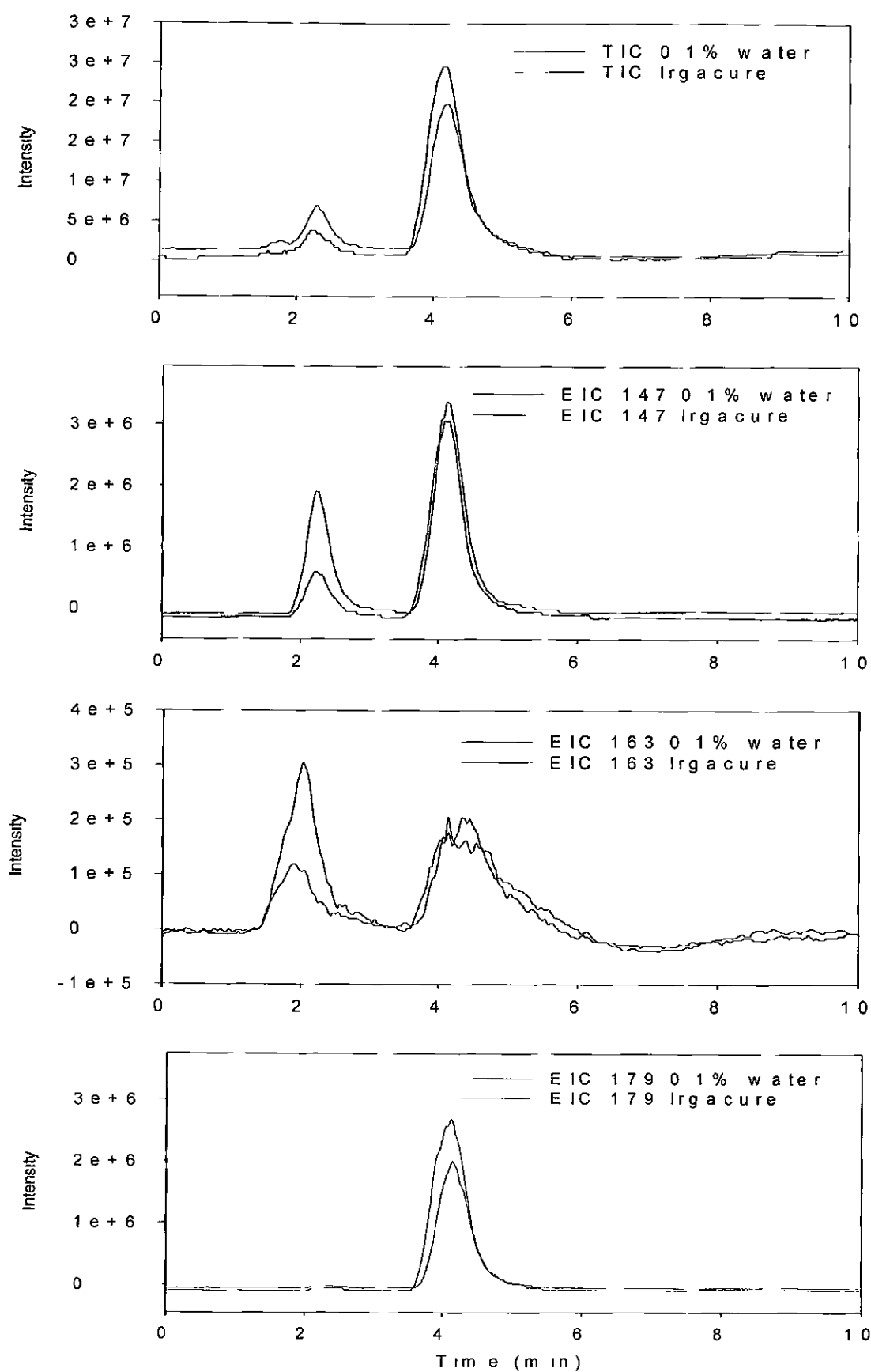


**Figure 2.30** TIC and EIC's for Irgacure 819 (0 min. sample) in MeOH. Unless stated otherwise all operating conditions as in Fig 2.13

The addition of the strong acid, MSA, and the weak acid,  $\text{BF}_3 \cdot 2\text{H}_2\text{O}$ , to the 0 min. and 24 hour sample, was not found to significantly affect the degradation of the Irgacure. Ions of  $m/z$  147, 163 and 179 were also obtained for the 0 min. and 24 hour samples, with the same trend observed as that shown in Fig. 2.30 for the Irgacure sample with and without water added. When 0.1% water was added in conjunction with MSA and  $\text{BF}_3 \cdot 2\text{H}_2\text{O}$ , again the fragment ions of  $m/z$  147, 163 and 179 were obtained with the same trend also obtained as that illustrated in Fig. 2.30.

From the HPLC-UV investigations, it was determined that the addition of ferrocene to the Irgacure sample resulted in a decrease in the rate of degradation of the Irgacure samples exposed to light. With the addition of ferrocene, ions of  $m/z$  147, 163 and 179 were obtained. A comparison of the 0 min. and 24 hour samples was performed and Fig. 2.31 represents the TIC's and EIC for  $m/z$  163 for both samples.

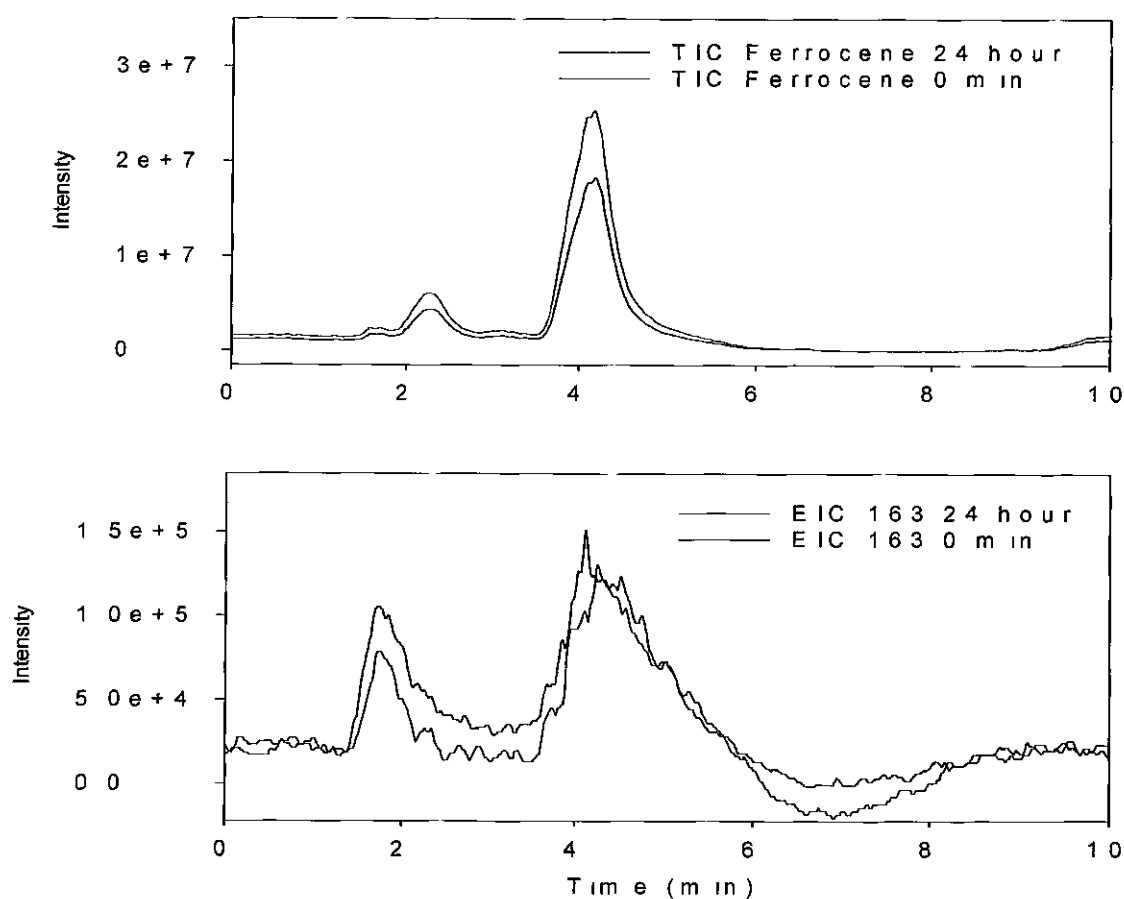


**Figure 2.31** TIC and EIC for  $m/z$  163 for Irgacure 819 (0 min. and 24 hour sample) in MeOH  
Unless stated otherwise all operating conditions as in Fig. 2.13

It was found from the TIC in Fig. 2.31, that degradation of the Irgacure had occurred, however, after 24 hours degradation was not complete. This was not expected, as complete photodegradation had occurred by 24 hours in the HPLC-UV analysis of light samples with ferrocene added, as discussed in Section 2.4.3.4. This was due in part to the increased sensitivity and also to the decreased light in the MS laboratory. However, it was not expected even taking these two factors into account that such high concentrations of Irgacure would remain. Also, from the EIC of  $m/z$  163, it appears that the peak at 1.8 min., has decreased slightly in intensity, Fig. 2.31.

The addition of a strong acid, MSA, versus a weak acid,  $\text{BF}_3 \cdot 2\text{H}_2\text{O}$ , in combination with ferrocene in the Irgacure sample was investigated for the 24 hour samples. Again ions of  $m/z$  147, 163 and 179 were acquired, as shown in the TIC and EIC's in Fig. 2.32. An overlay of the TIC's and EIC's obtained for the Irgacure sample with no additives, ferrocene, and ferrocene with MSA and  $\text{BF}_3 \cdot 2\text{H}_2\text{O}$  is illustrated in Fig. 2.32. Complete photodegradation was expected, however, only slight degradation was achieved, as discussed above, Fig. 2.32.

The ion of  $m/z$  147 corresponded to the benzoyl radical, as discussed in Section 2.4.5.1, which was also present in the internal standard, as it eluted at 2.2 min. The addition of MSA into the sample resulted in a reduction of the intensity of the Irgacure peak, which represented a 16% reduction. In contrast the weak acid caused only a slight reduction in intensity (6.6%), as shown in Fig. 2.32. The ion of  $m/z$  163 was present in the Irgacure sample and also in the peak at 1.8 min., which corresponds to the degradation of the Irgacure. In a comparison with the Irgacure sample with MSA added, this peak at 1.8 min. possessed a greater intensity than in the sample with no additives or  $\text{BF}_3 \cdot 2\text{H}_2\text{O}$  added, which indicates that the presence of MSA affected the rate of Irgacure degradation, as illustrated in Fig. 2.32. The ion of  $m/z$  179 eluted at 4.1 min., and was therefore present in the Irgacure.

The addition of CHP, BQ and HQ in conjunction with ferrocene was investigated for both 0 min. and 24 hour samples. Their addition did not considerably affect the rate of degradation of the Irgacure, with fragment ions of  $m/z$  147, 163 and 179 again obtained. In order to help identify these ions, an investigation of the cure chemistry of the Irgacure was performed and is discussed in Section 2.4.4.4.

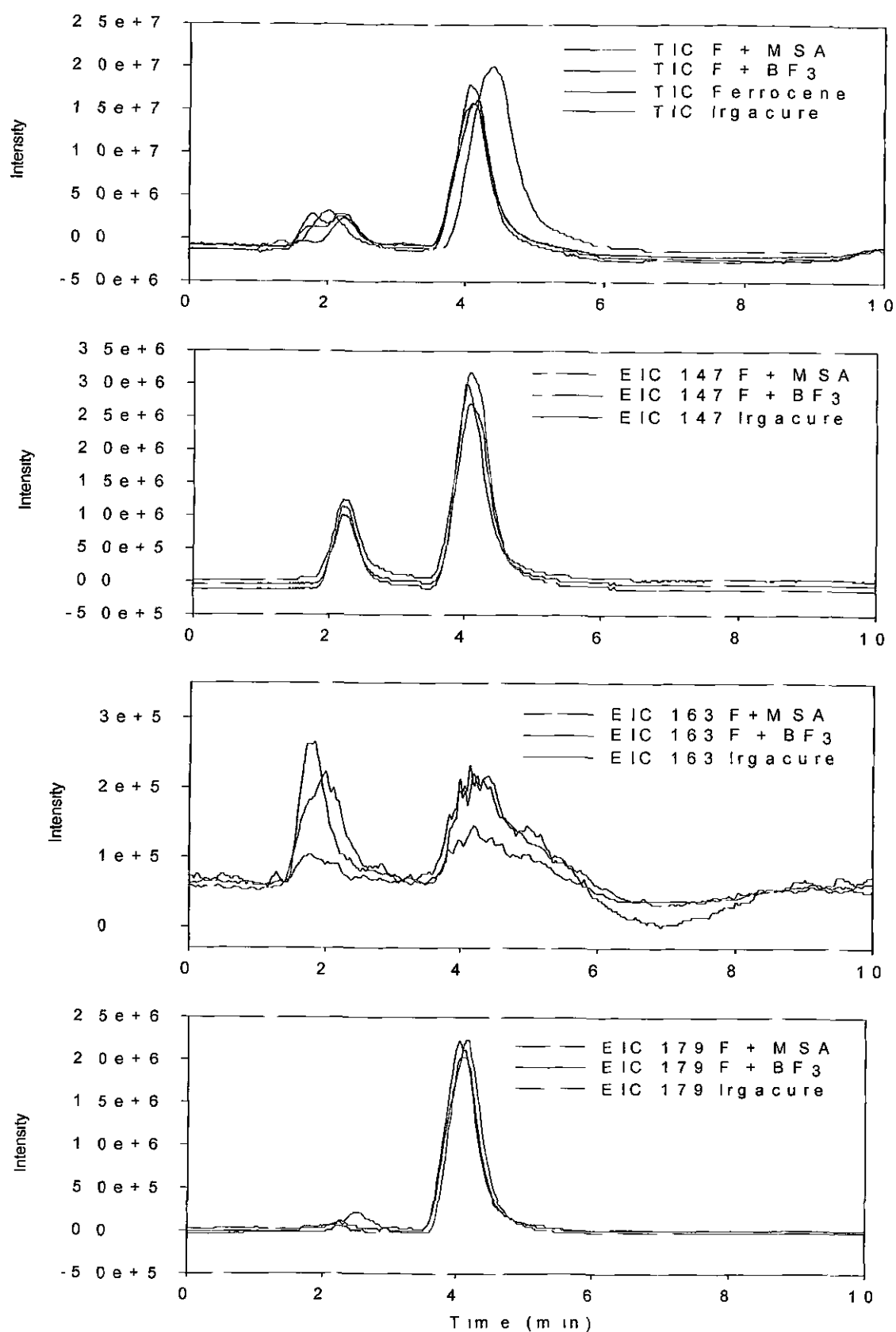
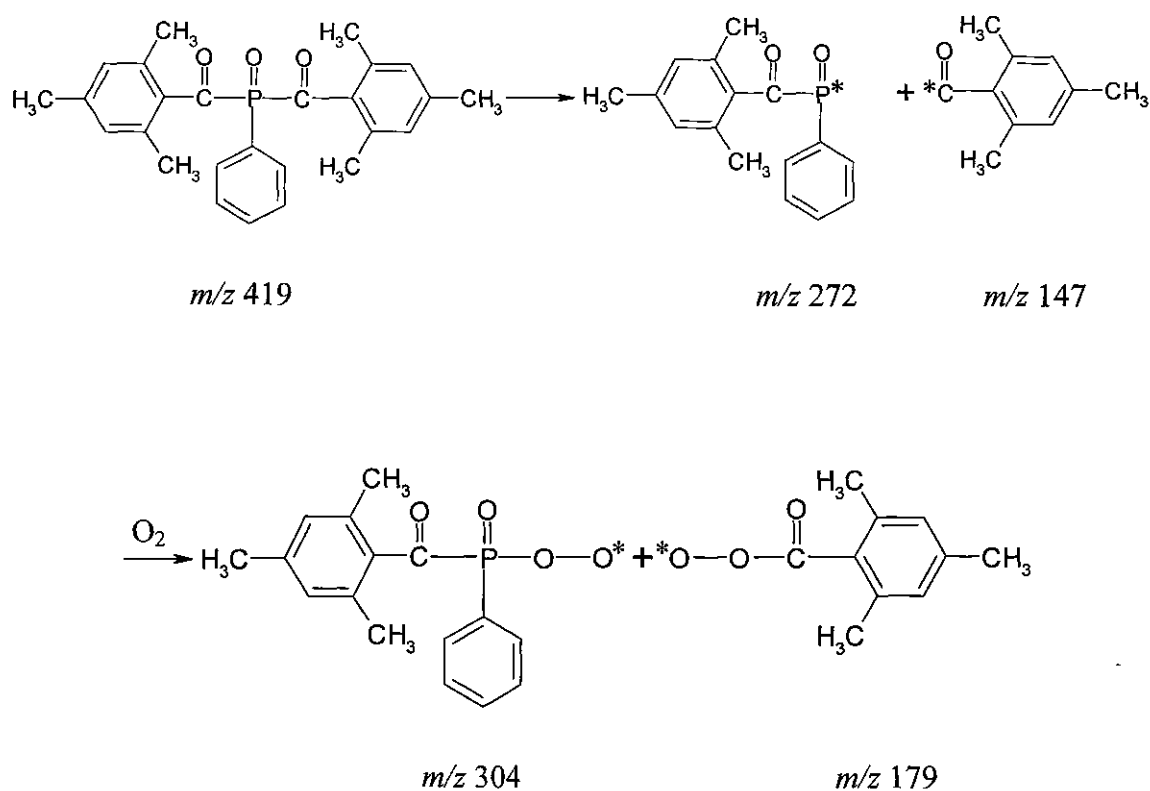


**Figure 2.32** TIC and EIC's for Irgacure 819 (24 hour samples) in MeOH, with ferrocene, ferrocene and MSA and ferrocene and BF<sub>3</sub>·2H<sub>2</sub>O Where F: ferrocene and BF<sub>3</sub>: BF<sub>3</sub>·2H<sub>2</sub>O. All operating conditions as in Fig. 2.13

From the HPLC-UV investigation it was determined that the ethyl cyanoacetate matrix eluted in the same region of the chromatogram in which the products of degradation of the Irgacure occurs, Fig. 2.23. The ethyl cyanoacetate matrix was not used for HPLC-APCI-MS analysis due to concerns about contamination of the ionisation source by the matrix. Consequently, the analysis of the Irgacure samples in an ethyl cyanoacetate matrix was not performed using HPLC-APCI-MS.

#### 2.4.5.3 Investigation of the Irgacure cure mechanism

It is reported in literature that the Irgacure undergoes  $\alpha$ -cleavage to produce the benzoyl and phosphinoyl radicals.<sup>[24]</sup> This reaction is shown in Fig. 2.28. From the mass spectrometry investigation, fragment ions of  $m/z$  147, 163 and 179 were obtained for the analysis of the Irgacure with and without additives in the sample. Based on both the fragment ions observed and potential reaction schemes supplied by Henkel Loctite (Irl.) the following mechanism has been proposed for the Irgacure 819, as illustrated in Fig. 2.33.



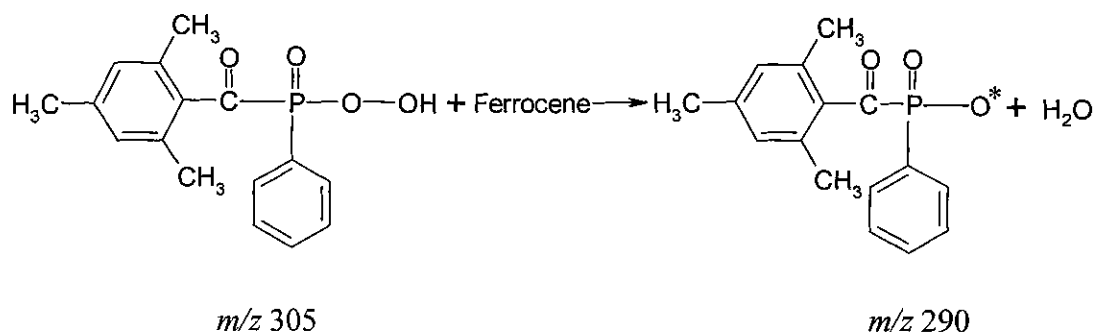


**Figure 2.33** Proposed cure mechanism for the Irgacure 819

The fragment ion of  $m/z$  179 was identified as a peroxy radical, produced from the reaction of the benzoyl and phosphinoyl radicals with oxygen. The appearance of the fragment ion  $m/z$  163 was also identified, which did not produce additional fragment ions upon further fragmentation. Fig. 2.34 illustrates the mechanism for the formation of  $m/z$  163, through the presence of water.

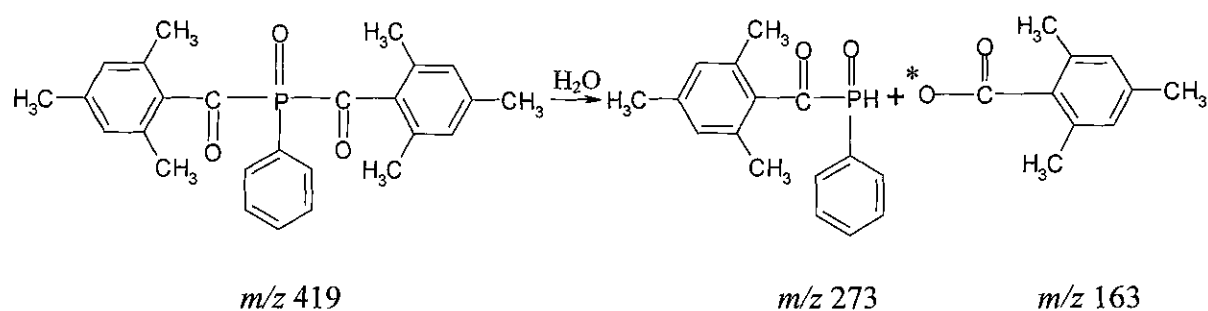


**Figure 2.34** Proposed cure mechanism for the Irgacure 819 with the presence of water

From the HPLC-UV investigations, it was determined that the rate of Irgacure degradation was not dependent upon the water content. However, the curing mechanism of cyanoacrylate adhesives is initiated by the presence of a weak base, such as water, on the surface of the materials being bonded.<sup>[25]</sup> From the analysis of the Irgacure with and without 0.1% water added, as shown in Fig. 2.30, it was also determined that the

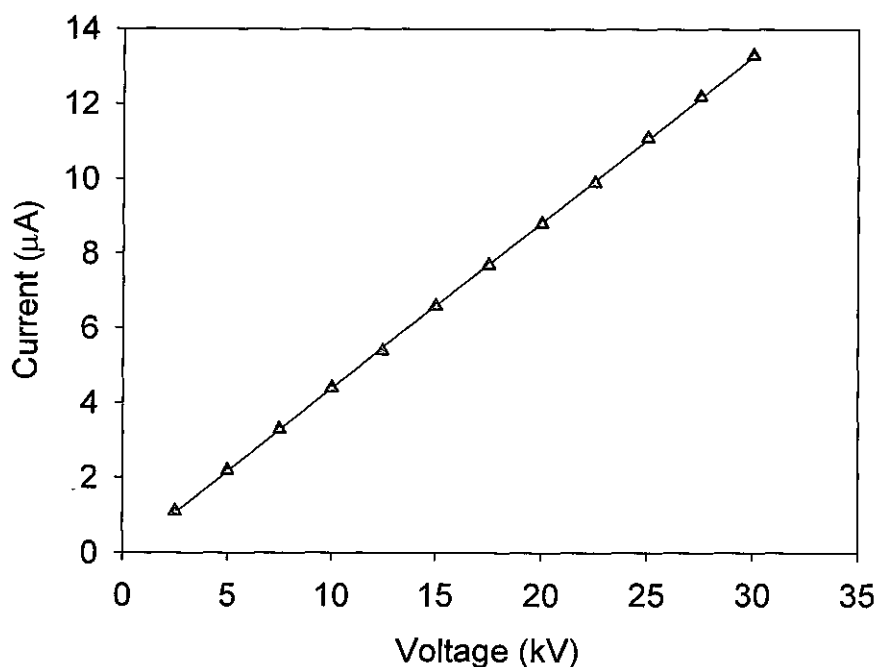


presence of water in the sample did not affect the rate of degradation of the Irgacure, *i.e.*, the curing of the Irgacure. This is shown in the EIC of  $m/z$  163, where the trace of the Irgacure sample with no water added possesses a greater intensity, than that with water added. It would be expected that the EIC with water added, would have a higher intensity, according to the reaction mechanism proposed in Fig. 2.34. As a result, the curing mechanism proposed for the Irgacure 819 is a free radical mechanism.

## 2.4.6 Development of CE method for Irgacure analysis

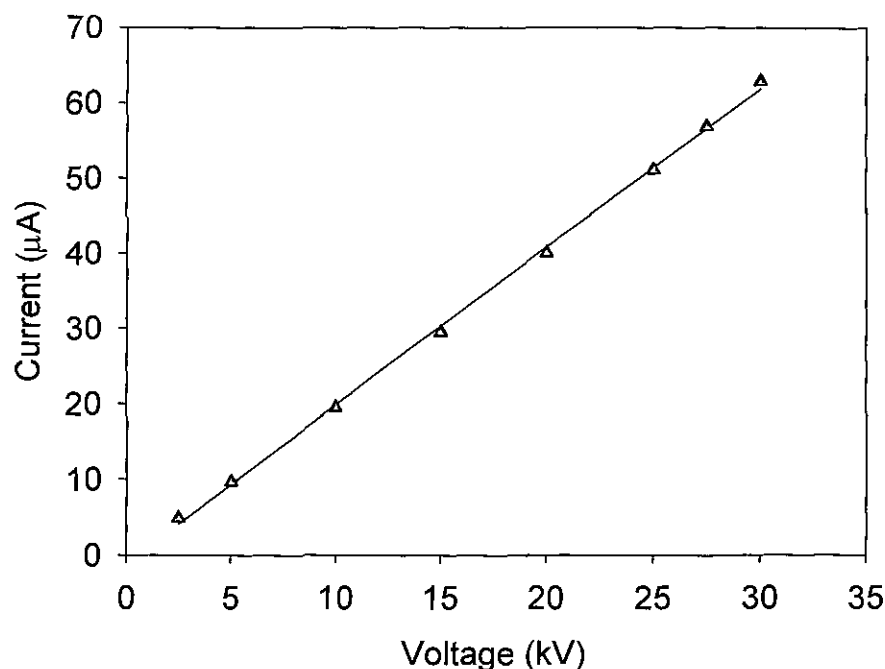
### 2.4.6.1 CE buffer selection

The CE analysis of the Irgacure was performed using a borate based buffer, which has a  $pK_a$  value of 9.24. Two buffer systems were investigated, *i.e.*, a 50 and 250 mM borate buffer at pH 9.0. In order to determine the optimum separation voltage for the analysis of the Irgacure an Ohm's law plot was obtained, as described by Nelson *et al* , and plotted in Fig.'s 2.36 and 2.37.



**Figure 2.36** Ohm's Law plot for 50 mM borate, pH 9.0. Effective capillary length 0.58 m

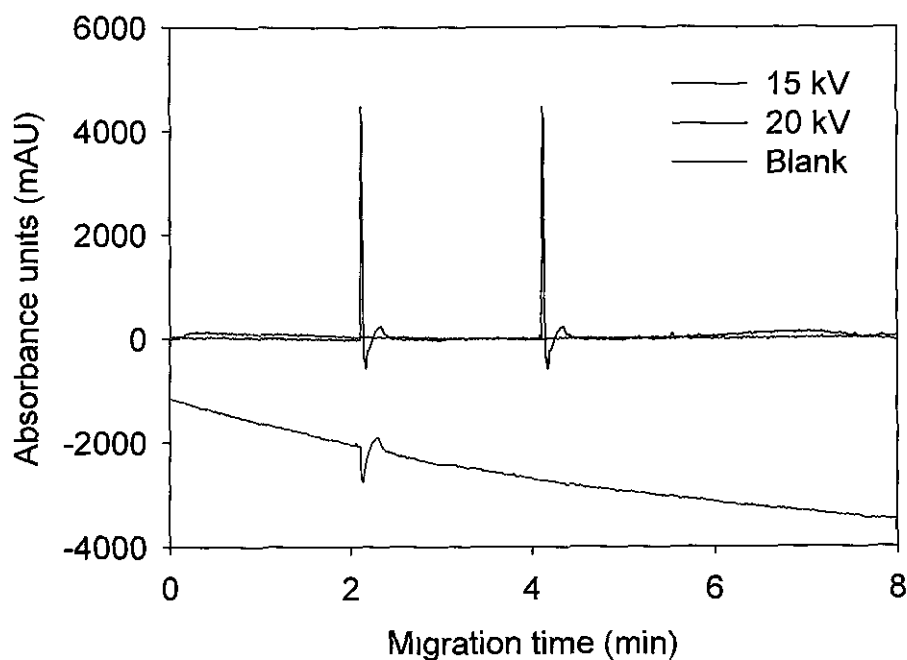
From the Ohm's Law plot in Fig. 2.36, it was evident that a linear relationship between current and voltage existed and that the analysis could be performed at separation voltages as high as 30 kV for the 50 mM borate buffer. Increasing the borate concentration increased the currents generated, as shown in Fig. 2.37, and Joule heating resulted. From Fig. 2.37, it was determined that a linear relationship between current and voltage existed from 2.5-27.5 kV, after which Joule heating was evident.



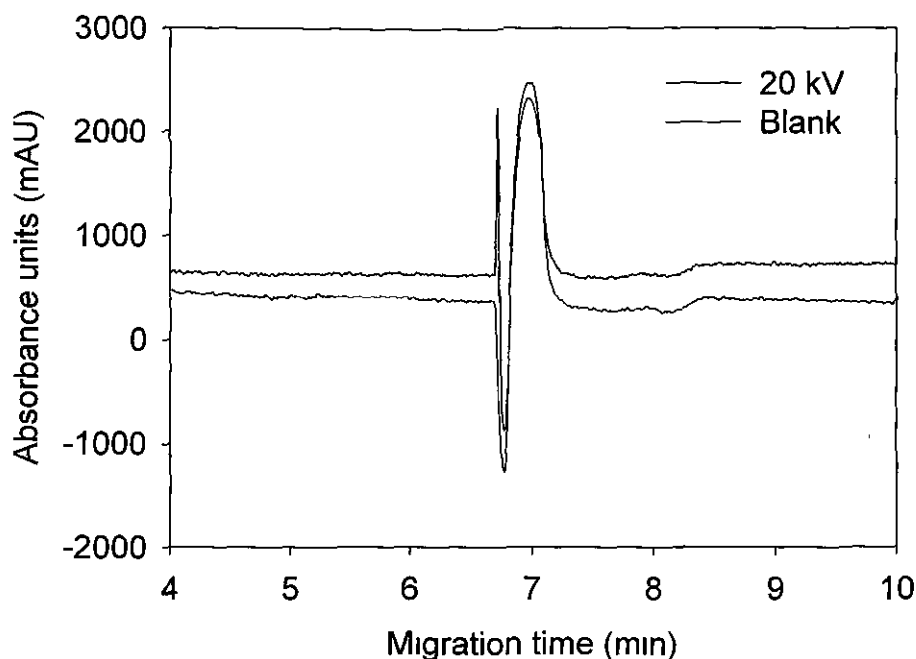
**Figure 2.37** Ohm's Law plot for 250 mM borate, pH 9.0. Effective capillary length 0.58 m

Fig 2.38 illustrates a separation of the Irgacure in a MeOH sample matrix using 50 mM borate buffer. It was evident from Fig. 2.38, that using the separation voltage of 20 kV, the separation was complete by 3 min., including rinse times, and a total analysis time of 6 min. was obtained. This was a reduction of 4 min. from the total analysis time achieved by HPLC. Also, increased separation efficiencies of 411,280 plates  $m^{-1}$  were obtained. However, the Irgacure migrates with the electroosmotic flow (EOF), which indicates that it is a neutral analyte at this pH. As a result, an alternative mode of CE more suited to the analysis of neutrals should be employed for further analysis, such as micellar electrokinetic chromatography (MEKC). Using the borate buffer of 250 mM, the separation time of the Irgacure was increased to 8 min., with a total analysis time of

11 min. Using this buffer, the absorbance response of the Irgacure was reduced and as a result, the peak absorbance of the blank was greater than that of the Irgacure, as shown in Fig. 2.39. Due to the increased total analysis time with the higher concentration of borate, and also the decreased absorbance response obtained with this buffer, a buffer of 50 mM borate at pH 9.0 was employed for further analysis.



**Figure 2.38** Effect of separation voltage for the CE analysis of the Irgacure 819 ( $1000 \mu\text{g ml}^{-1}$ ). Separation voltages 15 and 20 kV employed with direct UV detection at 280 nm, pressure injection 0.5 psi / 5 s. BGE: 50 mM borate, pH 9.0. Effective capillary length 0.58 m



**Figure 2.39** CE separation for the analysis of the Irgacure 819 ( $1000 \mu\text{g mL}^{-1}$ ). Separation voltage 20 kV, pressure injection 0.5 psi / 5 s with direct UV detection at 280 nm. BGE: 250 mM borate, pH 9.0. Effective capillary length 0.58 m

A time stability study of the Irgacure was performed, over a 24 hour time frame, using the optimised CE method, for samples exposed to the light and maintained in the dark. For the samples maintained in the dark, no degradation of the Irgacure sample occurred and Fig. 2.40 illustrates the separation of the Irgacure samples exposed to the light. From Fig. 2.40, it was found that complete photodegradation of the Irgacure had occurred by 24 hours, which validated the results obtained in the HPLC method.

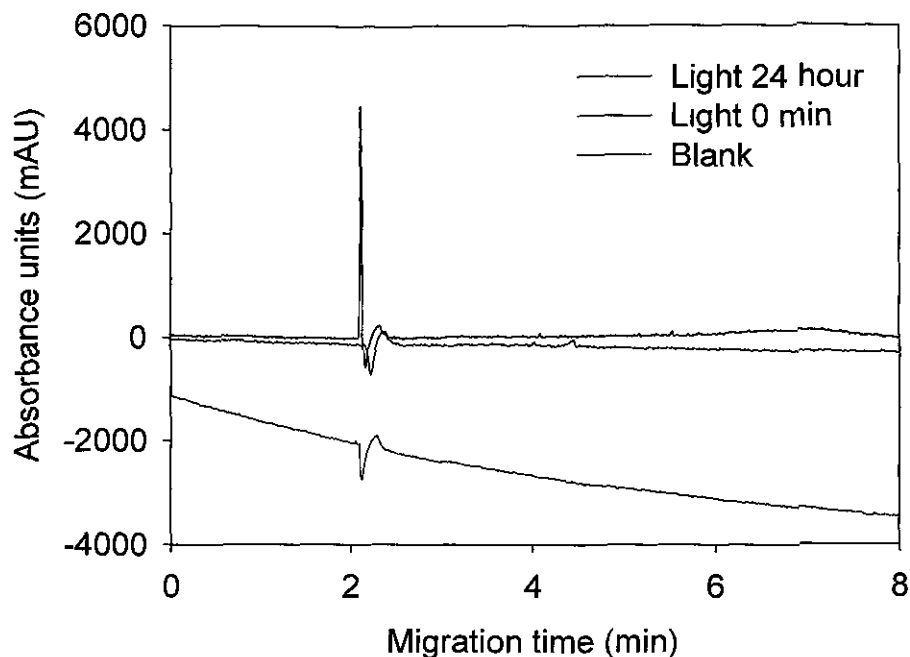


**Figure 2.40** CE separation for the analysis of the Irgacure 819 sample exposed to the light ( $1000 \mu\text{g mL}^{-1}$ ). Separation voltage 20 kV, with direct UV detection at 280 nm. Unless stated otherwise all operating conditions as in Fig 2.37. Effective capillary length 0.58 m

The CE method developed, with its reduced total analysis times and increased separation efficiencies, ( $411,280 \text{ plates m}^{-1}$ ) demonstrates its ability as an alternative method of analysis for the degradation of the Irgacure. The addition of an internal standard, however, is required, as this would provide an illustration of the degradation of the Irgacure.

## 2.5 CONCLUSION

A HPLC method was developed and was successfully applied to the analysis of the photoinitiator, bis(2,4,6-trimethylbenzoyl)phenyl-phosphine oxide, (Irgacure 819). A comparison of its stability in samples, which were kept in the dark and exposed to the light, was performed using the optimised HPLC-UV method. From this it was determined that the degradation of the Irgacure had almost completely occurred by 60 min. for the samples exposed to the light. For the samples maintained in the dark, only an 8% reduction in the Irgacure peak height was obtained. The addition of various analytes added such as stabilisers and weak and strong acids, was performed and it was determined that complete degradation of the Irgacure had not occurred by 60 min. with the addition of a stabiliser into the Irgacure sample exposed to the light. An investigation of the curing mechanism of the Irgacure was performed using APCI-MS, and it was determined that the Irgacure undergoes a free radical curing reaction. This mechanism assignment was based on a number of factors. The addition of water did not affect the rate of degradation, which occurs for anionic initiation. As shown in Fig. 2.33, ferrocene reacted with the free radicals generated from the free radical initiation. These free radicals of  $m/z$  147, 163 and 179, were all identified as free radical intermediates produced by the outlined mechanism. The application of CE to the analysis of the Irgacure was shown. This is the first time that this analysis has been reported. The CE method developed demonstrated its ability as an alternative mode of analysis with increased separation efficiencies obtained, 2130 plates  $m^{-1}$  with HPLC and 411,280 plates  $m^{-1}$  with CE, and also a reduced total analysis time of 6 min. achieved.

## 2.6 REFERENCES

- [1] Decker, C., *Prog. Polym. Sci.*, **1996**, *21*, 593.
- [2] Decker, C., Zahouily, K., Decker, D. Nguyen, T., Viet, T., *Polymer*, **2001**, *42*, 7551.
- [3] Jacobi, M., Henne, A., *J. Radiation Curing*, **1983**, *19*, 16.
- [4] Jacobi, M., Henne, A., *Polym. Paint Colour J.*, **1985**, *175*, 636.
- [5] Rutsch, W., Dietliker, K., Leppard, D., Kohler, M., Misev, L., Kolczak, U., Rist, G., *Prog Org Coatings*, **1996**, *27*, 227.
- [6] Kolczak, U., Rist, G., Dietliker, K., Wirz, J., *J. Am. Chem. Soc.*, **1996**, *118*, 6477.
- [7] Gatlik, I., Rzadek, P., Gescheidt, G., Rist, G., Hellrung, B., Wirz, J., Dietliker, K., Hug, G., Kunz, M., Wolf, J-P., *J. Am. Chem Soc* , **1999**, *121*, 8332.
- [8] Jockusch, S., Turro, N. J., *J. Am. Chem. Soc.*, **1998**, *120*, 11773.
- [9] Jockusch, S., Koptug, I. V., Mc Garry, P. F., Sluggett, G. W., Turro, N. J., Watkins, D. M., *J Am. Chem. Soc* , **1997**, *119*, 11495.
- [10] Baxter, J. E., Davidson, R. S., Hageman, H. J., *Eur. Polym J*, **1988**, *24*, 419.
- [11] Baxter, J. E., Davidson, R. S., Hageman, H. J., *Eur. Polym. J*, **1988**, *24*, 551.
- [12] Baxter, J. E., Davidson, R. S., Hageman, H. J., *Polymer*, **1988**, *29*, 1569.
- [13] Baxter, J. E., Davidson, R. S., Hageman, H. J., Hakvoort, G. T. M., Overeem, T., *Polymer*, **1988**, *29*, 1575.
- [14] Sluggett, G. W., Turro, C., George, M. W., Koptug, I. V., Turro, N. J., *J Am. Chem. Soc.*, **1995**, *117*, 5148.
- [15] Sluggett, G. W., Mc Garry, P. F., Koptug, I. V., Turro, N. J., *J. Am Chem Soc* , **1996**, *118*, 7367.
- [16] Snyder Index of Polarities.
- [17] Puig, D., Barcelo, D., *Trends in Anal. Chem.*, **1996**, *15*, 362.
- [18] Sacher, F., Lange, F. T., Brauch, H-J., Blankenhorn, I., *J. Chromatogr. A*, **2001**, *938*, 199.
- [19] Mahnik, S. N., Rizovski, B., Fuerhacker, M., Mader, R. M., *Chemosphere*, **2006**, *65*, 1419.
- [20] Badea, I., Lazar, L., Moja, D., Nicolescu, D., Tudose, A., *J. Pharm. Biomed. Anal* , **2005**, *39*, 305.
- [21] [www.sgc.com](http://www.sgc.com)

- [22] Pereira, L., *ThermoElectron Corporation Manual*.
- [23] Agilent Technologies, *Basics of LC/MS Primer Manual*.
- [24] Corrales, T., Catalina, F., Peinado, C., Allen, N. S., *J. Photochem. Photobiol. A Chem.*, **2003**, 159, 103.
- [25] Mc Cullagh, N., *MSc. Thesis*, Dublin City University, **2002**.



### ***Chapter Three***

#### ***Development and Application of a CE method for the analysis of Cyanoacrylate Adhesives***

### 3.1 INTRODUCTION

This work describes the development of a Capillary Electrophoresis (CE) method for the simultaneous determination of both inorganic and acidic anions, which may be present in cyanoacrylate adhesives. Cyanoacrylate adhesives, commonly known as superglues, are single component instant bonding adhesives, that are capable of forming and maintaining a bond between surfaces.<sup>[1]</sup> A flow chart providing a broad overview of the manufacturing process is illustrated in Fig. 3.1. The alkyl cyanoacetic acid is condensed with formaldehyde in the reaction vessel. The productions of this reaction “crack” are heated, leading to a crude monomer and a crack residue, which is discarded. The pure monomer is produced from the distillation of the crude monomer and the residue remaining from this distillation is recycled back into the reaction vessel to complete the production cycle.

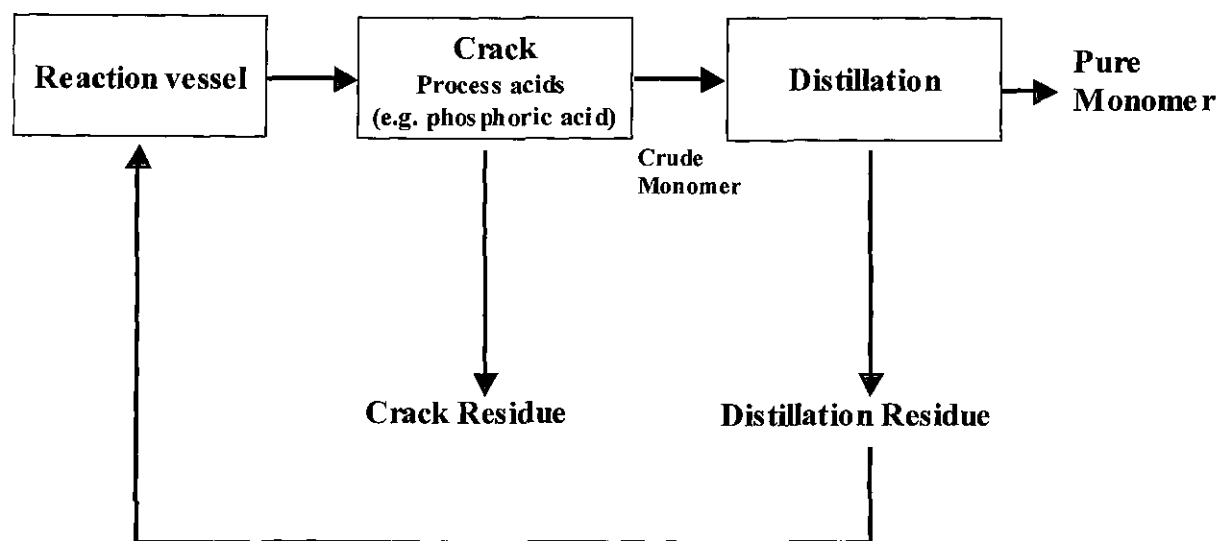
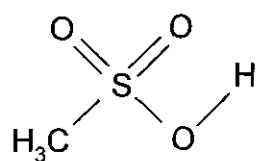
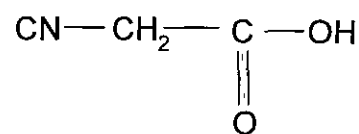


*Figure 3.1 Illustration of the cyanoacrylate production process*

A variety of inorganic and acidic anions may be present at different stages of the production process, such as sulphate and methyl sulphonic acid (MSA), and in order to maintain the quality of the product, sensitive methods for their quantification are required.<sup>[1]</sup> A CE method was developed previously for their separation by Kincaid.<sup>[2]</sup> Using this method the following anions were successfully separated: chloride, nitrate, sulphate, malonate, maleate, formic acid, phosphate, MSA, cyanoacetic acid and hydroxyl propane sulphonic acid (HPSA). A run time of under 7 min. achieved baseline separation for these species.<sup>[2]</sup> The analytes which were under investigation for this study were slightly different to those separated by Kincaid, namely phosphate, chloride, nitrate, sulphate, *fluoride*<sup>\*</sup>, formic acid, cyanoacetic acid, *diethylphosphate* (DEP) and MSA, Fig. 3.2.



I



II

**Figure 3.2** Structures of I-MSA and II-cyanoacetic acid, which are two of the organic acids present in cyanoacrylate adhesives

The analyses of anions have previously been carried out using traditional chromatography techniques, such as Ion Chromatography (IC) and High Performance Liquid Chromatography (HPLC).<sup>[3,4]</sup> Two IC methods were developed for the simultaneous separation of inorganic anions and cations. In one method, two ion-exchange columns were connected in series, and with ultra-violet (UV) detection the simultaneous separation of anions and cations was achieved in a run time of 20 min.

\* Anions not previously determined by Kincaid

However, with conductivity detection, the analysis of cations was only achieved. In the method with the switching valves, the simultaneous analysis of anions and cations was achieved with UV detection. A run time of 30 min. was obtained and in a comparison with the previous method, improved peak shapes were achieved. Detection limits in the range 0.01-0.4  $\mu\text{g ml}^{-1}$  and 0.09-7.1  $\mu\text{g ml}^{-1}$  were obtained with UV and conductivity detection respectively. The method incorporating the switching valves was successfully applied to the simultaneous determination of anions and cations in river, pond and tap water.<sup>[5]</sup>

A suppressed conductimetric method was also developed for the simultaneous determination of common inorganic anions, calcium and magnesium, by anion exchange chromatography. Using this method their determination was achieved in a run time of 20 min., and was applied to the analysis of drinking water samples. Limits of detection (LOD) in the range 8-40  $\text{ng ml}^{-1}$  were obtained.<sup>[6]</sup> A liquid chromatography method was developed for the analysis of 11 organic acids, such as oxalic, lactic and maleic acid, in dairy products with a reduced run time of 18 min. achieved when compared to previous literature methods.<sup>[7]</sup>

CE has recently been developed as an alternative method for the analysis anions.<sup>[8-11]</sup> It is an ideal method for the determination of anions because of its high separation efficiency, low material and sample consumption and short analysis times. However, there are drawbacks in the application of CE, such as poor injection reproducibility and precision.<sup>[11]</sup>

Most anions exhibit a very weak absorbance in the UV region, *i.e.*, they do not possess a chromophore. As a result, indirect UV detection was the mode of detection employed. Indirect UV detection was first introduced for the analysis of inorganic anions by Jones and Jandik.<sup>[12-14]</sup> The electrophoretic mobility of the probe ion should approximately match the mobilities of the sample ions as closely as possible, to avoid fronting or tailing in the sample peaks as the discrepancy in the mobilities becomes larger.<sup>[15]</sup> Fig. 3.3 represents an illustration of the electrophoretic mobility of some UV absorbing anions and analyte anions.

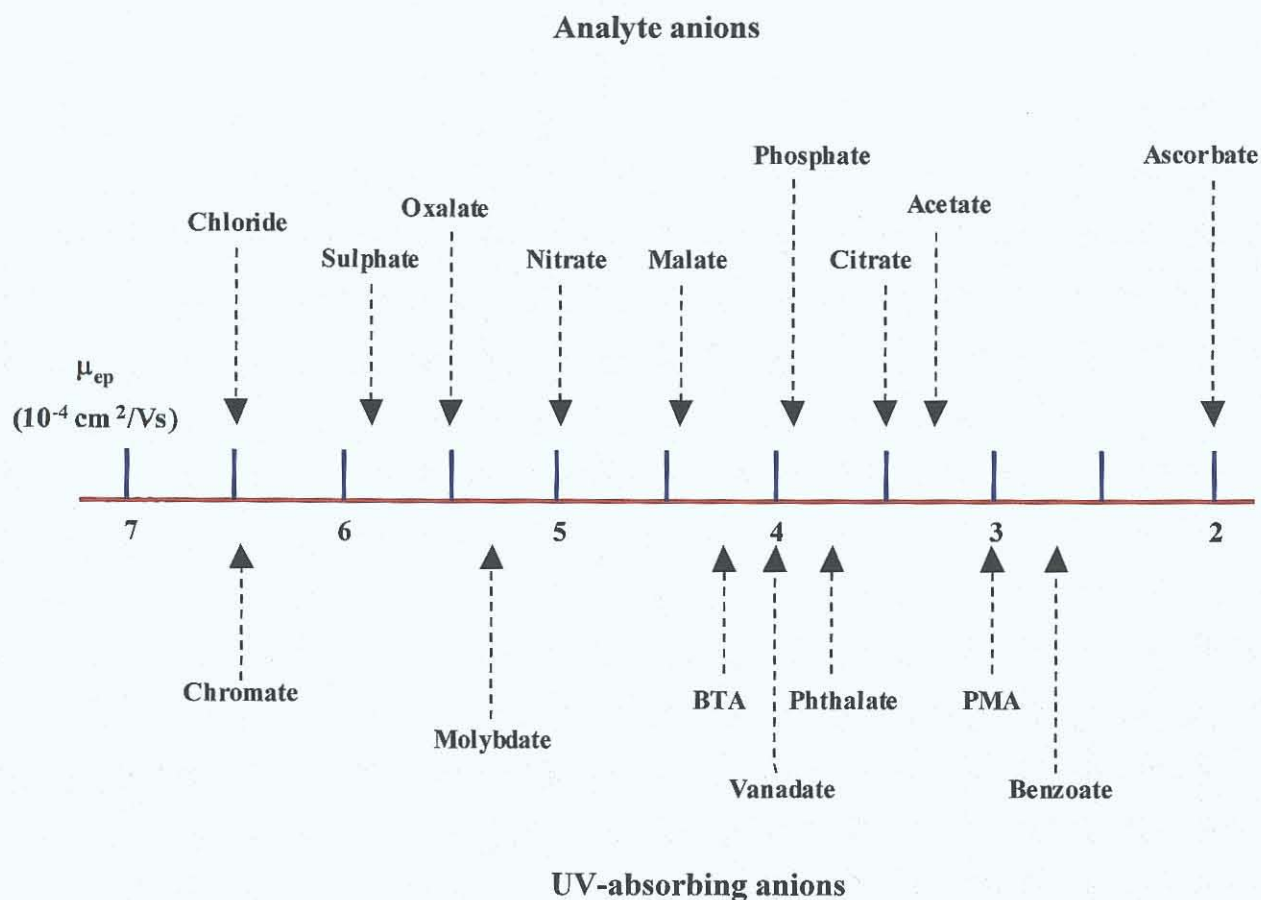


**Figure 3.3** Representation of the electrophoretic mobilities of some UV absorbing anions and analyte anions<sup>[16]</sup>

### 3.1.1 Choice of probe ion

Chromate is a highly chromophoric species, and is an ideal background electrolyte (BGE), resulting in fast (< 5 min.) and efficient (600,000 plates  $\text{m}^{-1}$ ) separations.<sup>[17,18]</sup> An alternative probe, pyridinedicarboxylic acid (PDCA), has been employed for the simultaneous determination of inorganic anions, organic acids and metal cations, with highly reproducible separations achieved in less than 15 min.,<sup>[19]</sup> and for the analysis of organic acids in waste waters.<sup>[20]</sup> PDCA has also been employed in the simultaneous determination of anions, organic and amino acids, nucleotides and carbohydrates with LOD's in the range of 6-12  $\mu\text{g ml}^{-1}$  obtained.<sup>[21,22]</sup>

A method was successfully developed for the simultaneous determination of both organic and inorganic anions in rainwater, using molybdate as the BGE. A run time of 7 min., which was a reduction of 8 min. from the developed IC method, was achieved. Detection limits in the  $\text{ng ml}^{-1}$  range were obtained and the CE method developed was applied to the analysis of rainwater samples.<sup>[23]</sup> Recently, a new counterion buffered molybdate electrolyte was developed for the quantitative determination of up to eight anions, such as chloride, sulphate and succinate, with detection limits in the range of  $0.17 \mu\text{g ml}^{-1}$ - $0.51 \mu\text{g ml}^{-1}$  achieved.<sup>[24]</sup> The analysis of organic acids in plant samples has also been reported using phthalate as the BGE with LOD of  $0.008$ - $0.08 \mu\text{g ml}^{-1}$  achieved.<sup>[25]</sup> In a comparison with IC, the CE separation of 17 acids was obtained within 3.2 min., whereas with IC, the separation was obtained in 30 min.<sup>[26]</sup>

The probe, pyromellitic acid (PMA), was utilised for the quantification of anions in environmental water samples with limits of quantification (LOQ) between  $0.02$ - $0.1 \mu\text{g ml}^{-1}$  achieved<sup>[27]</sup> and also for the determination of anions in atmospheric aerosols.<sup>[28]</sup> A cationic probe, imidazole, was employed for the successful separation of 16 metal ions, with high separation efficiencies achieved ( $650,000 \text{ plates m}^{-1}$ ).<sup>[29]</sup> Imidazole has also recently been applied to the indirect determination of cations, with its counter ion employed for the simultaneous separation of high mobility cations and anions.<sup>[30]</sup>

In the analysis of anions, the probe ion employed must have a high a molar absorptivity to enable their indirect detection. As the analyte anion passes through the detector, the response is generated as a decrease in absorbance, in relation to the BGE. Chromate is suited to the analysis of high mobility anions, such as chloride and nitrate, whereas phthalate has a lower mobility and is therefore more suited to the analysis of low migrating anions, *e.g.* phosphate and fluoride as shown in Fig. 3.3.<sup>[15]</sup> In order to enable the rapid simultaneous determination of high and low mobility anions, chromate was chosen as the probe ion. It is a suitable probe ion choice and has been widely employed for the indirect UV determination of anions in liquor samples<sup>[18]</sup> and was also applied to the analysis of anions with a run time of 2.5 min. and LOD's in the range of  $0.09$ - $0.12 \mu\text{g ml}^{-1}$  achieved.<sup>[31]</sup> Chromate has also been employed for the analysis of

trace inorganic anions, such as chloride, nitrate and bromide, in geological samples with the separation achieved in less than 6 min.<sup>[32]</sup>

### **3.2 SCOPE OF RESEARCH**

This chapter illustrates the development of a CE method for the simultaneous determination of some inorganic and acidic anions that may be present in cyanoacrylate adhesives, with indirect UV detection using chromate as BGE. Following optimisation of the separation conditions, such as electrolyte and surfactant concentrations, the method was applied to the analysis of cyanoacrylate adhesives, and enabled the monitoring of their production process. The CE method developed was compared with ion chromatography for the separation of the same analytes, to demonstrate the advantages over IC for the analysis of cyanoacrylate adhesives.



### 3.3 MATERIALS AND METHODS

#### 3.3.1 Instrumentation

##### 3.3.1.1 Capillary electrophoresis separations

All separations were performed on Beckman P/ACE MDQ instrument (Fullerton, CA), equipped with a UV absorbance detector. Polyimide-coated fused silica capillaries of 50  $\mu\text{m}$  internal diameter (i.d.) were employed. The effective length of the capillary utilised was 0.50 m, with a total length of 0.56 m (Composite Metal Services Ltd., England). All sample analyses were carried out using indirect UV detection at 254 nm with a deuterium lamp. Sample introduction was performed hydrodynamically (0.5 psi) for 5 s. Data analysis was performed using Beckman (version 3.4) software. Separations were performed with reverse polarity at -10 kV and the temperature maintained at 25 °C.

##### 3.3.1.2 Ion Chromatography separations

The Ion Chromatographic instrumentation consisted of a Dionex eluant degas module with a Dionex gradient pump, an IonPac AS11 anion separator column (250 x 4 mm I.D.), an IonPac ATC-1 Anion Trap Column, an IonPac AG11 guard column (4 mm) and a Dionex ASRS-ULTRA regenerating suppressor (4 mm). Detection was supplied by a Dionex Conductivity Detector CD20. The Rheodyne injection loop was 10  $\mu\text{l}$ . All samples were analysed in triplicate with a flow rate of 2  $\text{ml min}^{-1}$ .

#### 3.3.2 Chemicals

Chloroform (HPLC grade) was purchased from Labscan Ltd. (Dublin, Ireland). All other chemicals were of reagent grade. Sodium chromate (30,7831), sodium hydroxide (48,0878, NaOH), chloroacetic acid (C-0266), citric acid (25,1275), cetyltrimethylammonium bromide (85,5820, CTAB), tetradecyltrimethyl ammonium bromide (86,0425, TTAB), didodecylammonium bromide (35,9025, DDAB), N-tris [Hydroxymethyl]methyl-3-amino-propane sulphonic acid (T-5130, TAPS), Trizma hydrochloride (T-3253), Trizma base (T-1503), sodium sulphate (23,9313), sodium

nitrate (22,1341), sodium dihydrogenphosphate (22,9903), methacrylic acid (39,5374), *p*-toluene sulphonic acid (16,1993, PTSA), potassium chloride (31,0123), potassium bromide (24,3418) and cyanoacetic acid (23,9976) were obtained from Sigma Aldrich (Tallaght, Dublin). Potassium fluoride (60239) was obtained from Fluka (Buchs, Switzerland). Deionised water was treated with a Hydro Nanopure system to specific resistance > 18 M $\Omega$  cm (Millipore, Bedford, MA, USA). Stock solutions of anions were prepared using deionised water. Diethyl phosphate (98% purity, 40742-0050, and 99.3% purity, MET 90C, DEP), MSA, formic acid and cyanoacrylate adhesive samples were obtained from Henkel Technologies (Irl.) Ltd.

### **3.3.3 Procedures**

#### **3.3.3.1 CE Background electrolyte (BGE) preparation**

Electrolytes were prepared using deionised water. Three BGE solutions were prepared, which consisted of a sodium chromate electrolyte and an electroosmotic flow (EOF) modifier. A stock solution of 50 mM sodium chromate was prepared, from which 15 mM and 5 mM sodium chromate solutions were obtained by dilution of the stock with deionised water. The EOF modifiers employed were CTAB, DDAB and TTAB. Concentrations of 1 mM CTAB, 2.65 mM and 1 mM DDAB and 2.35 mM and 5 mM TTAB were prepared by dilution of stock solutions with deionised water. Buffered electrolytes were prepared using 10 mM TAPS and 50 mM Tris at pH 8.5. The pH of the unbuffered electrolyte was adjusted to 8.5 using 1 mM sulphuric acid (H<sub>2</sub>SO<sub>4</sub>). All electrolyte solutions were filtered with 0.45  $\mu$ m swinny filter (Gelman Nylon Acrodisc, 4438) prior to use.

#### **3.3.3.2 Preconditioning of the CE separation capillary**

Separation capillaries were preconditioned as described in Chapter 2 in Section

#### **2.3.3.3**

### **3.3.3.3 Preparation of IC eluent**

A sodium hydroxide gradient eluent was employed, utilising concentrations of 5 mM and 50 mM.

### **3.3.3.4 Preparation of stock solutions and standards**

A stock ( $1000\ \mu\text{g ml}^{-1}$ ) solution of each anion was prepared using deionised water, from which standards of known concentration were obtained, by dilution of the stock with deionised water.

### **3.3.3.5 Quantification of Analytes in the Adhesive Sample**

The quantification of analytes in the adhesive samples was carried out using both analyte spiking and the internal standard method. A range of standards, composed of different anion concentrations, were prepared and analysed by CE and IC in triplicate.

### **3.3.3.6 Adhesive sample preparation**

A 1 g quantity of the adhesive sample was dissolved in 20 ml chloroform and 10 ml of an aqueous internal standard was added. The CE internal standard employed was chloroacetic acid ( $\text{pH}=3.5$ ,  $50\ \mu\text{g ml}^{-1}$ ) and for IC was citric acid ( $\text{pH}=3$ ,  $1200\ \mu\text{g ml}^{-1}$ ). The solution was mixed thoroughly and left to stand to allow complete separation of the two layers (*i.e.* the aqueous and organic layers). The upper aqueous layer was removed and filtered through a  $0.45\ \mu\text{m}$  swinny filter (Gelman Nylon Acrodisc, 4438) prior to analysis by CE. Three replicate extractions and a blank were performed for each sample and the % recovery of each extraction was obtained.

### 3.4 RESULTS AND DISCUSSION

#### 3.4.1 Development of CE separation

As discussed in Section 3.1, the analysis of high mobility anions, such as chloride and sulphate, is widely reported employing chromate as the probe ion.<sup>[32,33]</sup> Whereas phthalate has a lower mobility and is therefore more suited to the analysis of low migrating anions, *e.g.* phosphate and fluoride.<sup>[15]</sup> In this work, the rapid simultaneous determination of high and low mobility anions, with improved run times when compared to IC was required. Chromate is a suitable probe ion and has been regularly utilised for the indirect UV determination of anions.<sup>[32,34]</sup>

Initially the optimisation of the separation of the five inorganic anions, in their order of migration, chloride, sulphate, nitrate, fluoride and phosphate was performed. The results are shown in Fig. 3.4. The separation efficiency values calculated were greatest at the lower voltage of -10 kV, and are plotted in Fig 3.5. However, the increased separation efficiency does not suggest an improved separation and at this low voltage the analysis time is longer. A separation voltage of -15 kV was employed and at this voltage, baseline resolution was obtained for all analytes, as shown in Fig 3.4.

The method shown in Fig. 3.4 was applied to the simultaneous separation of the five inorganic and also the acidic anions, formic acid, MSA, cyanoacetic acid, methacrylic acid and DEP and inorganic anions, Fig. 3.6.

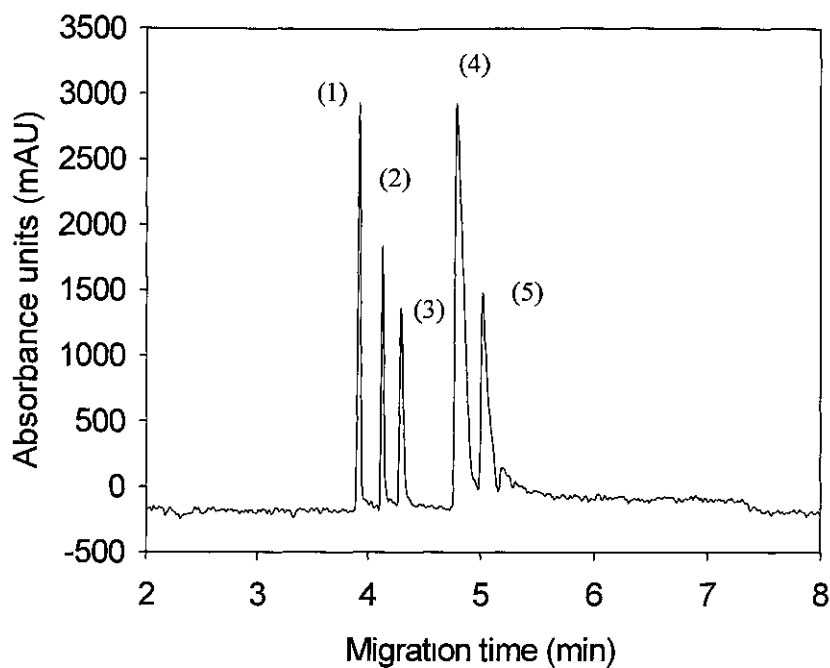


**Figure 3.4** Optimised CE separation for the analysis of the inorganic anions (1) chloride, (2) sulphate, (3) nitrate, (4) fluoride and (5) phosphate. All standards were  $100 \mu\text{g mL}^{-1}$ . Separation voltage  $-15 \text{ kV}$ , pressure injection  $0.5 \text{ psi} / 5 \text{ s}$ , with indirect UV detection at  $254 \text{ nm}$ . BGE:  $10 \text{ mM chromate}$ ,  $1 \text{ mM CTAB}$ ,  $\text{pH } 8.0$ . Effective capillary length  $0.50 \text{ m}$

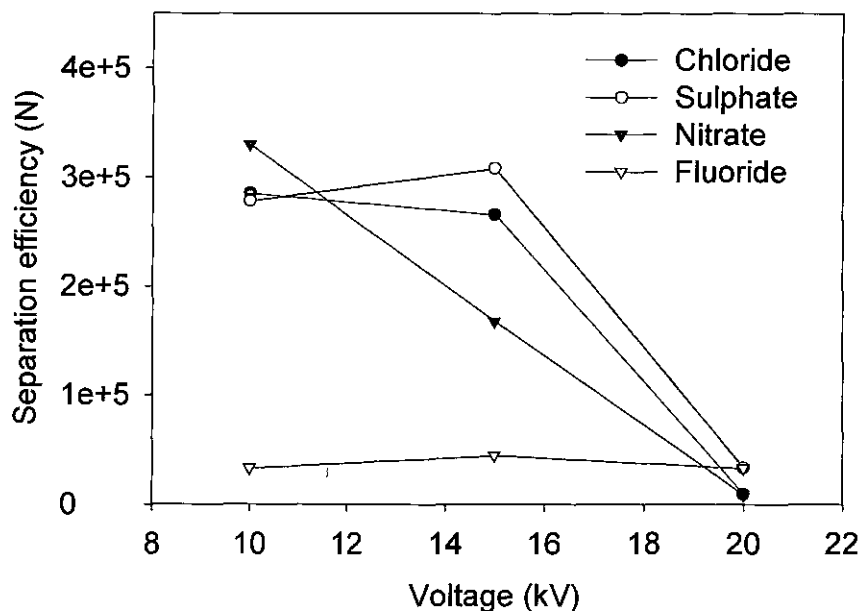


**Figure 3.5** Graphical illustrations of the separation efficiencies calculated for chloride, sulphate, nitrate and fluoride. All operating conditions as in Fig. 3.4

The order of migration was determined to be chloride, sulphate, nitrate, fluoride, formic acid, phosphate, MSA, cyanoacetic acid, methacrylic acid and DEP, as illustrated in Fig. 3.6. As fluoride and formic acid migrated at very similar times, a resolution value of 0.2 was achieved. In order to improve the resolution between these analytes, several separation parameters were altered, Section 3.4.2.

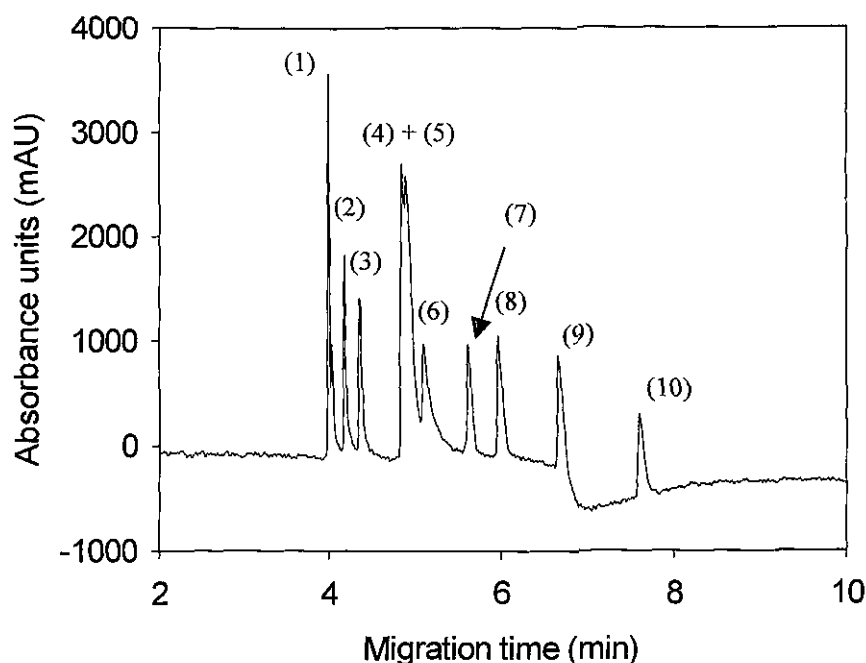


**Figure 3.6** CE separation for the analysis of (1) chloride, (2) sulphate, (3) nitrate, (4) fluoride, (5) formic acid, (6) phosphate, (7) MSA, (8) cyanoacetic acid, (9) methacrylic acid and (10) DEP. All standards were  $100 \mu\text{g ml}^{-1}$ . Separation voltage  $-15 \text{ kV}$ , pressure injection  $0.5 \text{ psi} / 5 \text{ s}$ , with indirect UV detection at  $254 \text{ nm}$ . BGE:  $10 \text{ mM}$  chromate,  $1 \text{ mM}$  CTAB,  $\text{pH } 8.0$ . Effective capillary length  $0.50 \text{ m}$

### 3.4.2 Optimisation of separation

#### 3.4.2.1 Effect of injection pressure and time

Samples were introduced by pressure injection. This mode of injection is more precise than electrokinetic injection, as electrokinetic sample introduction is dependent upon the EOF and also the electrophoretic mobilities of the analytes.<sup>[35]</sup> Whereas, for pressure injection the conditions are dependent upon the capillary dimensions, the viscosity of the electrolyte and the applied pressure and time.

The volume of sample injected onto the capillary was determined using the Hagen-Poiseuille Equation (Eqn. 3.1). With pressure injection, nanolitre (nl) levels of sample are introduced. The volumes injected for the various injection parameters are shown in Table 3.1.

$$V = \frac{\Delta P D^4 \pi t}{128 \eta L} \quad \text{Eqn. 3.1}$$

Where:	$V$	=	volume injected (nl)
	$\Delta P$	=	pressure drop (Pa)
	$D$	=	internal diameter of the capillary (cm)
	$t$	=	injection time (s)
	$\eta$	=	viscosity of the electrolyte (Pa s)
	$L$	=	total capillary length (cm)

At both the higher levels of pressure and time, the calculated volume of sample injected was larger; Table 3.1; however, the separation efficiencies calculated were less than those at the reduced values, and are plotted in Fig.'s 3.7 and 3.8. Therefore, samples were introduced by applying a pressure of 0.5 psi and 5 s.

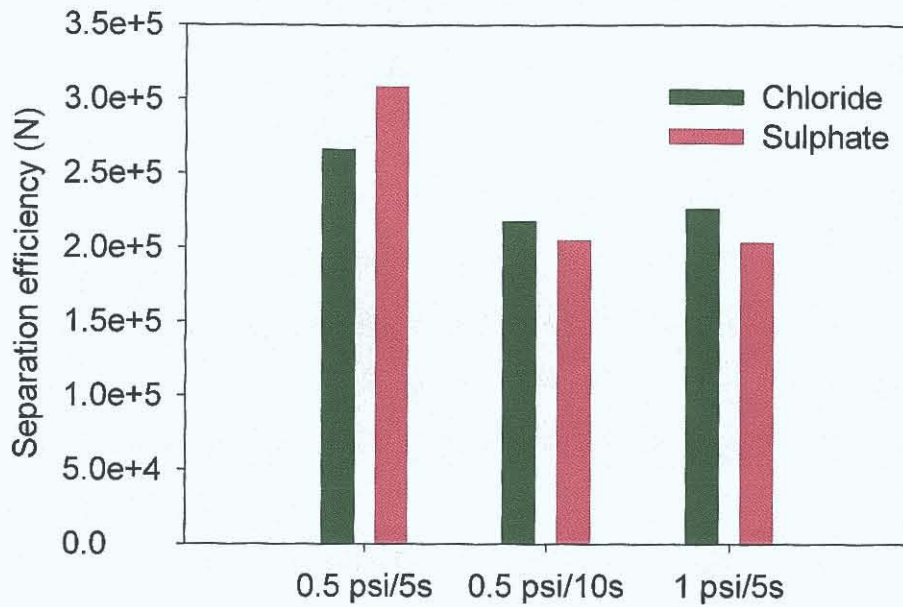


**Figure 3.7** Graphical illustrations of the changing separation efficiencies for chloride, and sulphate. Unless stated otherwise all operating conditions as in Fig. 3.4

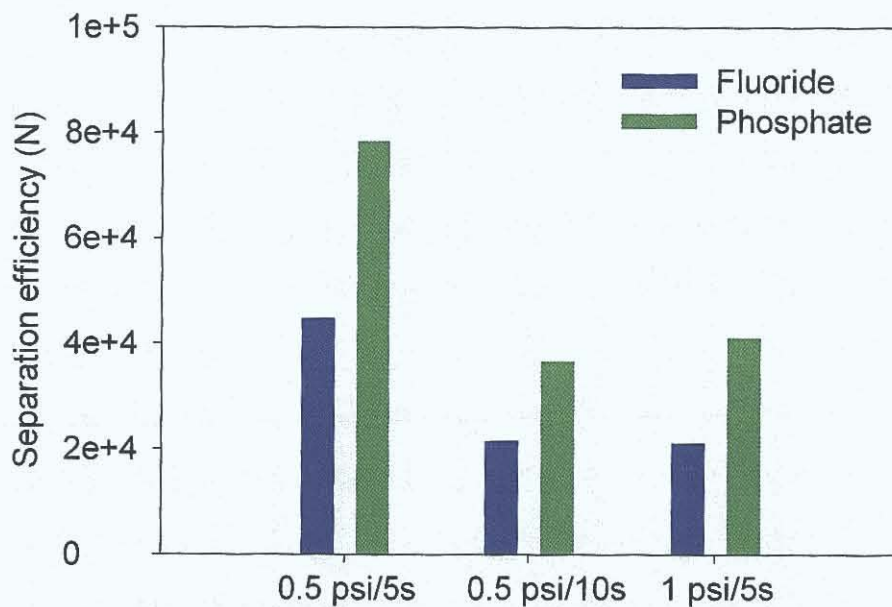


**Figure 3.8** Graphical illustrations of the changing separation efficiencies for fluoride and phosphate. Unless stated otherwise all operating conditions as in Fig. 3.4



**Table 3.1** Volume (nl) injected for varying times and pressure, where  $\eta = 0.88 \text{ Pa s}$  (water value at  $25^\circ \text{C}$ , where  $3.48 \times 10^{-3} \text{ Pa} = 0.5 \text{ psi}$  and  $6.89 \times 10^{-3} \text{ Pa} = 1 \text{ psi}$ , calculated using the Hagen-Poiseuille Equation

Injection pressure (Pa)	Injection time (s)	Volume injected (nl)
$3.48 \times 10^{-3}$	5	5.2
$6.89 \times 10^{-3}$	5	10.4
$3.48 \times 10^{-3}$	10	10.4

#### 3.4.2.2 Electrolyte pH

In CE separations, the EOF is advantageous; however, in many cases it needs to be controlled. Significant changes occur by altering the pH of the electrolyte. Any changes in pH will influence the effective charge and mobility and therefore selectivity of the analytes.<sup>[36]</sup>

The effect of varying the pH in the range 7.8-8.5 was studied. Precipitation of chromate electrolytes occurs in the presence of an EOF modifier, e.g. CTAB at pH levels less than 8.0.<sup>[37]</sup> This can result in inaccurate absorbance, but also results in the blockage of the capillary rendering it useless for further analysis. Increase of the pH, even by a factor of 0.2, can reverse the precipitation that occurs, and therefore render the chromate solution useful as a BGE.<sup>[37]</sup> At pH 7.8 the chromate precipitated out of solution and results were only obtained at pH values of 8.0, 8.2 and 8.5. A pH value of 8.5 was chosen as this resulted in the optimum resolution of all analytes, such as an increase from 1.33 at pH 8.0 to 1.89 at pH 8.5 between chloride and sulphate peaks. The

resolution calculated between fluoride and formic acid had also increased slightly, from 0.29 at pH 8.0 to 0.33 at pH 8.5.

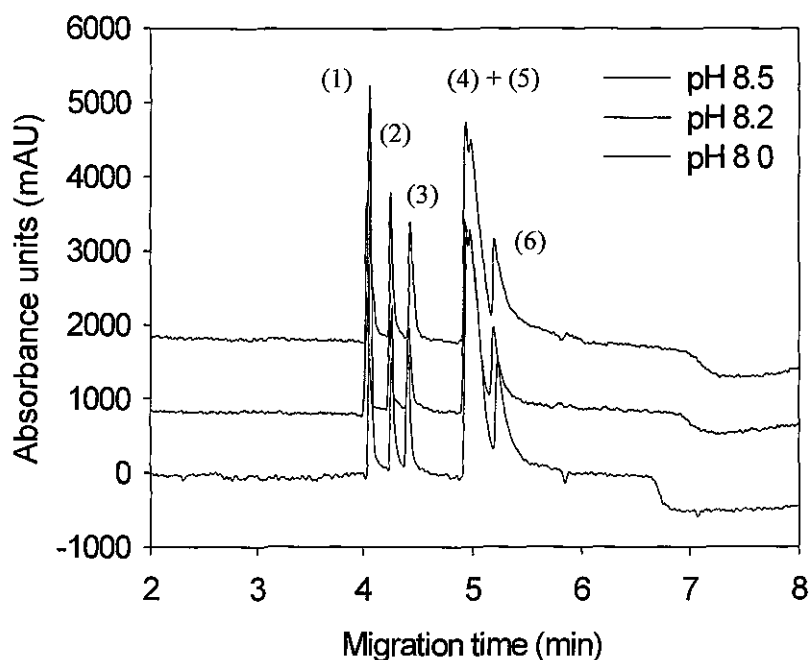


**Figure 3.9** Effect of pH on the separation of (1) chloride, (2) sulphate, (3) nitrate, (4) fluoride, (5) formic acid and (6) phosphate. All standards were  $100 \mu\text{g ml}^{-1}$ . Unless stated otherwise, all operating conditions as in Fig. 3.4, indirect UV detection at 254 nm. Effective capillary length 0.50 m. The pH 8.2 and 8.5 electropherograms are offset by 1000 and 2000 mAU respectively

### 3.4.2.3 Electrolyte concentration

The useful electrolyte concentration range is limited by a number of factors, namely the capillary length and diameter and the applied electric field.<sup>[38]</sup> A number of papers have been published describing the effect of chromate concentration on anion selectivity.<sup>[13,39,40]</sup>

In this work the chromate concentration was varied between 5 and 15 mM. At high concentrations of electrolyte high currents are generated and Joule heating results. Excessive Joule heating affects both the resolution and analyte stability. Joule heating may be limited by either reducing the internal diameter of the capillary, lengthening the capillary or decreasing the concentration of the electrolyte.<sup>[38]</sup> In order to determine the

maximum voltage at which Joule heating was not excessive and at which the separation could occur, Ohm's Law plots were performed for the different concentrations of chromate, such as that shown in Fig. 3.15. From the resolution and separation efficiencies ( $330,000 \text{ plates m}^{-1}$ ) calculated, 15 mM was chosen as the chromate concentration employed, as illustrated in Fig. 3.10 and Table 3.2.

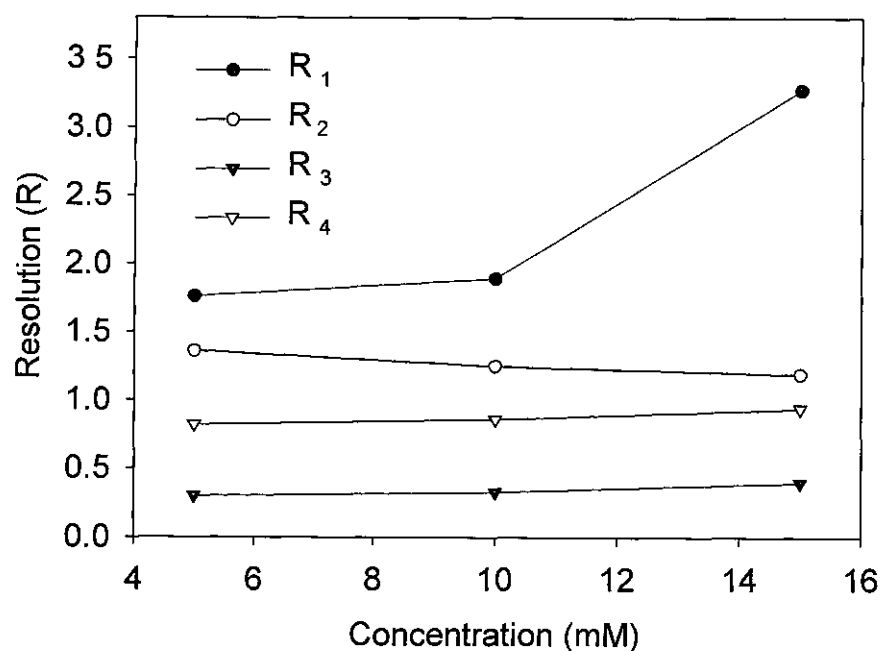


**Figure 3.10** Graphical illustrations of the changing resolutions calculated at various electrolyte concentrations, where  $R_1$  corresponds to the resolution calculated between chloride and sulphate,  $R_2$  is the resolution calculated between sulphate and nitrate,  $R_3$  is the resolution calculated between fluoride and formic acid and  $R_4$  is the resolution calculated between formic acid and phosphate. Unless stated otherwise all operating conditions as in Fig. 3.4, and BGE at pH 8.5 with 1 mM CTAB

**Table 3.2** Separation efficiencies ( $N/m$ ) calculated at various chromate concentrations and % Relative Standard Deviation values (%RSD) for migration time, where  $n = 3$  and total length = 0.58m. All operating conditions as in Fig. 3.4

Anion	5 mM Chromate	% RSD	15 mM Chromate	% RSD
Chloride	226,504	17	330,069	0.94
Sulphate	196,580	15.3	305,255	4.8
Nitrate	62,016	6.6	168,849	6.2

At the higher concentration of chromate, the %RSD values calculated were found to be less than those at the lower concentration of 5 mM, as shown in Table 3.2. Also, the resolution values had increased slightly for the higher concentration, due to the increased current generated. Any differences in migration times were due to changes in EOF caused by the variation of the electrolyte concentration.

#### 3.4.4.4 Electrolyte surfactant composition and concentration

In order to reverse the EOF, surfactants, such as TTAB, DDAB and CTAB, were added to the electrolyte. A combination of TTAB and DDAB was employed; <sup>[41,42]</sup> however, the system peak induced by bromide interfered with the sulphate determination and nitrate and fluoride were co-migrating. The results from this investigation are shown in Fig.'s 3.11 and 3.12.

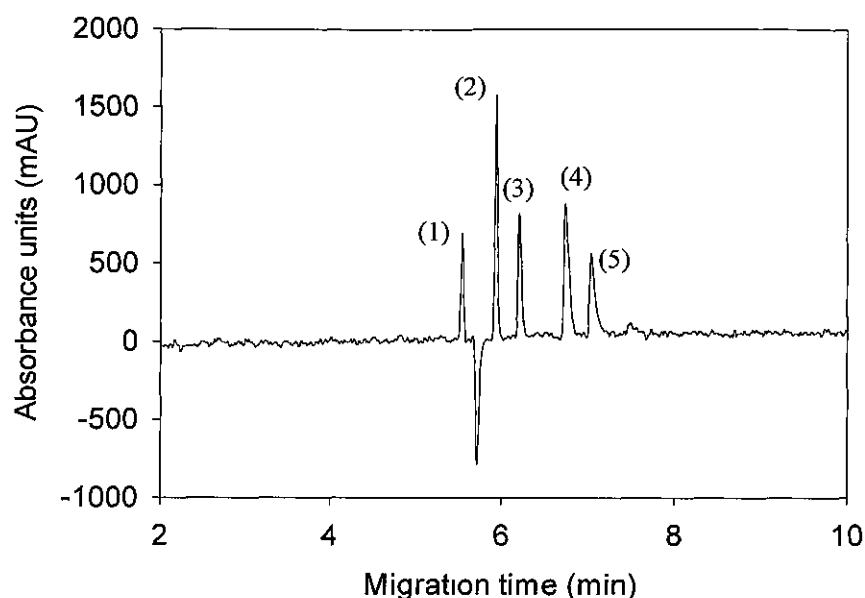


**Figure 3.11** Effect of surfactant composition on the separation of (1) chloride, (2) sulphate, (3) nitrate, (4) fluoride and (5) phosphate. All standards were  $100 \mu\text{g ml}^{-1}$ . Separation voltage  $-10 \text{ kV}$ , pressure injection  $0.5 \text{ psi} / 5 \text{ s}$ , with indirect UV detection at  $254 \text{ nm}$ . BGE:  $5 \text{ mM}$  chromate,  $2.35 \text{ mM}$  TTAB,  $2.65 \text{ mM}$  DDAB,  $\text{pH } 8.5$ . Effective capillary length  $0.50 \text{ m}$

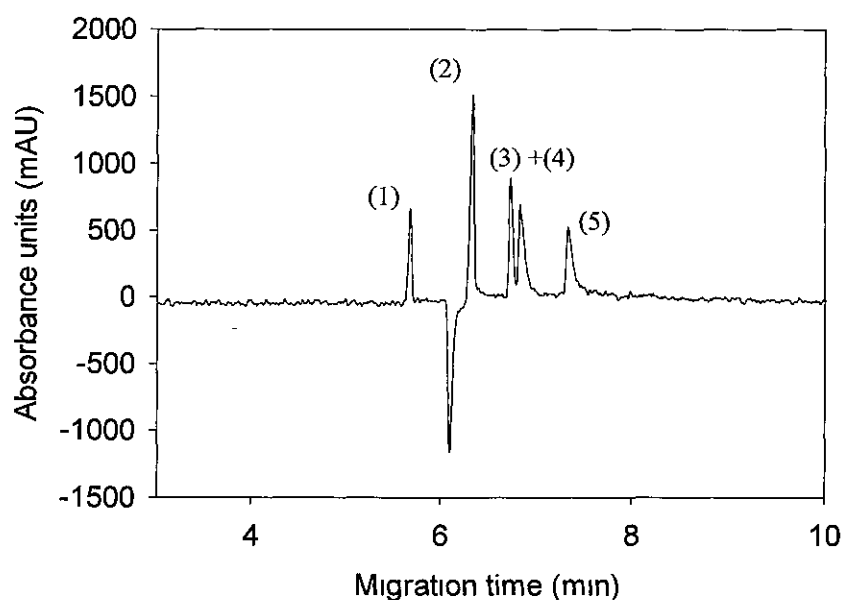


**Figure 3.12** Effect of surfactant composition on the separation of (1) chloride, (2) sulphate, (3) nitrate, (4) fluoride and (5) phosphate. All standards were  $100 \mu\text{g ml}^{-1}$ . Separation voltage  $-10 \text{ kV}$ , pressure injection  $0.5 \text{ psi} / 5 \text{ s}$ , with indirect UV detection at  $254 \text{ nm}$ . BGE:  $5 \text{ mM}$  chromate,  $5 \text{ mM}$  TTAB,  $1 \text{ mM}$  DDAB,  $\text{pH } 9.0$ . Effective capillary length  $0.50 \text{ m}$

A bromide peak was also expected from the surfactant CTAB and in order to determine this, bromide and CTAB were injected individually. A peak from bromide was observed at 4.1 min., and a bromide peak was detected at the same migration time when CTAB was injected. When the electrolyte containing CTAB and chromate at pH 8.5 was injected, no bromide peak was observed. Ten successive injections of the electrolyte also showed no peak for bromide. In order to investigate this further, an electrolyte containing a lower concentration of chromate (10 mM) with CTAB, was injected and a bromide peak at 4.1 min. was detected in the analysis of anions, as shown in Fig. 3.6. Therefore, it was clear from these investigations, that the appearance of a bromide peak was dependent upon the concentration of the electrolyte. As a result, it was determined that this surfactant (CTAB) was a suitable choice for the analysis of the anions present in cyanoacrylate adhesives as no bromide interference was observed when the electrolyte containing 15 mM chromate was employed.

Below its critical micelle concentration (CMC), CTAB adheres to the wall of the capillary through ionic interactions and therefore changes the EOF. At concentrations above the CMC, the separation mechanism is altered and results in micellar electrokinetic chromatography (MEKC). In a direct comparison of CZE with MEKC, the surfactant was added at concentrations above and below its CMC, as shown in Fig. 3.13. The CMC of CTAB is 1.3 mM.<sup>[36]</sup> At the lower concentration of 1 mM both sulphate and nitrate and fluoride and phosphate co-migrated, as illustrated in Fig. 3.13. At 1.5 mM CTAB, baseline resolution was not achieved between either fluoride and formic acid and formic acid and phosphate. From these investigations, a surfactant concentration of 1 mM resulted in the optimum separation.

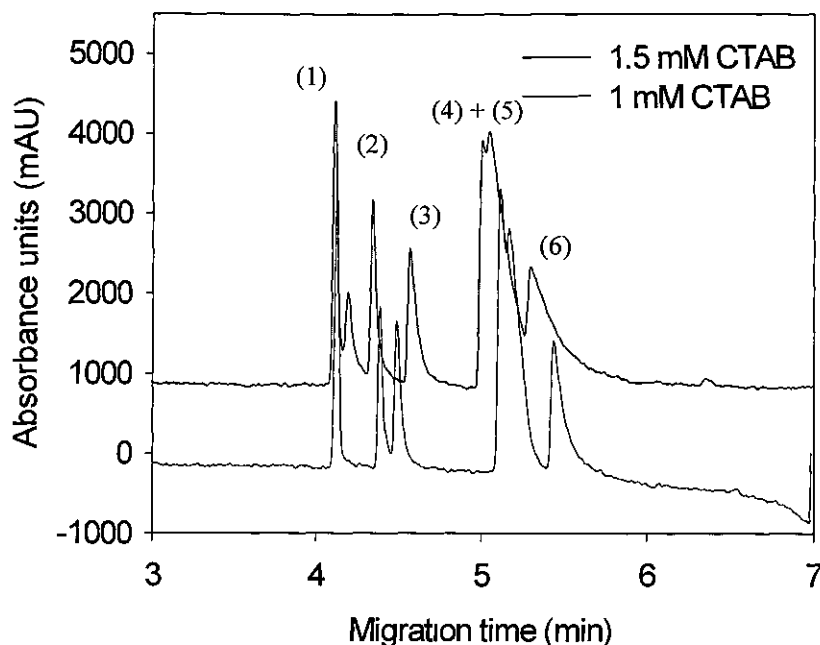


**Figure 3.13** Effect of CTAB concentration on the separation of (1) chloride, (2) sulphate, (3) nitrate, (4) fluoride, (5) formic acid and (6) phosphate. All standards were  $100 \mu\text{g ml}^{-1}$ . Unless stated otherwise, all operating conditions as in Fig. 3.4, with indirect UV detection at 254 nm. Effective capillary length 0.50 m. BGE. 15 mM chromate at pH 8.5. The 1.5 mM CTAB electropherogram is offset by 1000 mAU

#### 3.4.2.5 Development of chromate-based buffered electrolytes

As previously stated in Section 3.4.2.2, the EOF is advantageous in CE separations; however, in most cases it needs to be controlled. Significant changes occur by altering the pH of the electrolyte. One method of controlling the pH of the electrolyte is the addition of a buffer to the electrolyte system. Two chromate-based buffered electrolyte systems were investigated, namely TAPS and Tris, and results are illustrated in Fig. 3.14.

In the study with a TAPS buffer, ( $\text{pK}_a$  8.51) system peaks were obtained (6.4 min., and 8.2 min.) during the analysis, which interfered with the analytes of interest. When buffering chromate with Tris ( $\text{pK}_a$  8.06) the co-migration of sulphate and nitrate occurred, and at lower voltages (-8 kV), the separation of these anions was not achieved, Fig. 3.14. There are alternative methods for the buffering of electrolytes in

indirect detection, *e.g.* the incorporation of a lower mobility probe ion or a counterion in the BGE. However, there are disadvantages too in the application of these approaches, such as the introduction of system peaks and poor peak shape.<sup>[37]</sup> Therefore, as the buffering of chromate resulted in either the development of system peaks or additional co-migrating peaks, an unbuffered electrolyte was employed. The pH of the electrolyte was adjusted to 8.5 with 1 mM H<sub>2</sub>SO<sub>4</sub>. In order to prevent any instability of the electrolyte, the latter was changed regularly during analysis (after six separations), and most importantly the electrolyte was prepared daily to prevent changes in pH. Any changes in migration times were due to differences in EOF caused by the variation of the buffer in the electrolyte.

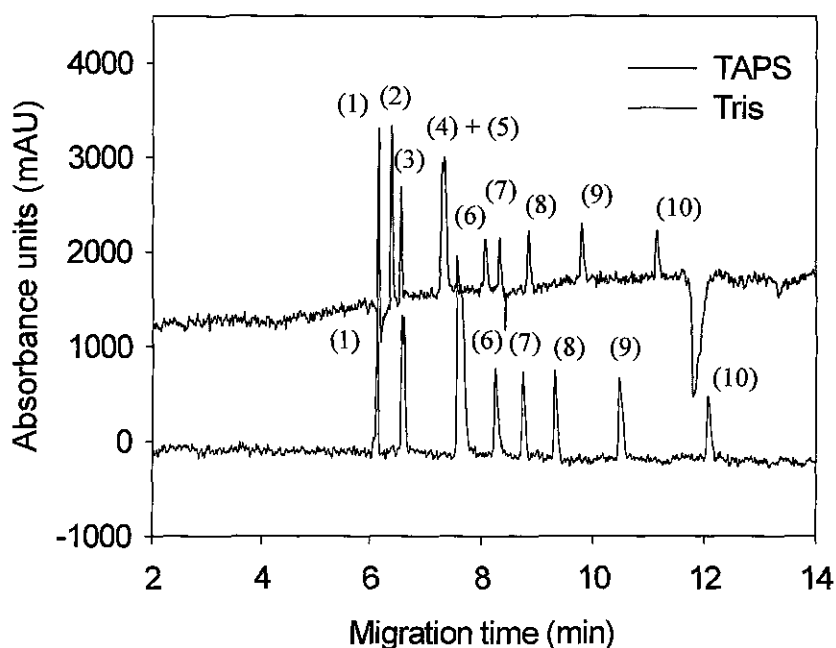


**Figure 3.14** An investigation of chromate-based electrolytes buffered with either 0.01M TAPS or 0.05 M Tris for the separation of (1) chloride, (2) sulphate, (3) nitrate, (4) fluoride, (5) formic acid, (6) phosphate, (7) MSA, (8) cyanoacetic acid, (9) methacrylic acid and (10) DEP. All standards were 100  $\mu\text{g mL}^{-1}$ . Separation voltage  $-10\text{ kV}$ , pressure injection 0.5 psi / 5 s, with indirect UV detection at 254 nm. BGE: 15 mM chromate, 1 mM CTAB at pH 8.5. Effective capillary length 0.50 m



### 3.4.2.6 Effect of separation voltage

The optimum separation voltage for the analysis of the inorganic and acidic anions, was determined using an Ohm's Law plot, as described by Nelson *et al.*, with the electrolyte conditions of 15 mM chromate, 1 mM CTAB at a pH value of 8.5, as shown in Fig. 3.15.<sup>[43]</sup>

From the Ohm's Law plot it was evident that a linear relationship between current and voltage existed and that the analysis could be performed at separation voltages as high as -27.5 kV. However, at this high voltage an increase in EOF and ion mobility occurred which may lead to band broadening.

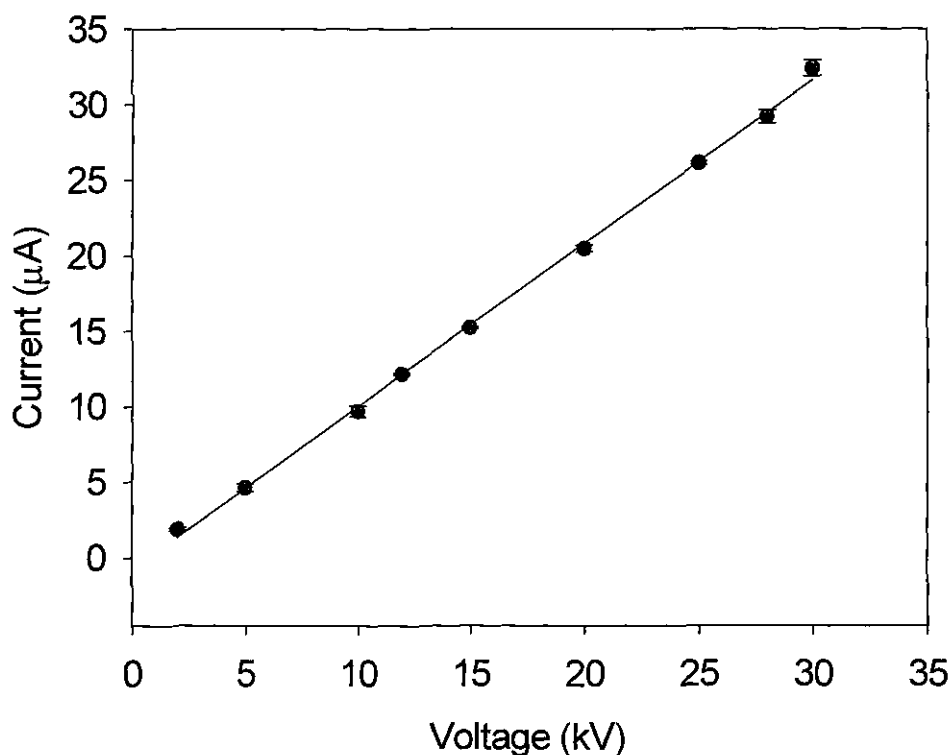


**Figure 3.15** Ohm's Law plot for 15 mM chromate, 1 mM CTAB and pH 8.5

The separation voltage of -10 kV was employed, from the resolution and separation efficiency values calculated, as plotted in Fig.'s 3.16 and 3.17. At -6 kV, greater resolution between fluoride and formic acid was obtained; however, the run time

was excessively long and separation voltage of  $-10$  kV was employed for subsequent optimisation, Fig. 3.23. Also, at  $-6$  kV, the resolution calculated between chloride and sulphate ( $R_1$ ) was reduced. This was not expected and was probably due to tailing of the chloride peak.

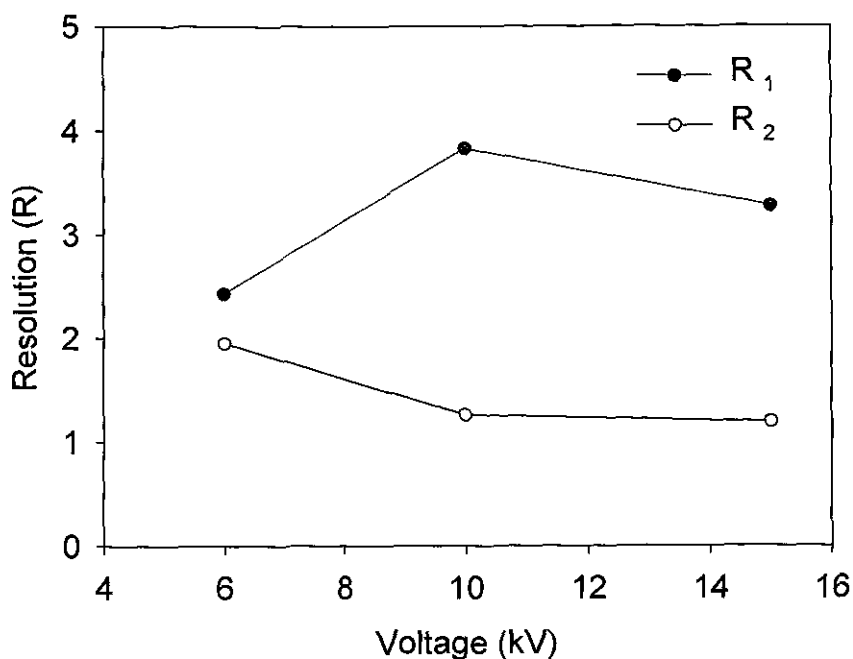


**Figure 3.16** Graphical illustrations of the resolution values calculated at various separation voltages Resolution assignments as in Fig. 3.10 Unless stated otherwise, all operating conditions as in Fig. 3.4 and BGE: 15 mM chromate at pH 8.5

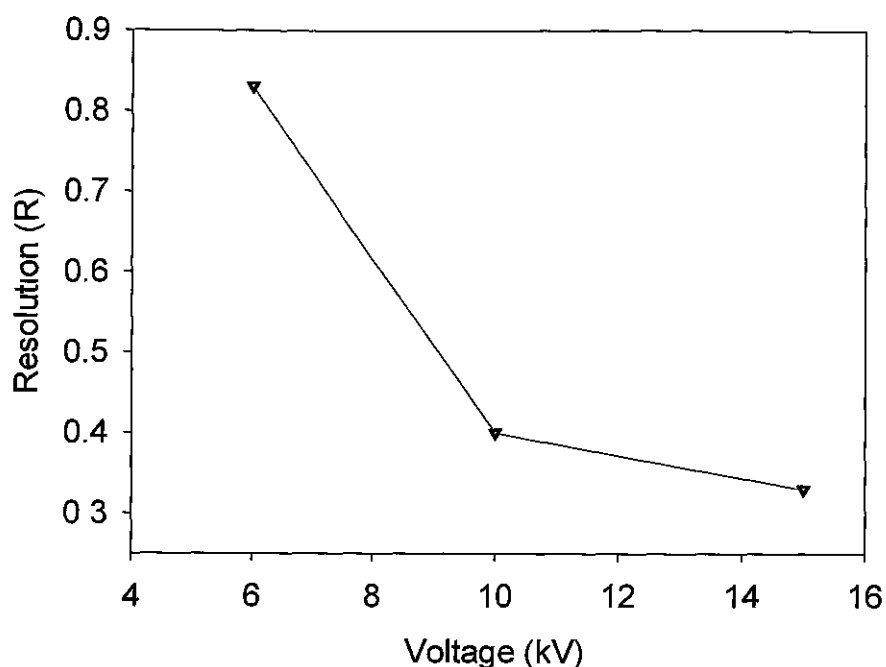


**Figure 3.17** Graphical illustration of the variation with voltage of resolution calculated between fluoride and formic acid. Unless stated otherwise, all operating conditions as in Fig. 3.4 and BGE. 15 mM chromate at pH 8.5

#### 3.4.2.7 Effect of separation temperature

It is possible to control the temperature at which a separation occurs on all commercial instruments. At elevated temperatures, the pH and viscosity of the electrolyte will change. If the viscosity of the electrolyte has changed this may effectively lead to errors in quantification of the analytes due to variable injection volumes. Also, at high temperatures the conductivity of the electrolyte increases, which results in a rise in current and a further increase in temperature.<sup>[35]</sup>

An increase in temperature may also result in a reduction of the total analysis times and may lead to a decrease in resolution, as shown in Fig.'s 3.18-3.20.

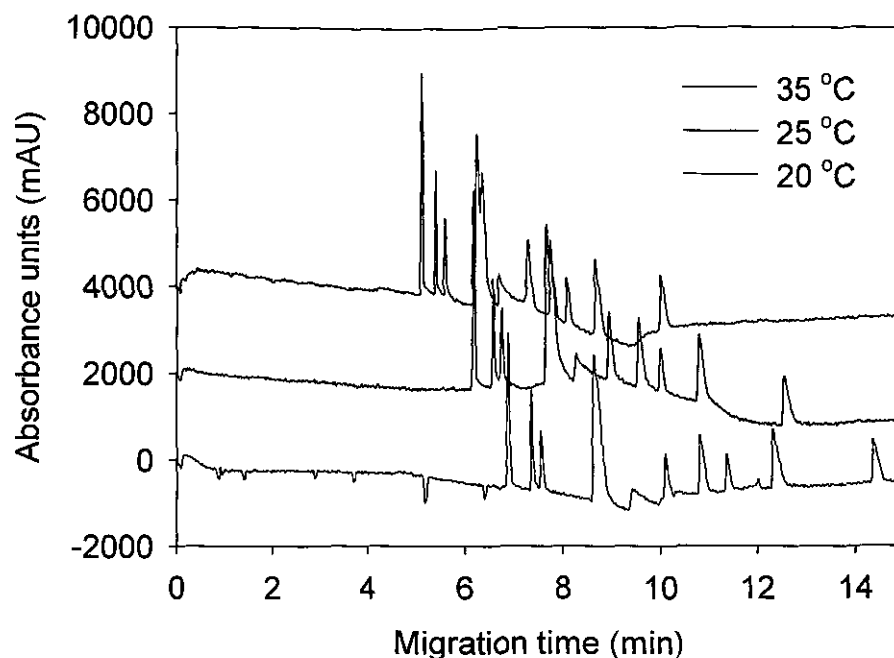


**Figure 3.18** Effect of operating temperature on the separation of chloride, sulphate, nitrate, fluoride, formic acid, phosphate, MSA, cyanoacetic acid, chloroacetic acid, methacrylic acid and DEP at different separation temperatures. All standards were  $50 \mu\text{g ml}^{-1}$ . Separation voltage  $-10 \text{ kV}$ , pressure injection  $0.5 \text{ psi} / 5 \text{ s}$  with indirect UV detection at  $254 \text{ nm}$ . BGE.  $15 \text{ mM}$  chromate,  $1 \text{ mM}$  CTAB at  $\text{pH } 8.5$ . Effective capillary length  $0.50 \text{ m}$ . The  $25^\circ\text{C}$  and  $35^\circ\text{C}$  electropherograms are offset by  $1000$  and  $2000 \text{ mAU}$  respectively

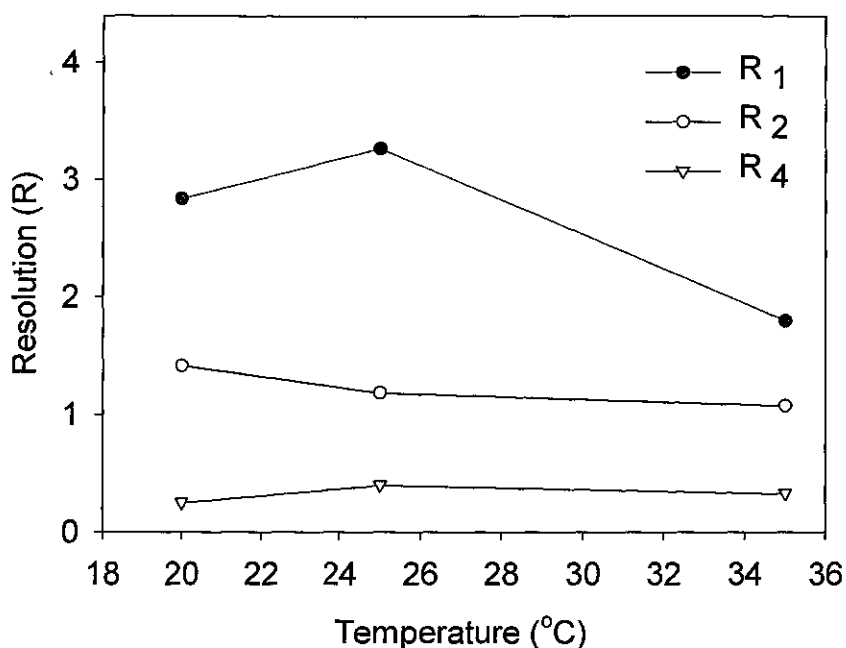


**Figure 3.19** Graphical illustration of the changing resolution values at various separation temperatures. Resolution assignments as in Fig. 3.10. Unless stated otherwise, all operating conditions as in Fig. 3.18

From Fig. 3.19, it was evident that there was a significant decrease in resolution between sulphate and nitrate ( $R_2$ ) from 25 °C to 35 °C. The resolution was greatest between sulphate and nitrate at 20 °C; however, this increase at this separation temperature was only evident for these analyte anions, as illustrated in Fig.'s 3.19 and 3.20.

The electrophoretic mobility ( $\mu_e$ ) of a charged species is dependent upon the mobility of the analyte and the EOF. It was calculated, at different separation temperatures, as shown in Fig.'s 3.21 and 3.22, using Equation 3.2. It should be noted that  $\mu_e$  will be negative for anions as the capillary electrophoresis system is under reverse polarity control, *i.e.*, the detector is at the anode and the analytes migrate against the EOF. It was evident that from 20 °C to 35 °C there was a significant increase in the mobilities calculated for chloride, sulphate, fluoride and formic acid, as plotted in Fig.'s 3.21 and 3.22 at 25 °C.

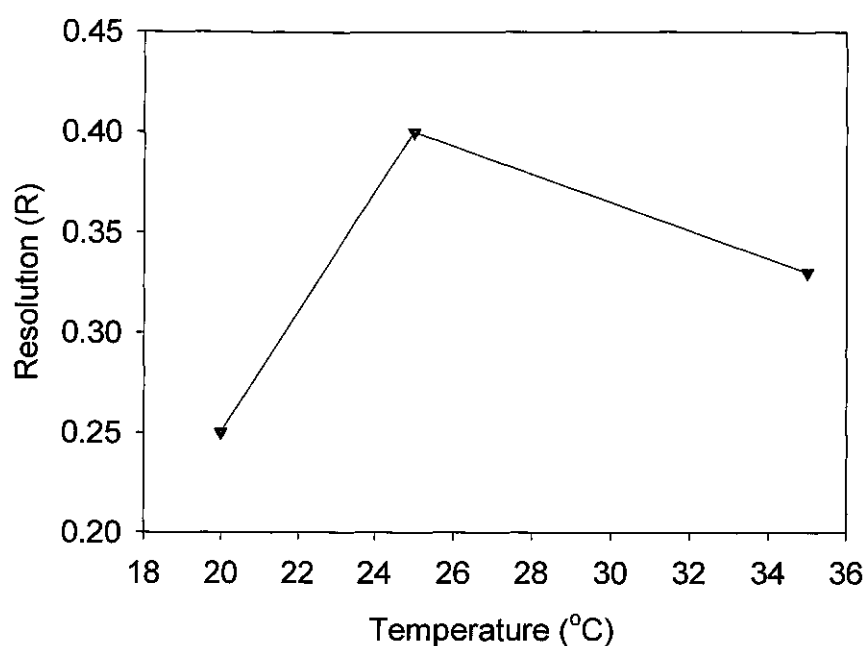


**Figure 3.20** Graphical illustration of the changing resolution values between fluoride and formic acid at various separation temperatures. Unless stated otherwise, all operating conditions as in Fig 3.18

$$\mu_a = \frac{1}{tE} = \frac{lL}{tV} \quad \text{Eqn. 3.2}$$

Where:

$\mu_a$	=	$\mu_e + \mu_{EOF}$
$t$	=	migration time (s)
$E$	=	electric field
$l$	=	effective capillary length (cm)
$L$	=	total capillary length (cm)
$V$	=	applied voltage (V)

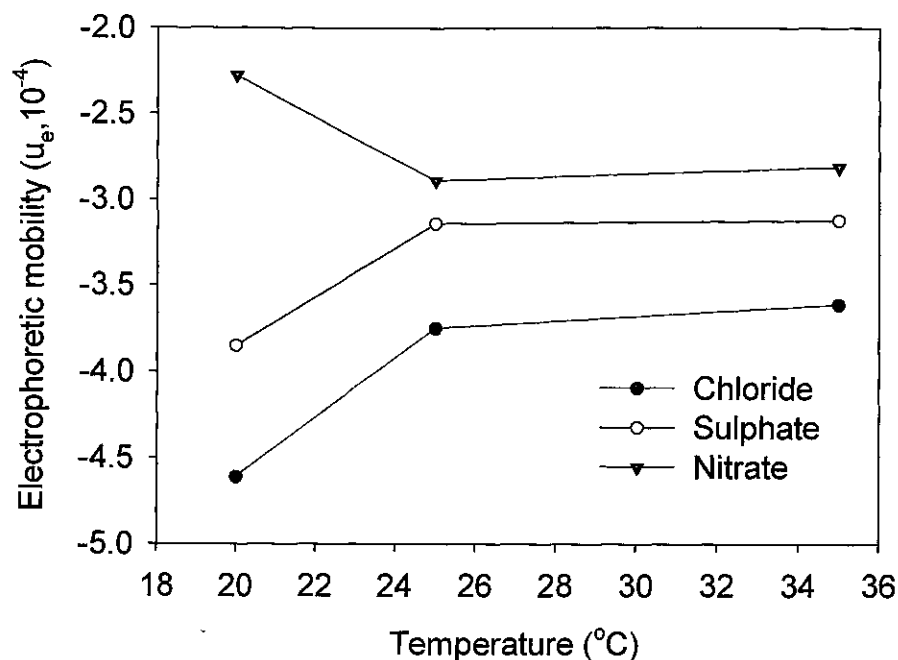


**Figure 3.21** Electrophoretic mobilities ( $\mu_e, \text{cm}^2 / \text{Vs}$ ) calculated for chloride, sulphate and nitrate at different separation voltages, where  $\mu_{\text{EOF}}$  = electrophoretic mobility of the internal standard. Unless stated otherwise, all operating conditions as in Fig. 3.18

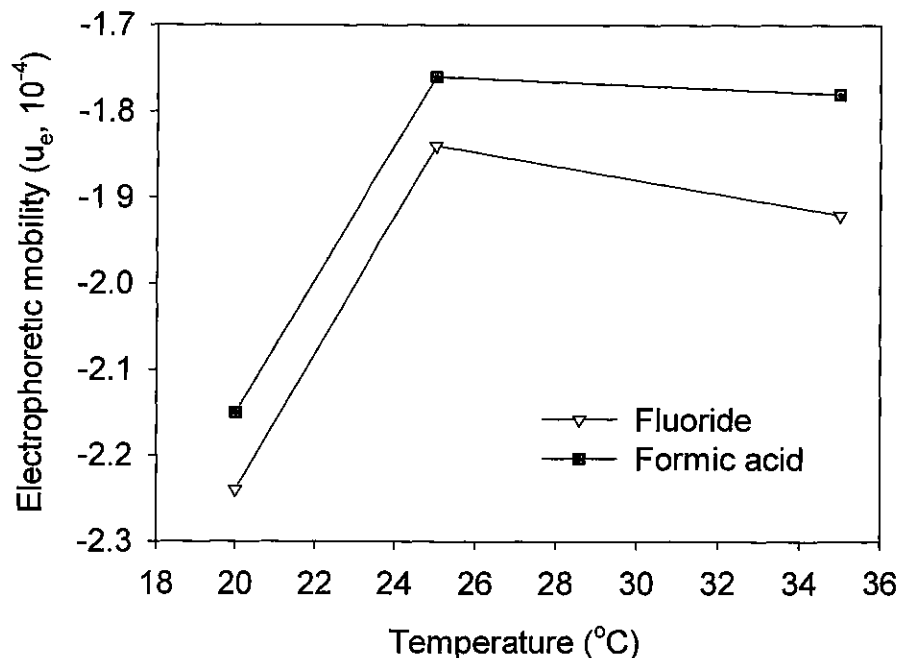


**Figure 3.22** Electrophoretic mobilities ( $\mu_e, \text{cm}^2 / \text{Vs}$ ) calculated for fluoride and formic acid at different separation voltages, where  $\mu_{\text{EOF}}$  = electrophoretic mobility of the internal standard. Unless stated otherwise, all operating conditions as in Fig. 3.18

The mobility calculated for nitrate was greatest at 20 °C; however, taking into account the increased resolutions obtained and the increase in mobility of all the other anions at 25 °C, this was employed as the operating temperature. The effective mobilities calculated also confirmed the order of migration of the analytes under investigation.

### 3.4.3 Optimum separation conditions

From the investigation carried out for the separation of the acidic and inorganic anions the optimum conditions determined were 15 mM chromate, 1 mM CTAB, at pH 8.5. All separations were performed at -10 kV separation voltage, a pressure injection of 0.5 psi/ 5 s, a separation temperature of 25 °C with indirect detection of 254 nm, as shown in Fig. 3.23. Following optimisation of the separation, the quantification of the analytes was performed using the internal standard method, Section 3.4.4.

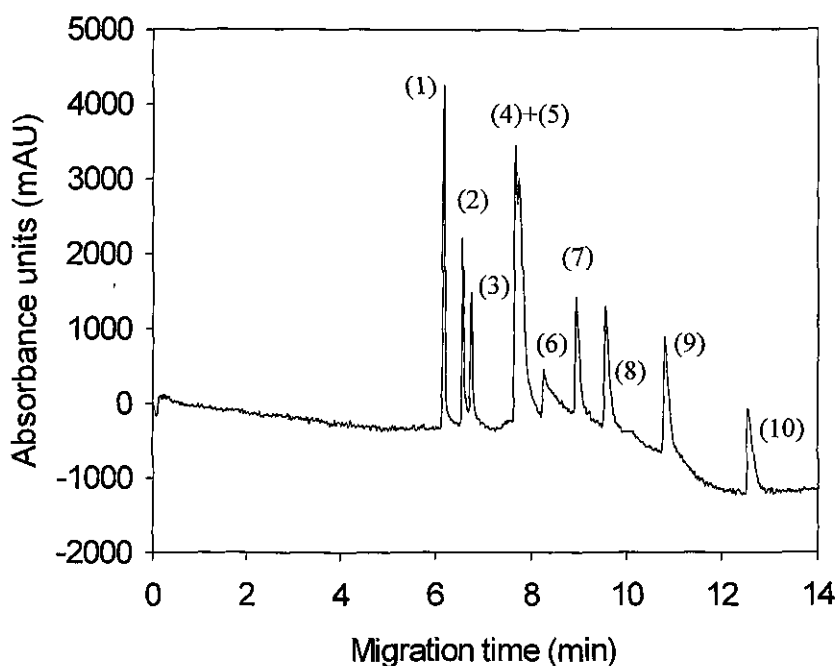


**Figure 3.23** Optimum CE separation for the analysis of (1) chloride, (2) sulphate, (3) nitrate, (4) fluoride, (5) formic acid, (6) phosphate, (7) MSA, (8) cyanoacetic acid, (9) methacrylic acid and (10) DEP. All standards were 100  $\mu\text{g mL}^{-1}$ . Separation voltage -10 kV, pressure injection 0.5 psi/5 s, with indirect detection 254 nm. BGE 15 mM chromate, 1 mM CTAB, pH 8.5. Effective capillary length 0.50 m.



### 3.4.4 Quantification of the Analytes

#### 3.4.1.1 Internal Standard Method

The quantification of the anions in the samples was performed using the internal standard method. Peak identification was performed by peak spiking. The use of an internal standard involves adding a fixed amount of a known substance to all standard samples before analysis. The internal standard must be similar to the analyte, to ensure that it suffers similar losses during the process. It also must be completely resolved from the other components present in the sample. When using an internal standard, quantification is achieved by taking the ratio of the analyte peak areas to internal standard peak areas and plotting this against standard analyte concentration. Taking the ratio compensates for any variation in conditions as both the analyte and internal standard will be similarly affected. The use of an internal standard eliminates all injection volume-related sources of error and results in improved precision.<sup>[44]</sup>

Previously, oxalic acid was employed as the internal standard; <sup>[2]</sup> however, as this co-migrated with nitrate an alternative internal standard was required. Based on  $pK_a$  values, chloroacetic acid was utilised as the internal standard, Table 3.3. The order of migration is also illustrated in Table 3.3, and from this it was found that as the molecular weight is increased, so too is the migration time. The charge on the anion also affects the migration time. Sulphate and chloroacetic acid have similar molecular weights; however, sulphate migrates over 2 min. earlier due to its charge of  $-2$ . Using chloroacetic acid, calibration plots of all ten anions were obtained. The calibration plots for chloride and DEP are shown in Fig. 3.24. From the  $R^2$  values it was evident that the inorganic anion, chloride, was more stable than the acidic anion, DEP, as illustrated in Fig. 3.24. All ten anions showed a linear response with increasing concentration, *i.e.*, all  $R^2$  values were greater than 0.97, with the exception of DEP. Therefore this method was suitable for their quantification. The  $R^2$  value for DEP at 0.9576 was significantly lower than the  $R^2$  values for chloride and sulphate. The purity level of DEP employed in these investigations was 98%, and in order to improve its  $R^2$  value a higher grade was employed (99%). However, this increased level of purity did not significantly enhance either the separation or its linearity. The LOD's and LOQ's for all analytes were obtained at a signal to noise ratio of 3:1, as shown in Table 3.7.

**Table 3.3** The migration order,  $pK_a$  values, charge and molecular weight for all 11 analytes analysed<sup>[45]</sup>

Migration order	$pK_a$	Charge	Molecular Weight ( $g \cdot mol^{-1}$ )
Chloride	2.86	-1	35.5
Sulphate	2-4	-2	96
Nitrate	2-4	-1	62
Fluoride	2.66	-1	19
Formic acid	3.75	-1	46
Phosphate	6.82	-3	94
MSA	1.92	-1	80
Cyanoacetic acid	2.47	-1	85
Chloroacetic acid	2.87	-1	94.5
Methacrylic acid	4.66	-1	76
DEP	6.8-12.5	-1	153

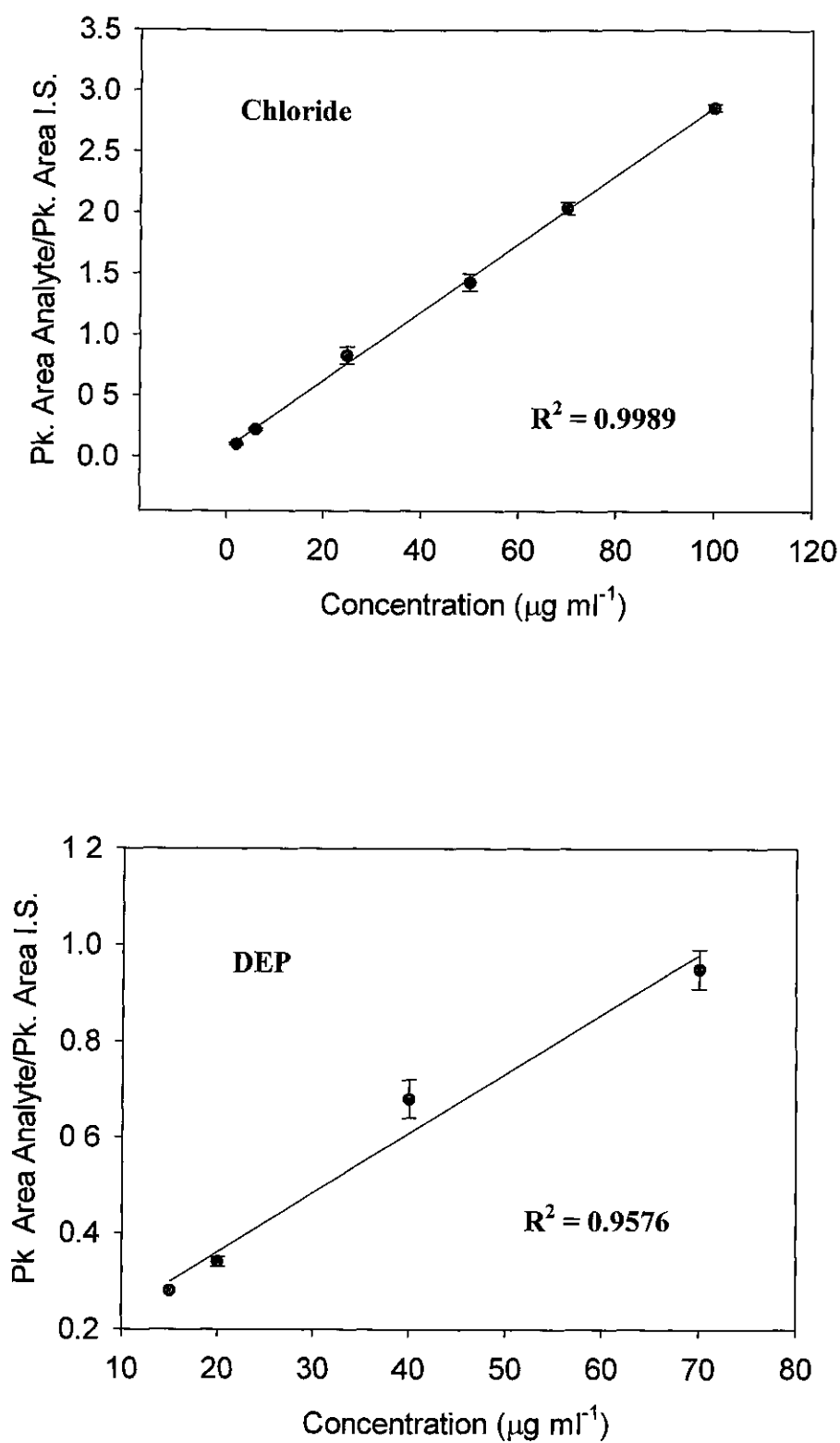


**Figure 3.24** Calibration plots for chloride (2-100  $\mu\text{g ml}^{-1}$ ,  $R^2$  0.9989) and DEP (15-70  $\mu\text{g ml}^{-1}$ ,  $R^2$  0.9576) with chloroacetic acid (50  $\mu\text{g ml}^{-1}$ ) as the internal standard

An electropherogram of the separation of all analytes with the internal standard, using the optimised separation conditions is shown in Fig. 3.25.

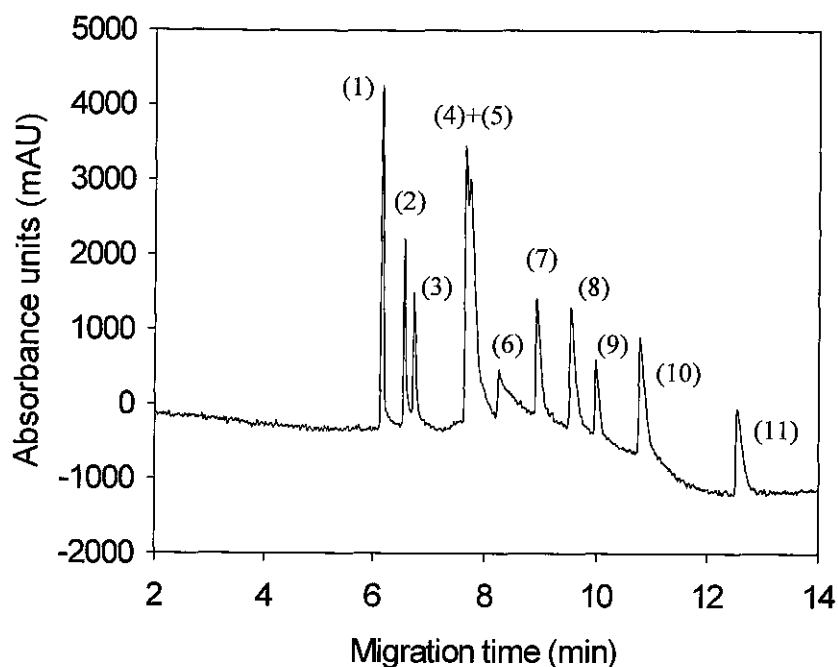


**Figure 3.25** Optimised CE separation, with internal standard, for the analysis of (1) chloride, (2) sulphate, (3) nitrate, (4) fluoride, (5) formic acid, (6) phosphate, (7) MSA, (8) cyanoacetic acid, (9) chloroacetic acid, internal standard ( $50 \mu\text{g mL}^{-1}$ ), (10) methacrylic acid and (11) DEP. All standards were  $100 \mu\text{g mL}^{-1}$ . Separation voltage  $-10 \text{ kV}$ , pressure injection  $0.5 \text{ psi} / 5 \text{ s}$  with indirect UV detection at  $254 \text{ nm}$ . BGE:  $15 \text{ mM}$  chromate,  $1 \text{ mM}$  CTAB at  $\text{pH } 8.5$ . Separation temperature  $25^\circ\text{C}$ . Effective capillary length  $0.50 \text{ m}$ .

### 3.4.5 Limits of detection (LOD) and quantification (LOQ)

The limit of detection (LOD) is described as the minimum mass or concentration of an analyte that can be detected at a suitable signal to noise ratio. The limit of quantification (LOQ) is defined as the lowest level at which an acceptable level of accuracy is achieved for the measured analyte.<sup>[38]</sup>

The LOD's and LOQ's were calculated from the blank plus three times the standard deviation and the blank plus ten times the standard deviation respectively, Table 3.7 in Section 3.4.7.

The CE method developed was applied to the simultaneous determination of these inorganic and acidic anions, which may be present at different stages of the ethyl cyanoacrylate production process, as discussed in Section 3.4.6.

### **3.4.6 Application of CE method to Cyanoacrylate adhesives**

The aim of the CE method development was ultimately the application to the determination of inorganic and acidic anions that may be present during the production process of cyanoacrylate adhesives. Sample preparation was performed using liquid-liquid extraction (LLE), which is based upon the transfer of solutes from one liquid phase, the aqueous phase, to another liquid phase, organic phase. The % recovery of chloroacetic acid for each sample analysis in the region 80-90%, were obtained, as illustrated in Table 3.4.

The aqueous phase employed was the internal standard, chloroacetic acid. The pH of the aqueous phase will affect the extraction. However, the pH employed was 3.5, which was above its  $pK_a$  of 2.87.<sup>[45]</sup> At this pH, chloroacetic acid was present, and therefore, the % recoveries were not affected by the pH. An additional pH of 6.5 was also investigated to establish if pH affected the % recovery. As expected no change in % recovery was obtained at pH 6.5 compared with pH 3.5. Chloroform was employed as the organic phase, as this enabled the full dissolution of the adhesive sample.

Samples from the ethyl cyanoacrylate process, at different stages of production were analysed, as shown in Table 3.5. Samples were taken from the crude monomer, which on distillation produces the pure monomer and the residue remaining from the distillation was also analysed, as illustrated in Fig. 3.1. All samples investigated were from the same batch.

**Table 3.4** The % recoveries obtained for analysis of ethyl cyanoacrylate adhesive samples. Operating conditions as in Fig. 3.25<sup>[1]</sup>

Sample	% Recovery of chloroacetic acid	% RSD (n=3)
Crude monomer	88.3	4.7
Distillation residue	84.7	1.3
Pure monomer	89.0	1.4

**Table 3.5** Samples analysed for the ethyl cyanoacrylate production process

Production Process	Sample name
Ethyl Cyanoacrylate	<ul style="list-style-type: none"> <li>• Crude monomer</li> <li>• Distillation residue</li> <li>• Pure monomer</li> </ul>

### 3.4.6.1 Ethyl Cyanoacrylate Adhesive Samples

As described in Section 3.4.6, the samples were analysed from three different stages of the production process, *i.e.*, a crude monomer sample, a distillation residue sample and a pure monomer sample. The distillation of the crude monomer is a purification process that removes any impurities and results in the production of the pure monomer. The three electropherograms in Fig. 3.26 illustrate the difference both quantitatively and qualitatively between the three stages of the production process.

It was expected that the crude monomer sample would contain higher quantities of the analytes, as this stage is prior to the purification step. The pure monomer sample, as the sample which undergoes purification was expected to contain lower levels of these analytes. The concentrations of the analytes determined and the various analytes present within the samples are illustrated in Table 3.6 and Fig. 3.28.

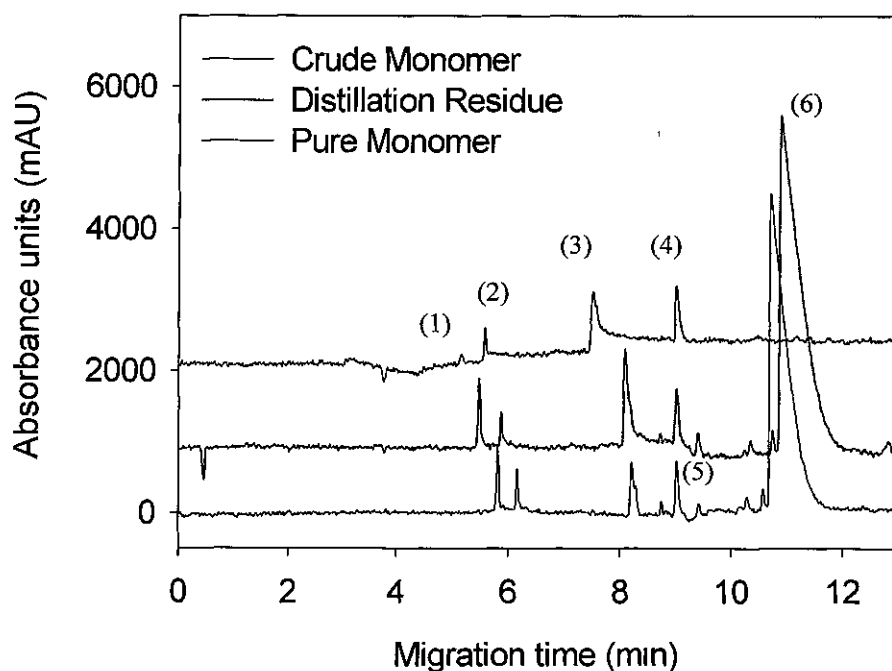


**Figure 3.26** Analysis of ethyl cyanoacrylate adhesive samples at different stages of the production process with the optimised CE method. The components have been identified as follows (1) chloride, (2) sulphate, (3) MSA, (4) chloroacetic acid, internal standard, (5) cyanoacetic acid (in crude monomer analysis only) and (6) DEP. The distillation residue and pure monomer electropherograms are offset by 1000 and 2000 mAU respectively. All operating conditions as in Figure 3.25, indirect UV detection at 254 nm. Effective capillary length 0.50 m

The concentrations of the analytes in the crude monomer sample were expected to be present at a higher level than those in the pure monomer sample, as the pure monomer was subjected to a distillation process. This was evident in the determination of the chloride concentration, as it has decreased from  $26.1 \mu\text{g ml}^{-1}$  in the crude monomer to  $2.1 \mu\text{g ml}^{-1}$  in the pure monomer sample. However, the concentrations determined for sulphate were found to be at a similar level for both monomers, as shown in Table 3.6. This illustrates the limitations of the purification process as the concentration was expected to be reduced. Also, as the pure monomer sample undergoes a purification step, the sample contains less analytes (both DEP and cyanoacetic acid were not present in the pure monomer sample, Fig. 3.26) and the absorbance response was lower for this sample.

For the pure monomer sample it was only possible to determine the analyte MSA qualitatively. This was due to the poor stability of both the MSA standard and the cyanoacrylate adhesive sample. It was initially thought that this peak was due to PTSA, and when spiked with this analyte there was an increase in both peak area and height. However, the same occurred when the sample was spiked with a standard of known concentration of MSA. To determine whether the standards were co-migrating they were analysed individually and with the internal standard, as shown in Fig 3.27. From this, it was evident that PTSA and MSA did not co-migrate; however, when analysed with the sample they were co-migrating. As a result, the analysis of the pure monomer samples was also performed at a lower voltage (-5 kV). Nevertheless, at this low voltage, the analytes were still co-migrating. From discussions with the suppliers of the adhesive samples, they were confident that this peak was due to the presence of MSA and not PTSA. It was not expected that PTSA would be present at this stage of the production process as PTSA was not present in the crude monomer sample. Therefore, the peak was identified as MSA and could not be quantified. Due to the problems with the identity of this peak, further identification would benefit in the future from mass spectral analysis. A schematic showing the concentrations of analyte anions present during various stages of the production process is illustrated in Fig. 3.28.



**Table 3.6** The concentrations of the analytes determined for the various stages of the production process for ethyl cyanoacrylate adhesive samples

Sample	Analyte	Concentration ( $\mu\text{g.ml}^{-1}$ )	%RSD (n=3)
Crude Monomer	Chloride	$26.1 \pm 2.3$	8.8
Distillation residue		$25.7 \pm 1.5$	5.7
Pure Monomer		$2.1 \pm 0.1$	4.1
Crude Monomer	Sulphate	$19.3 \pm 1.2$	6.0
Distillation residue		$21.5 \pm 3.0$	13.8
Pure Monomer		$21.9 \pm 0.2$	1.0
Crude Monomer	MSA	$39.9 \pm 1.8$	4.6
Distillation residue		> 100	N/A
Pure Monomer		MSA	N/A
Crude Monomer	Cyanoacetic acid	$6.2 \pm 0.4$	6.3
Distillation residue		None detected	N/A
Pure Monomer		None detected	N/A
Crude Monomer	DEP	> 100	N/A
Distillation residue		> 100	N/A
Pure Monomer		None detected	N/A

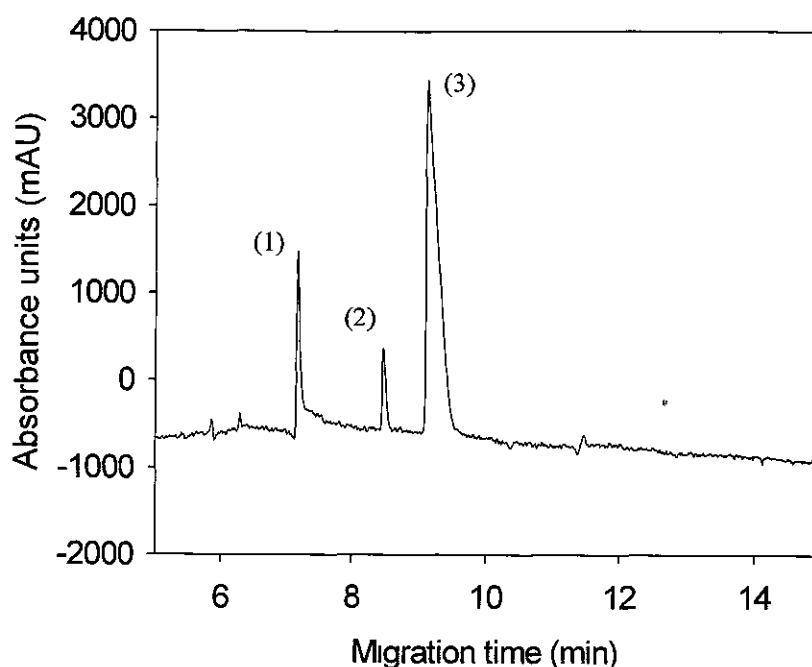


**Figure 3.27** CE separation of (1) PTSA standard ( $80 \mu\text{g ml}^{-1}$ ), (2) MSA standard ( $50 \mu\text{g ml}^{-1}$ ) and the internal standard (3) chloroacetic acid ( $50 \mu\text{g ml}^{-1}$ ). All operating conditions as in Figure 3.25 with indirect UV detection at 254 nm. Effective capillary length 0.50 m

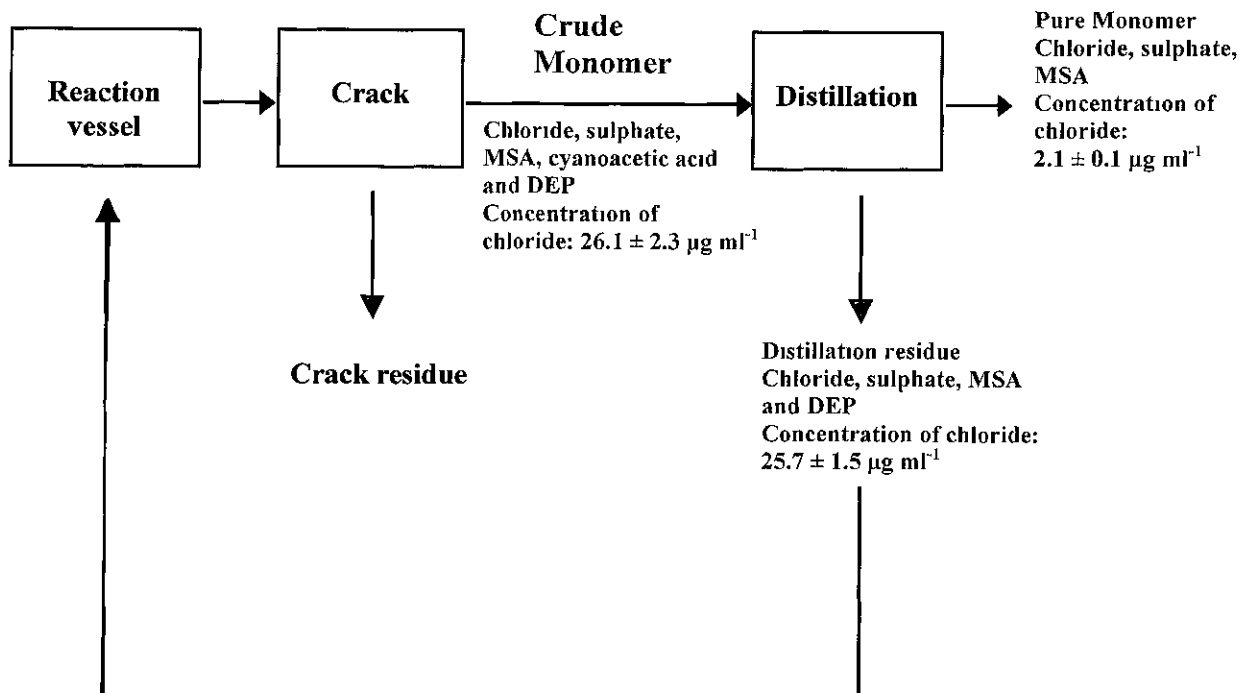


**Figure 3.28** Schematic of the production process for ethyl cyanoacrylate adhesives, showing the different analytes found to be present and the concentration of chloride in each stage of the production process

### 3.4.7 Ion Chromatography (IC) Comparison

The CE method developed was compared with IC, the separation technique traditionally employed for the analysis of anions.<sup>[6,46]</sup> For IC analysis, the method traditionally employed for the analysis of anions, the internal standard employed was citric acid. For analysis by CE, citric acid could not be utilised as its mobility was not suitably matched by the electrolyte and it therefore co-migrated with some analytes. However, for IC determination, it was an ideal choice for internal standard, as it did not co-elute with any of the analytes of interest. The IC gradient method is shown in Appendix 1b.

The precision and repeatability of the method were demonstrated through the investigation of parameters, such as migration time and peak height. Table 3.7 demonstrates the high separation efficiency obtained with the CE method. It was apparent from these results that high separation efficiencies, with reduced error, were achieved with the developed CE method. Table 3.7 also shows the detection limits, calculated at a  $S/N = 3$ , and the linear ranges, for all analytes by CE and IC literature values. The linear ranges are comparable for both CE and IC. The LOD's determined by the IC method were lower than those obtained by the developed CE method.<sup>[1]</sup> This was expected, as indirect UV detection suffers from poor sensitivity due to its high background noise and as a result exhibits a limited dynamic range.<sup>[47]</sup> However, the detection limits obtained by CE were capable of determining the typical concentration ranges of anions found in the cyanoacrylate adhesives.

**Table 3.7** The separation efficiencies (*N*) calculated for the capillary electrophoresis analyses and a comparison of the linear range and LOD's calculated for the analytes present in cyanoacrylate adhesives by CE and IC. All operating conditions as in Fig. 3.23

Analyte	N for CE (plates/m)	% RSD (n=3)	Linear Range ( $\mu\text{g mL}^{-1}$ ) for CE	LOD for CE ( $\mu\text{g mL}^{-1}$ ), n=3	Linear Range ( $\mu\text{g mL}^{-1}$ ) for IC	LOD for IC ( $\mu\text{g mL}^{-1}$ )
Chloride	330,069	2.4	2-100	$1.0 \pm 0.3$	0-100	0.006
Sulfate	305,255	2.6	6-100	$4.6 \pm 0.6$	0-100	0.01
Nitrate	168,849	1.7	6-100	$2.6 \pm 0.3$	0-100	0.006
Fluoride <sup>a</sup>	N/A	N/A	5-100	$0.8 \pm 0.1$	0-20	0.008
Formic acid <sup>a</sup>	N/A	N/A	5-100	$1.8 \pm 0.5$	N/A	N/A
Phosphate	57,654	1.8	20-100	$2.5 \pm 0.7$	0-20	0.03

Analyte	N for CE (plates/m)	% RSD (n=3)	Linear Range ( $\mu\text{g ml}^{-1}$ ) for CE	LOD for CE ( $\mu\text{g ml}^{-1}$ ) n=3	Linear Range ( $\mu\text{g ml}^{-1}$ ) for IC	LOD for IC ( $\mu\text{g ml}^{-1}$ )
MSA <sup>b</sup>	251,240	4.2	8-100	$2.2 \pm 0.4$	N/A	N/A
Cyanoacetic acid <sup>b</sup>	307,096	2.57	8-100	$2.4 \pm 0.5$	N/A	N/A
Methacrylic acid <sup>b</sup>	250,243	4.75	5-100	$0.7 \pm 0.1$	N/A	N/A
DEP <sup>b</sup>	222,818	3.42	15-120	$3.4 \pm 0.8$	N/A	N/A

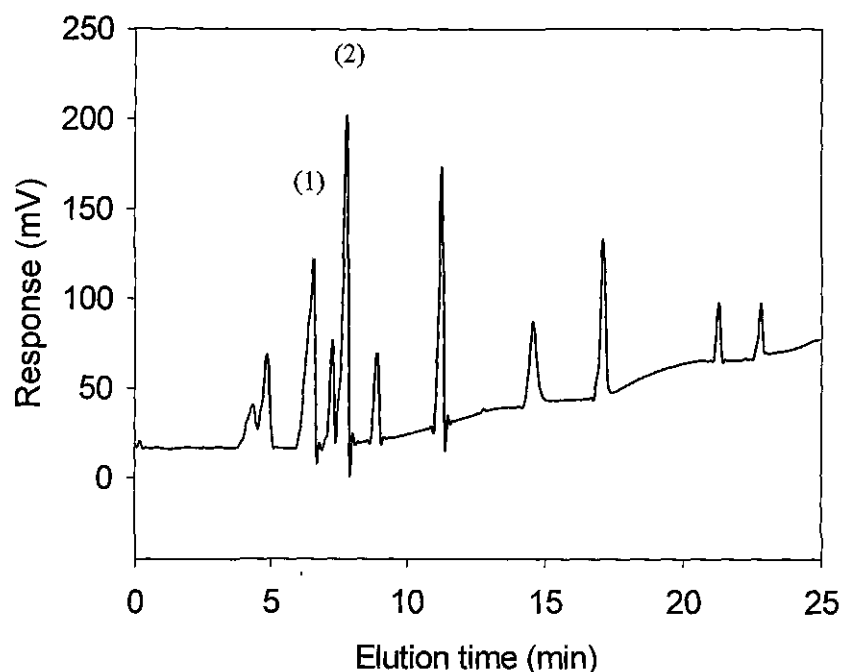
All IC results reproduced from reference <sup>[6]</sup>

Table reproduced from reference <sup>[1]</sup>

<sup>a</sup> Analytes co-migrate in CZE

<sup>a</sup> Analytes co-elute in IC

An IC separation for the analysis of a standard analyte mixture by IC is represented in Fig. 3.29, showing the order of elution. The order of elution was determined to be DEP, fluoride, DEP and formic acid, MSA, cyanoacetic acid and methacrylic acid, chloride, nitrate, PTSA, sulphate, phosphate and the internal standard, citric acid. It was evident from Fig. 3.29, that the order of elution differed from CE, due to the different separation principles, and that some of the analytes co-eluted, *e.g.* cyanoacetic acid and methacrylic acid. The analytes which co-elute are identified in Fig. 3.29. In CE analysis only two analytes co-migrate, fluoride and formic acid. Also, the total length of analysis with CE was significantly less, namely 23 min. with CE and 45 min with IC.



**Figure 3.29** IC separation with conductometric detection for the analysis of DEP ( $50 \mu\text{g ml}^{-1}$ ), fluoride ( $10 \mu\text{g ml}^{-1}$ ), (1) DEP and formic acid ( $50 \mu\text{g ml}^{-1}$ ), MSA ( $10 \mu\text{g ml}^{-1}$ ), (2) cyanoacetic acid ( $50 \mu\text{g ml}^{-1}$ ) and methacrylic acid ( $80 \mu\text{g ml}^{-1}$ ), chloride ( $30 \mu\text{g ml}^{-1}$ ), nitrate ( $50 \mu\text{g ml}^{-1}$ ), PTSA ( $80 \mu\text{g ml}^{-1}$ ) sulphate ( $30 \mu\text{g ml}^{-1}$ ), phosphate ( $25 \mu\text{g ml}^{-1}$ ), citric acid, internal standard ( $50 \mu\text{g ml}^{-1}$ ). Operating conditions as illustrated in Appendix 1b

CE offers advantages over the traditional chromatography methods, namely reduced sample volumes and waste and rapid separations, and is also less expensive than IC, which is currently used. The application of CE to the determination of anions in ethyl cyanoacrylate adhesive samples has not been reported in the literature previously. The developed CE method with its increased separation efficiencies, low RSD values and faster overall analysis times demonstrate its effectiveness as a viable and powerful alternative separation technique compared to the traditional IC.

### 3.5 CONCLUSION

A novel CE method was successfully developed for the simultaneous determination of inorganic and acidic anions, which are present in ethyl cyanoacrylate adhesive samples. High separation efficiencies were obtained for CE, such as 330,000 plates  $m^{-1}$  for chloride, and also reduced total analysis times, notably 23 min. for CE compared with 45 min. for IC. The detection limits obtained with IC were lower than those determined by CE. Nevertheless, the limits obtained by CE were capable of determining the expected concentrations in the adhesive samples. CE generates less waste than chromatographic methods and is also less expensive than IC, which is currently used. The CE method developed, with its high separation efficiencies and precision demonstrates that it is a powerful alternative for the simultaneous analysis of inorganic and acidic anions in complex matrices.



### 3.6 REFERENCES

- [1] Whitaker, G., Kincaid, B. J., Raftery, D. P., Van Hoof, N., Regan F., Smyth, M. R., Leonard, R. G., *Electrophoresis*, **2006**, Article in Press.
- [2] Kincaid, B., *Ph D. Thesis*, Dublin City University, **1999**.
- [3] Nesterenko, P., *Trends in Anal. Chem.*, **2001**, 20, 311.
- [4] Gennaro, M. C., Angelino, S., *J. Chromatogr. A*, **1997**, 789, 181.
- [5] Abd Karim, K. J. B., Jin, J. Y., Takeuchi, T., *J. Chromatogr. A*, **2003**, 995, 153.
- [6] Fernandez-Garcia, R., Alonso-Garcia, J. I., Sanz-Medel, A., *J. Chromatogr. A*, **2004**, 1033, 127.
- [7] Tormo, M., Izco, J. M., *J. Chromatogr. A*, **2004**, 1033, 305.
- [8] Mikkers, F. P., Everaerts, F. M., Verheggen, Th. P. E. M., *J. Chromatogr.*, **1979**, 169, 11.
- [9] Isaaq, H. J., *Electrophoresis*, **2000**, 21, 1921.
- [10] Doble, P., Haddad, P. R., *J. Chromatogr. A*, **1999**, 834, 189.
- [11] Paull, B., King, M., *Electrophoresis*, **2003**, 24, 1892.
- [12] Jones, W. R., Jandik, P., *American Laboratory*, **1990**, 22, 51.
- [13] Jones, W. R., Jandik, P., *J. Chromatogr.*, **1991**, 546, 445.
- [14] Jones, W. R., Jandik, P., *J. Chromatogr.*, **1992**, 608, 385.
- [15] Fritz, J. S., *J. Chromatogr. A*, **2000**, 884, 261.
- [16] Fung, Y. S., Lau, K. M., *Electrophoresis*, **2003**, 24, 3224.
- [17] King, M., Paull, B., Haddad, P. R., Macka, M., *Analyst*, **2002**, 127, 1564.
- [18] Sullivan, J., Douek, M., *J. Chromatogr. A*, **2004**, 1039, 215.
- [19] Soga, T., Ross, G. A., *J. Chromatogr. A*, **1999**, 834, 65.
- [20] Kallio, M. P., Kuitunen, M., Manninen, P. K. G., *Chemosphere*, **1997**, 35, 1509.
- [21] Soga, T., Ross, G. A., *J. Chromatogr. A*, **1999**, 837, 231.
- [22] Soga, T., Ross, G. A., *Electrophoresis*, **2001**, 22, 3418.
- [23] Fung, Y. S., Lau, K. M., *Talanta*, **1998**, 45, 641.
- [24] Chovancék, M., Choo, P., Macka, M., *Electrophoresis*, **2004**, 25, 437.
- [25] Wang, M., Qu, F., Shan, X. Q., Lin, J. M., *J. Chromatogr. A*, **2003**, 989, 285.
- [26] Chen, J., Preston, B. P., Zimmerman, M. J., *J. Chromatogr. A*, **1997**, 781, 205.
- [27] Hiissa, T., Siren, H., Kotiaho, T., Snellman, M., Hautajarvi, A., *J. Chromatogr. A*, **1999**, 853, 403.

- [28] Dabek-Zlotorzynska, E., Piechowski, M., Liu, F., Kennedy, S., Dlouhy, J. F., *J. Chromatogr. A*, **1997**, 770, 349.
- [29] Shakulashvili, N., Faller, T., Engelhardt, H., *J. Chromatogr. A*, **2000**, 895, 205.
- [30] Johns, C., Yang, W., Macka, M., Haddad, P. R., *J. Chromatogr. A*, **2004**, 1050, 217.
- [31] Diress, A. G., Lucy, C. A., *J. Chromatogr. A*, **2005**, 1085, 155.
- [32] Santoyo, E., Garcia, R., Abella, R., Aparicio, A., Verma, S. P., *J. Chromatogr. A*, **2001**, 920, 325.
- [33] Krivacsy, Z., Molnar, A., Tarjanyi, E., Gelencser, A., Kiss, G., Hlavay, J., *J. Chromatogr. A*, **1997**, 781, 223.
- [34] Kuban, P., Kuban, P., Kuban, V., *J. Chromatogr. A*, **1999**, 836, 75.
- [35] Mayer, B. X., *J. Chromatogr. A*, **2001**, 907, 21.
- [36] Heiger, D., *High Performance Capillary Electrophoresis-An Introduction*, Agilent Manual, Germany, **2000**.
- [37] Macka, M., Johns, C., Doble, P., Haddad, P. R., *LCGC*, **2001**, 19, 178.
- [38] Landers, J. P., *Handbook of Capillary Electrophoresis*, CRC Press, Boca Raton, **1997**.
- [39] Buchberger, W., Haddad, P. R., *J. Chromatogr.*, **1992**, 608, 59.
- [40] Jimidar, M., Massart, D. L., *Anal. Chim. Acta*, **1994**, 294, 165.
- [41] Harakuwe, A. H., Haddad, P. R., Buchberger, W., *J. Chromatogr. A*, **1994**, 685, 161.
- [42] Haddad, P. R., Harakuwe, A. H., Buchberger, W., *J. Chromatogr. A*, **1995**, 706, 571.
- [43] Nelson, R. J., Paulus, A., Cohen, A. S., Guttman, A., Karger, B. L., *J. Chromatogr.*, **1989**, 480, 111.
- [44] Altria, K. D., *LCGC*, **2002**, 1.
- [45] Lide, D. R., *CRC Handbook of Chemistry and Physics*, 8th Ed., Taylor and Francis, London, **2000**.
- [46] Kapinus, E. N., Revelsky, I. A., Ulogov, V. O., Lyalikov, Y. A., *J. Chromatogr. A*, **2004**, 800, 321.
- [47] Pacakova, V., Stulik, K., *J. Chromatogr. A*, **1999**, 834, 257.

## ***Chapter Four***

### ***An Investigation of the Stability of Cyanoacrylate Adhesive Samples Using the Developed CE method***

## 4.1 INTRODUCTION

In Chapter 3, a Capillary Electrophoresis (CE) method was developed for the simultaneous determination of some anions present in cyanoacrylate adhesives. Cyanoacrylate adhesives are defined as substances which are capable of forming and maintaining a bond between two surfaces. They are single component, instant bonding adhesives that cure at ambient temperatures to form strong bonds between surfaces by addition polymerisation initiated by adsorbed water.<sup>[1]</sup> Cyanoacrylate adhesives were first discovered by H. W. Coover, at Eastman in the 1950s, with ethyl cyanoacrylate being one of the monomers under investigation. In 1958, Eastman Kodak produced its first commercially available cyanoacrylate adhesive under the name Eastman 910.<sup>[2]</sup>

Cyanoacrylate adhesives initially had limited success. This was attributed primarily to two factors. Firstly, they were unstable during manufacture and storage; and secondly, consumers were slow to recognise the advantages of these adhesives. These problems were addressed in the 1970s with the introduction of new manufacturers into the market and rapid growth resulted.<sup>[3]</sup> Due to their properties, cyanoacrylates may be used in a wide range of industries. They are widely used in the automotive and electronics industry and also in household appliances. Cyanoacrylates also have applications in medicine and dentistry.<sup>[4]</sup>

In this chapter, the trace acid profile of cyanoacrylate adhesives was investigated using the developed CE method. Preparation of the adhesive samples was performed using liquid-liquid extraction (LLE).

### 4.1.1 Cure Chemistry of Cyanoacrylate Adhesives

Cyanoacrylate adhesives consist of a mixture of the following elements: monomers, initiators, accelerators and inhibitors / stabilisers. They also contain some performance enhancing components such as modifiers, plasticisers, fillers and thickeners. The monomer is normally the principal component in the mixture and forms the backbone of the resulting polymer. An initiator will start the reaction, which forms the polymer, *i.e.*, “curing” reaction. Accelerators and inhibitors are used to control the

curing rate. An accelerator, will as its name suggests, speed up the curing process, while an inhibitor will stop the curing reaction completely.

Monomers in cyanoacrylate adhesive formulations are classified according to their odour; either high or low. Low odour monomers are less volatile but more expensive. Examples of low odour monomers include  $\beta$ -methoxyethyl cyanoacrylate and  $\beta$ -ethoxyethyl cyanoacrylate. However, due to their faster cure profile and lower costs the more volatile (hence higher odour) esters such as methyl and ethyl cyanoacrylate are the most widely used.<sup>[5]</sup>

As cyanoacrylates consist mainly of the monofunctional monomer, (Fig. 4.1), they are able to homopolymerise rapidly at room temperature and do not require large amounts of co-reactants.<sup>[6]</sup>

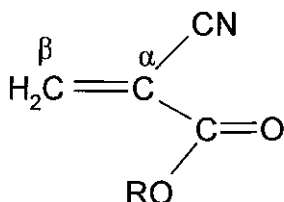
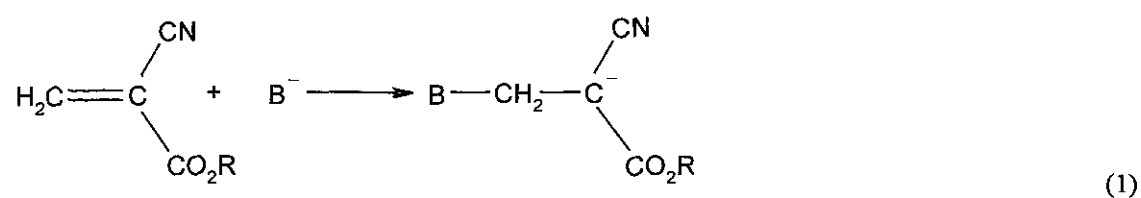


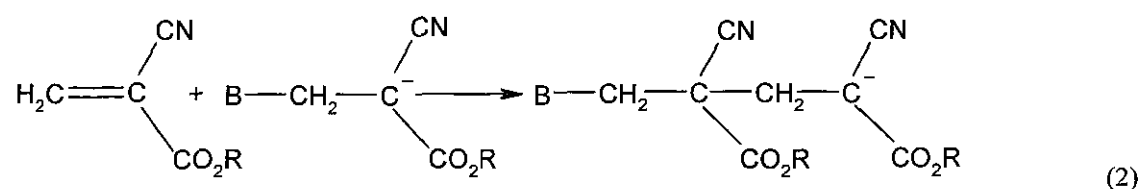
**Figure 4.1** The structure of a cyanoacrylate monomer, where R denotes an alkyl group, for example methyl, ethyl or butyl<sup>[6]</sup>

Cyanoacrylates are known to cure either by a free radical or an anionic mechanism; however, the latter mechanism has attracted more attention due to the ease of initiation and the rapid rates of polymerisation that occur.<sup>[4]</sup> The reactivity of cyanoacrylates is caused by the presence of the cyano and carbonyl groups, two strong electron-withdrawing groups, on the  $\alpha$ -carbon atom. This leaves the C=C double bond vulnerable to attack by weak bases (*e.g.* water). This mechanism is initiated by the presence of a weak base, on the surface of the materials being bonded.<sup>[6]</sup> The cure process for the anionic polymerisation of cyanoacrylates consists of three steps, initiation of the reaction, propagation and termination as shown in Fig. 4.2.

*Step 1: Initiation*



*Step 2. Propagation*



*Step 3: Termination*

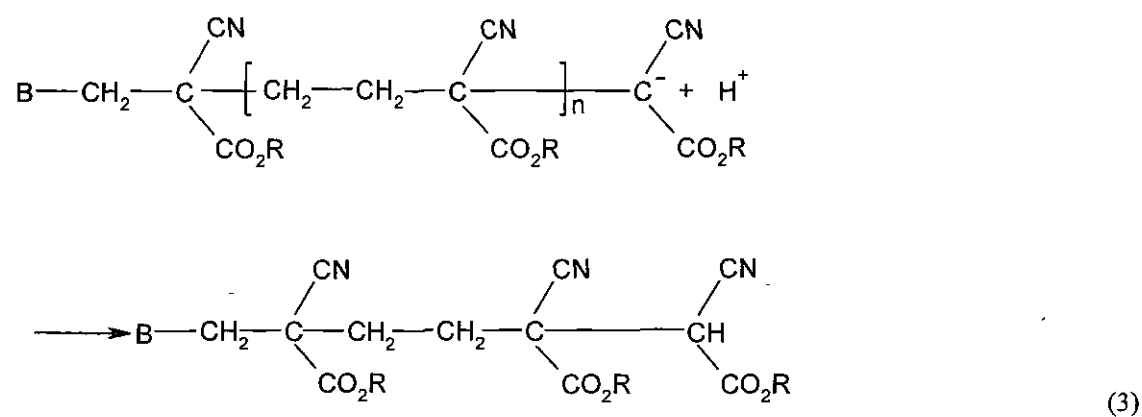


**Figure 4.2** The cure mechanism for cyanoacrylate adhesives<sup>[5]</sup>

Generally, any anion present on the surface of the substrate can act as an initiator for polymerisation. Epoxides and secondary and tertiary amines have been used as cure initiators for cyanoacrylate adhesives.<sup>[2]</sup>

The rate of reaction can be terminated either by chain transfer or the addition of a strong acid. In chain transfer the polymer chain attacks another species to form an inert polymer and a new anion, which will initiate the growth of a new polymer chain. The addition of a strong acidic gas (*e.g.* SO<sub>3</sub>, BF<sub>3</sub>) will complex the anion and slow down or terminate the polymerisation.<sup>[6]</sup> These acidic gases can also be employed as inhibitors, in order to improve the stability of the cyanoacrylate adhesives during storage. Alternative non-volatile acidic inhibitors, such as benzene sulphonic acid or *p*-toluene sulphonic acid (*p*-TSA, Fig. 4.3), have also been employed.

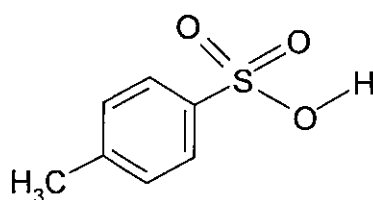


**Figure 4.3** Structure of organic acid inhibitor *p*-TSA

The curing process for cyanoacrylates can be accelerated by the addition of crown ethers, oligomers of poly (ethylene) oxide or prodands.<sup>[7]</sup> Accelerators do not affect the overall stability of cyanoacrylate adhesives. At low temperatures, the humidity is decreased, which reduces the amount of water available for the cure process and therefore reduces the curing rate. In order to improve the curing rate, accelerators such as crown ethers may be added. The addition of crown ethers increases the amount of water available and therefore the rate of cure is enhanced.<sup>[6]</sup>

Other components present in cyanoacrylates include modifiers, which are added to adhesives in order to obtain the desired physical property and appearance required. Some examples of modifiers are tougheners and plasticisers. Tougheners are added to enhance the resistance and strength of adhesives, whilst plasticisers (*e.g.* aliphatic diesters and alkyl phthalates), reduce brittleness.<sup>[6]</sup> As cyanoacrylate adhesives consist of numerous components, both a sensitive and selective method for their analysis is required.

A flow chart, Fig. 3.1, illustrating the cyanoacrylate production process is shown in Chapter 3. In Figure 4.4 the production process for cyanoacrylate adhesives is shown in greater detail. The condensation of the alkyl cyanoacetate with formaldehyde, results in a prepolymer that by heating is depolymerised into a liquid monomer, (crude monomer). For the reaction to occur smoothly, the base catalyst is removed by the addition of appropriate acids (*e.g.* phosphoric acid, sulphuric acid). The crude monomer undergoes a purification process, *i.e.* a distillation, whereby impurity anions will be removed. This distillation results in the formation of a pure monomer. Upon exposure to air, the pure monomer cures and forms strong bonds between surfaces by the addition polymerisation initiated by adsorbed water. The addition of a free radical inhibitor, *e.g.* hydroquinone, prevents the monomer undergoing a free radical polymerisation during storage.

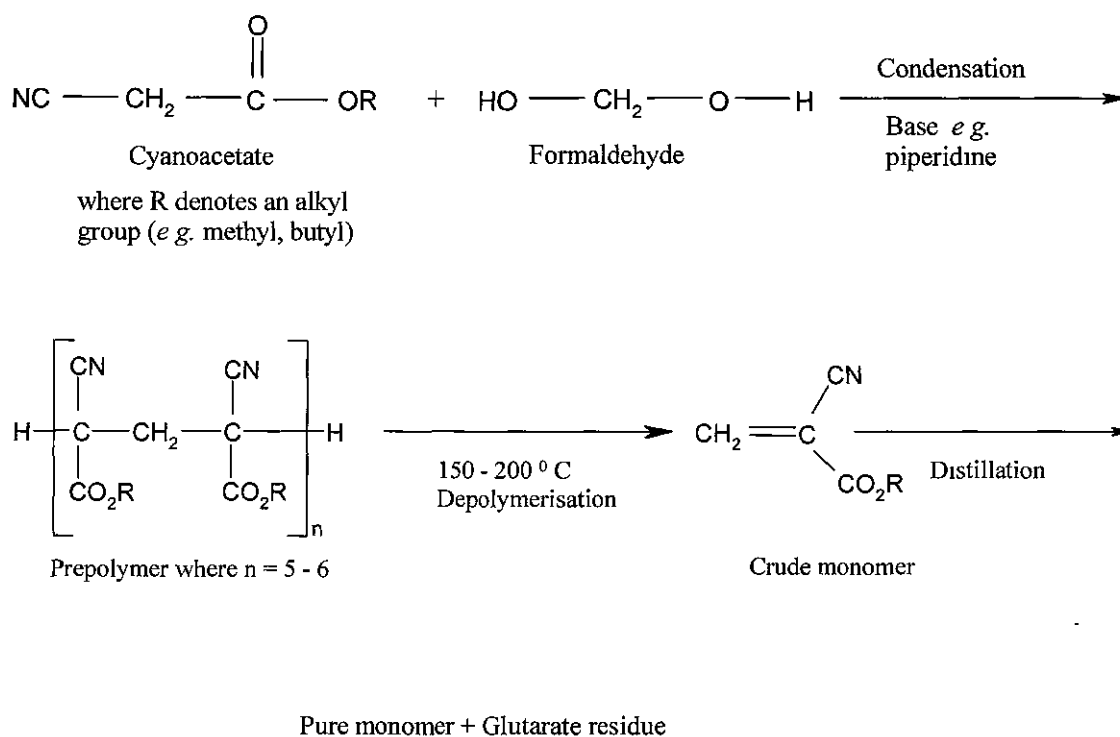


**Figure 4.4** Schematic of the cyanoacrylate manufacturing process



As previously discussed in Chapter 3, a wide range of inorganic and acidic anions may be present at different stages of the production process, such as sulphate, nitrate and formic acid. In order to maintain the quality of the product, a sensitive and selective method for their quantification is required.

CE has recently emerged as a powerful analytical separation technique for the determination of small charged species, such as inorganic anions and organic acids <sup>[8-12]</sup> due to its low sample consumption and rapid and highly efficient separations. In Chapter 3, a suitable sensitive and selective CE method was developed for the quantification of inorganic and acidic anions at different stages of their production process. This method is also suited to the analysis in the  $\beta$ -methoxyethyl cyanoacrylate adhesives production process.

## 4.2 SCOPE OF RESEARCH

The analysis of  $\beta$ -methoxyethyl cyanoacrylate adhesives, at different stages of their production process (*i.e.* crude monomer, distillation residue and pure monomer samples) was performed using the developed CE method. Sample pre-treatment was performed using LLE with chloroform. The solubility of the adhesives was investigated using various organic solvents, *e.g.* hexane, dichloromethane, and chloroform and the optimum sample preparation method was determined. The trace acid profile of the cyanoacrylate adhesive was investigated using the optimised CE method from Chapter 3.

## **4.3 MATERIALS AND METHODS**

### **4.3.1 Instrumentation**

#### ***4.3.1.1 Capillary electrophoresis separations***

Capillary electrophoresis separations were performed as described in Chapter 3 in Section 3.3.3.1.

### **4.3.2 Chemicals**

Chloroform (650471, Chromasolv grade) was purchased from Sigma Aldrich (Dublin, Ireland). High Performance Liquid Chromatography (HPLC) grade chloroform was obtained from Labscan Ltd. (Dublin, Ireland). All other chemicals were of reagent grade and as described in Chapter 3 in Section 3.3.2. Cyanoacrylate adhesive samples were obtained from Henkel Technologies (Irl.) Ltd.

### **4.3.3 Procedures**

#### ***4.3.3.1 CE Background electrolyte (BGE) preparation***

Electrolytes were prepared using deionised water. All electrolyte solutions consisted of a sodium chromate electrolyte and an electroosmotic flow (EOF) modifier. A stock solution of 50 mM sodium chromate was prepared, from which a 15 mM sodium chromate solution was obtained by dilution of the stock with deionised water. The EOF modifier employed was cetyltrimethylammonium bromide (CTAB). A concentration of 1 mM CTAB was prepared by dilution of a stock solution with deionised water. The pH of the unbuffered electrolyte was adjusted to 8.5 using 1 mM sulphuric acid (H<sub>2</sub>SO<sub>4</sub>). The BGE consisted of 15 mM chromate, 1 mM CTAB at pH 8.5. All electrolyte solutions were filtered with 0.45 µm swinny filter (Gelman Nylon Acrodisc, 4438) prior to use.

#### ***4.3.3.2 Preconditioning of the CE separation capillary***

Separation capillaries were preconditioned as described in Chapter 2 in Section 2.3.3.3.

#### ***4.3.3.3 Quantification of Analytes in the Adhesive Sample***

The quantification of analytes in the adhesive samples was performed as described in Chapter 3 in Section 3.3.3.5.

#### ***4.3.3.4 Adhesive sample preparation***

Adhesive samples were prepared as described in Chapter 3 in Section 3.3.3.6. using HPLC and Chromasolv grade chloroform.

## 4.4 RESULTS AND DISCUSSION

In this investigation, the analysis of  $\beta$ -methoxyethyl cyanoacrylate adhesives was performed using a developed CE method.<sup>[13]</sup> Samples were taken from the crude monomer, which on distillation produces the pure monomer and the residue remaining from the distillation was also analysed, as shown in Fig. 3.1. In the crude monomer sample, the analytes determined were chloride, sulphate, methyl sulphonic acid (MSA), cyanoacetic acid and di(methoxyethyl)phosphate (DMEP). The same analytes were present in the distillation residue. In the pure monomer sample the presence of chloride, sulphate, formic acid, cyanoacetic acid and MSA was determined. The electropherograms obtained are shown in Fig.'s 4.5-4.7. The % recovery of chloroacetic acid (internal standard) for each sample analysis was obtained and determined to be in the region 77-84%, as shown in Table 4.1.

The quantification of the anions in the samples was performed using both the internal standard method and by peak spiking as described in Section 3.4.4 in Chapter 3, using the developed CE method. The concentrations of the analytes determined and the various analytes present within the samples are presented in Table 4.2.

### 4.4.1 Sample preparation procedure

The anions expected to be present in the adhesive sample include chloride, sulphate and cyanoacetic acid. In order to quantify these anions using CE the adhesive sample must be present as an aqueous solution. Therefore, a sample pre-treatment process was required. In this study sample pre-treatment was performed by LLE. LLE is one of the most extensively studied sample preparation techniques due to its simplicity and convenience. In LLE, sample constituents are extracted into an aqueous phase from a water-immiscible organic phase. Organic solvents employed include diethyl ether, hexane and chloroform.<sup>[14]</sup> In this study, for the analysis of adhesives, LLE was performed using chloroform as the organic phase and the internal standard, chloroacetic acid as the aqueous layer. A blank LLE extraction, *i.e.* of chloroacetic acid, was performed in triplicate and from a known standard the % recovery of chloroacetic acid for each sample analysis was obtained, and are shown in Table 4.1.

**Table 4.1** The % recoveries and % Relative Standard Deviation values (%RSD) obtained for analysis of  $\beta$ -methoxyethyl cyanoacrylate adhesives. Operating conditions as in Fig. 4.5

Sample	% Recovery of chloroacetic acid	% RSD (n=3)
Crude monomer	77.3	4.4
Distillation residue	79.5	3.2
Pure monomer	84.2	1.4

Triplicate LLE's were carried out for each sample. Once extracted each sample was analysed in triplicate by CE. Typical electropherograms of  $\beta$ -methoxyethyl cyanoacrylate adhesive samples are illustrated in Fig.'s 4.5-4.7. The distillation of the crude monomer is a purification process that removes any impurities and results in the production of the pure monomer.

**Table 4.2** The concentrations of the analytes determined for the various stages of the production process for  $\beta$ -methoxyethyl cyanoacrylate adhesive samples

Sample	Analyte	Concentration ( $\mu\text{g ml}^{-1}$ )	% RSD (n=3)
Crude monomer	Chloride	$31.3 \pm 1.4$	1.9
Distillation residue		$60.5 \pm 3.4$	4.7
Pure monomer		$9.4 \pm 1.1$	12.1
Crude monomer	Sulphate	$44.6 \pm 3.7$	8.3
Distillation residue		$82.3 \pm 3.0$	3.7
Pure monomer		$22.6 \pm 1.5$	6.6
Crude monomer	MSA <sup>a</sup>	MSA	N/A
Distillation residue		MSA	N/A
Pure monomer		$22.5 \pm 0.6$	2.6
Crude monomer	Cyanoacetic acid	$11.3 \pm 0.85$	7.5
Distillation residue		None detected	N/A
Pure monomer		None detected	N/A
Crude monomer	DMEP	> 100	N/A
Distillation residue		> 100	N/A
Pure monomer		None detected	N/A

<sup>a</sup> Not quantified by CE

The concentrations of the analytes chloride, sulphate and DMEP, in the crude monomer sample were expected to be present at a higher level than those in the pure monomer sample, as shown in Table 4.2. This is because the crude monomer sample was prior to the distillation stage, *i e*, the purification of the sample. As the pure monomer was subjected to a distillation, the sample contained less analytes (DMEP not present in pure monomer), and the absorbance response was lower for this sample, as illustrated in Fig. 4.7 and Table 4.2.

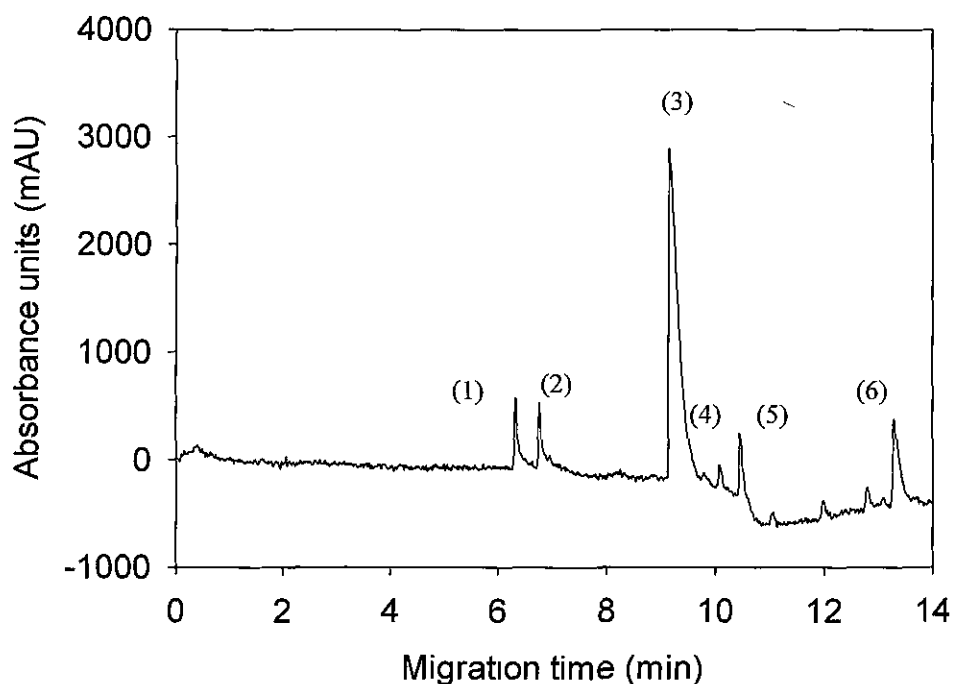


**Figure 4.5** CE analysis of a  $\beta$ -methoxyethyl crude monomer. The components have been identified as follows (1) chloride, (2) sulphate, (3) MSA, (4) cyanoacetic acid, (5) chloroacetic acid, internal standard and (6) DMEP. Separation voltage -10 kV, pressure injection 0.5 psi / 5 s, with indirect UV detection at 254 nm. BGE. 15 mM chromate, 1 mM CTAB at pH 8.5. Separation temperature 25 °C. Effective capillary length 0.50 m



The concentration of chloride in the crude monomer sample was determined to be  $31.3 \mu\text{g ml}^{-1}$  whereas in the pure monomer sample this was reduced to  $9.4 \mu\text{g ml}^{-1}$ . There was a decrease, too in the amount of sulphate determined in the crude monomer sample to the final pure monomer sample, i.e., a reduction of 49% from the crude monomer sample to the pure monomer sample. This demonstrates the effectiveness of the manufacturing method in the removal of impurities from the adhesive.

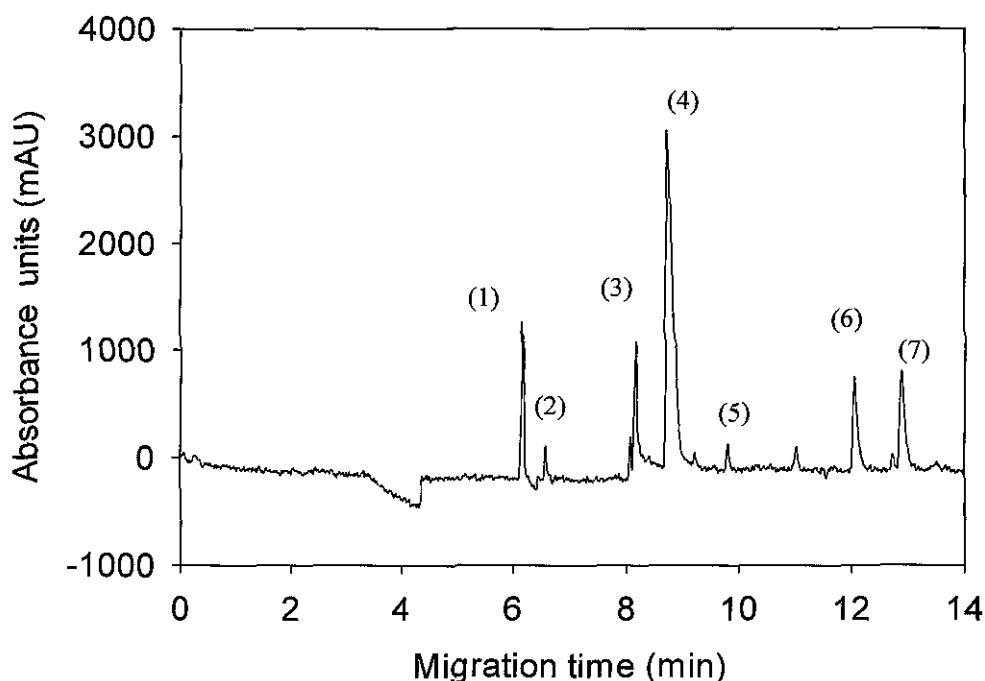


**Figure 4.6** CE analysis of a  $\beta$ -methoxyethyl distillation residue. The components have been identified as follows (1) chloride, (2) sulphate, (3) MSA, (4) unidentified peak, (5) chloroacetic acid, internal standard, (6) DMEP and (7) unidentified peak. All operating conditions as in Figure 4.5, indirect UV detection at 254 nm Effective capillary length 0.50 m

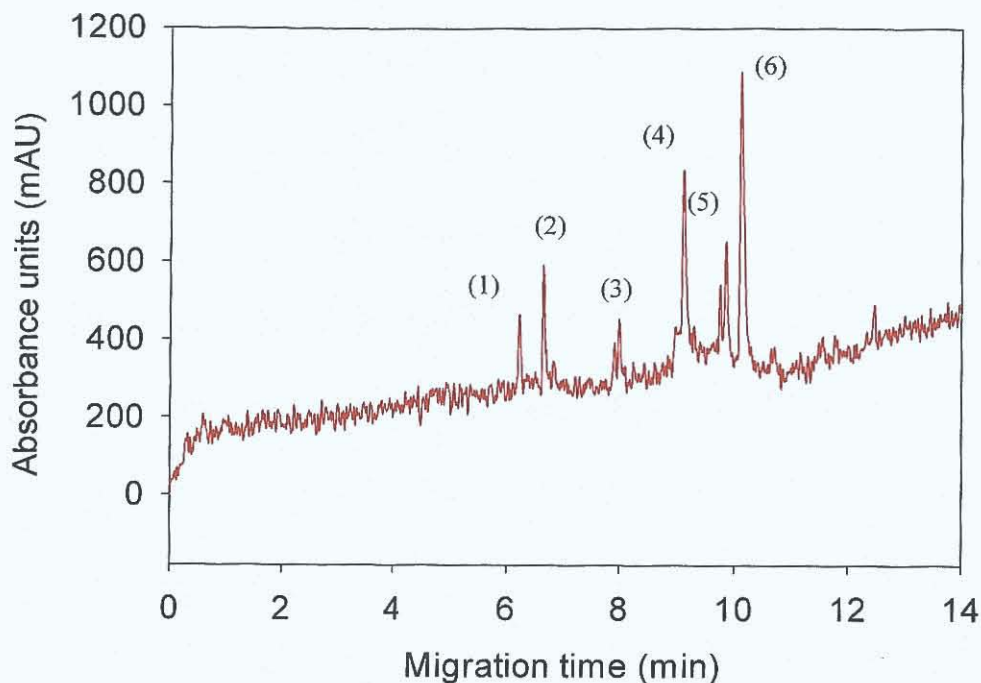


**Figure 4.7** CE analysis of a  $\beta$ -methoxyethyl pure monomer. The components have been identified as follows (1) chloride, (2) sulphate, (3) formic acid, (4) MSA, (5) cyanoacetic acid and (6) chloroacetic acid, internal standard. All operating conditions as in Figure 4.5, indirect UV detection at 254 nm. Effective capillary length 0.50 m

#### 4.4.2 Chloride determination

The presence of chloride in the sample was initially thought to be due an artefact of sample pre-treatment. In order to investigate this, a range of solvents were employed to dissolve the cyanoacrylate sample, such as hexane, dichloromethane and toluene. However, none of these solvents provided satisfactory extractions and chloroform was employed for all extractions, as this was the only solvent, which enabled the full dissolution of the adhesives.

The analysis of the adhesives was also performed using a higher grade of chloroform, (Chromasolv), and the % recoveries obtained for both grades of chloroform were comparable, 73-85%, with slightly reduced %RSD values obtained with HPLC chloroform, Table 4.3.

**Table 4.3** The % recoveries obtained for analysis of  $\beta$ -methoxyethyl cyanoacrylate adhesives using Chromasolv chloroform Operating conditions as in Fig 4 5

Sample	% Recovery of chloroacetic acid	% RSD (n=3)
Crude monomer	73.4	4.9
Distillation residue	73.2	5.2
Pure monomer	85.7	2.6

The influence of Chromasolv chloroform on the concentration of chloride in the adhesive samples was also investigated, as shown in Table 4.4. A decreased quantity of chloride was determined with the higher grade of chloroform for the distillation residue and crude monomer samples, with no chloride detected in the pure monomer sample. For the distillation residue sample, this was as a direct result of a reduced % recovery, with a higher %RSD obtained with Chromasolv chloroform than the % recovery obtained with the HPLC grade. It can also be concluded that the reduced quantity of chloride in the sample was due to the increased quality of chloroform in the sample pre-treatment.

**Table 4.4** Chloride concentrations determined for the  $\beta$ -methoxyethyl cyanoacrylate distillation residue with HPLC and Chromasolv grade chloroform. Operating conditions as in Fig. 4.5

Sample	Concentration, ( $\mu\text{g ml}^{-1}$ ) HPLC Grade	Concentration ( $\mu\text{g ml}^{-1}$ ) Chromasolv Grade
Crude monomer	$31.3 \pm 1.4$	$31.1 \pm 1.4$
Distillation residue	$60.5 \pm 3.4$	$49.8 \pm 4.7$
Pure monomer	$9.4 \pm 1.1$	None detected

#### 4.4.3 Stability of cyanoacrylate adhesives

The stability of the adhesive samples was investigated over a three-year period using CE. As previously stated, CE is an ideal method for the analysis of anions due to its low sample consumption and its rapid and highly efficient separations.<sup>[15]</sup> Fig.'s 4.8-4.10 illustrate the trace acid profiles obtained for the analysis of the  $\beta$ -methoxyethyl cyanoacrylate adhesive samples within this time frame. The acid profiles from year 1 and year 2 are similar and therefore the profiles from year 1 and year 3 are shown in Fig.'s 4.8-4.10. From this it was apparent that firstly, the concentration of the analytes decreased from the first year of analysis, for example in the crude monomer sample, the concentration of sulphate decreased from  $44.6 \mu\text{g ml}^{-1}$  in year 1, to  $12 \mu\text{g ml}^{-1}$  in the final year. It was also evident that there were extra unidentified peaks in the electropherograms, and that some analytes had been eliminated from the final year analysis, such as chloride, sulphate and cyanoacetic acid, in the crude and pure monomer samples. This suggests that the adhesive sample had destabilised over time, possibly due to the addition of the process acids during the production. Therefore, this illustrates that the methoxyethyl adhesive samples were stable over a two-year period,

after which degradation of the sample occurred. From Fig. 4.10, it was found that the acid MSA was generated over time. This was expected as the acid MSA is a by-product of extended storage over time.

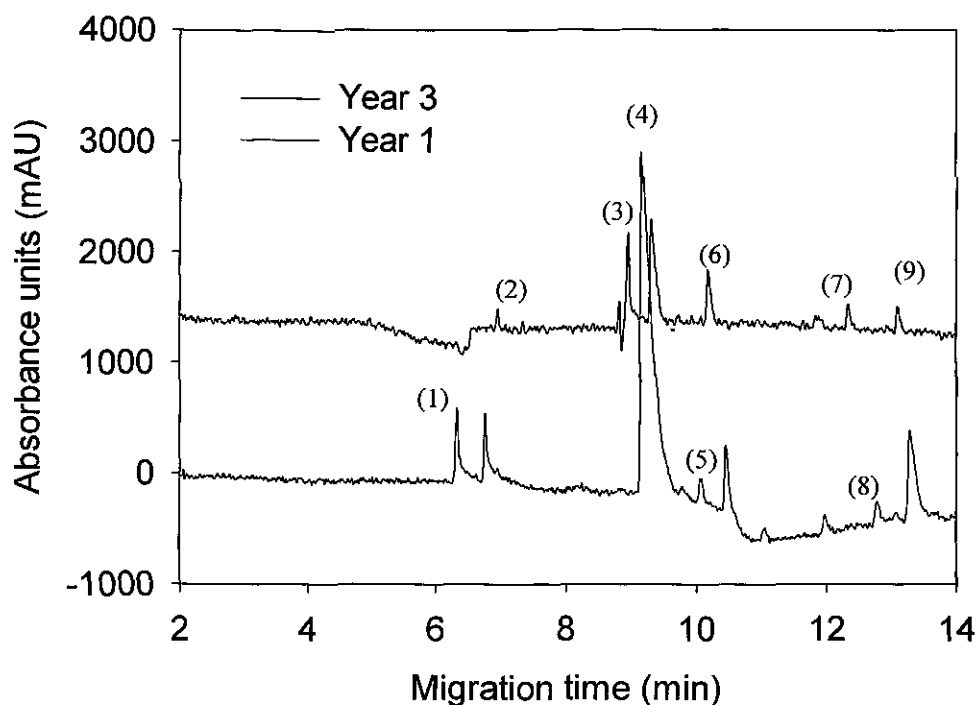


**Figure 4.8**  *$\beta$ -methoxyethyl cyanoacrylate crude monomer stability over a three year period. The components have been identified as follows (1) chloride, (2) sulphate, (3) unidentified peak, (4) MSA, (5) cyanoacetic acid, (6) chloroacetic acid, internal standard, (7) unidentified peak, (8) unidentified peak and (9) DMEP. The year 3 electropherogram is offset by 1000 mAU. All operating conditions as in Figure 4.5. Effective capillary length 0.50 m*

From these investigations it was found that, using CE, the efficiency of the manufacturing method in the removal of impurities from the adhesive could be monitored. The ability of CE to effectively monitor the cyanoacrylate production process was illustrated. Moreover, CE was shown to be suitable for the in-depth stability studies of the adhesives in question.

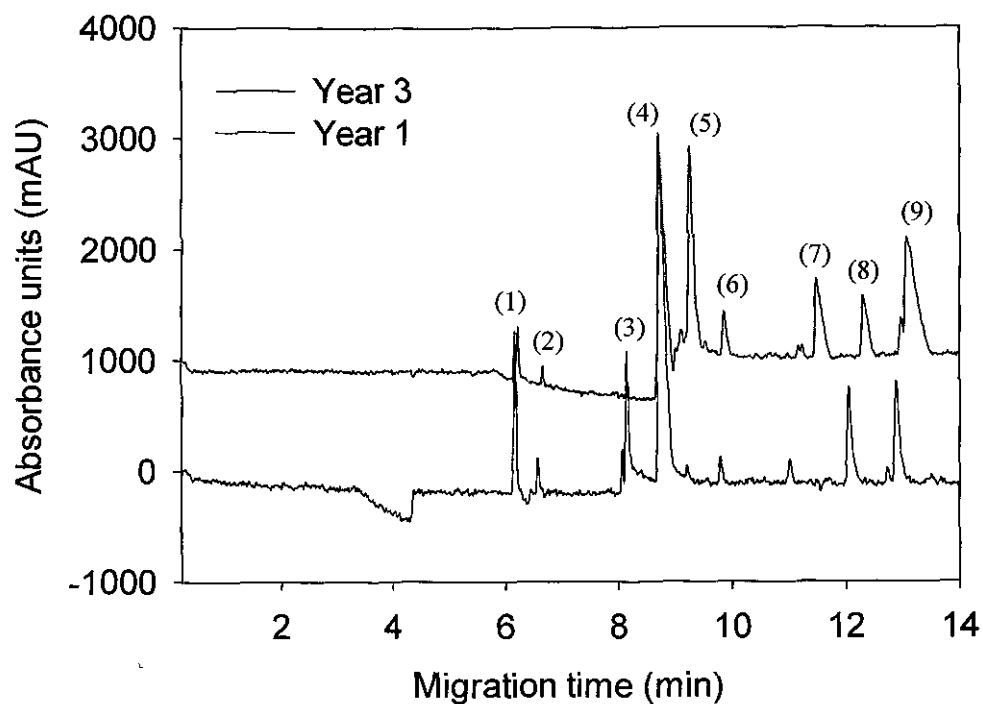


**Figure 4.9**  *$\beta$ -methoxyethyl cyanoacrylate distillation residue stability over a three-year period. The components have been identified as follows (1) chloride, (2) sulphate, (3) MSA, (4) unidentified peak, (5) unidentified peak, (6) chloroacetic acid, internal standard, (7) unidentified peak, (8) DMEP and (9) unidentified peak. The year 3 electropherogram is offset by 1000 mAU. All operating conditions as in Figure 4.5. Effective capillary length 0.50 m*

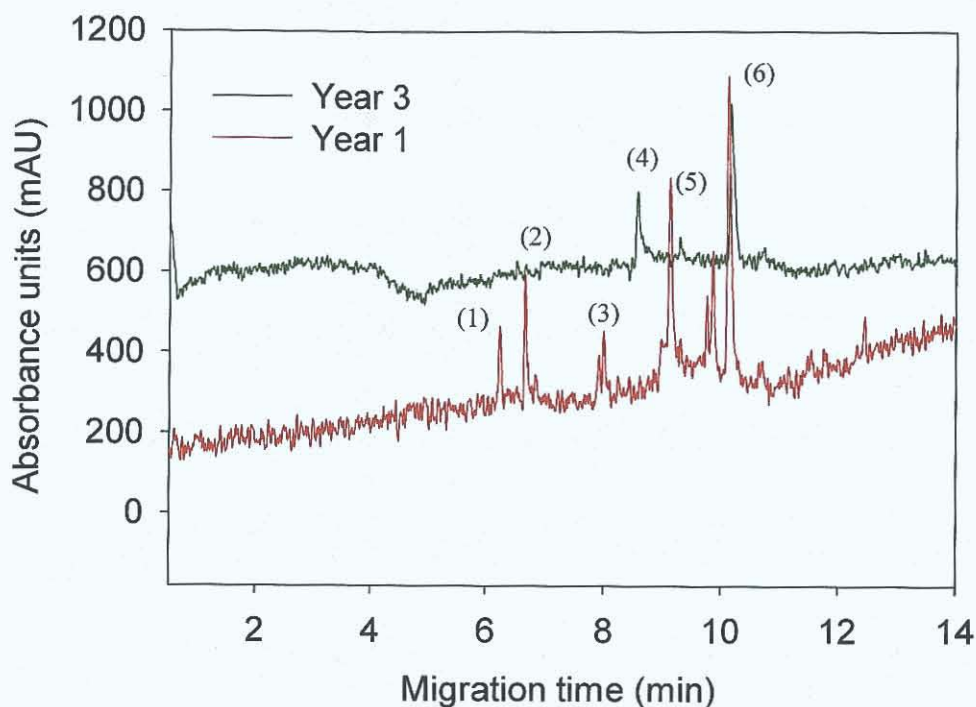


**Figure 4.10**  $\beta$ -methoxyethyl cyanoacrylate pure monomer stability over a three-year period. The components have been identified as follows (1) chloride, (2) sulphate, (3) formic acid, (4) MSA, (5) cyanoacetic acid, and (6) chloroacetic acid, internal standard. The year 3 electropherogram is offset by 750 mAU. All operating conditions as in Figure 4.5. Effective capillary length 0.50 m

## **4.5 CONCLUSION**

A simple and reproducible sample preparation method was developed and successfully applied to the analysis of cyanoacrylate adhesives. Chloroform was determined to be the optimum solvent for their extraction as it enabled full dissolution of the sample. A comparison was made between two grades of chloroform, HPLC and Chromasolv, and the optimum method developed with HPLC grade resulted in decreased % RSD values, <8% and large % recoveries, 77-84%. The presence of chloride in the pure monomer sample was determined to be an artefact of the sample preparation procedure. The relationship between the type and concentration of the trace acids present in the cyanoacrylate adhesive and the stability and performance attributes of the adhesive was monitored. Samples were shown to be stable for 2 years, after which degradation occurred. This investigation illustrated the capability of CE as a powerful alternative for the simultaneous analysis of inorganic and acidic anions in a cyanoacrylate matrix. The efficiency of the production process was demonstrated and shows its effectiveness in the purification of the adhesive samples.



## 4.6 REFERENCES

- [1] Comyn, J., *Int. J. of Adhesion and Adhesives*, **1998**, 18, 247.
- [2] Coover, H. W., Dreifus, D. W., O' Connor, J. T., *Handbook of Adhesives*, Reinhold, New York, **1977**.
- [3] Mc Manus, M. G., *MSc. Thesis*, Dublin City University, **1995**.
- [4] Tomlinson, S. K., Ghita, O. R., Hooper, R. M., Evans, K. E., *Vib. Spec.*, **2006**, 40, 133.
- [5] Kincaid, B., *Ph.D. Thesis*, Dublin City University, **1999**.
- [6] Mc Cullagh, N., *MSc. Thesis*, Dublin City University, **2002**.
- [7] Millet, G. H., *Structural Adhesives*, Plenum Press, New York, **1986**.
- [8] Mikkers, F. P., Everaerts, F. M., Verheggen, Th. P. E. M., *J Chromatogr.*, **1979**, 169, 11.
- [9] Haumann, I., Boden, J., Mainka, A., Jegle, U., *J Chromatogr. A*, **2000**, 895, 269.
- [10] Galli, V., Barbas, C., *J. Chromatogr. A*, **2004**, 1032, 299.
- [11] Johns, C., Yang, W., Macka, M., Haddad, P. R., *J. Chromatogr. A*, **2004**, 1050, 217.
- [12] Breadmore, M. C., Haddad, P. R., Fritz, J. S., *J. Chromatogr. A*, **2001**, 920, 31.
- [13] Whitaker, G., Kincaid, B., Raftery, D. P., Van Hoof, N., Regan, F., Smyth, M. R., Leonard, R. G., *Electrophoresis*, **2006**, *Article in Press*.
- [14] Bjergaard, S. P., Rasmussen, K. E., Halvorsen, T. G., *J. Chromatogr. A*, **2000**, 902, 91.
- [15] Paull, B., King, M., *Electrophoresis*, **2003**, 24, 1892.

## ***Chapter Five***

### ***Analysis of Anthracycline Antibiotics by CE and HPLC***

## 5.1 INTRODUCTION

From the previous chapters, the advantages and applicability of Capillary Electrophoresis (CE) were demonstrated for the analysis of industrial samples. The CE method developed, with its high separation efficiencies and precision, illustrated its ability for the simultaneous analysis of inorganic and acidic anions in adhesive samples. Taking into account the advantages of CE and also its low solvent usage, the separation technique was applied to the analysis of another complex matrix, *i.e.*, rat plasma. CE has been widely reported in the determination of pharmaceuticals in biological matrices, such as anthracyclines in plasma samples.<sup>[1-4]</sup> Anthracyclines are antibiotics that are regularly used in the treatment of cancers, such as lung and ovarian cancers. Daunorubicin (DAN) and doxorubicin (DOX) were the first identified anthracyclines and are isolated from pigment producing *Streptomyces* species.<sup>[5]</sup> Due to the cardiotoxic nature of these anthracyclines, epirubicin (4'-epidoxorubicin) is one of a series of anthracyclines produced that has fewer side effects.<sup>[6]</sup> Epirubicin (EPI) differs from doxorubicin in the orientation of the 4'OH group, as shown in Fig. 5.1.

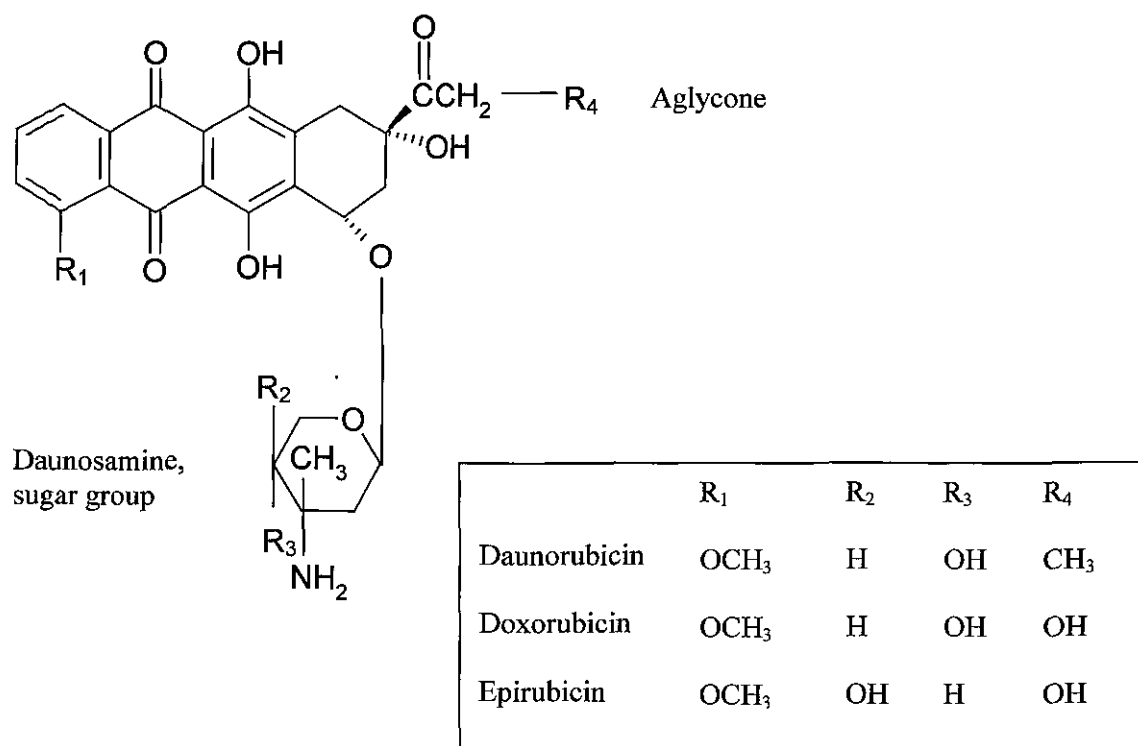


**Figure 5.1** Structures of the anthracyclines, daunorubicin, doxorubicin and epirubicin

All anthracyclines have a tetracycline ring structure with an amino sugar group, daunosamine, attached by a glycosidic link. The anthracyclines have proton-accepting quinone carbonyl groups and proton donating phenolic groups on adjacent rings that allow them to behave as electron accepting and donating species.<sup>[7]</sup>

The chemotherapeutic activity of anthracyclines has been attributed to three functions. Firstly, binding to DeoxyriboNucleic Acid (DNA) through intercalation. DAN contains two electroactive sites; the aglycone moiety intercalates between the  $\pi$  stacked base pairs of DNA and daunosamine binds to the major groove of the DNA double helix, stabilising the normally reversible topoisomerase II DNA complex. Fig. 5.2 represents the DNA helical structure. As a result of intercalation, DAN forms strong bonds with DNA and hinders the synthesis of DNA.<sup>[8]</sup> The intercalation of DOX has also been reported.<sup>[9]</sup>

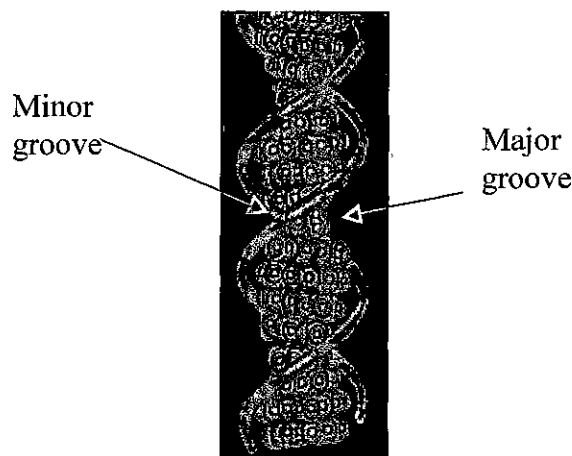


**Figure 5.2** Representation of the DNA double helical structure, with  $\pi$  stacked bases shown in grey and the sugar phosphate backbone in blue<sup>[10]</sup>

Anthracyclines also bind to cell membranes, modifying their fluidity and ion transport.<sup>[11]</sup> The cell is a highly functional unit whose membrane components have a number of functions. It is a highly protective functional unit, which regulates transport between the extracellular and intracellular layers. The survival of the cell is dependent

upon maintaining the difference between these two layers and any change, which alters the fluidity and ion transport of cell membranes, can be detrimental to the cell. Finally, the quinone structure is highly susceptible to generation via one-electron reduction of the semiquinone radical. This radical results in the production of oxygen radicals and hydrogen peroxide ( $\text{H}_2\text{O}_2$ ), which are both cardiotoxic and may lead to cell death.<sup>[12]</sup>

DAN and DOX are both known to cause myelosuppression and cardiotoxicity, which is the dose limiting factor for these drugs.<sup>[13]</sup> There is an ongoing discussion about the best schedule for anthracyclines, as reduced acute cardiotoxicity was determined with prolonged infusions compared to bolus injections.<sup>[14]</sup> The dose regimen of anthracyclines is dependant upon the age, size and gender of the patient. The potential for DOX cardiotoxicity is age related, and younger children are at a higher risk.<sup>[15]</sup> DOX ( $40\text{-}50\text{ mg m}^{-2}$ ) was administered in combination with docetaxel ( $50\text{-}75\text{ mg m}^{-2}$ ) to patients with breast cancer and resulted in an overall remission of 71-81%. The use of EPI in combination with docetaxel<sup>[16]</sup> and also in combination with vinorelbine and 5-fluorouracil<sup>[17]</sup> was also reported in the treatment of breast cancer. The therapeutic concentrations of anthracyclines are in the range  $5\text{-}50,000\text{ ng ml}^{-1}$  and Fig. 5.3 illustrates a pharmacokinetic (PK) profile for DOX and its metabolites in plasma.<sup>[18]</sup>

Both DAN and DOX are active against acute leukaemias; however, DOX has a wider range of activity against solid human tumours such as tumours of the breast, lung, ovary and bladder. It is most effective against soft-tissue sarcomas in adults.<sup>[13]</sup> DAN and DOX are administered intravenously and metabolised in the liver to their active metabolites daunorubicinol and doxorubicinol.<sup>[1]</sup>

EPI, meanwhile, possesses similar response rates to DOX in small cell lung and ovarian cancer. There are fewer incidences of cardiotoxicity associated with EPI and it is also less myelotoxic. It is also administered intravenously and is rapidly and extensively metabolised by the liver and red blood cells.<sup>[19]</sup> The cardiotoxicity of these drugs is related to the concentration of the dose administered and anthracycline induced cardiomyopathy is frequently irreversible and could potentially result in clinical congestive heart failure.<sup>[20]</sup> As a result, sensitive methods for their analysis, in different biological matrices, are required.

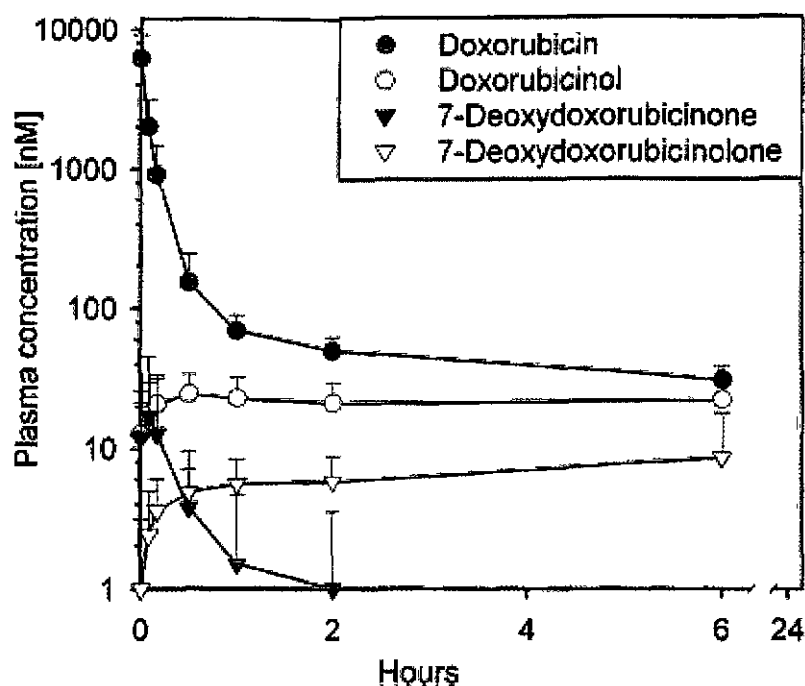


**Figure 5.3** Pharmacokinetic profile of DOX and its metabolites doxorubicinol, 7-deoxydoxorubicinone and 7-deoxydoxorubicinolone after administration of DOX ( $50 \text{ mg m}^{-2}$ ) as 10 min. infusions<sup>[18]</sup>

The peak plasma concentrations of anthracyclines play an important role in their cardiotoxicity.<sup>[14]</sup> The anthracyclines, DAN, DOX and EPI, are highly protein bound in plasma, (60-90%).<sup>[21]</sup> Therefore, methods for the determination of the free drug and bound drug concentrations are required. Separation techniques, such as High Performance Liquid Chromatography (HPLC) and CE, have been used for protein binding studies, and also in drug stability and PK and metabolic studies.<sup>[14,22-24]</sup> In this section, the analysis and separation of anthracyclines will be discussed in detail in Section 5.2 and alternative methods for their analysis will be also be outlined.

## 5.2 ANALYSIS OF ANTHRACYCLINES

The determination of anthracycline antibiotics has been reported in the literature using both HPLC<sup>[25-28]</sup> and CE.<sup>[2,29,30]</sup> DAN, DOX and EPI are most suited to analysis by fluorescence and electrochemical detection due to their native electroactive and fluorescent properties.<sup>[31-33]</sup> The HPLC methods of determination are discussed in Section 5.2.1.

### 5.2.1 HPLC Analysis

HPLC, coupled with electrochemical (EC), fluorescence and laser-induced fluorescence (LIF) is regularly employed for the detection of anthracyclines in biological fluids.<sup>[2,34-36]</sup> The EC detection of anthracyclines was possible due to the presence of oxidisable (phenolic) and reducible (quinone) functional groups. In Section 5.2.1.1, the determination of these anthracyclines with HPLC-EC detection is discussed in detail.

#### 5.2.1.1 HPLC-Electrochemical (HPLC-EC) detection

The simultaneous separation of the anthracycline DAN from its metabolites (*e.g.* daunorubicinol and daunorubicin-aglycone) in human plasma was demonstrated by Akpofure *et al.*, with electrochemical and fluorescence detection.<sup>[37]</sup> In this method, the separation of all analytes was achieved in less than 25 min., with DOX employed as the internal standard. HPLC coupled with EC detection was also applied for the separation of DOX from its metabolites and also DAN from its metabolites in plasma samples.<sup>[33]</sup> From their detection limits, calculated as three times the noise level, this method was reported to be five times more sensitive than the previous method proposed by Akpofure *et al.*<sup>[37]</sup>

The separation of six anthracycline antibiotics in plasma, was reported by Riley using a reversed-phase column.<sup>[31]</sup> For this method a short column was employed (7.5 cm) which resulted in shorter analysis times (10 min.) and also improved sensitivity, with detection limits between 1 and 2 ng ml<sup>-1</sup> obtained.

More recently, Ricciarello *et al.*,<sup>[36]</sup> demonstrated the use of an amperometric-coulometric detection, with two working electrodes for the determination of EPI, DOX and their principal metabolites, as shown in Fig. 5.4. This method was applied to the analysis of EPI, with DOX as the internal standard, in human plasma. Quantitation limits, calculated at  $S/N = 3$ , of  $1 \text{ ng ml}^{-1}$  were obtained for all analytes under investigation.

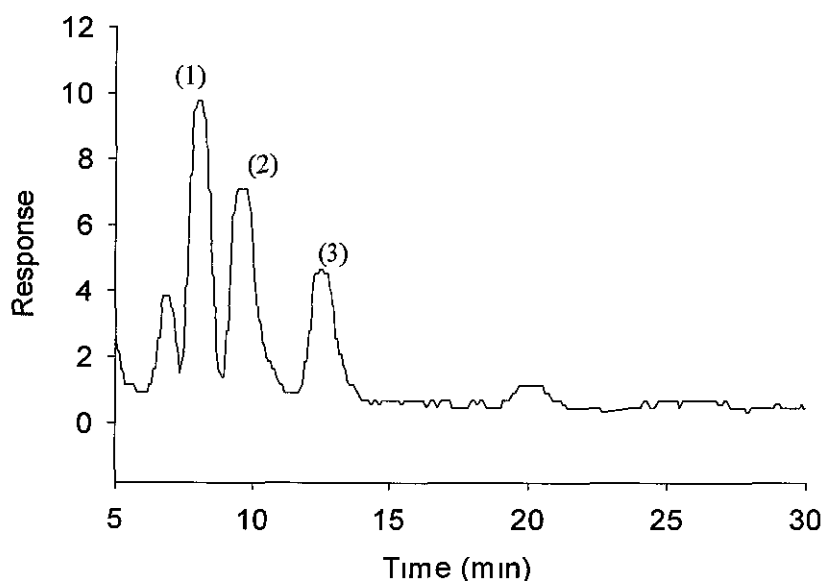


**Figure 5.4** HPLC separation with EC detection of an extract of blank plasma containing (1)  $12 \text{ ng ml}^{-1}$  of 13-*S*-dihydroepirubicin, (2)  $40 \text{ ng ml}^{-1}$  of EPI and (3)  $29.8 \text{ ng ml}^{-1}$  of DOX<sup>[36]</sup>

The methods of analysis discussed in Section 5.2.1.1 demonstrate the ability of electrochemical detection for the determination of anthracyclines in biological samples.<sup>[36,38]</sup> An alternative mode of detection employed for their analysis is fluorescence. Fluorescence detection is ideal as anthracyclines possess native fluorescent properties and therefore do not require derivatisation. HPLC coupled with fluorescence detection is discussed in Section 5.2.1.2.



### 5.2.1.2 HPLC-Fluorescence detection

The analysis of anthracyclines and their metabolites in different biological matrices, such as plasma,<sup>[25,27,39-42]</sup> serum,<sup>[43-45]</sup> urine<sup>[32,46-50]</sup> and murine specimens<sup>[51]</sup> was performed by fluorescence detection. Fluorescence detection provides 1000 times more sensitivity than absorption spectroscopy and is ideally suited for the therapeutic monitoring of anthracyclines.<sup>[35,52-55]</sup> The first report of the analysis of DAN and its metabolite daunorubicinol in plasma was published by Hulhoven and Desager in 1976.<sup>[27]</sup> In this method, their simultaneous separation and quantification was achieved by HPLC-fluorescence with detection limits of 10 ng ml<sup>-1</sup> obtained. The liquid chromatographic analysis of DOX and its metabolites in biological fluids was also achieved by Israel *et al.*, with picomolar limits of detection (LOD) achieved.<sup>[25]</sup> Coupled-column liquid chromatography has also been applied to the analysis of EPI and its metabolites in plasma with an excitation and emission wavelengths of 445 nm and 560 nm respectively, as illustrated in Fig. 5.5. The method developed was applied to the pharmacokinetic monitoring of EPI and its metabolites in biological samples, such as human plasma.<sup>[56]</sup>

A technique for the extraction of anthracyclines from biological fluids, which enabled their HPLC-fluorescence analysis, was developed by Robert.<sup>[26]</sup> This extraction technique was applied to the analysis of both plasma and serum samples. A method was developed for the quantification of cellular concentrations of DOX, with good linearity and reproducibility obtained.<sup>[57]</sup> Fluorescence detection was also successfully applied to the analysis of DOX and its metabolites, in serum samples with detection limits in the ng ml<sup>-1</sup> range obtained,<sup>[43]</sup> in plasma<sup>[58-60]</sup> and in hospital samples.<sup>[61]</sup>

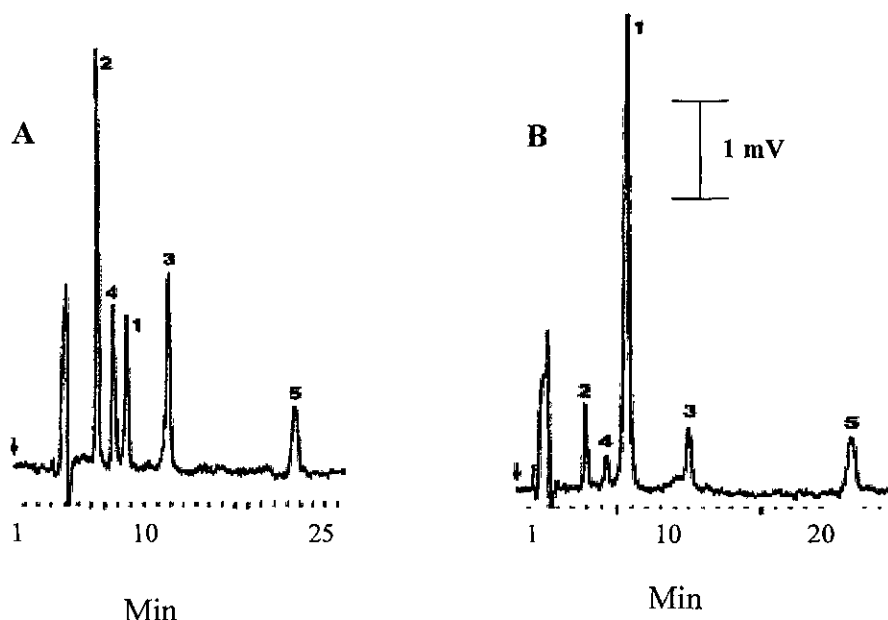


**Figure 5.5** HPLC separation with fluorescence detection for (A) EPI and its metabolites where, 1 = EPI ( $12.4 \text{ ng ml}^{-1}$ ), 2 = epirubicinol ( $16.4 \text{ ng ml}^{-1}$ ), 3 = epirubicin aglycone ( $11.2 \text{ ng ml}^{-1}$ ), 4 = epirubicinol aglycone ( $12.8 \text{ ng ml}^{-1}$ ), 5 = 7-deoxy epirubicinol aglycone ( $16.0 \text{ ng ml}^{-1}$ ), (B) Patient's plasma 15 min. after chemoembolisation, concentrations are 1 =  $40.6 \text{ ng ml}^{-1}$ , 2 =  $3.8 \text{ ng ml}^{-1}$ , 3 =  $5.3 \text{ ng ml}^{-1}$ , 4 =  $2.8 \text{ ng ml}^{-1}$  and 5 =  $7.1 \text{ ng ml}^{-1}$  [56]

The HPLC fluorescence analysis of DOX and EPI and their respective metabolites was reported by Nicholls *et al.* [45] This method enabled low LOD's in serum ( $1 \text{ ng ml}^{-1}$ ) and sample preparation was performed by SPE onto C<sub>8</sub> Bond-Elut cartridges. The use of a microbore column for the analysis of DOX has been reported which allows for enhanced sensitivity and resolution and also results in reduced solvent consumption and waste generation as compared to conventional packed columns. [62] The plasma concentrations of EPI and its metabolites were determined by HPLC coupled with fluorescence detection. The method developed was successfully applied to the analysis of human plasma samples taken during a 96 hour infusion of EPI in a patient with multiple myeloma. [63] Recently, a method was developed for the simultaneous analysis of DOX and its metabolite doxorubicinol in parrot plasma. [63] Fluorescence detection was also employed for the separation of DOX and DAN in urine with detection limits in the low picogram level obtained. [64]

HPLC-fluorescence detection was also applied to the sensitive and selective analysis of DOX, pirarubicin and doxorubicinol in serum. Doxorubicinol is a major metabolite of DOX and as it also causes cardiotoxic effects, a method to detect both of these analytes was desired. Low LOD's ( $2 \text{ ng ml}^{-1}$ ) and limits of quantification (LOQ) ( $0.5 \text{ ng ml}^{-1}$ ) were obtained.<sup>[65]</sup> Recently, a method was developed for the detection of EPI and epirubicinol in plasma and saliva.<sup>[61]</sup>

The analysis of anthracyclines has also been reported using ultra-violet (UV) and mass spectrometry (MS) detection, which are discussed in Sections 5.2.1.3 and 5.2.1.4 respectively.

#### 5.2.1.3 HPLC-Ultra violet (HPLC-UV) detection

A method was developed by Eksborg *et al.*, for the liquid chromatographic determination of DAN and daunorubicinol in plasma from leukaemic patients.<sup>[66]</sup> The separation of DAN and DOX from their respective metabolites was performed, incorporating sodium dodecyl sulphate (SDS) into the mobile phase.<sup>[67]</sup> The addition of SDS into the mobile phase enabled the separation of eight anthracycline derivatives, with improved resolutions, in an isocratic run. Recently, a HPLC method was developed for the simultaneous determination of seven anthracyclines, with high precision and accuracy obtained. The detection limits determined were in the range  $42\text{-}128 \text{ ng ml}^{-1}$ .<sup>[28]</sup>

The determination of bound and free DOX in methacrylamide polymer-drug conjugates was performed by Configliacchi *et al.*, incorporating a diode array detector.<sup>[68]</sup> Polymer-drug conjugates, which possess reduced toxicity and have improved availability at the tumour site, are at the forefront of cancer chemotherapy. Linearity of the method was achieved between  $1$  and  $50 \text{ } \mu\text{g ml}^{-1}$  with detection limits of  $0.5 \text{ } \mu\text{g ml}^{-1}$  obtained. However, the LOD's obtained with UV detection do not represent the PK levels required for the analysis of DOX in plasma, Fig. 5.2. The LOD obtained from this method is sensitive to  $\mu\text{g ml}^{-1}$  concentration levels; however, this does not reflect the therapeutic concentrations ( $5\text{-}50,000 \text{ ng ml}^{-1}$ ) of these antibiotics in biological matrices.

Despite the limitations of UV detection, with respect to sensitivity, it has been regularly been applied to the analysis of anthracyclines in plasma,<sup>[69]</sup> spiked human plasma,<sup>[70]</sup> in blood and urine<sup>[71]</sup> and for hospital samples.<sup>[72]</sup>

#### 5.2.1.4 HPLC Mass spectrometry (HPLC-MS) detection

The simultaneous analysis of the anthracyclines DAN, DOX, EPI and idarubicin, and their respective metabolites, in human serum, was performed using HPLC-electrospray mass spectrometry.<sup>[73]</sup> The compounds were detected in the selected ion monitoring mode, using for quantitation ions  $m/z$  291 for idarubicin and idarubicinol,  $m/z$  321 for DAN and daunorubicinol,  $m/z$  361 for DOX and EPI and  $m/z$  363 for doxorubicinol. The anthracycline aclarubicin was employed as the internal standard, with  $m/z$  of 812, as shown in Fig. 5.6. Low LOD's were obtained (*e.g.* 0.5 ng ml<sup>-1</sup> for DAN and 1 ng ml<sup>-1</sup> for DOX) and the developed method was successfully applied to the simultaneous separation of anthracyclines in serum. Recently, a liquid chromatography-tandem mass spectrometry method was developed for the trace determination of these anthracyclines in urine.<sup>[74]</sup>

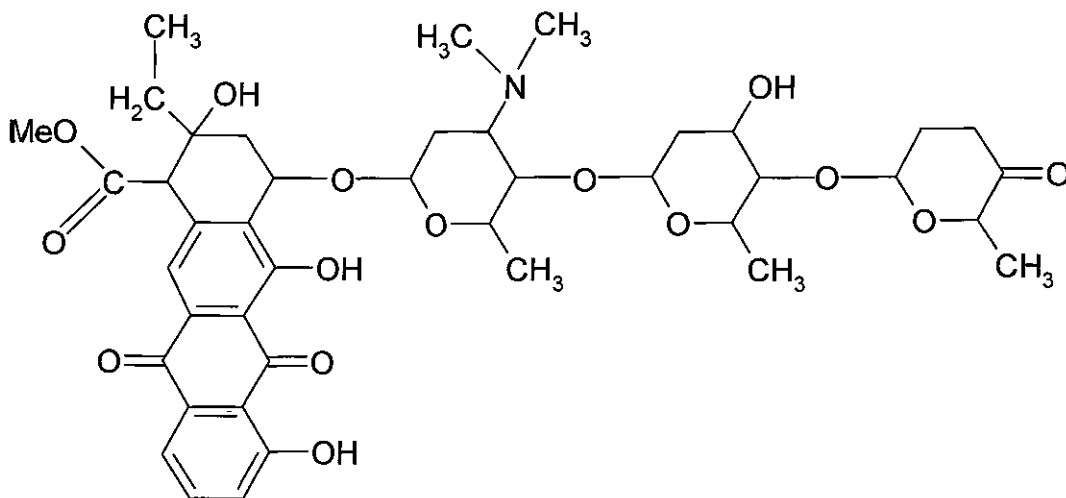


**Figure 5.6** Structure of the internal standard, aclarubicin<sup>[73]</sup>

A liquid chromatography-tandem mass spectrometry (LC-MS/MS) method was developed to identify and quantify DOX in *e.g.*, rat plasma. Low LOQ's of 1.44 ng ml<sup>-1</sup> were obtained and the method was linear over the PK relevant range (0.728-58,300 ng ml<sup>-1</sup>).<sup>[75]</sup> LC-MS/MS was also applied to the analysis of DAN in rat plasma<sup>[76]</sup>, the determination of a prodrug and the active metabolites of DOX<sup>[77]</sup> and EPI in human plasma<sup>[78]</sup> with detection limits of 0.1 ng ml<sup>-1</sup> achieved.

HPLC is the most prevalent method of analysis of anthracyclines. However, CE has recently been employed and offers advantages over the traditional chromatography methods, namely reduced sample volumes and waste and rapid separations. Their analysis by CE is discussed in Section 5.2.2

### 5.2.2 CE Analysis

The most common mode of detection for CE analysis of anthracyclines is fluorescence. As previously discussed in Section 5.2, the analysis of anthracyclines is ideally suited to fluorescence detection due to their native fluorescent properties and the sensitivity of fluorescence enables the therapeutic monitoring of DAN,<sup>[79]</sup> DOX,<sup>[18]</sup> and EPI.<sup>[16]</sup> Recently, the analysis of anthracyclines by CE coupled with EC has been reported, which is discussed in Section 5.2.2.1.

#### 5.2.2.1 Capillary Electrophoresis-Electrochemical (CE-EC) detection

During the extensive literature search for this study, the analysis of anthracyclines by CE-EC was only reported by one research group. In this paper the analysis of the anthracycline DAN by CE coupled with amperometric detection was reported.<sup>[29]</sup> A carbon disk electrode was used as the working electrode (WE), and the electrochemical behaviour of DAN was initially investigated by cyclic voltammetry (CV) in phosphate buffer solution (pH 7.8, 0.15 M). A typical CV of DAN is shown in Fig. 5.6.

In buffer solution only, no anodic peak was observed; however, after the addition of DAN an anodic peak with a peak potential of 0.66 V was detected. This peak was attributed to the oxidation of the double phenolic groups (-OH) on DAN, as

illustrated in Fig. 5.1. From the hydrodynamic voltammogram of DAN, a peak potential of 0.95 V was employed as the detection potential for subsequent analysis.<sup>[29]</sup>

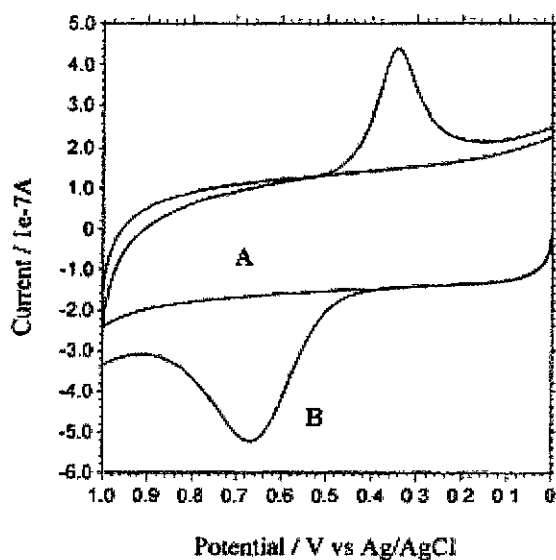


**Figure 5.6** Cyclic voltammogram of DAN at carbon disk electrode in phosphate buffer (pH 7.8, 0.15 M, WE) Reference Electrode (RE): Ag/AgCl (0.03 mM KCl), Auxiliary Electrode (AE): platinum electrode. (A) Buffer solution and (B)  $2 \times 10^{-4}$  M DAN. Scan rate  $0.1 \text{ V s}^{-1}$  <sup>[29]</sup>

The optimum separation conditions were determined to be 0.95 V detection potential, a separation voltage of 8 kV, electrokinetic sample introduction of 8 kV for 10 s employing a phosphate buffer solution (pH 7.8, 0.15 M). A detection limit of  $4.5 \mu\text{g ml}^{-1}$  was obtained and this method was successfully applied to the determination of DAN in human urine, without any sample modification.<sup>[29]</sup>

The application of Laser Induced Fluorescence (LIF) detection to the analysis of anthracyclines is discussed in Section 5.2.2.2.

### 5.2.2.2 Capillary Electrophoresis-Laser-Induced Fluorescence (CE-LIF) detection

The simultaneous separation of DAN, DOX and EPI in human plasma was obtained using CE-LIF detection with a phosphate buffer (100 mM, pH 4.2). An argon-ion excitation laser of 488 nm was employed. The buffer was modified with 70% acetonitrile (ACN), which decreases the interaction with the capillary wall and improved both the peak shape and resolution of DAN, DOX and EPI. The addition of ACN also decreased the conductivity of the buffer and therefore resulted in reduced heat generation inside the capillary. Detection limits of all three anthracyclines were reported in the range of 125 – 250 pg ml<sup>-1</sup>.<sup>[30]</sup>

The therapeutic monitoring of DAN, DOX, idarubicin and their metabolites was obtained by CE-LIF detection for their therapeutic monitoring in human plasma with LOQ of 2 ng ml<sup>-1</sup> obtained.<sup>[80]</sup> Based on work previously carried out by Hempel *et al.*,<sup>[81]</sup> idarubicin was employed as the internal standard, as shown in Fig. 5.7. The method developed enabled the monitoring of DOX plasma levels for several days after dosing,<sup>[80]</sup> and in a recent method by Hempel *et al.*, the quantification of DAN and daunorubicinol in plasma was developed, which enabled their accurate determination in small sample volumes with concentrations as low as 2 ng ml<sup>-1</sup>.<sup>[1]</sup>

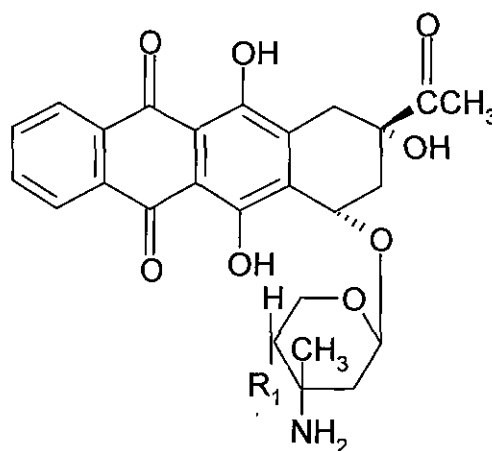


**Figure 5.7** Structure of the internal standard, idarubicin where R<sub>1</sub> is OH functional group<sup>[81]</sup>

Recently, the determination of free and liposomal associated DAN (daunoxome) in plasma was performed. Plasma samples were pre-treated by solid-phase extraction with Sep-Pak C<sub>18</sub> cartridges. Low LOQ's were obtained (1 µg ml<sup>-1</sup>) which is within the acceptable range for PK analysis of this drug.<sup>[82]</sup> In another application of LIF, the stability of DOX and idarubicin in heparin plasma and whole blood was performed and it was determined that DOX and idarubicin concentrations decrease rapidly with time.<sup>[83]</sup>

In a comparison of HPLC-LIF with CE-LIF, the latter was determined to be a more sensitive technique in the detection of DAN and enabled the monitoring of the kinetics of DAN release in Kaposi sarcoma.<sup>[2]</sup> The simultaneous separation of DOX, DAN and idarubicin was performed using a borate buffer which contained 30% ACN.<sup>[7]</sup> The presence of ACN in the buffer improved the separation and also helped decrease the conductivity of the buffer. This method was applied to the analysis of the three anthracyclines in serum samples, as shown in Fig. 5.8. Detection limits of less than 0.9 ng ml<sup>-1</sup> were obtained.

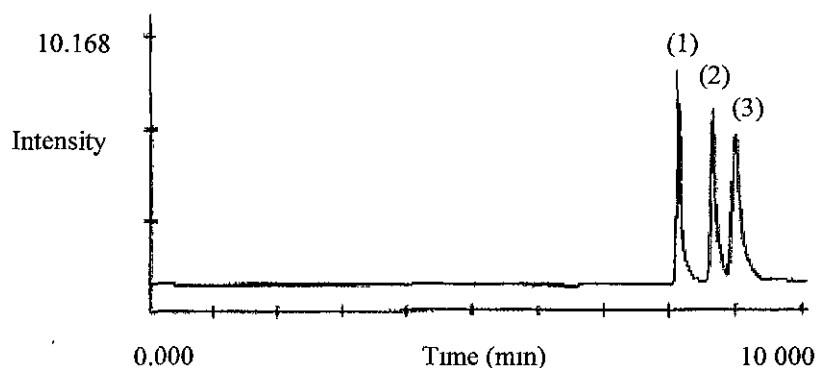


**Figure 5.8** CE-LIF separation, excitation laser 488 nm, of a serum sample spiked with (1)-DAN, (2)-idarubicin and (3)-DOX. (25 ng ml<sup>-1</sup>). Separation voltage 15 kV. Pressure injection (3.45 kPa/5-15 s). Electrophoretic buffer 100 mM borate, pH 9.5, 30% ACN. Effective capillary length 0.5 m x 75 µm internal diameter (i.d.).<sup>[7]</sup>



MEKC and CEC have also been coupled with LIF for the detection and quantification of DOX in cell extracts, single cells, individual nuclei and plasma.<sup>[84-86]</sup> The LOD's were in the zeptomole ( $10^{-21}$  mole) range that enabled the detection of a larger number of metabolites, which will aid in the identification of more efficient and less harmful chemotherapeutic agents. The fluorescence detection of DOX in plasma was also performed using pressurised capillary electrochromatography (CEC)<sup>[87]</sup> with detection limits of  $1.7 \text{ ng ml}^{-1}$  obtained.<sup>[87]</sup>

The application of UV detection to the analysis of anthracyclines is discussed in Section 5.2.2.3. UV detection is a universal mode of detection and is regularly employed for method development.

#### **5.2.2.3 Capillary Electrophoresis-Ultra violet (CE-UV) detection**

In the search for literature for the analysis of anthracyclines by CE-UV only one paper was found. In the analysis of anthracyclines, UV detection is primarily used for method development, due to the lack of sensitivity associated with it. However, sweeping techniques have been incorporated with UV, to further enhance the sensitivity of the separation.<sup>[88]</sup>

Using a sweeping preconcentration step, the anthracycline antibiotic DOX was analysed and quantified incorporating SDS in the buffer electrolyte. The sweeping step preconcentrates a long injected zone of cationic anthracyclines into a narrow zone of negatively charged SDS micelles. The application of this step reduced adsorption of the anthracyclines on the capillary wall, improved the reproducibility of the migration times and the sensitivity of detection. Under these conditions, positively charged anthracyclines migrate towards the zone of SDS micelles. On the boundary of these zones, anthracyclines are solubilised by SDS micelles and the analytes migrate in reverse polarity to the detector. As the sensitivity is enhanced, this method was successfully applied to the determination of therapeutic levels of DOX in real plasma samples. However, there were limitations with this method, which undermined its applicability as a practical CE method. This method did not allow for the simultaneous separation of DAN and DOX and an excessively large sample volume was required for analysis (approx.  $10 \mu\text{l}$ ).<sup>[88]</sup>

#### 5.2.2.4 Alternative methods of analysis

The analysis of DOX hydrochloride by visible spectrophotometry has been reported using four sensitive visible spectrophotometric methods, *e.g.* the first method was based upon the oxidation of the drug with Fe(III) to produce Fe(II). All of the methods developed resulted in concentration measurements, which were reproducible within a Relative Standard Deviation (RSD) of 1%.<sup>[89]</sup>

The fluorescence characteristics of DAN and DOX were investigated by Karukstis *et al.*, in order to assess their distribution in cell membranes.<sup>[90]</sup> Fluorescence detection of DOX was also performed using a fibre optic based fluorescence sensor<sup>[91]</sup> and by excitation-emission matrix fluorescence and multi-way analysis.<sup>[92]</sup> With the fibre optic sensor, detection limits of  $0.057 \mu\text{g ml}^{-1}$  were obtained which were comparable with traditional fluorescence methods of analysis.<sup>[91]</sup> The feasibility of the quantitative determination of DOX by surface-enhanced Raman spectroscopy was performed by Loren *et al*<sup>[93]</sup> This method has illustrated the potential of quantifying DOX in complex sample matrices without sample pretreatment.<sup>[93]</sup>

### 5.3 SCOPE OF RESEARCH

Fundamental to this research is the development of a method for the separation and quantification of anthracyclines that occur in biological matrices, *e.g.* serum and plasma in real time. This will allow for a more accurate and individualised dose regimen. CE has been selected as the separation method as it offers rapid and efficient separations and generates little solvent waste. Most importantly, analysis by CE requires small sample volumes and this is ideal for the detection of anthracyclines as they are carcinogenic and extremely toxic.

In this work, UV detection was employed for the development of the separation of DAN, DOX and EPI in a single run. A comparison of detection limits was performed using both CE-LIF, and CE-EC, with improved detection limits obtained with LIF detection. The CE method developed was applied to the analysis of plasma samples, using various sample preparation steps, such as acetonitrile precipitation and vacuum ultrafiltration (VUF), for the detection of free drug. The determination of bound drug was performed in rat plasma samples using microdialysis with CE-LIF. This method was illustrated to be capable of real time monitoring of DAN, DOX and EPI at therapeutic levels in plasma samples.

## 5.4 MATERIALS AND METHODS

### 5.4.1 Instrumentation

#### 5.4.1.1 *CE-Ultra violet (CE-UV) separations*

All separations were performed on a home built capillary electrophoresis system, equipped with CZE 1000R high voltage power supply (Spellman High Voltage Electronics, NY, USA). The capillary inlet and electrical connections were housed in a Plexiglas safety container with fitted safety interlock. Detection was supplied by UV-vis detector (Thermo Electron Spectra System UV 1000) at 234 nm with a 1 mm flow cell modified for CE. Polyimide-coated fused silica capillaries, (Polymicro Technologies Inc., Phoenix, AZ, USA) of 50  $\mu\text{m}$  internal diameter (i.d.) were employed. The effective length of the capillary utilised was 0.60 m, with a total length of 0.70 m. Sample introduction was performed electrokinetically (17.5 kV) for 5 s. Data acquisition was performed using Chrom and Spec (version 1.5) software. All analysis with the home built system were at ambient temperature.

#### 5.4.1.2 *CE-Electrochemical (CE-EC) separations*

Electrochemical detection was facilitated by LC-4C amperometric detector (Bioanalytical Systems, West Lafayette, IN, USA). A carbon fiber, 33  $\mu\text{m}$  i.d. WE, Ag/AgCl RE and platinum (Pt) wire AE were employed. Data acquisition was performed using Lab View (version 5.1) software.

#### 5.4.1.3 *CE-Laser-Induced Fluorescence (CE-LIF) separations*

All separations were performed on a Beckman P/ACE MDQ instrument (Fullerton, CA, USA), equipped with a modular ZetaLIF 2000 LIF detector (Picometrics, Toulouse, France). A He/Cd 442 nm (33mW) laser with an emission wavelength of 490 nm was employed for all sample analyses (Omnichrome). Polyimide-coated fused silica capillaries, (Polymicro Technologies Inc., Phoenix, AZ, USA) of 50  $\mu\text{m}$  i.d. were employed. The effective length of the capillary utilised was 0.60 m, with a total length of 0.70 m. Sample introduction was performed

electrokinetically (5 kV) for 5 s. Data acquisition was performed using 32 Karat (version 5.0) software.

#### ***5.4.1.4 HPLC-Ultra violet (HPLC-UV) separations***

The HPLC system consisted of a Varian ProStar 230 solvent delivery module, and a Varian ProStar 310 UV detector module (Palo Alto, CA, USA). The system was operated using Varian ProStar 6.0 chromatography software. A Waters Spherisorb ODS2 reversed phase column (4.0 x 250 mm, particle size 5  $\mu\text{m}$ , Waters Millipore, Milford, MA) was employed. An isocratic elution was employed at a flow rate of 1.5 ml  $\text{min}^{-1}$ . All sample analyses were carried out using UV detection at 230 nm with a deuterium lamp.

#### ***5.4.1.5 Electrochemical analysis***

Cyclic voltammetry experiments were performed on CHI 1000 potentiostat (Austin, TX, USA) with CHI 1000 software. A carbon fiber, 33  $\mu\text{m}$  i.d. WE, Ag/AgCl RE and Pt wire AE were employed.

#### ***5.4.1.6 UV-vis analysis***

All UV spectra were obtained on Cary Win UV, dual beam with 2 nm resolution.

### **5.4.2 Chemicals**

HPLC grade methanol (MeOH) and ACN were purchased from Labscan Ltd. (Dublin, Ireland). All other chemicals were of reagent grade. Sodium dodecyl sulphate (436143, SDS,) sodium dihydrogenphosphate (22,9903) and sodium hydroxide (48,0878, NaOH) were obtained from Sigma Aldrich (Tallaght, Dublin). Boric acid (B0394), daunorubicin hydrochloride (D8809), doxorubicin hydrochloride (D1515), 2-hydroxy propyl  $\beta$ -cyclodextrin (389145), methyl  $\beta$ -cyclodextrin (M7564), alpha ( $\alpha$ )-cyclodextrin (C4642), sodium chloride (S9625), potassium chloride (31,0123), magnesium chloride (M4880), calcium chloride (C8106), sodium dihydrogen phosphate

(22,990-3) and disodium hydrogen phosphate (S9763) were obtained from Sigma Aldrich (St. Louis, MO, USA). Epirubicin stock standard was provided by the National Institute of Cellular Biotechnology (N.I.C.B.), D.C.U. Sulfobutyl butyl ether (SBE)<sub>4</sub>  $\beta$ -cyclodextrin was provided by the University of Kansas, Lawrence, KS. Deionised water was treated with a Hydro Nanopure system to specific resistance > 18 M $\Omega$  cm (Millipore, Bedford, MA, USA).

### 5.4.3 Procedures

#### 5.4.3.1 CE Background electrolyte (BGE) preparation

Electrolytes were prepared using deionised water. Three BGE solutions were prepared, which consisted of a borate electrolyte and a chiral selector. A stock solution of 200 mM boric acid was prepared, from which a 105 mM boric acid solution was obtained by dilution of the stock with deionised water. The chiral selectors employed were 2-hydroxy propyl  $\beta$ -cyclodextrin, alpha ( $\alpha$ )-cyclodextrin and sulfobutyl butyl ether (SBE)<sub>4</sub>  $\beta$ -cyclodextrin. Concentrations of 1.75-7 mM 2-hydroxy propyl  $\beta$ -cyclodextrin, 5 mM  $\alpha$ -cyclodextrin and 5 mM sulfobutyl butyl ether (SBE)<sub>4</sub>  $\beta$ -cyclodextrin were prepared by dilution of stock solutions with deionised water. The electrolyte consisted of 30:70 ACN:electrolyte. The pH of the electrolyte was adjusted to 9.0 using 1 M NaOH. Once the buffer was prepared, it was necessary to filter using 0.22  $\mu$ m swinny filter before use.

#### 5.4.3.2 Preconditioning of the CE separation capillary

The separation capillaries were preconditioned as described in Chapter 2 in Section 2.3.3.3.

#### 5.4.3.3 Preparation of HPLC mobile phase

The mobile phase for HPLC-UV was prepared by mixing buffer A (phosphate, pH 2.0) with SDS in the range 0.2-0.4%, with solvent B (MeOH:ACN, 50:50). The composition of the mobile phase was buffer A:solvent B= 40/60.<sup>[28]</sup> All mobile phases

were vacuum filtered using 47 mm Pall Nylaflo nylon membranes with 0.45  $\mu\text{m}$  pore size and stirred overnight prior to use to ensure complete degassing.

#### **5.4.3.3 Preparation of plasma samples**

The analysis of anthracyclines was performed in rat plasma samples. Blood samples were centrifuged (Fisher Scientific, Microcentrifuge 235C) at 4000 g for 10 min. The supernatant layer (plasma) was removed and transferred to microcentrifuge vials (Fisher Scientific, NC966056) for analysis.

#### **5.4.3.4 Determination of free drug by Vacuum ultrafiltration (VUF)**

Ultrafiltration probes were made from polyacrylonitrile (PAN) membrane (250  $\mu\text{m}$  i.d, 150  $\mu\text{m}$  outer diameter (o.d.) with a molecular weight cut off 30 kDa, Filtral AN 69HF, 10 mm). The PAN membrane was cut at an angle and to both ends of this; polyimide tubing (175.3  $\mu\text{m}$  i.d., 223.5  $\mu\text{m}$  o.d., 15 cm, Microlumen, Tampa, FL) was inserted. This was UV cured in place by UV glue and lamp (ELC-450 UV Light System).

Once the polyimide tubing was UV cured, both ends were placed in tygon tubing (Norton Performance Plastics) and also UV cured in place. The probe was now successfully made and threaded through a hub assembly (Bioanalytical Systems, West Lafayette, IN, USA). The hub assembly consisted of a needle, through which the tygon tubing was threaded, into the sample collection container. Sample collection was performed under vacuum, using a BD vacutainer (Fisher Scientific, 366397, 10.25 x 64 mm, 3 ml draw). The probe was placed in the plasma sample and samples were left overnight in fridge. The flow of the sample through the tubing was determined to be 0.25 ml/hr. Once the samples were filtered, they were stored in microcentrifuge tubes (Fisher Scientific, NC966056) at  $-20\text{ }^{\circ}\text{C}$  until required.

#### **5.4.3.5 Determination of bound drug by microdialysis**

Microdialysis probes were made as in Section 5.4.3.4, with the exception that only one end of the polyimide tubing was inserted into tygon tubing (Norton Performance Plastics, 1 cm) and this was UV cured in place. The tygon tubing was inserted into a syringe needle, which was placed on a CMA/100 microsyringe pump (CMA/Microdialysis AB, Stockholm, Sweden). The probe was perfused with an artificial Cerebrospinal Fluid (aCSF) solution (147 mM NaCl, 3 mM KCl, 1 mM MgCl<sub>2</sub>, 1.3 mM CaCl<sub>2</sub>, 0.2 mM NaH<sub>2</sub>PO<sub>4</sub> and 1.3 mM Na<sub>2</sub>HPO<sub>4</sub> dissolved in deionised water) at a flowrate of 2 µl min<sup>-1</sup>. Microdialysate samples were collected in plastic vials and analysed at 10 min. intervals.

#### **5.4.3.6 Preparation of stock solutions and standards**

Stock solutions of DAN and DOX (2 mg ml<sup>-1</sup>) were prepared in MeOH and stored at -20 °C. Stock solutions of EPI (2 mg ml<sup>-1</sup>) were prepared in water and stored at 4 °C and were stable for one month. From this stock solution of EPI, a 1 mg ml<sup>-1</sup> standard was prepared in methanol and stored at -20 °C. Standards of known concentration were prepared by dilution of the stock standards with 10:90 ACN / buffer.



## 5.5 RESULTS AND DISCUSSION

### 5.5.1 Development of CE separation

The choice of electrolyte is critical to the success of separations by CE. Based on work reported by Perez-Ruiz *et al.*, a borate buffer was employed.<sup>[7]</sup> It is essential that the pH of the electrolyte approximates to the  $pK_a$  of the electrolyte, which for borate was 9.24.<sup>[94]</sup> All anthracyclines possess a sugar amino group, daunosamine, which undergoes protonation, and phenolic groups which are liable to ionisation in alkaline media. The  $pK_a$  values of the anthracyclines are shown in Table 5.1. From the  $pK_a$  values, it is evident that DOX has a higher  $pK_a$  than its epimer. As a result, under physiological conditions, a higher proportion of DOX will be in the ionised form and therefore its uptake by cells will be reduced. In contrast EPI, will have a higher proportion of non-ionised drug than DOX at any pH. The implication of this is that EPI will penetrate cells more easily than DOX under the same conditions. DOX and EPI differ in the configuration of the 4'OH group. In DOX, this group undergoes hydrogen bonding with the amino,  $NH_2$  group. This interaction allows for the ionisation of the  $NH_2$  group and therefore gives DOX a higher  $pK_a$  than EPI.<sup>[95]</sup>

**Table 5.1** The  $pK_a$  values for DAN, DOX and EPI<sup>[95]</sup>

Anthracycline	$pK_a$
DAN	8.43, 8.5
DOX	8.22, 8.34
EPI	7.7, 8.08

The order of migration was determined to be DAN, DOX and EPI. A pH of 9.0 resulted in the greatest resolution ( $R$ ) between DOX and EPI, ( $R = 0.3$ ) and was therefore used in subsequent optimisation of the separation, Fig. 5.9. As DOX and EPI are epimers of each other, they migrate at very similar times, and as a result baseline resolution was not achieved using conventional CE. In order to improve the resolution between these analytes, a chiral selector was added to the electrolyte, Section 5.5.1.1.

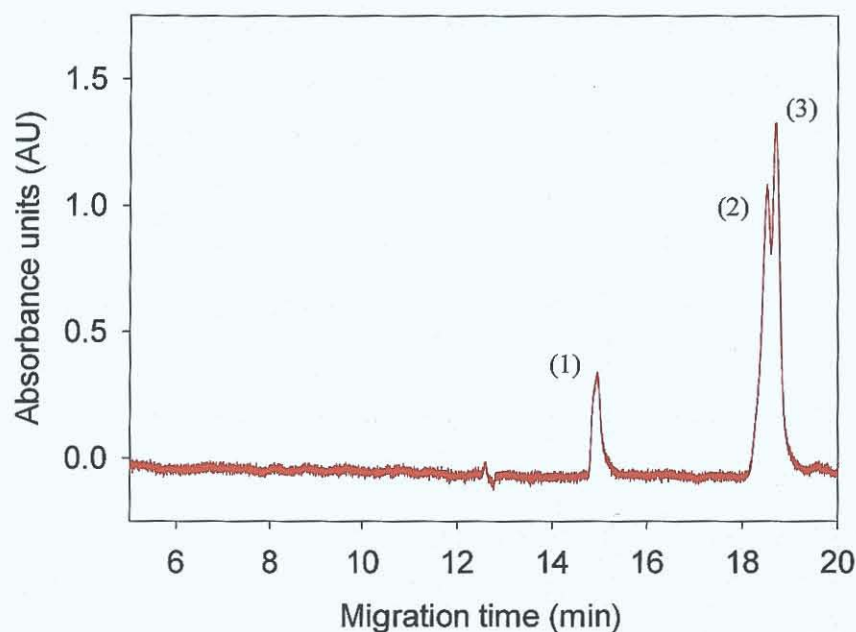


**Figure 5.9** CE separation with direct UV detection at 234 nm for the analysis for the analysis (1) DAN ( $95 \mu\text{g mL}^{-1}$ ), (2) DOX ( $100 \mu\text{g mL}^{-1}$ ), and (3) EPI ( $100 \mu\text{g mL}^{-1}$ ). Separation voltage 17.5 kV, electrokinetic injection 17.5 kV / 5 s. Buffer: 105 mM borate, 30% ACN, pH 9.0. Effective capillary length 0.60 m.

#### 5.5.1.1 Addition of chiral selectors

Cyclodextrins (CD) are the most regularly employed chiral selectors in CE.<sup>[96]</sup> They are non-reducing oligosaccharides consisting of six, seven or eight glucose units, which correspond to  $\alpha$ -,  $\beta$ - and  $\gamma$ -respectively.<sup>[97]</sup> These are known as the native CD's that are capable of forming inclusion complexes with other hydrophobic molecules. Fig. 5.10 illustrates the structure of  $\beta$ -CD. Native CD's may be derivatised with hydrophobic

(e.g. methyl or propyl) or hydrophilic groups (e.g. sulphate, phosphate) which improves further the complex forming ability and selectivity towards certain analytes.<sup>[98]</sup>

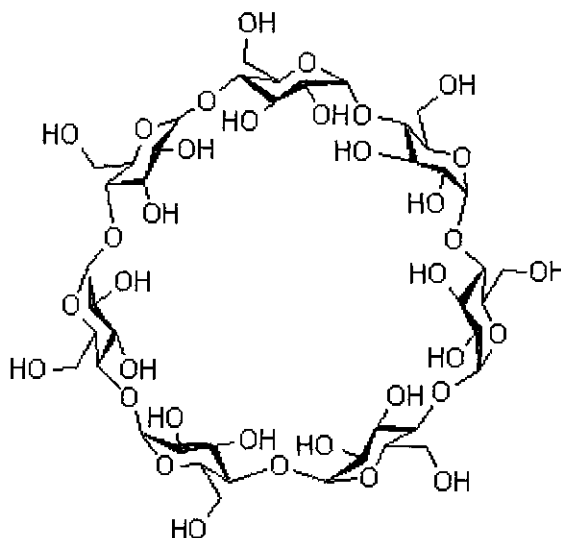


**Figure 5.10** Structure of  $\beta$ -cyclodextrin (reproduced from [www.chemblink.com](http://www.chemblink.com))

The use of charged CD's as chiral selectors has been reported,<sup>[99,100]</sup> and in order to help in the separation of DOX and EPI, the addition of a charged and derivatised CD was investigated, as illustrated in Fig. 5.11. In the analysis of the anthracyclines with the charged CD, the separation of DOX and EPI was improved somewhat but baseline resolution was not obtained, ( $R=0.6$ ), as shown in Fig. 5.11.

Alpha ( $\alpha$ ) CD was added to the electrolyte and its effect on the separation is shown in Fig. 5.12. Poor peak shape of DAN, DOX and EPI was obtained with  $\alpha$ -CD, and following this, their analysis was performed with varying concentrations of the derivatised CD, 2-hydroxy propyl  $\beta$ -CD.

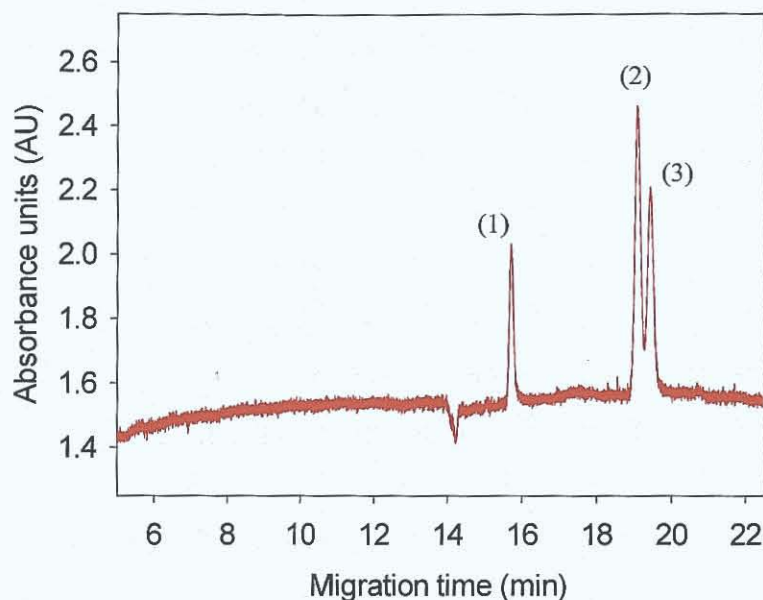


**Figure 5.11** Effect of the addition of chiral selectors on the separation of (1) DAN ( $95 \mu\text{g mL}^{-1}$ ), (2) DOX ( $30 \mu\text{g mL}^{-1}$ ), and (3) EPI ( $20 \mu\text{g mL}^{-1}$ ). Separation voltage 17.5 kV, electrokinetic injection 17.5 kV / 5 s with direct UV detection at 234 nm. Buffer: 105 mM borate, 5 mM SBE<sub>4</sub>  $\beta$ -CD, 6 mM methyl  $\beta$ -CD, 30% ACN, pH 9.0. Effective capillary length 0.60 m

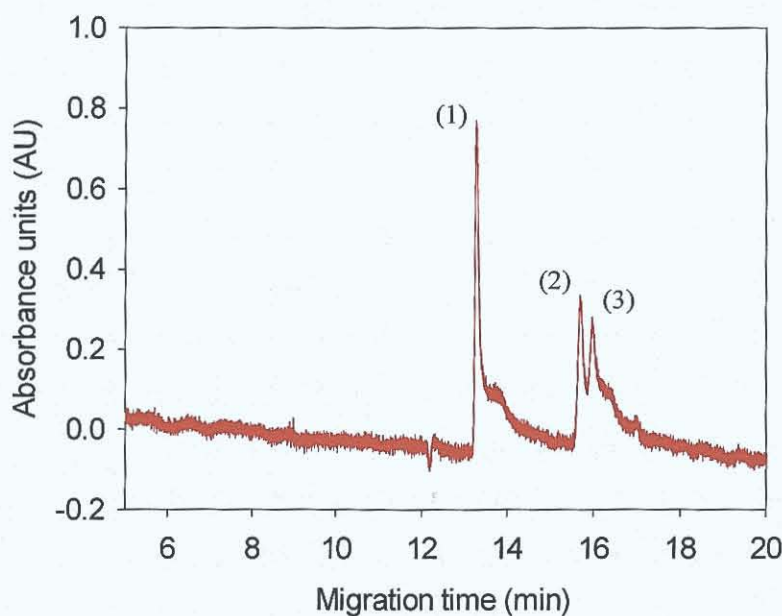


**Figure 5.12** Effect of the addition of a chiral selector on the separation of (1) DAN ( $95 \mu\text{g mL}^{-1}$ ), (2) DOX ( $30 \mu\text{g mL}^{-1}$ ), and (3) EPI ( $20 \mu\text{g mL}^{-1}$ ). Separation voltage 17.5 kV, electrokinetic injection 17.5 kV / 5 s with direct UV detection at 234 nm. Buffer: 105 mM borate, 5 mM  $\alpha$ -CD, 30% ACN, pH 9.0. Effective capillary length 0.60 m

Derivatised CE's are suited to the analysis of anionic and cationic compounds and the effect of the addition of the CD 2 hydroxy-propyl  $\beta$ -CD, in the range 1.75-7 mM on the resolution of the anthracyclines was studied, the results of which are shown in Fig. 5.13. The solubility of the CD was reached at 7 mM and above this concentration the CD was not soluble in deionised water. It was found that the optimum concentration of 2-hydroxy propyl  $\beta$ -CD was 3.5 mM and therefore this was employed for subsequent work, Fig. 5.14.

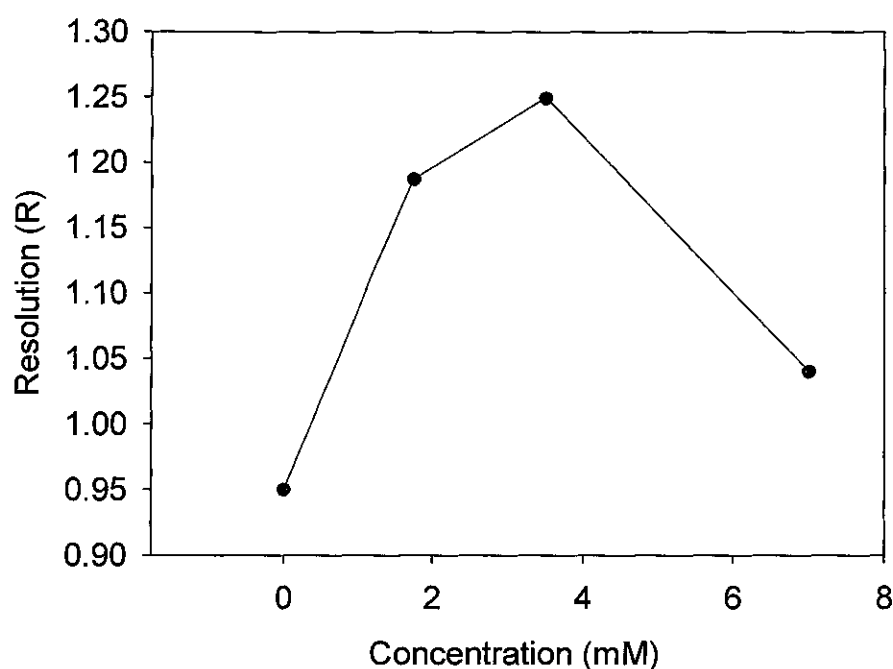


**Figure 5.13** Graphical illustration of the resolution calculated at various concentrations of 2-hydroxy propyl  $\beta$ -CD. Unless stated otherwise all operating conditions as in Fig 5 9

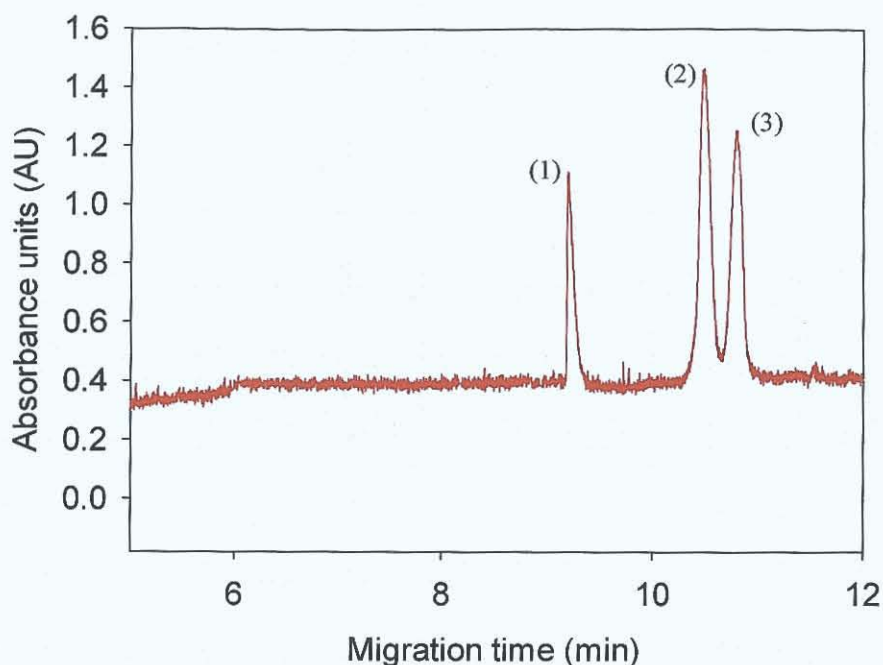


**Figure 5.14** Optimised CE separation of (1) DAN ( $95 \mu\text{g mL}^{-1}$ ), (2) DOX ( $30 \mu\text{g mL}^{-1}$ ), and (3) EPI ( $20 \mu\text{g mL}^{-1}$ ). Separation voltage 17.5 kV, electrokinetic injection 17.5 kV / 5 s with direct UV detection at 234 nm. Buffer: 105 mM borate, 3.5 mM 2-hydroxy propyl  $\beta$ -CD, 30% ACN, pH 9.0. Effective capillary length 0.60 m

#### 5.5.1.2 Optimum separation conditions

From the resolution values calculated, the optimum separation conditions determined were 105 mM borate, 30% ACN, 3.5 mM 2-hydroxy propyl  $\beta$ -CD, pH 9.0, a separation voltage of 17.5 kV. Sample introduction was performed electrokinetically (17.5 kV / 5 s). From a study of the UV spectra, direct detection at 234 nm was employed, as shown in Fig.'s 5.14 and 5.15, for their determination.

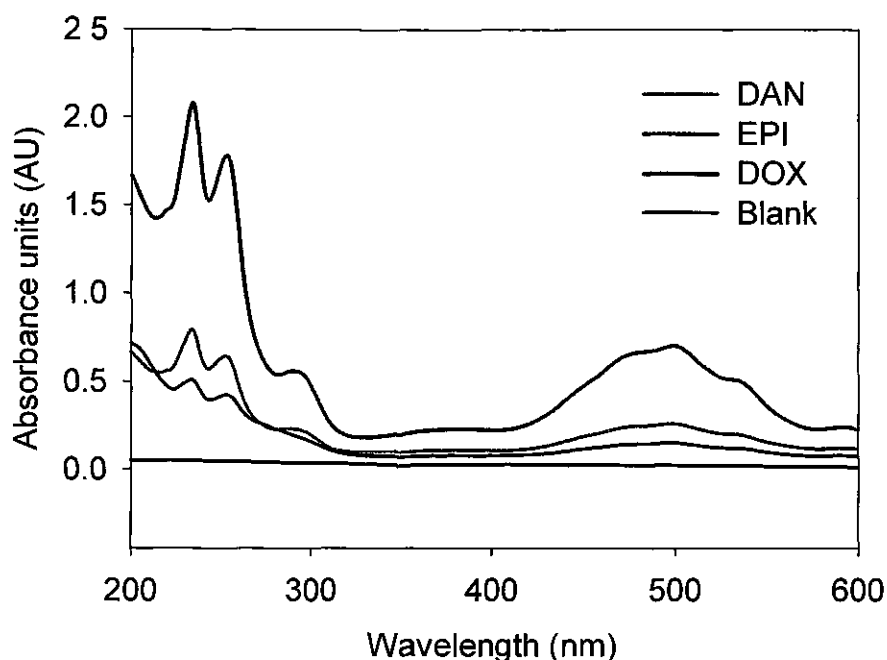


**Figure 5.15** UV spectra of DAN ( $28 \mu\text{g ml}^{-1}$ ), DOX ( $29 \mu\text{g ml}^{-1}$ ) and EPI ( $29 \mu\text{g ml}^{-1}$ ), in electrolyte. Buffer electrolyte was 105 mM borate, 3.5 mM 2-hydroxy propyl  $\beta$ -CD, 30% ACN, pH 9.0

The CE-UV method developed was then applied to the analysis of rat plasma samples.

## 5.5.2 Application to plasma samples

### 5.5.2.1 Direct injection of plasma samples

For real time monitoring, it was preferred that minimum sample pre-treatment was carried out. As a result, the direct injection of rat plasma spiked samples of anthracyclines was investigated, Fig. 5.16. However, it was evident from this investigation that the length of analysis was greater (35 min.), and the separation of DOX and EPI was not obtained. This was a direct result of the extensive protein binding of anthracyclines.<sup>[21]</sup> Therefore, for the analysis of anthracyclines in plasma, a sample preparation step was required, which would remove the protein content from the sample without affecting the anthracyclines. In this work, vacuum ultrafiltration (VUF) was employed, Section 5.5.2.2, to investigate the free drug concentration.

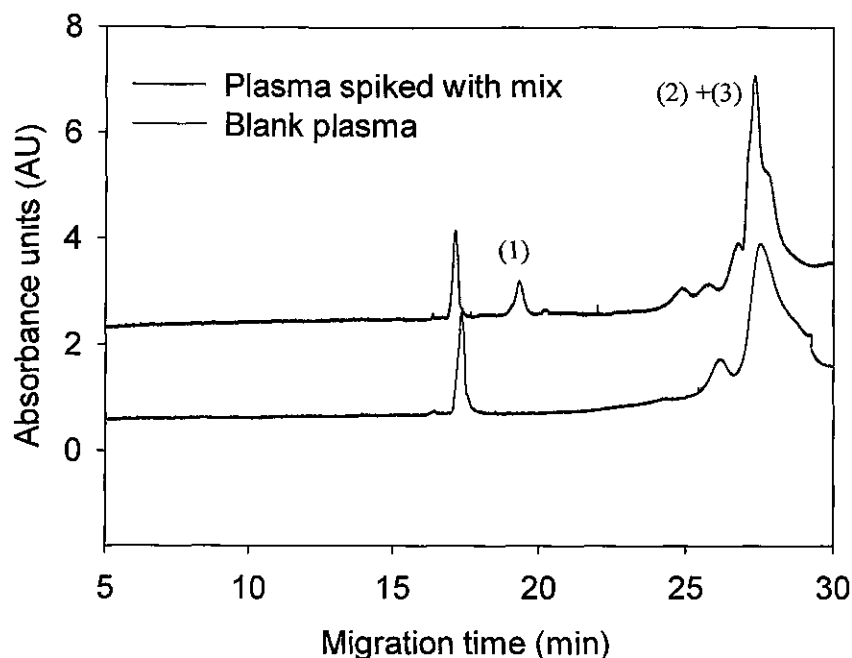


**Figure 5.16** Analysis of rat plasma spiked with (1) DAN ( $95 \mu\text{g mL}^{-1}$ ), (2) DOX ( $100 \mu\text{g mL}^{-1}$ ), and (3) EPI ( $100 \mu\text{g mL}^{-1}$ ) All operating conditions as in Fig. 5.14, direct UV detection at 234 nm. Effective capillary length 0.60 m. The spiked plasma trace is offset by 2 AU

#### 5.5.2.2 Vacuum Ultrafiltration (VUF) of plasma samples

The driving force for VUF sampling is the application of a vacuum, to pull the bulk solution into the ultrafiltration probe.<sup>[101]</sup> An illustration of the VUF process is shown in 5.17. The polyacrylonitrile (PAN) membrane contains tiny pores, which allowed smaller molecules, *e.g.* DOX and EPI, to flow through the probe. DOX and EPI were carried with the bulk flow of the solution. The PAN membrane employed had a molecular weight cut off of 30 kDa. The application of VUF to the analysis of free drug concentration of anthracyclines has not been reported previously in literature.



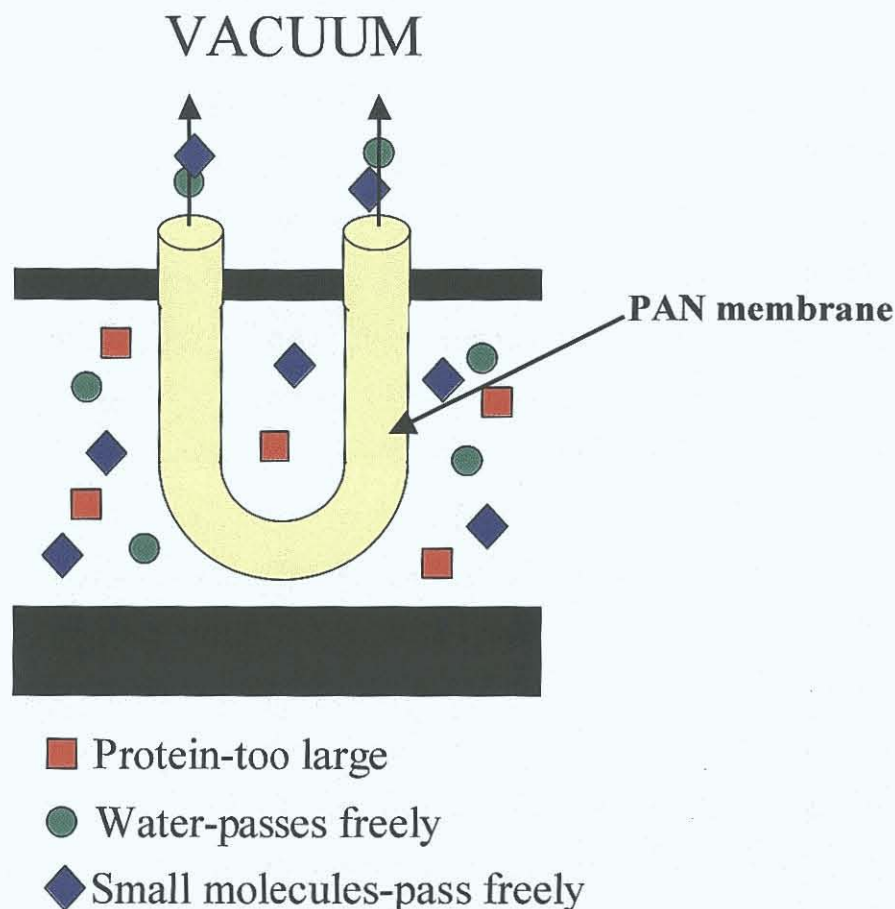


**Figure 5.17** Illustration of the VUF process, showing the flow of smaller molecules and water through the PAN membrane (reproduced from [www.bioanalytical.com](http://www.bioanalytical.com))

The plasma samples were spiked with known concentrations of DAN, DOX and EPI prior to VUF, Fig. 5.18. However, free drug concentrations of DAN, DOX and EPI were not detected using VUF coupled with CE-UV as shown in Fig. 5.18. Therefore, a more sensitive mode of detection was required, which would reflect the therapeutic concentrations (5-50,000 ng ml<sup>-1</sup>) of anthracyclines in plasma.<sup>[18]</sup> Anthracyclines are electroactive species that possess electron donating phenolic groups and an electron accepting quinone group,<sup>[7]</sup> and as a result the potential of applying electrochemical detection, which is a rapid and inexpensive technique, to their analysis was investigated.

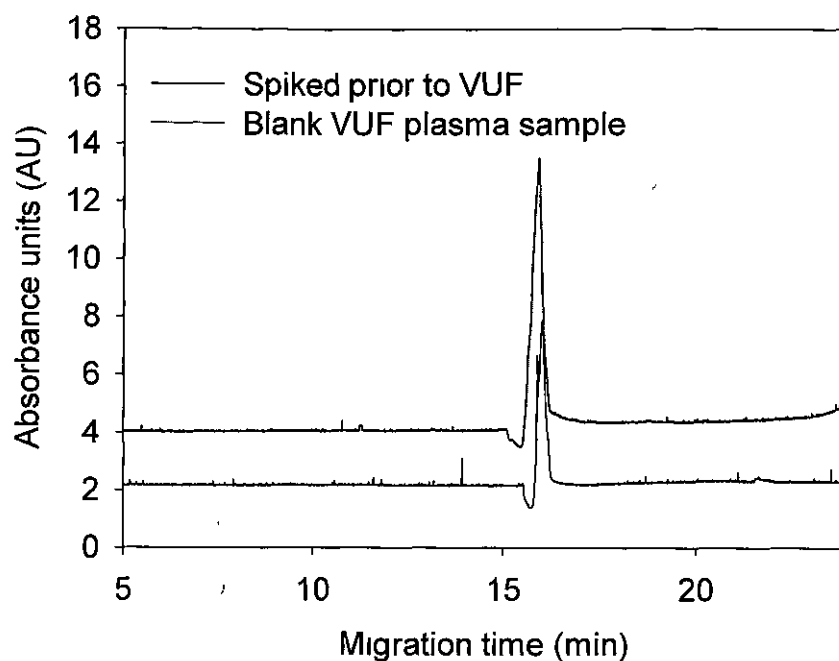


**Figure 5.18** CE analysis of rat plasma spiked with DAN ( $95 \mu\text{g mL}^{-1}$ ), DOX ( $100 \mu\text{g mL}^{-1}$ ) and EPI ( $100 \mu\text{g mL}^{-1}$ ) prior to VUF. No analytes were detected. Unless stated otherwise all operating conditions as in Fig.5 14, with direct UV detection at 234 nm. Effective capillary length 0.60 m. The spiked plasma sample is offset 2 AU

### 5.5.3 Electrochemical (EC) detection

There is only one report in literature on the CE-EC analysis of anthracyclines. In this paper, the electrochemical detection of DAN was performed using a carbon disk electrode as the WE. In this research, on-column detection with a cellulose acetate decoupler and a carbon fiber WE was employed. An illustration of the electrochemical detection employed is shown in Fig. 5.19.

In EC detection, it is necessary to separate the separation ( $\mu\text{A}$ ) and detection current (pA). This is achieved on-column with the addition of a decoupler. The working electrode is inserted into the capillary and the distance between this and the decoupler must be controlled, too short and the resistance is too high and too long and band-broadening starts to occur. However, most decouplers cannot shunt all of the current with the most effective decouplers maximising their surface area. With on-column CE-EC low LOD's have been reported. <sup>[102,103]</sup>

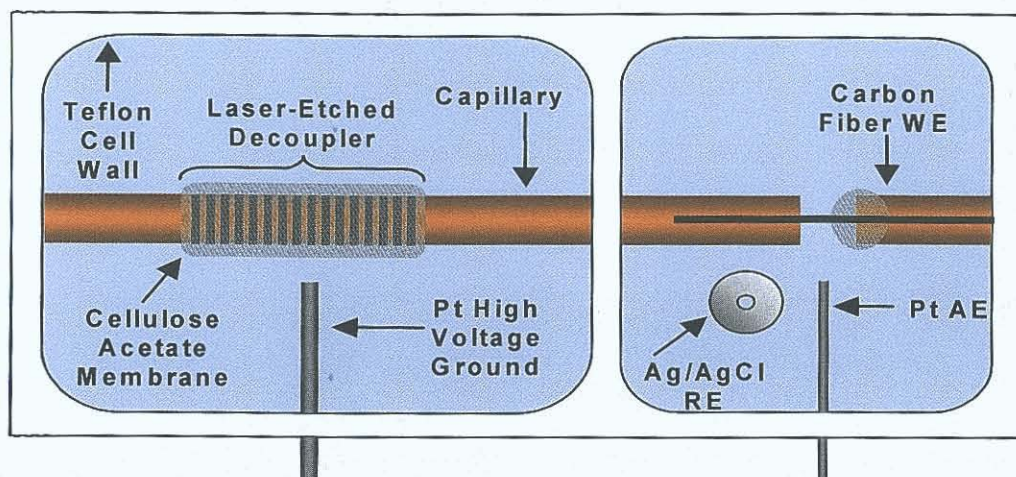


**Figure 5.19** Illustration of an electrochemical cell with an on-column decoupler and carbon fiber WE, (33  $\mu\text{m}$  i.d.)<sup>[104]</sup>

An electrochemical characterisation of the anthracyclines was performed using cyclic voltammetry. Cyclic voltammograms (CV) were performed for each individually and are shown in Fig. 5.20. From Fig. 5.20, it was found that each of the anthracyclines are electrochemically active and undergo irreversible oxidation between 0.2 and 0.6 V vs Ag/AgCl.

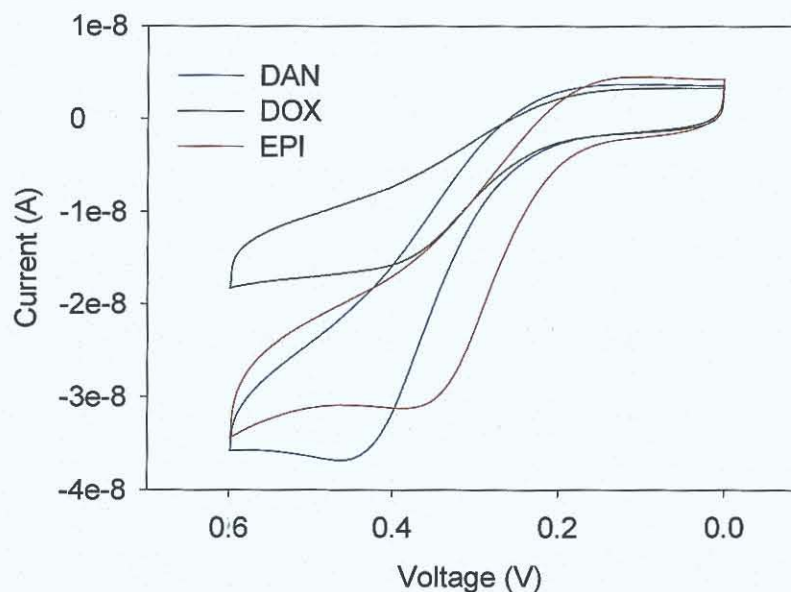


**Figure 5.20** CVs of DAN, DOX and EPI in buffer electrolyte of 105 mM borate, 3.5 mM 2-hydroxy propyl  $\beta$ -CD, 30% ACN, pH 9.0, with carbon fiber WE vs. Ag/AgCl RE at a scan rate of  $50 \text{ mV s}^{-1}$

As DAN, DOX and EPI are never administered together, the optimisation was initially carried out with DAN and DOX, with DAN as the internal standard.<sup>[36]</sup> Also, as DOX and EPI were not present in the same sample, the CD was removed from the buffer electrolyte. A hydrodynamic voltammogram (HDV) was performed to determine the optimum detection potential for their separation, as illustrated in Fig. 5.21. A detection potential of 300 mV was employed and the optimum separation is shown in Fig. 5.22.

A comparison of the LOD's determined with UV and EC detection is illustrated in Table 5.2. The LOD's were calculated from the blank plus three times the standard deviation. However, EC detection did not facilitate the therapeutic monitoring (5-50,000 ng ml<sup>-1</sup>) of the anthracyclines because of the LOD's obtained. Therefore, it was necessary to apply an alternative mode of detection with even lower LOD, *i.e.* fluorescence, to their analysis. Anthracyclines possess native fluorescence and their analysis by fluorescence is widely reported.<sup>[1,19,80]</sup>

**Table 5.2** The LOD's and LOQ's calculated for DAN, DOX and EPI for UV and EC detection

Analyte	UV ( $\mu\text{g ml}^{-1}$ )	% RSD (n=3)	EC ( $\mu\text{g ml}^{-1}$ )	% RSD (n=3)
DAN	14.0	6.2	2.8	2.1
DOX	12.0	7.3	1.2	2.9
EPI	13.6	5.7	N/A	N/A

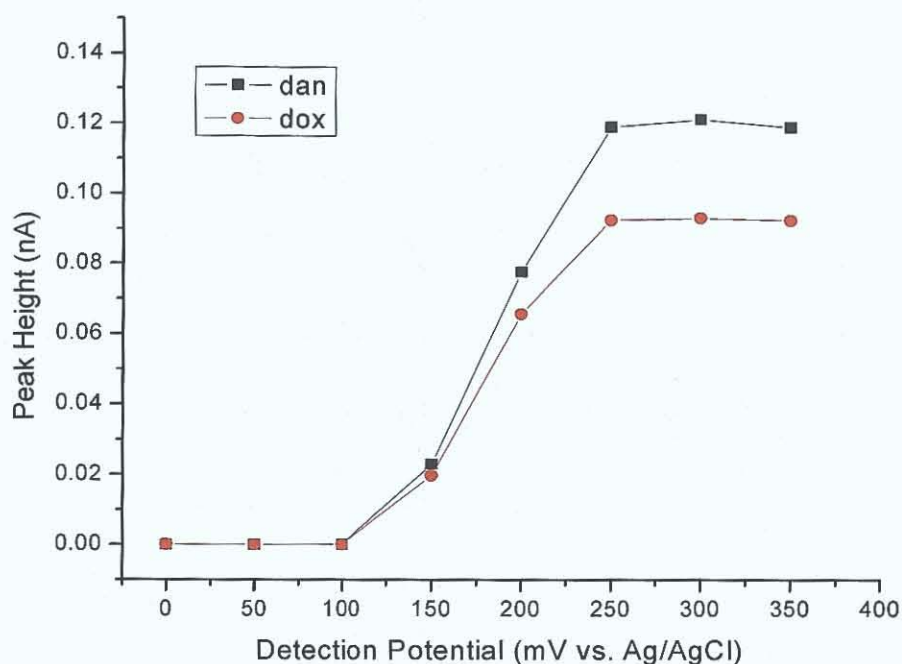


**Figure 5.21** Hydrodynamic voltammogram of DAN ( $5.6 \mu\text{g mL}^{-1}$ ) and DOX ( $2.9 \mu\text{g mL}^{-1}$ ) with carbon fiber WE vs. Ag/AgCl RE. Buffer: 50 mM borate, 10% ACN, pH 9.0. Effective capillary length 0.65 m

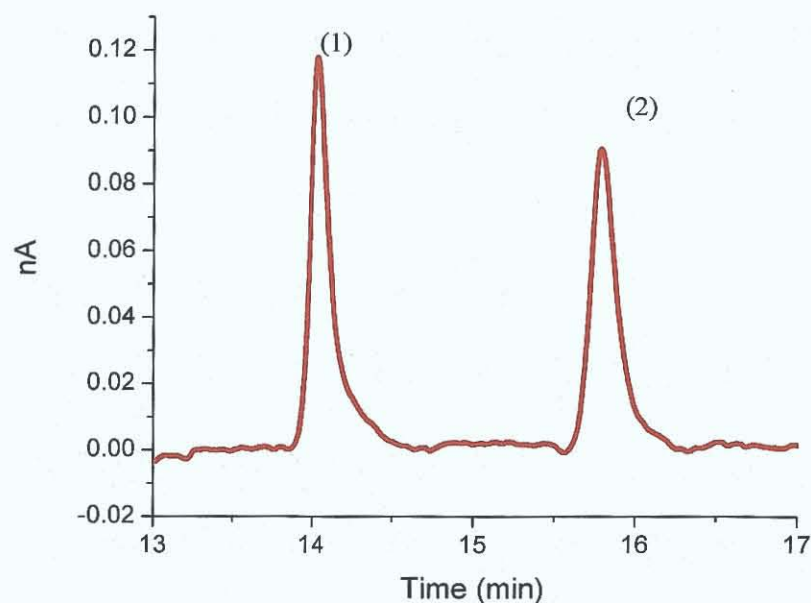


**Figure 5.22** CE separation with EC detection at a detection potential of 300 mV vs. Ag/AgCl RE of (1) DAN ( $5.6 \mu\text{g mL}^{-1}$ ) and (2) DOX ( $2.9 \mu\text{g mL}^{-1}$ ) with carbon fiber WE. Separation voltage 17.5 kV, electrokinetic injection 17.5 kV / 5 s. Buffer: 50 mM borate, 10% ACN, pH 9.0. Effective capillary length 0.65 m

#### 5.5.4 Laser-Induced Fluorescence (LIF) detection

Fluorescence detection is ideal as anthracyclines possess native fluorescent properties and therefore do not require derivatisation.<sup>[7,90]</sup> Using the conditions optimised for UV detection the analysis of DAN, DOX and EPI was performed and is illustrated in Fig. 5.23.

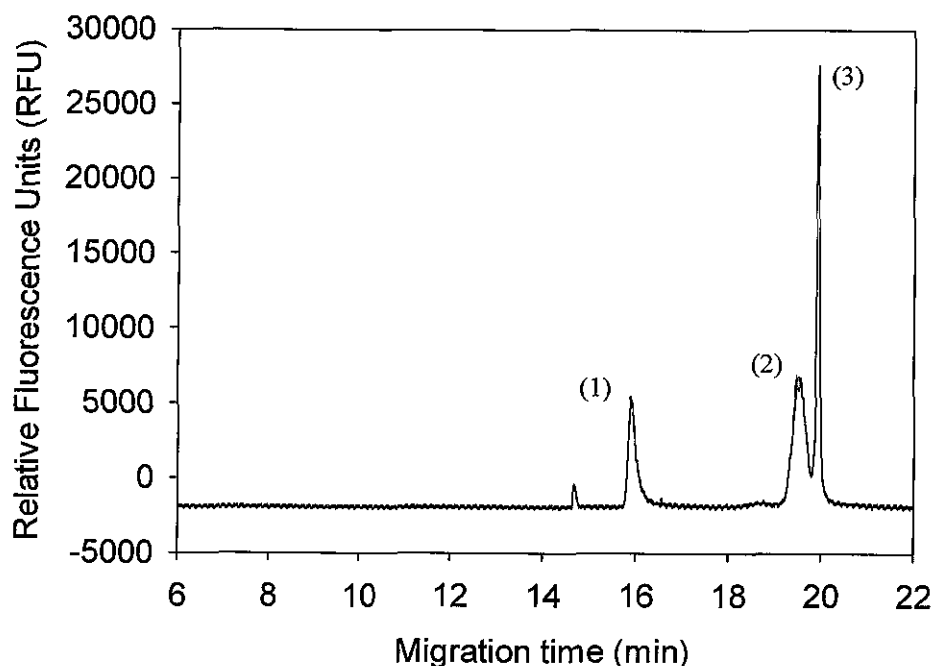


**Figure 5.23** CE-LIF separation, excitation laser 442 nm of (1) DAN ( $5.6 \mu\text{g ml}^{-1}$ ), (2) DOX ( $5.8 \mu\text{g ml}^{-1}$ ) and (3) EPI ( $8.7 \mu\text{g ml}^{-1}$ ). Separation voltage 17.5 kV, electrokinetic injection 5 kV / 5 s. Buffer: 105 mM borate, 3.5 mM 2-hydroxy propyl  $\beta$ -CD, 30% ACN, pH 9.0. Effective capillary length 0.60 m

A comparison of the LOD's determined with UV, EC and LIF detection are illustrated in Table 5.3. Improved detection limits in the range of 150-1400  $\text{ng ml}^{-1}$  were obtained with LIF detection, which were low enough to allow for the therapeutic monitoring of the anthracyclines. However, the LOD's determined were not capable of detection in the 5-150  $\text{ng ml}^{-1}$  range. The developed method was applied to the analysis of plasma samples. Using microdialysis, the extent of protein binding in plasma was performed, Section 5.5.5.



**Table 5.3** The LOD's calculated for DAN, DOX and EPI for UV, EC and LIF detection

Analyte	UV ( $\mu\text{g ml}^{-1}$ )	EC ( $\mu\text{g ml}^{-1}$ )	LIF ( $\mu\text{g ml}^{-1}$ )
DAN	14.0	2.8	1.4
DOX	12.0	1.2	0.3
EPI	13.6	N/A	0.15

### 5.5.5 Determination of protein binding in plasma

The extent of protein binding of drugs in plasma has previously been determined using ultrafiltration and equilibrium dialysis.<sup>[105-108]</sup> CE requires a small sample volume for analysis, and is therefore an ideal separation technique to couple to microdialysis, which produces only a few  $\mu\text{l}$  of sample. Microdialysis is a membrane based sampling technique, which is based upon the concentration gradient alone, *i.e.*, either an electrical field or an ionic strength gradient across the membrane. The dialysate contains the sample under investigation, so the sampled system may be a living system or even a portion into which the microdialysis probe is inserted. The probe is perfused slowly with a sampling solution, (the perfusate), whose ionic strength and pH are close to that of the system under investigation. The flow rate was maintained by a syringe pump, and in this study, the perfusate employed was an aCSF solution, which is a saline solution. The dialysis membrane, *i.e.*, the polyacrylonitrile (PAN) membrane, which had a molecular weight cut off of 30 kDa, was permeable to small molecules, (*e.g.* DAN, DOX and EPI), but did not allow macromolecules such as proteins to pass through. A digital image of the PAN membrane employed (10 mm) is illustrated in Fig. 5.24. Analytes that diffuse through were collected into a collection vial.<sup>[109]</sup> VUF differs from microdialysis in that a vacuum is constantly applied to the probe, in contrast for

microdialysis sampling a solution is pumped through the probe at a constant flow rate. The coupling of CE to microdialysis for the determination of protein binding of anthracyclines in plasma has not been reported in the literature previously.

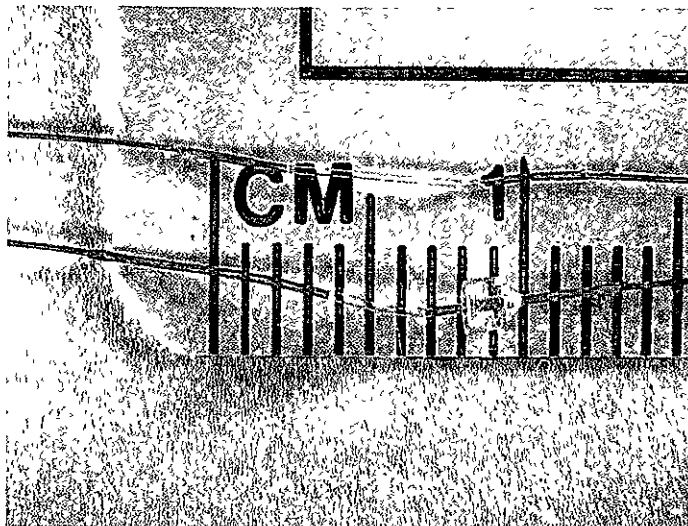
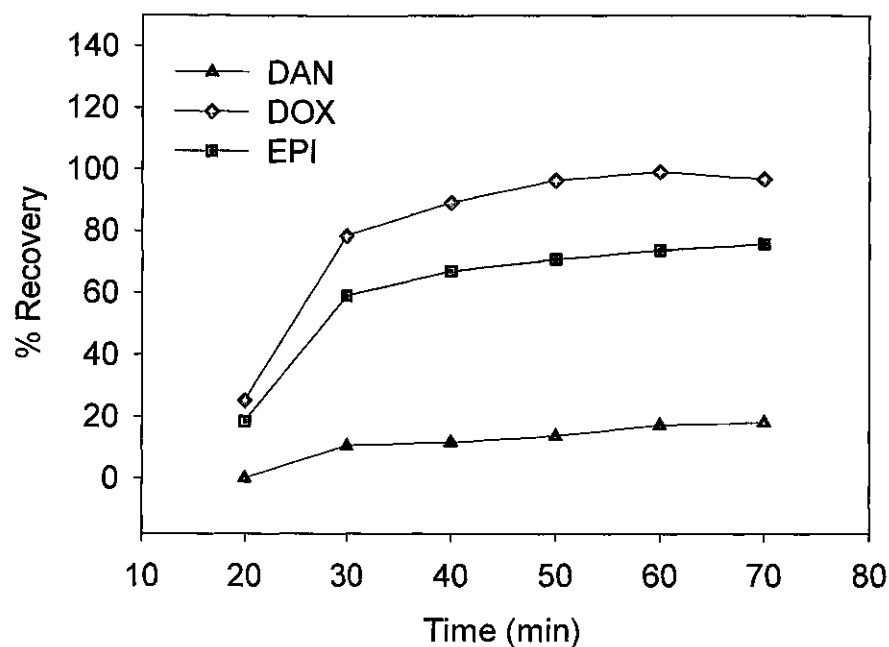


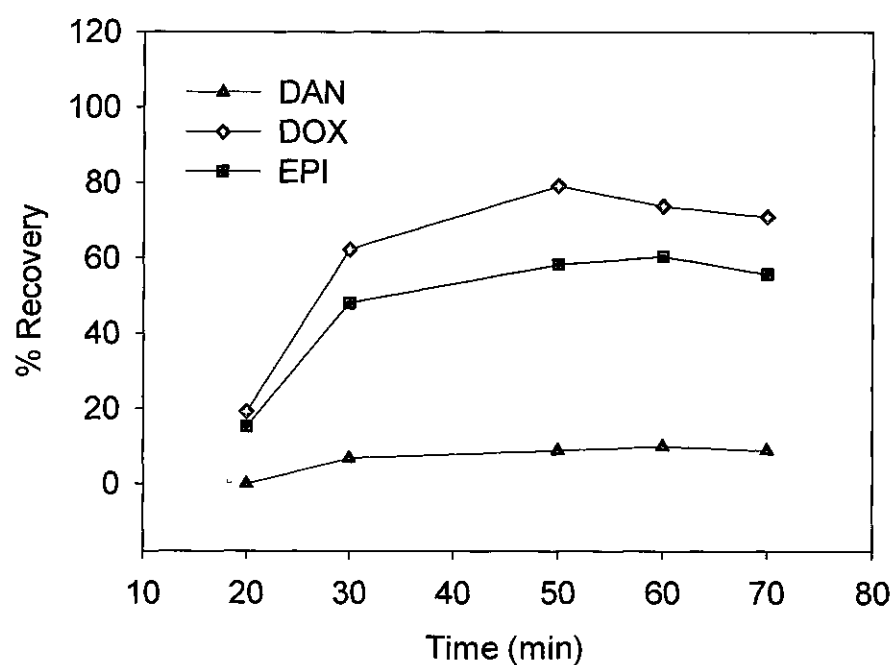
**Figure 5.24** Digital image of a microdialysis probe

Initially, the % recoveries of DAN, DOX and EPI were obtained in plasma and in an aCSF solution, Fig.'s 5.25 (A) and (B). % recoveries were calculated according to literature methods.<sup>[104]</sup> From these % recoveries, the estimated protein binding obtained was in the 25-45%. However, from literature it is known that the % protein binding of anthracyclines is higher, between 60-90%,<sup>[21]</sup> therefore in order to verify this result, this experiment should be repeated.





(A)



(B)

**Figure 5.25** (A) % recoveries obtained for DAN ( $56 \mu\text{g mL}^{-1}$ ), DOX ( $58 \mu\text{g mL}^{-1}$ ) and EPI ( $58 \mu\text{g mL}^{-1}$ ) in plasma. (B) % recoveries obtained for DAN ( $56 \mu\text{g mL}^{-1}$ ), DOX ( $58 \mu\text{g mL}^{-1}$ ) and EPI ( $58 \mu\text{g mL}^{-1}$ ) in aCSF. Flow rate  $2 \mu\text{L min}^{-1}$ , samples collected every 10 min. Separation conditions as in Fig 5.23

### 5.5.6 Comparison of CE method with HPLC-UV

The CE method developed was compared with HPLC, the separation technique regularly employed for the analysis of anthracyclines.<sup>[48,53,68]</sup> Based on a literature method, the analysis of DAN, DOX and EPI was performed, with UV detection.<sup>[28]</sup> A chromatogram showing their separation with various amounts of SDS in the mobile phase is illustrated in Fig. 5.26. It is evident from Fig. 5.26 that increasing the content of SDS reduces the length of analysis from 30 min. to 18 min. The analysis time is similar to CE; however, increased sample volumes were required for analysis by HPLC ( $\mu\text{l}$ ), compared to nl volumes required for CE. The anthracyclines are carcinogenic and highly toxic, therefore CE is an ideal separation technique as the small sample volume required reduces the exposure to them.

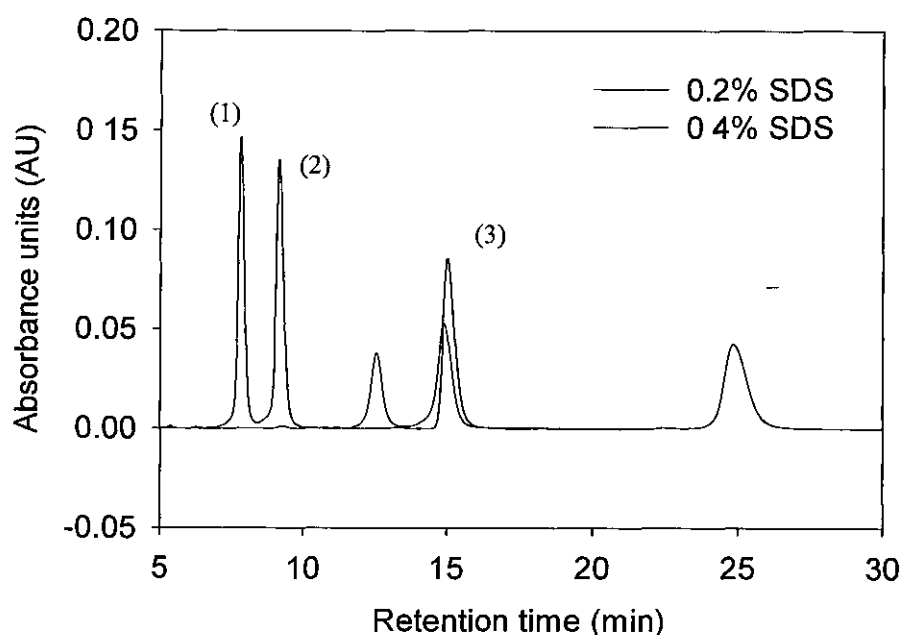


**Figure 5.26** HPLC separation with UV detection at 230 nm of (1) DOX ( $58 \mu\text{g ml}^{-1}$ ), (2) EPI ( $58 \mu\text{g ml}^{-1}$ ) and (3) DAN ( $56 \mu\text{g ml}^{-1}$ ). Mobile phase prepared by mixing the buffer A (phosphate, pH 2.0, with either 0.2 % or 0.4 % SDS), with solvent B (mixture of MeOH:ACN, 50:50). The composition of the mobile phase was buffer A:solvent B = 40/60. Flow rate  $1.5 \text{ ml min}^{-1}$

## **5.6 CONCLUSION**

A CE method was successfully developed for the separation of the anthracyclines DAN, DOX and EPI coupled with UV, EC and LIF detection. Detection limits in the range of 12-14  $\mu\text{g ml}^{-1}$  were obtained with UV detection. The CE-UV method was applied to the analysis of rat plasma samples, using VUF for the determination of the free drug concentration. However, due to the extent of plasma protein binding of anthracyclines, no free drug was detected. Improved detection limits (150-1400  $\text{ng ml}^{-1}$ ) were obtained with LIF detection, which were capable of monitoring the therapeutic levels (5-50,000  $\text{ng ml}^{-1}$ ) of anthracyclines. The degree of plasma protein binding of anthracyclines was determined using microdialysis, however, the results obtained conflicted with literature data. Nonetheless the potential of this technique for the real time monitoring of plasma samples with on-line microdialysis coupled with CE was demonstrated. Microdialysis is suitable for coupling to CE as it generates sample volumes that are ideal for CE analysis. There is the capability too for the miniaturisation of CE, which will further reduce the waste generated and also potentially enable point of care testing. The CE method developed was compared to HPLC, and further demonstrates the advantages of CE for their analysis. The exposure to the anthracyclines, which are carcinogenic and extremely toxic, is significantly reduced through analysis by CE.

## 5.7 REFERENCES

- [1] Hempel, G., Schulze-Westhoff, P., Flege, S., Boos, J., *J. Chromatogr. B*, **2001**, 758, 221.
- [2] Simeon, N., Chatelut, E., Canal, P., Nertz, M., Couderc, F., *J. Chromatogr. A*, **1999**, 853, 449.
- [3] Kunkel, A., Gunter, S., Watzig, H., *J. Chromatogr. A*, **1997**, 768, 125.
- [4] Altria, K. D., *LCGC*, **December 2001**, 2.
- [5] Weiss, R. B., *Seminars In Oncology*, **1992**, 19, 670.
- [6] Dodde, W., Maring, J. G., Hendriks, G., Wachters, F. M., Groen, H. J. M., De Vries, E. G. E., Uges, D. R. A., *Ther. Drug Monit.*, **2003**, 25, 433.
- [7] Perez-Ruiz, T., Martinez-Lozano, C., Sanz, A., Bravo, E., *Electrophoresis*, **2001**, 22, 134.
- [8] Wang, J., Ozsoz, M., Cai, X., Rivas, G., Shiraishi, H., Grant, D. H., Chicharro, M., Palecek, E., *Bioelectrochem. and Bioenerg.*, **1998**, 45, 33.
- [9] Oliveira-Brett, A. M., Vivan, M., Fernandes, I. R., Piedade, J. A. P., *Talanta*, **2002**, 56, 959.
- [10] Taubes, G., *Science*, **1997**, 275, 1420.
- [11] Turker, L., *J. Molecular Structure*, **2002**, 583, 81.
- [12] Zucchi, R., Danesi, R., *Curr. Med. Chem-Anti-Cancer Agents*, **2003**, 3, 151.
- [13] Loadman, P. M., Calabrese, C. R., *J. Chromatogr. B*, **2001**, 764, 193.
- [14] Hempel, G., Flege, S., Wurthwein, G., Boos, J., *Cancer Chemother. Pharmacol.*, **2002**, 49, 133.
- [15] Booser, D. J., Hortobagyi, G. N., *Drugs*, **1994**, 47, 223.
- [16] Ceruti, M., Tagini, V., Recalenda, V., Arpicco, S., Cattel, L., Airolidi, M., Bumma, C., *Il Farmaco*, **1999**, 54, 733.
- [17] Berruti, A., Bitossi, R., Bottini, A., Bonardi, S., Donadio, M., Nigro, C., Bertetto, O., Danese, S., Bertone, E., Sarobba, M. G., Farris, A., Katsaros, D., Castiglione, F., Volpe, T., Lattuada, S., Mancarella, S., Dogliotti, L., *J. Pharm. Biomed. Anal.*, **2005**, 41, 249.
- [18] Andersen, A., Holte, H., Slordal, L., *Cancer Chemother. Pharmacol.*, **1999**, 44, 422.
- [19] Zagotto, G., Gatto, B., Moro, S., Sissi, C., Palumbo, M., *J. Chromatogr. B*, **2001**, 764, 161.

- [20] Hortobagyi, G. N., *Drugs*, **1997**, 54, 1.
- [21] [www.rxlist.com](http://www.rxlist.com)
- [22] Celio, L. A., Digregorio, G. J., Ruch, E., Pace, J. N., Piraino, A. J., *Arch. Int. Pharmacodyn.*, **1982**, 260, 180.
- [23] Chassany, O., Urien, S., Claudepierre, P., Bastian, G., Tillement, J-P., *Cancer Chemother. Pharmacol.*, **1996**, 38, 571.
- [24] Sandstrom, M., Simonsen, L. E., Freijis, A., Karlsson, M. O., *Cancer Chemother Pharmacol* , **1999**, 44, 469.
- [25] Israel, M., Pegg, W. J., Wilkinson, P. M., Garnick, M. B., *J. Liq. Chrom.*, **1978**, 1, 795.
- [26] Robert, J., *J. Liq. Chrom.*, **1980**, 3, 1561.
- [27] Hulhoven, R., Desager, J. P., *J. Chromatogr.*, **1976**, 125, 369.
- [28] Badea, I., Lazar, L., Moja, D., Nicolescu, D., Tudose, A., *J Pharm. Biomed. Anal* , **2005**, 39, 305.
- [29] Hu, Q., Zhang, L., Zhou, T., Fang, Y., *Anal. Chim. Acta*, **2000**, 416, 15.
- [30] Reinhoud, N. J., Tjaden, U. R., Irth, H., Van Der Greef, J., *J. Chromatogr. B*, **1992**, 574, 327.
- [31] Riley, C. M., Runyan, A. K., *J. Pharm. Biomed. Anal.*, **1987**, 5, 33.
- [32] Rossi, D. T., Philips, B. A., Baldwin, J. R., Narang, P. K., *Anal. Chim. Acta*, **1993**, 271, 59.
- [33] Dubois, J., Hanocq, M., Atassi, G., *Anal. Lett.*, **1987**, 20, 1611.
- [34] Oosterbaan, M. J. M., Dirks, R. J. M., Vree, T. B., Van Der Kleijn, E., *J. Chromatogr.*, **1984**, 306, 323.
- [35] De Bruijn, P., Verweij, J., Loos, W. J., Kolker, H. J., Planting, A. S. T., Nooter, K., Stoter, G., Sparreboom, A., *Anal. Biochem.*, **1999**, 266, 216.
- [36] Ricciarello, R., Pichini, S., Pacifici, R., Altieri, I., Pellegrini, M., Fattorossi, A., Zuccaro, P., *J. Chromatogr. B*, **1998**, 707, 219.
- [37] Akpofure, C., Riley, C. A., Sinkule, J. A., Evans, W. E., *J. Chromatogr. B*, **1982**, 232, 377.
- [38] Mou, C., Ganju, N., Sridhar, K.S., Krishan, A., *J. Chromatogr. B*, **1997**, 703, 217.
- [39] Brown, J E., Wilkinson, P. A., Brown, J. R., *J. Chromatogr.*, **1981**, 226, 521.
- [40] Buehler, P.W., Robles, S. J., Adami, G. R., Gajee, R., Negrusz, A., *Chromatographia*, **1999**, 49, 557.

- [41] Beijnen, J. H., Meenhorst, P. L., Van Gijn, R., Fromme, M., Rosing, H., Underberg, W. J. M., *J Pharm Biomed. Anal.*, **1991**, 9, 995.
- [42] Kummerle, A., Krueger, T., Dusmet, M., Vallet, C., Pan, Y., Ris, H. B., Decosterd, L. A., *J. Pharm. Biomed. Anal.*, **2003**, 33, 475.
- [43] Cummings, J., Stuart, J. F. B., *J Chromatogr.*, **1984**, 311, 125.
- [44] Cummings, J., *J. Chromatogr.*, **1985**, 341, 401.
- [45] Nicholls, G., Clark, B.J., Brown, J. E., *J. Pharm. Biomed. Anal.*, **1992**, 10, 949.
- [46] Hahn, K. A., Chan, T. C. K., Morrison, W. B., Hahn, E. A., *J. Amer. Animal Hospital Assoc.*, **1994**, 30, 276.
- [47] Erb, N., Erttmann, R., Landbeck, G., *Cancer Chemother. Pharmacol.*, **1986**, 17, 53.
- [48] Camaggi, C., Comparsi, R., Strocchi, E., Testoni, F., Pannuti, F., *Cancer Chemother Pharmacol.*, **1988**, 21, 216.
- [49] Cassinelli, G., Configliacchi, E., Penco, S., Rivola, G., Arcamone, F., Pacciarini, A., Ferrari, L., *Drug Metabolism and Disposition*, **1984**, 12, 506.
- [50] Weenen, H., Osterop, A. P. R. M., Van Der Poort, S. E. J. M., Lankelma, J., Van Der Vijgh, W. J. F., Pinedo, H. M., *J. Pharm. Sci.*, **1986**, 75, 1201.
- [51] Van Asperen, J., Van Telligen, O., Beijnen, J. H., *J. Chromatogr. B*, **1998**, 712, 129.
- [52] Palm, C., Bjork, O., Bjorkholm, M., Eksborg, S., *Anti-Cancer Drugs*, **2001**, 12, 859.
- [53] Fogli, S., Danesi, R., Innocenti, F., Di Paolo, A., Bocci, G., Barbara, C., Del Tacca, M., *Ther. Drug Monit.*, **1999**, 21, 367.
- [54] Dine, T., Brunet, C., Luyckx, M., Cazin, M., Gosselin, P., Cazin, J. L., *Biomed. Chrom.*, **1990**, 4, 20.
- [55] Alvarez-Cedron, L., Sayalero, M. L., Lanao, J. M., *J. Chromatogr. B*, **1999**, 721, 271.
- [56] Rudolphi, A., Vielhauer, S., Boos, K-S., Seidel, D., Bathges, I-M., Berger, H., *J Pharm. Biomed. Anal.*, **1995**, 13, 615.
- [57] Andersen, A., Warren, D. J., Slordal, L., *Cancer Chemother. Pharmacol.*, **1994**, 34, 197.
- [58] Deesen, P. E., Leyland-Jones, B., *Drug Metabolism and Disposition*, **1984**, 12, 9.
- [59] Riley, C. A., Crom, W. R., Evans, W. E., *Ther. Drug Monit.*, **1985**, 7, 455.

- [60] Andersen, A., Warren, D. J., Slordal, L., *Ther. Drug Monit.*, **1993**, *15*, 455.
- [61] Mahnik, S. N., Rizovski, B., Fuerhacker, M., Mader, R. M., *Chemosphere*, **2006**, *65*, 1419.
- [62] Zhao, P., Dash, A. K., *J. Pharm. Biomed. Anal.*, **1999**, *20*, 543.
- [63] Gilbert, C. M., Mc Geary, R. P., Filippich, L. J., Norris, R. L. G., Charles, B. G., *J. Chromatogr. B*, **2005**, *816*, 273.
- [64] Sepaniak, M. J., Yeung, E.S., *J. Chromatogr.*, **1980**, *190*, 377.
- [65] Jacquet, J. M., Galtier, M., Bressolle, F., Jourdan, J., *J. Pharm. Biomed. Anal.*, **1992**, *10*, 343.
- [66] Eksborg, S., Ehrsson, H., Andersson, B., Beran, M., *J. Chromatogr.*, **1978**, *153*, 211.
- [67] Van Lancker, M. A., Nelis, H. J. C. F., Leenheer, A. P. De, *J. Chromatogr.*, **1983**, *254*, 45.
- [68] Configliacchi, E., Razzano, G., Rizzo, V., Vigevari, A., *J. Pharm. Biomed. Anal.*, **1996**, *15*, 123.
- [69] Mikan, A., Martinez Lanao, J., Lopez Gonzalez, F., Dominguez-Gil Hurle, A., *Biomed. Chrom.*, **1990**, *4*, 154.
- [70] Fahmy, O., Korany, M. A., Maher, H. M., *J. Pharm. Biomed. Anal.*, **2004**, *34*, 1099.
- [71] Cummings, J., Morrison, J. G., Willmott, N., *J. Chromatogr.*, **1986**, *381*, 373.
- [72] Larson, R. R., Khazaeli, M. B., Dillon, H. K., *App. Occupational Envtl. Hygiene*, **2003**, *18*, 109.
- [73] Lachatre, F., Marquet, P., Ragot, S., Gaulier, J. M., Cardot, P., Dupuy, J. L., *J. Chromatogr. B*, **2000**, *738*, 281.
- [74] Scottani, C., Tranfo, G., Bettinelli, M., Faranda, P., Spagnoli, M., Minola, C., *Rapid Commun. Mass Spec.*, **2004**, *18*, 2426.
- [75] Arnold, R. D., Slack, J. E., Straubinger, R. M., *J. Chromatogr. B*, **2004**, *808*, 141.
- [76] Yang, Y., *Talanta*, **2006**, *Article in Press*.
- [77] Mazuel, C., Grove, J., Gerin, G., Keenan, K. P., *J. Pharm. Biomed. Anal.*, **2003**, *33*, 1093.
- [78] Li, R., Dong, L., Huang, J., *Anal. Chim. Acta*, **2005**, *546*, 167.
- [79] Callies, S., De Alwis, D. P., Mehta, A., Burgess, M., Aarons, L., *Cancer Chemother. Pharmacol.*, **2004**, *54*, 39.

- [80] Hempel, G., Schulze-Westhoff, P., Flege, S., Laubrock, N., Boos, J., *Electrophoresis*, **1998**, *19*, 2939.
- [81] Hempel, G., Haberland, S., Schulze-Westhoff P., Mohling, N., Blaschke, G., Boos, J., *J. Chromatogr. B*, **1997**, *698*, 287.
- [82] Griese, N., Blaschke, G., Boos, J., Hempel, G., *J. Chromatogr. A*, **2002**, *979*, 379.
- [83] Laubrock, N., Hempel, G., Schulze-Westhoff, P., Wurthwein, G., Flege, S., Boos, J., *Chromatographia*, **2000**, *52*, 9.
- [84] Anderson, A. B., Gergen, J., Arriaga, E. A., *J. Chromatogr. B*, **2002**, *769*, 97.
- [85] Anderson, A. B., Ciriacka, C. M., Fuller, K. M., Arriaga, E. A., *Anal. Chem* , **2003**, *75*, 8.
- [86] Xiong, G., Chen, Y., Arriaga, E. A., *Anal. Chem.*, **2005**, *77*, 3488.
- [87] Nagaraj, S., Karnes, H. T., *Biomed. Chrom.*, **2000**, *14*, 234.
- [88] Gavenda, A., Sevic, J., Psotova, J., Bednar, P., Bartak, P., Adamovsky, P., Simanek, V., *Electrophoresis*, **2001**, *22*, 2782.
- [89] Sastry, C. S. P., Rao, J., *Talanta*, **1996**, *43*, 1827.
- [90] Karukstis, K. K., Thompson, E. H. Z., Whiles, J. A., Rosenfeld, R. J., *Biophys. Chem* , **1998**, *73*, 249.
- [91] Wen-Xu, L., Jian, C., *Anal. Chem.*, **2003**, *75*, 1458.
- [92] Trevisan, M. G., Poppi, R. J., *Anal. Chim. Acta*, **2003**, *493*, 69.
- [93] Loren, A., Eliasson, C., Murty, K. V. G. K., Kall, M., Abrahamsson, J., Abrahamsson, K., *J. Raman Spec.*, **2001**, *32*, 971.
- [94] Landers, J. P., *Handbook of Capillary Electrophoresis*, CRC Press, Boca Raton, **1997**.
- [95] Launchbury, A. P., Habboubit, N., *Cancer Treatment Reviews*, **1993**, *19*, 197.
- [96] Phinney, K. W., Jackson, J. W., Sander, L. C., *Electrophoresis*, **2002**, *23*, 1308.
- [97] Emara, S., Morita, I., Tamura, K., Razee, S., Masujima, T., Mohamed, H. A., El-Gizaway, S-M., El-Rabbat, N. A., *Talanta*, **2000**, *51*, 359.
- [98] Schneiderman, E., Stalcup, A. M., *J. Chromatogr. B*, **2000**, *745*, 83.
- [99] Rodriguez, M. A., Liu, Y., McCulla, W. S., Jenks, W. S., Armstrong, D. W., *Electrophoresis*, **2002**, *23*, 1561.
- [100] Andersen, S., *J. Pharm. Biomed. Anal.*, **2003**, *33*, 263.
- [101] Lam, H., Davies, M., Lunte, C. E., *J. Pharm. Biomed. Anal.*, **1996**, *14*, 1753.
- [102] Osbourn, D.M., Lunte, C.E., *Anal. Chem.*, **2001**, *73*, 5961.



- [103] Park, S., Lunte, C. E., *Anal. Chem.*, **1995**, 67, 4366.
- [104] Arnett, S. D., Osbourn, D. M., Moore, K. D., Vandaveer, S. S., Lunte, C. E., *J. Chromatogr. B*, **2005**, 827, 16.
- [105] Oravcova, J., Bohs, B., Lindner, W., *J. Chromatogr. B*, **1996**, 677, 1.
- [106] Lin, Z. J., Musiano, D., Abbot, A., Shum. L., *J. Pharm. Biomed. Anal.*, **2005**, 37, 757.
- [107] Singh, S. S., Mehta, J., *J. Chromatogr. B*, **2006**, 834, 108.
- [108] Wan, H., Rehngren, M., *J. Chromatogr. A*, **2006**, 1102, 125.
- [109] Jimenez, J.-R., Luque De Castro, M. D., *Trends in Anal. Chem.*, **2006**, 25, 563.

## ***Chapter Six***

### ***Conclusions and Future Work***

## 6.1 COMPARISON OF ELECTROPHORESIS Vs CHROMATOGRAPHY

The separation principles of electrophoresis and chromatography are very different. However, they are complementary techniques, *e.g.* separation in CE is dependant upon the size to charge ratio of the analyte ion; in contrast, HPLC is based upon the hydrophobicity of the analytes. In the preceding four chapters, a comparison was made between these modes of separation. The limitations and advantages of both techniques are outlined below.

### 6.1.1 Sample matrix

The application of Capillary Electrophoresis (CE) to the analysis of complex matrices, such as plasma samples, was demonstrated. For the real time monitoring of anthracyclines in plasma, it is preferred that minimal sample pre-treatment was carried out. The feasibility of analysing plasma samples without sample pre-treatment was demonstrated using CE, and with further method development the direct injection of plasma could potentially be applied to the determination of anthracyclines in plasma. This possibility does not exist for chromatographic techniques and so the superior ruggedness of CE is a major advantage for plasma analysis.

Microdialysis is a sampling technique, which removes the need for a separate sample pre-treatment step. The degree of plasma protein binding of anthracyclines was determined using microdialysis. The potential of this technique for the real time monitoring of plasma samples with on-line microdialysis coupled with CE was also demonstrated. This highlights another advantage of CE over chromatographic techniques, which are not as readily amenable to microdialysis coupling, and therefore not as suitable for real time monitoring.

In the analysis of cyanoacrylate adhesives, preparation of the adhesive samples was performed using liquid-liquid extraction. This sample pre-treatment was required for the chromatographic analysis of the samples too. In this study, as a sample pre-treatment was required for both separation techniques, neither mode of separation offered distinct advantages in the analysis of adhesives.

### 6.1.2 Sample volume

The exposure to the anthracyclines, which are carcinogenic and extremely toxic, is significantly reduced through analysis by CE, as nl sample volumes are required for analysis by CE, compared to  $\mu\text{l}$  sample volumes required for analysis by High Performance Liquid Chromatography (HPLC). The anthracyclines are carcinogenic and highly toxic, and therefore CE is an ideal separation technique as the small sample volume required reduces the exposure to them.

The sampling technique, microdialysis, was applied to the analysis of anthracyclines, and this is an ideal sampling technique for coupling to CE as it generates sample volumes that are suited for CE analysis. There is the capability too for the miniaturisation of CE, which will further reduce the waste generated and also potentially enable point-of-care testing. Also, the cost of removal of waste generated through either the chromatographic analysis of industrial or clinical samples is decreased due to the reduced waste generated by CE.

### 6.1.3 Length of Analysis

The CE method developed for the analysis of anthracyclines was compared with HPLC, the separation technique regularly employed for the analysis of anthracyclines. The length of analysis in this study was similar to CE; however, the coupling microdialysis to CE should help improve the temporal resolution of the analysis.

The electrophoretic analysis of ethyl cyanoacrylate adhesives, resulted in high separation efficiencies, such as 330,000 plates  $\text{m}^{-1}$  for chloride, and also reduced total analysis times, namely 23 min. for CE compared with 45 min. for Ion Chromatography (IC). The application of CE to the analysis of the irgacure was also shown and demonstrated its ability as an alternative mode of analysis with increased separation efficiencies obtained, 2130 plates  $\text{m}^{-1}$  with HPLC and 411,280 plates  $\text{m}^{-1}$  with CE. A reduced total analysis time of 6 min. was also achieved with CE, with the potential of applying higher separation voltages to further reduce the analysis time. CE therefore resulted in a superior analysis time when compared to both HPLC and IC.

#### 6.1.4 Detection Methods

Detection modes, such as fluorescence, electrochemical (EC) and mass spectrometric (MS) detection, were successfully applied to the analysis of industrial and clinical samples with both CE and HPLC. Ultra-violet (UV) detection is the preferred mode for method development; nevertheless, it does not enable the therapeutic monitoring of pharmaceuticals in biological matrices. However, UV is still an important mode of detection both for method development and also for the analysis of samples where the LOD's are not the deciding factor, such as in the analysis of inorganic and acidic anions in cyanoacrylate adhesives.

For the analysis of anthracyclines, UV, EC and Laser-Induced Fluorescence (LIF) detection was employed. Improved detection limits ( $150\text{-}1400\text{ ng ml}^{-1}$ ) were obtained with LIF detection, which were capable of monitoring the therapeutic levels ( $5\text{-}50,000\text{ ng ml}^{-1}$ ) of anthracyclines. Therefore, for anthracycline analysis, LIF was shown to be the preferred mode of detection.

The application of HPLC coupled with MS detection enabled the structural elucidation of the irgacure and it was determined that the irgacure undergoes free radical curing reaction. The structural elucidation was not possible with any of the other modes of detection used in this thesis.

#### 6.1.5 Conclusion

In this work, electrophoresis was compared with chromatography in terms of the matrix of the sample to be analysed, the volume of sample required, the length of analysis developed and the detection methods preferred. CE was clearly demonstrated as an alternative mode of separation capable of equalling, and in many cases improving on the corresponding chromatographic analysis.

## ***Chapter Seven***

## ***Appendices***

**7.1 APPENDIX 1a – MS Parameters for APCI-MS**

<b><u>Mode</u></b>		<b><u>Trap</u></b>	
Mass Range mode	Std/Normal	Scan Begin	50.00 m/z
Ion Polarity	Positive	Scan End	1000.0 m/z
Ion Source Type	APCI	Averages	20 Spectra
Current Alternating Ion Pol	N/A	Charge Control	On
Alternating Ion Polarity	N/A	ICC Target	20000
		ICC Actual	16261
<b><u>Detector &amp; Block Voltages</u></b>		Accumulation Time	5215 µs
Multiplier Voltage	1750 V	Max. Acc. Time	30000 µs
Dynode Voltage	7.0 kV		
Scan Delay	0 µs	<b><u>MS/MS Manual Mode</u></b>	
Skimmer 1 Block	100.0 V	Fast Calc	On
Skimmer 2 Block	300.0 V	ISTD	Off
<b><u>Tune Source</u></b>		<b><u>MS/MS Automatic</u></b>	
Trap Drive	38.3	Auto MS/MS	Off
Skim 1	15.0 V		
Skim 2	6.4 V	<b><u>Rolling Average</u></b>	
Octopole RF Amplitude	91.0 Vpp	Rolling	On
Octopole Delta	2.05 V		
Lens 1	-3.2 V	<b><u>Compressed Spectra</u></b>	
Lens 2	-46.1 V	Compressed Spectra	Off
Octopole	2.38 V		
Capillary Exit	65.0 V		
Cap Exit Offset	50.0 V		
HV End Plate Offset	-993 V		
Current End Plate	2177.151 nA		
HV Capillary	2828 V		
Current Capillary	77.214 nA		
Dry Temp (Measured)	326 °C		
Dry Gas (Measured)	8.02 l/min		
Nebuliser (Measured)	30.34 psi		

**7.2 APPENDIX 1b-IC Gradient method**

Time (min.)	50 mM NaOH (%)	H <sub>2</sub> O (%)	5 mM NaOH (%)	MeOH (%)
0-2	0	80	50	150
3	0	77.5	7.5	150
4-5	0	75	10.0	150
6	1.7	66.7	16.7	150
7	3.3	58.3	23.3	150
8	5.0	50.0	30.0	150
9	7.5	37.5	40.0	150
10	10.0	25.0	50.0	150
11	12.5	12.5	60.0	150
12	15.0	0.0	70.0	150
13	16.2	0.0	68.5	150
14	17.5	0.0	67.5	150
15	18.8	0.0	66.2	150
16.0	20.0	0.0	65.0	150
17.0	30.0	0.0	55.0	150
18.0	40.0	0.0	45.0	150
19.0	50.0	0.0	35.0	150
20.0	60.0	0.0	25.0	150
21.0	70.0	0.0	15.0	150
22-25	80.0	0.0	5.0	150
26.0	0	80.0	5.0	150



### 7.3 Publications

*"The Potential of Capillary Electrophoresis for the Analysis of Inorganic and Acidic Anions in Cyanoacrylate Adhesives"*

*Electrophoresis*, Article in Press, **2006**

Gillian Whitaker, Brendan J. Kincaid, Nicole Van Hoof, Fiona Regan, Malcolm R. Smyth, Raymond G. Leonard

*"An investigation into the stability of cyanoacrylate adhesives using capillary electrophoresis"*

*Intl. J. of Adhesion and Adhesives*, Manuscript in preparation

Gillian Whitaker, Brendan J. Kincaid, Nicole Van Hoof, Fiona Regan, Malcolm R. Smyth, Raymond G. Leonard

*"A Study of the Mechanisms of Oxidative DNA Damage by Nickel"*

*Free Radical Biology and Medicine*, Article in submission **2006**

Michele Kelly, Gillian Whitaker, Blánaid White, Malcolm R. Smyth

## 7.4 Oral Presentations

### **4th Biennial Conference on Analytical Sciences in Ireland, April 11-12, 2006, DIT, Kevin St., Dublin, Ireland**

**"The Capillary Electrophoretic Determination of some Inorganic and Acidic Anions Present in Cyanoacrylate Adhesives"**

**Gillian Whitaker, Brendan J. Kincaid, Declan P. Raftery, Nicole Van Hoof, Fiona Regan, Malcolm R. Smyth, Raymond G. Leonard**

### **Analytical Research Forum, July 17-19, 2006, University College Cork, Ireland**

**"The potential of capillary electrophoresis for the determination of anthracyclines"**

**Gillian Whitaker, Stacy D. Arnett, Robert O'Connor, Fiona Regan, Craig E. Lunte, Malcolm R. Smyth**

## 7.5 Poster Presentations

### **18th International Symposium on MicroScale Bioseparations (MSB)**

**February 12 – 17, 2005, New Orleans**

*"Quantification of anthracycline antibiotics in plasma by capillary electrophoresis"*

Gillian Whitaker, Stacy D. Arnett, Robert O'Connor, Fiona Regan, Craig E. Lunte, Malcolm R. Smyth

### **Responses to DNA Damage: Insights from Chemical, Biochemical, Structural Biology and Cellular Studies, September 19-21, 2005, Sussex, United Kingdom**

*"Generation of 8-oxoguanine by carcinogenic metal Nickel"*

Michele Kelly, Gillian Whitaker, Blánaid White, Malcolm R. Smyth

### **Separations in the Biosciences, 4th International Symposium on Separations in the Biosciences, September 18-21, 2005, Amsterdam**

*"The Potential of Capillary Electrophoresis for the Determination of Anthracyclines"*

Gillian Whitaker, Stacy D. Arnett, Robert O'Connor, Fiona Regan, Craig E. Lunte, Malcolm R. Smyth

### **4th Biennial Conference on Analytical Sciences in Ireland, April 11-12 2006, DIT, Kevin St., Dublin, Ireland**

*"A Study of the Mechanisms of Oxidative DNA Damage by Nickel using Electrochemical Detection"*

Michele Kelly, Gillian Whitaker, Blánaid White, Malcolm R. Smyth

### **11<sup>th</sup> International Conference on Electroanalysis, June 11-15, 2006, Bordeaux, France**

*"An Electrochemical Study of 8-oxoguanine oxidation"*

Michele Kelly, Blánaid White, Gillian Whitaker, Malcolm R. Smyth